The transcriptional cofactor PCAF as mediator of the interplay between p53 and HIF-1 alpha and its role in the regulation of cellular energy metabolism

A thesis submitted to The University of Manchester for the degree of Doctor of Philosophy in the Faculty of Medical and Human Sciences

2011

Ramkumar Rajendran

School of Pharmacy and Pharmaceutical Sciences

Table of Contents

List of figures

List of tables

Word count: 54,869

Abstract

Energy production is a very important function for the cells to maintain homeostasis, survive and proliferate. Cellular energy can be produced either through oxidative phosphorylation (OXPHOS) in the presence of oxygen or glycolysis in its absence. Cancer cells, even in the presence of oxygen prefer to produce energy through glycolysis and this confers them a survival advantage. Energy metabolism has recently attracted the interest of several laboratories as targeting the pathways for energy production in cancer cells could be an efficient anticancer treatment. For that purpose the role of various transcription factors in determining the pathway of energy production has been investigated extensively and there is evidence to suggest that oncogenic transcription factors promote glycolysis whereas tumour suppressors demote it.

In line with this notion, the master regulator of cellular response to hypoxia, the Hypoxia Inducible Factor 1 (HIF-1) has been shown to induce the expression of a variety of genes encoding enzymes involved in glucose metabolism as well as OXPHOS favouring energy production through glucose metabolism in hypoxic cells. The tumour suppressor p53 on the other hand inhibits glycolysis and stimulates OXPHOS. One of the pathways through which p53 exerts these effects, is by inducing the inhibitor of glycolysis TIGAR and the cytochrome c oxidase assembly factor SCO2 gene expression under DNA damage conditions. However, the regulation of the expression of these genes in hypoxic conditions has been only partially elucidated.

We hypothesised that under hypoxic conditions, TIGAR and SCO2 gene expression might be differentially regulated in cells bearing mutated p53 and in these cells the involvement of HIF-1 could be crucial. Indeed under hypoxia mimicking conditions, the TIGAR and SCO2 protein and mRNA levels were found to be modulated differentially in p53 wild type and mutant cell lines. The bioinformatics analysis revealed the presence of hypoxia responsive elements (HREs) within the regulatory region of the promoters of TIGAR and SCO2 genes. Firefly reporter assays and chromatin immunoprecipitation (ChIP) assays have indicated that HIF-1 plays a crucial role in the regulation of TIGAR gene expression. The direct involvement of HIF-1 in the regulation of SCO2 gene expression requires further investigation.

We and others have recently reported that PCAF is a common cofactor for p53 and HIF-1α, regulating the protein stability and transcription target selectivity of both transcription factors thereby orchestrating the balance between life and death in cancer cells. We hypothesised that PCAF plays a similar role in the regulation of cellular energy metabolism by differentially targeting HIF-1α and p53 to the promoter of TIGAR and SCO2 genes. In this study we present evidence to support the notion that PCAF plays an import role in the regulation of TIGAR and SCO2 gene expression under hypoxic mimicking conditions. This conclusion was supported by assessing the functional consequences of PCAFwt and PCAFΔHAT overexpression on the intracellular lactate production, cellular oxygen consumption, NAD+/NADH ratio and ROS generation in cells under hypoxia mimicking conditions.

Declaration

No part of this thesis has been submitted in support of an application for any degree or qualification of The University of Manchester or any other university or institute of learning.

Copyright statement

This thesis is dedicated to my Mom

for being with me forever

Acknowledgements

First, I would like to thank my Supervisor Dr. Costas Demonacos for his support, guidance and for the opportunity to do PhD in his lab. I would also like to thank Dr. Marija Krstic-Demonacos for her valuable suggestions and help in this project. I also thank my Advisor Dr. Andrew McBain for his support during my course.

I specially thank My Wife Mahaalakshmi Muthusamy, my brother Mathan Samuvel Raj, My Supervisor Dr. Costas Demonacos and the University of Manchester for their financial support during the past four years. I also thank my friend Dr. Manikandan Kadirvel who encouraged me to come to research. I acknowledge with gratitude Professor Karen Vousden (Beatson Institute, Glasgow) and Professor Paul Hwang (NIH, Bethesda) for helping me with important expression vectors.

I thank my Parents and all my family members for their moral support for doing PhD. I remember with gratitude my Wife's struggles for being alone for the sake of me doing PhD. I thank all the past and present lab members, the graduate students who helped me in the lab especially, Dr. Georgia Xenaki, Dr. James Lynch, Ilhem Berrou, Travis Leung, Kleopatra Andreou, Muhammad Atif Chaudhry, Manjula Doddananjaiah, Richa Garva, Hassan Ashour and si nce the list is very big I am stopping here.

I also thank my friends in neighbouring labs for their helps in the lab and for making my life easier. I remember the support from all my friends in the past four years, Dr. Vijaykumar Karuppiah, Dr. Yamini Arthanari, Rajasimhan Sivakumar to name a few.

Abbreviations

ADM	Adrenomedullin
ADP	Adenosine diphosphate
AMP	Adenosine mono phosphate
AMPK	AMP-activated protein kinase
Apaf-1	Apoptotic peptidase activating factor-1
ARD1	Arrest defective 1
ARF	Alternate reading frame
ARF-BP1	ARF binding protein 1
ARNT	Aryl hydrocarbon receptor nuclear translocator
Asn	Asparagine
ATM	Ataxia telangiectasia mutated
ATP	Adenosine triphosphate
ATR	ATM and Rad3-related
Bax	Bcl-2-associated X protein
Bcl-2	B cell lymphoma-2
BH3	Bcl-2 homology domain 3
bHLH	Basic helix loop helix
BNIP3	BCL2/adenovirus E1B 19 kDa protein-interacting protein
CBP	cAMP responsive element binding (CREB) binding protein
Cdc	Cell division cycle
CDK	Cyclin dependent kinase
Chk	Checkpoint kinase
CITED	CBP/p300-interacting transactivator ED-rich tail 2
CK	Casein kinase
CoCl2	Cobalt chloride
COP1	Constitutively Photomorphogenic 1
COX	Cytochrome c oxidase
CSN-K	COP9 signalosome (CSN) associated kinase
C-TAD	C-terminal transactivation domain
Cul-2	Cullin-2
DNA	Deoxyribonucleic acid
DNA-PK	DNA dependent protein kinase
DSFX	Desferrioxamine
DUB	Deubiquitinase
DYRK	Dual specificity tyrosine-phosphorylation-regulated kinase
ERK	Extra cellular signal-regulated protein kinase
ET1	Endothelin 1
ETC	Electron transport chain
EPO	Erythropoietin
EPOR	Estrogen receptor/Progesterone receptor

F2,6-BP	Fructose 2,6-bisphosphate
F6P	Fructose 6-phosphate
FADH2	Flavin adenine dinucleotide (reduced form)
FDG	Flurodeoxyglucose
FH	Fumarate hydratase
FIH	Factor inhibiting HIF
G6Pase	Glucose 6-phosphatase
GADD45	Growth arrest and DNA damage 45
GAPDH	Glyceraldehyde 3-phosphate dehydrogenase
GK	Glucokinase
GLUT	Glucose transporter
GNAT	GCN-5 related N-acetyl transferase
GPI	Glucose phosphate isomerise
GSK	Glycogen synthase kinase
HAF	Hypoxia associated factor
HAT	Histone acetyl transferase
HAUSP	Herpesvirus-Associated Ubiquitin Specific Protease
HDAC	Histone deacetylase
HECT	Homologous to the E6-AP Carboxyl Terminus
HK2	Hexokinase2
HIF	Hypoxia inducible factor
HIPK	Homeodomain-interacting protein kinase
H-*Ras*	Harvey rat sarcoma
HRE	Hypoxia responsive element
HSP90	Heat shock protein 90
IGF	Insulin like growth factor
IKK	IkB kinase
IPAS	Inhibitory PAS domain protein
JNK	c-Jun N-terminal kinase
LDH-A	Lactate dehydrogenase-A
Lys	Lysine
MAPK	Mitogen-activated protein kinase
MDH	Malate dehydrogenase
MDM2	Murine double minute 2
MEF	Mouse embryonic fibroblast
MRG-1	Melanocyte-specific gene 1-related gene-1
mRNA	Messenger RNA
MXI1	MAX-interacting protein 1
mTOR	Mammalian target of rapamycin
NAD	Nicotinamide adenine dinucleotide
NADH	Nicotinamide adenine dinucleotide (reduced)
NADP	Nicotinamide adenine dinucleotide phosphate

NADPH	Nicotinamide adenine dinucleotide phosphate (reduced)
NES	Nuclear export signal
NLS	Nuclear localisation signal
NOS	Nitric oxide synthase
NQO1	NAD(P)H dehydrogenase (quinone) 1
N-TAD	N-terminal transactivation domain
OD	Oligomerization domain
ODDD	Oxygen dependent degradation domain
OXPHOS	Oxidative phosphorylation
P53R2	p53 –controlled ribonucleotide reductase
PAF	PCAF associated factor
PAS	Period-ARNT-Singleminded
PCAF	p300/CBP associated factor
PDH	Pyruvate dehydrogenase
PDK-1	Pyruvate dehydrogenase kinase-1
PEP	Phospho enol pyruvate
PET	Positron Emission Tomography
PFK-1	Phosphofructo kinase-1
PFKFB	Phosphofructokinase-2/Fructose 2,6-bisphosphatase
PGK	Phospho glycerate kinase
PGM	Phosphoglycerate mutase
PHD	Prolyl hydroxylase
PI3K	Phosphatidyl-inositol 3-kinase
PIRH2	p53 Induced protein with RING-H2
PKB	Protein kinase B
PKC	Protein kinase C
PPP	Pentose phosphate pathway
Pro	Proline
PTEN	Phosphatase and tensin homolog
PUMA	p53 upregulated modulator of apoptosis
pVHL	von Hippel-Lindau protein
RACK	Receptor activated protein kinase C
Ras	Rat sarcoma
RBX-1	Ring-Box-1
REG	Regulatory domain
RING	Really interesting new gene
RNA	Ribonucleic acid
ROS	Reactive oxygen species
SCO2	Synthesis of cytochrome c oxidase 2
SDH	Succinate dehydrogenase
siRNA	Small interfering RNA
SLC2A1	Solute carrier family 2, facilitated glucose transporter member 1

SOD2	Superoxide dismutase 2
SRC-1	Steroid receptor coactivator-1
SV40	Simian Virus 40
TAF	TBP associated factor
TBP	TATA-box binding protein
TCA cycle	Tricarboxylic acid cycle
TF	Transcription factor
TfR	Transferrin receptor
TGF	Transforming growth factor
TIGAR	Tp53 induced glycolysis and apoptosis regulator
TIF-1	Transcriptional intermediary factor 1
TPI1	Triose phosphate isomerase 1
TSC	Tuberous sclerosis protein
tRNA	Transfer RNA
VEGF	Vascular endothelial growth factor

1 Introduction

1.1 Cancer

Cancer is the result of the abnormal growth of cells caused by multiple changes in gene expression leading to dysregulated balance of cell proliferation and cell death and ultimately evolving into a population of cells that can invade tissues and metastasize to distant sites, causing significant morbidity and, if untreated, death of the host (Ruddon, 2007).

In 2000 Hanahan et al., proposed six biological features acquired during the multistep development of human tumours as hallmarks of cancer. The six phenotypes that a tumour requires in order to become a fully-fledged malignancy include self-sufficiency in growth signals, insensitivity to anti-growth signals, evading apoptosis, sustained angiogenesis, limitless replicative potential and tissue invasion and metastasis (Hanahan, 2000). However, in their recent update the authors have recognised two additional phenotypes as emerging hallmarks of cancer that include deregulated cellular energetics (reprogrammed energy metabolism) and evading immunological destruction (Hanahan and Weinberg, 2011).

Most of the genetic changes found in human cancers can be classified into two categories. They include gain-of-function mutations in proto-oncogenes, which lead to the activation of oncogenes that promote cell growth and cell survival; and loss-of-function mutations in tumour suppressor genes which lead to defective tumour suppressors which cannot perform their tumour suppressive activities such as prevention of unrestrained cellular growth and promotion of DNA repair and activation of cell cycle checkpoints (Lee and Muller, 2010). The gain-of-function mutation normally confers to cancer cells the proliferative advantage, the proto-oncogene H-*Ras*, for example, when activated induces MAPK mediated cellular proliferation as well as survival potential of the cancer cells (Karnoub and Weinberg, 2008). Other factors present in cancer cells such as the HIF-1α, regulate gene expression of genes encoding enzymes involved in glycolysis, promoting rapid utilization of glucose which is a

ubiquitously available energy source. As the glycolytic enzymes do not require oxygen to exert their function, high glycolysis enables cancer cells to survive in low oxygen conditions in which their normal counterparts cannot survive (DeBerardinis et al., 2008).

In contrast to oncogenes, mutations in tumour suppressors lead to either truncated proteins which lack tumour suppression activity or their expression is silenced due to epigenetic modifications (Ruddon, 2007). For example, the tumour suppressor p53 is mutated in more than 50% of the human cancers (Soussi et al., 2006). Mutated p53 lacks tumour suppressive activities such as cell cycle arrest, cell repair and apoptosis.

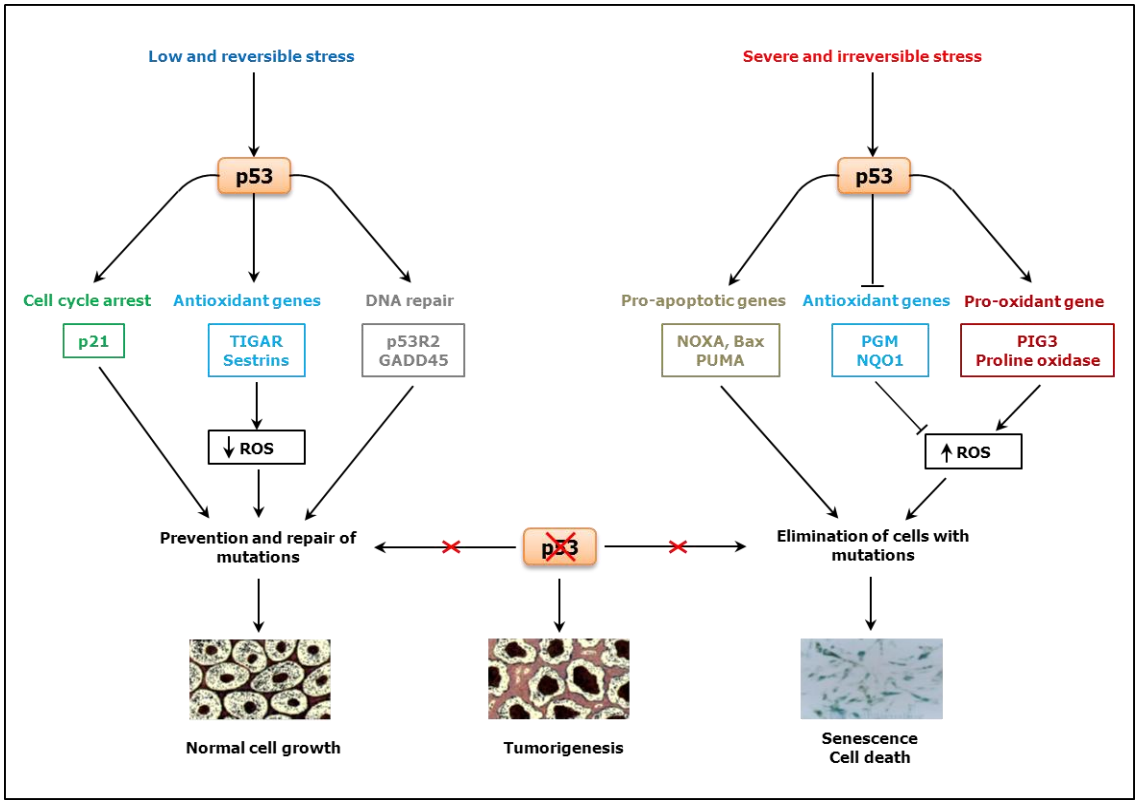

Figure 1.1.1: p53 differentially selects the target genes according to the stress conditions

Depending on the type and severity of stress, p53 modulates different subsets of its transcriptional target genes which can either induce cell survival or death. P53R2: p53 inducible ribonucleotide reductase; GADD45: Growth arrest and DNA damage 45; ROS: Reactive oxygen species; Bax: Bcl2 associated X protein; PUMA: p53 upregulated modifier of apoptosis; PGM: Phosphoglycerate mutase; NQO1: NAD(P)H dehydrogenase (quinone) 1; PIG3: p53 inducible gene 3; The figure is modified from (Bensaad and Vousden, 2007).

Apart from loss of function, mutations in tumour suppressor genes can lead to gain of function. For example, mutated p53 can promote tumorigenesis, poor prognosis and drug resistance (Seton-Rogers, 2009).

Activated by various cellular stress conditions wild type tumour suppressors are able to sense oncogenic signalling and in response promote cell protective functions. For example, when cells are exposed to mild or reversible stress, the p53 tumour suppressor will transcriptionally activate a particular subset of its target genes to stimulate cell cycle arrest ($p21^{WAF\text{-}1/CIP\text{-}1}$) (Tang et al., 1998), or antioxidant genes such as TIGAR and Sestrins to prevent ROS induced apoptosis (Bensaad et al., 2006; Budanov et al., 2004), or DNA damage repair genes (*p53R2*, *GADD45*) to repair damaged DNA (Figure 1.1.1) (Bensaad and Vousden, 2007). In the case of severe and irreversible genotoxic stress, p53 will turn on the gene expression of a different subset of its target genes to promote apoptosis (*NOXA*, *PUMA*, *Bax)* (Nakano and Vousden, 2001; Oda et al., 2000; Toshiyuki and Reed, 1995) and repress the expression of anti-oxidant genes (NQO1) (Bensaad and Vousden, 2007).

1.2 Glucose metabolism

The human diet is composed of complex nutrients such as proteins, lipids, and polysaccharides which must be broken down into smaller molecules before the cells can use them as a source of energy (Alberts et al., 2002). The digestive enzymes hydrolyse the most frequently used nutritive sugar, the disaccharide sucrose into the monosaccharide glucose. Glucose is actively transported into mammalian cells and subsequently converted to pyruvate which is either transformed to lactate in the cytoplasm or enters mitochondria where it is oxidized to carbon dioxide and water (Lehninger et al., 2005) and produces energy in the form of ATP (Figure 1.2.1)

1.2.1 Glycolysis

The cytoplasmic breakdown of glucose into pyruvate is called glycolysis. As all the enzymes of glycolysis are present in the cytoplasm and can function independent of oxygen availability, glycolysis can proceed in the cytoplasm both in the absence and presence of oxygen (Murray et al., 2003). In the first step of glycolysis, glucose is phosphorylated to glucose 6-phosphate (G6P) catalysed by hexokinase 2 (HK2) using

ATP as the phosphate donor. This is an irreversible reaction and hence one of the rate limiting reactions of glycolysis. G6P is then converted to fructose 6-phosphate (F6P) by glucose phosphate isomerase (GPI). Next F6P is phosphorylated to fructose 1,6-bisphosphate (F1,6-BP) catalysed by phosphofructokinase 1 (PFK-1) using ATP as another substrate. PFK-1 is functionally inactive in physiological conditions and requires fructose 2,6-bisphoshate to be activated. This reaction is another rate liming reaction in the glycolytic pathway (Lehninger et al., 2005; Murray et al., 2003; Singh and Costello, 2009).

F1,6-BP is cleaved by aldolase into two triose phosphates, glyceraldehyde 3-phosphate and dihydroxyacetone phosphate. Glyceraldehyde 3-phosphate and dihydroxyacetone phosphate are interconverted by the enzyme triose phosphate isomerase (TPI). The NAD dependent enzyme glyceraldehyde 3-phosphate dehydrogenase, converts glyceraldehyde 3-phosphate to 1,3-bisphosphoglycerate. Phosphoglycerate kinase catalyzes the transfer of one phosphate group from 1,3-bisphosphoglycerate to ADP to form ATP and 3-phosphoglycerate.

Since two molecules of triose phosphate are formed per molecule of glucose two molecules of ATP are formed at this stage per molecule of glucose. 3-phosphoglycerate is isomerized to 2-phosphoglycerate by Phosphoglycerate mutase (PGM). Enolase catalyzes the conversion of 2-phosphoglycerate into phosphoenol pyruvate (PEP). Pyruvate kinase enzyme catalyzes the transfer of a phosphate group from PEP to ADP to produce pyruvate and 2 ATP molecules. Under anaerobic conditions, pyruvate is reduced in the cytoplasm to produce lactate, a reaction catalysed by lactate dehydrogenase enzyme. However, in aerobic conditions, pyruvate is taken up into mitochondria and converted to acetyl CoA which is subsequently oxidized to CO_2 by the enzymes involved in the citric acid cycle. The 2 NADH produced in glycolysis, 2 molecules of NADH produced in oxidative decarboxylation of pyruvate and 8 NADH and $2FADH_2$ molecules produced in the citric acid cycle are oxidised to form electrons which flow through the electron transport chain subunits through which a proton gradient is created across the inner mitochondrial membrane.

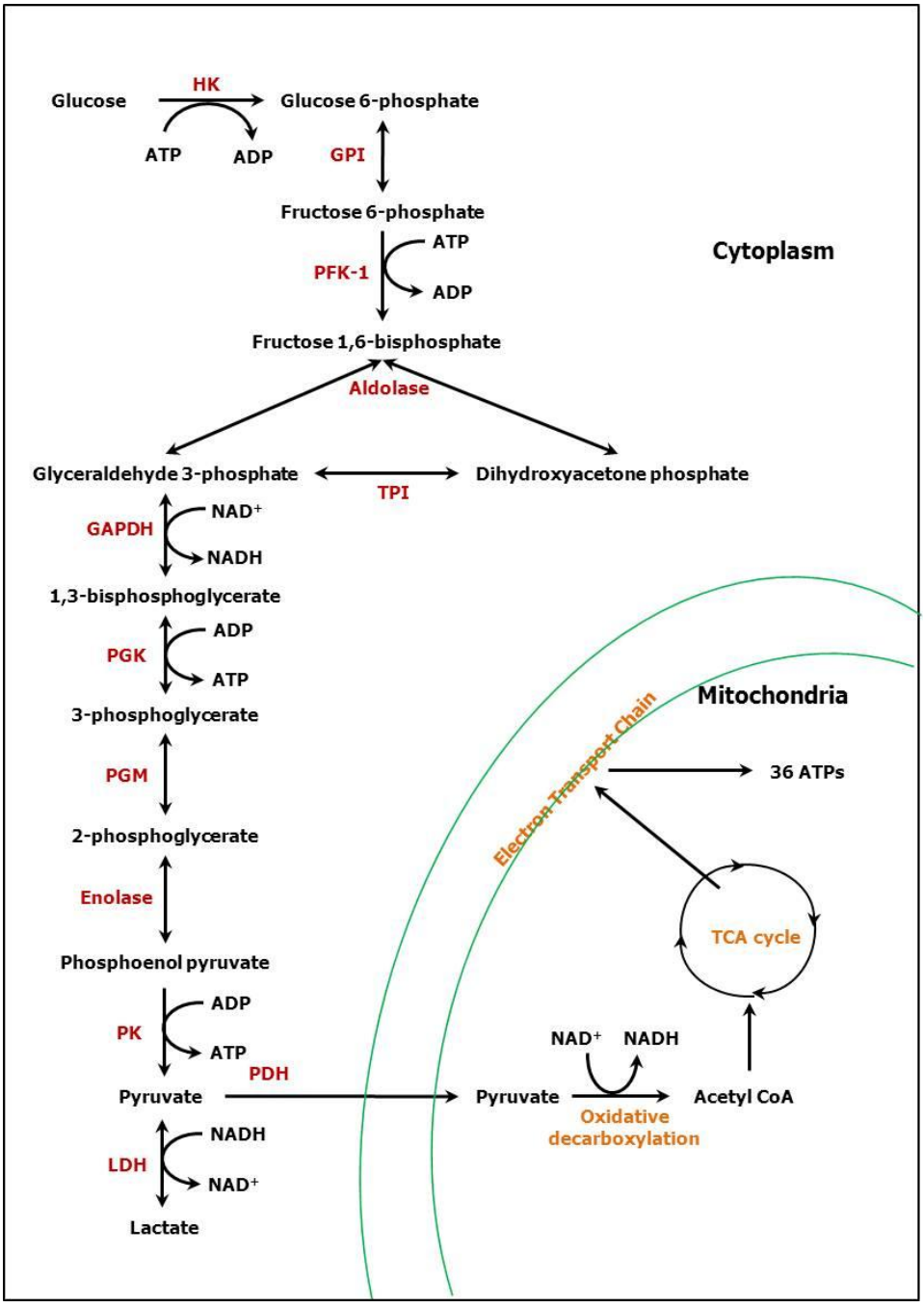

Figure 1.2.1: Cellular energy metabolisc pathways

In glycolysis, glucose is converted to pyruvate by glycolytic enzymes. Pyruvate is either converted to lactate in the cytoplasm or enters mitochondria where it undergoes oxidative decarboxylation, TCA cycle and electron transport chain to produce 36 ATP molecules. HK – hexokinase, GPI – glucose phosphate isomerase, PFK-1 – phosphofructokinase, TPI – triose phosphate isomerase, GAPDH – glyceraldehyde phosphate dehydrogenase, PGK – Phosphoglycerate kinase, PGM – Phosphoglycerate mutase, PK – pyruvate kinase, LDH – lactate dehydrogenase, PDH – pyruvate dehydrogenase. Mitochondrion is drawn in green colour and the enzymes are mentioned in red colour.

ATP is synthesised by the ATP synthase enzyme using the chemiosmotic gradient to drive phosphorylation of ADP. The electrons are finally accepted by the molecular oxygen and water is produced. Thus a net of 38 ATP molecules (including 2 ATPs from glycolysis) are synthesised from each molecule of glucose consumed by the cells (Lehninger et al., 2005; Murray et al., 2003; Singh and Costello, 2009). Figure 1.2.1 schematically represents the important steps of glycolysis and mitochondrial respiration.

1.3 Cancer metabolism

1.3.1 Background

The cells require ATP for their growth and survival, which is primarily obtained from catabolizing glucose in a two-step process. The first step is glycolysis, in which the glucose is converted to pyruvate in the cytoplasm to produce a net of 2 ATPs from each glucose molecule utilized. The second step occurs in the mitochondria and includes oxidative decarboxylation in which pyruvate is converted to acetyl CoA, tricarboxylic acid cycle (also known as citric acid cycle and Krebs cycle) in which acetyl CoA is converted to CO_2 and produces 2ATPs, 6NADH and $2FADH_2$ and oxidative phosphorylation in which NADH and FADH2 are oxidized to release the electrons which pass through a series of protein complexes called electron transport chain (ETC). The energy produced from the flow of electrons through ETC drives the synthesis of ATP by the phosphorylation of ADP hence known as oxidative phosphorylation (Lehninger et al., 2005).

In low oxygen conditions such as intense exercise, the end product of glycolysis pyruvate, instead of entering mitochondria and proceeding to OXPHOS is converted to lactic acid in the cytoplasm by lactate dehydrogenase in a process termed anaerobic glycolysis. Although the glycolytic flux provides less ATP (2 ATP molecules per one molecule of glucose) cells succeed to obtain enough ATP for their survival by rapidly consuming glucose. However this metabolic shift towards glycolysis is a temporary cellular adaptation to hypoxia which switches back to OXPHOS when oxygen levels return to normal (Garber, 2004). This inhibitory role of oxygen in the utilization of glucose was first noted by Louis Pasteur in 1857 and hence named Pasteur Effect (Gatenby and Gillies, 2004).

1.3.2 Warburg effect

In 1924 Otto Warburg observed that the cancer cells escape Pasteur Effect and convert glucose to lactic acid even in the presence of ample oxygen (Figure 1.3.1) (Warburg, 1956; Warburg et al., 1924). This phenomenon is known as Warburg effect or aerobic glycolysis. Warburg hypothesised that this metabolic change from OXPHOS to glycolysis is due to the impaired mitochondrial respiration, and this was the cause of cancer (Warburg, 1956). The lack of experimental evidence however for impaired mitochondrial respiration in cancer cells led his hypothesis to controversies (Racker, 1983; Weinhouse, 1976). However, more recent reports suggest that mutations in mitochondrial DNA that lead to defects in respiratory chain complexes and genes encoding TCA cycle enzymes such as succinate dehydrogenase (SDH) and fumarate hydratase (FH) might contribute to Warburg effect (Bayley and Devilee, 2010; Baysal et al., 2000).

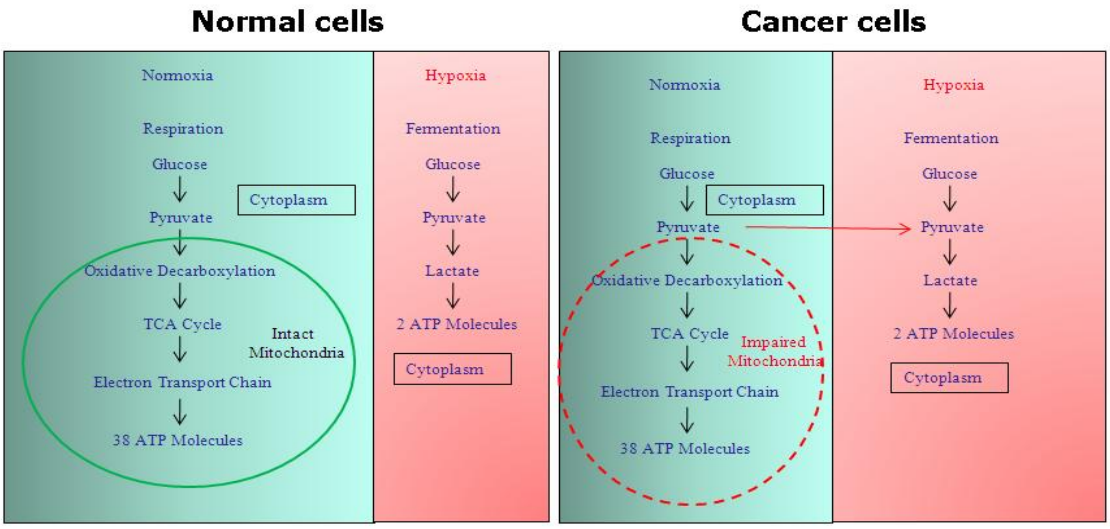

Figure 1.3.1: Energy production pathways in normal and cancer cells

The normal and cancer cells follow different cellular energy production pathways. In hypoxic conditions, both normal and cancer cells produce energy through glycolysis. In normoxic conditions, while normal cells produce energy through OXPHOS in intact mitochondria, cancer cells with their defective mitochondria prefer to produce energy through glycolysis. Intact mitochondria are denoted by green circle whereas impaired mitochondria are denoted by dotted red circle. The normoxia and hypoxia are denoted in green and red background respectively.

1.3.3 Warburg Effect and cancer cells

It has been shown that tumour cells benefit from high glycolytic shift in several ways. Pederson et al explain that glycolysis is a rich source of precursors which are essential for the biosynthesis of nucleic acids, phospholipids, fatty acids, porphyrins and cholesterol (Pedersen, 2007), thereby high glycolytic rates in cancer cells facilitate not only survival but also a high growth rate. Furthermore the low pH of lactic acid, the end product of aerobic glycolysis, creates acidic environment which assists tumour cells to protect themselves from the body's immune system. Cancer cells can survive producing energy through glycolysis even when there is no oxygen since the enzymes involved in glycolysis are not only oxygen independent but their expression can be stimulated in hypoxic environment (Murray et al., 2003; Pedersen, 2007). It has been assumed that increased glycolytic rate facilitates cells to overcome the destructive effects of reactive oxygen species (ROS) produced by oxidative phosphorylation, thereby imposing cell survival (Simon et al., 2000). The immortalization potential conferred to cancer cells by aerobic glycolysis could be a step towards tumorigenesis (Kim and Dang, 2006; Lu and Finkel, 2008).

1.3.4 Oncogenic activation of Warburg effect

In addition to the mutations of genes encoding the enzymes involved in energy metabolism, the Warburg effect can be induced by oncogenes such as *AKT*, *MYC* and *HIF-1α*. The oncoprotein AKT activates GLUT4, thereby enhances glucose uptake and induces HK2 to promote glycolysis (Elstrom et al., 2004; Kim and Dang, 2006). Myc contributes to the Warburg effect in cancer cells by regulating the gene expression of many glycolytic enzymes such as HK2, enolase1, LDH-A, PFK-M, glyceraldehyde phosphate dehydrogenase (GAPDH) and TPI1 (Kim et al., 2004a) and promoting glycolysis. Activation of Myc in human B cell model has been shown to be associated with mitochondrial biogenesis (Li et al., 2005), and to increase intracellular ROS levels which might cause mutations in the mitochondrial DNA leading to dysfunctional mitochondria (Kim and Dang, 2006).

HIF-1 has been shown to contribute to the Warburg effect by up-regulating the glucose uptake by GLUT1 and GLUT3 (Iyer et al., 1998) and promote glycolysis by regulating most of the glycolytic enzymes including HK2 and PFK1, aldolase, triose phosphate isomerase (TPI), GAPDH, phospho glycerate kinase (PGK1) enolase and lactate dehydrogenase (LDH) (Figure 1.4.4) (Dang and Semenza, 1999; Gess et al., 2004; Marín-Hernández et al., 2006; Semenza et al., 1994). In addition to enhance glycolysis, HIF-1 also inhibits mitochondrial respiration by up-regulating PDK-1, which phosphorylates and inactivates the PDH complex thereby inhibiting the conversion of pyruvate to acetyl-CoA, an important step of mitochondrial respiration (Figure 1.4.4) (Kim et al., 2006; Papandreou et al., 2006).

1.3.5 Warburg effect and tumorigenesis

Although aerobic glycolysis is induced due in part to oncogenic activation of glycolytic enzymes and mutations in genes encoding enzymes involved in OXPHOS, a recent report suggests that increased glycolysis could contribute to immortalization and subsequent malignant transformation. The study (Kondoh et al., 2005) identified two genes encoding glycolytic enzymes namely glucose phosphate isomerase (GPI) and phospho glycerate mutase (PGM) to contribute to immortalization in mouse embryonic fibroblast (MEF) cells. Mutated p53 has also been shown to up-regulate PGM and contribute to the immortalization of MEFs.

1.3.6 Exploiting Warburg effect in cancer therapy

The principle of Warburg effect has successfully been used as cancer diagnostic tool known as Positron Emission Tomography (PET). High glucose utilizing cells such as brain, kidney and cancer cells can uptake Flurodeoxyglucose (^{18}F-FDG or FDG) which is a glucose-analogue. Since FDG cannot be metabolized further and cannot move out of the cells is easily detected by scanning inside cancer cells which normally utilize high glucose.

Warburg proposed that increased glycolytic rate in cancer is connected to significant malfunction of the mitochondrial respiration due to various factors and for that reason tumour cells become more dependent on glycolysis. Elevated glycolysis is common in most of human cancers (Semenza, 2003), therefore understanding the molecular

pathways leading to up-regulated glycolysis in cancer cells may provide the means to design novel anticancer therapeutic approaches intervening at various steps of the process (Gatenby and Gillies, 2007). In addition, taking into account the fact that normal cells bearing competent mitochondrial respiration may produce energy through alternative energy sources such as fatty acids and amino acids, therapeutic approaches inhibiting glycolysis might prove to be selective in targeting cancer cells (Pelicano et al., 2006).

1.3.6.1 Known treatment strategies

Several reports have indicated that inhibition of glycolysis effectively kills cancer cells with defective mitochondria (Xu et al., 2005). The most effective way to inhibit glycolysis is by targeting the activity of the rate limiting enzymes of glycolysis such as HK, PFK, as well as GAPDH and lactate dehydrogenase (LDH) (Chen et al., 2007). PFK1 facilitates phosphorylation of fructose-6-phosphate and converts it to fructose-1, 6-bisphosphate. This rate limiting enzyme is inhibited by ATP, PEP, and citrate (Lehninger et al., 2005). PFK1 is allosterically activated by fructose 2,6-bisphosphate which is regulated by PFKFB. Recently Bensaad et al reported that the p53 target gene *TIGAR* inhibits the formation of fructose-2,6-bisphosphate and inhibits glycolysis (Bensaad et al., 2006). *TIGAR* as one of the genes that has been studied further in this thesis is discussed in details in section 1.7.

HK2 catalyses the first reaction of glycolysis, and is highly expressed in transformed cells. HIF-1α and mutated p53 stimulate HK2 expression (Pedersen et al., 2002) promoting glycolysis. Lack of HK2 enzymatic activity leads to the inhibition of both glycolysis and pentose phosphate pathway (PPP). In addition, HK2 inhibits apoptosis in cancer cells by binding to mitochondria and preventing the interaction of the pro-apoptotic Bax with the mitochondrial surface thereby preventing the release of cytochrome c (Pastorino et al., 2002). Therefore targeted inhibition of HK2 by 2-deoxyglucose, 3-bromo pyruvate, methyl jasmonate, 5-thioglucose and mannoheptulose (Chen et al., 2007; Goldin et al., 2008) results in decreased glycolysis, decreased PPP and increased apoptosis and these compounds are currently evaluated as anti-cancer therapeutics.

In addition glycolysis can be inhibited by GAPDH inhibitors α-chlorohydrin, ornidazole and iodoacetate (Bone and Cooper, 2000) and LDH inhibitor oxamate and butanedione (Wilkinson and Walter, 1972; Yang and Schwert, 1972).

1.4 Hypoxia Inducible Factor - 1α

1.4.1 Discovery

In 1988, Goldberg et al., provided evidence that the transcriptional regulation of gene expression of erythropoietin (*EPO*) was under the control of a heme protein responsive to low oxygen concentration (Goldberg et al., 1988). Later studies on the hypoxia mediated induction of *EPO* led to the identification of a *cis*-acting hypoxia responsive element (HRE) in the 3'-flanking region of this gene (Beck et al., 1991; Pugh et al., 1991; Semenza et al., 1991). In 1992 Semenza et al., identified a nuclear factor induced by hypoxia, that could bind with high efficiency to the HRE present within the regulatory region of the enhancer of *EPO* inducing its expression, which was named as hypoxia inducible factor 1 (HIF-1) (Semenza and Wang, 1992). Shortly after HREs were identified in several other hypoxia responsive genes such as *VEGF* (Levy et al., 1995), *GLUT-1* (Ebert et al., 1995), and genes encoding various glycolytic enzymes (Firth et al., 1994; Semenza et al., 1994). Other HIF family members were discovered later including HIF-2α (Ema et al., 1997; Flamme et al., 1997; Tian et al., 1997; Wenger and Gassmann, 1997), HIF-3α (Gu et al., 1998) and HIF-2β (also known as ARNT-2) (Hirose et al., 1996; Wines et al., 2001).

1.4.2 Structural Characteristics of HIF family members

HIF-1 is a heterodimer, composed of two different subunits, a hypoxia inducible HIF-1α and a constitutively expressed HIF-1β (also known as aryl hydrocarbon receptor nuclear translocator - ARNT) (Wang and Semenza, 1995). Both subunits of HIF-1 are basic-helix-loop-helix (bHLH) proteins containing a Per-ARNT-Sim (PAS) motif (Wang et al., 1995). Along with the wild type HIF-1α which comprise a protein of 826 amino acids, eight alternative splice variants of HIF-1α (HIF-$1\alpha^{827}$ (Gothié et al., 2000), HIF-$1\alpha^{736}$ (Gothié et al., 2000), HIF-$1\alpha^{557}$ (Chun et al., 2001), HIF-$1\alpha^{516}$ (Chun et al., 2002), HIF-$1\alpha^{785}$ (Chun et al., 2003), HIF-$1\alpha^{417}$ (Lee et al., 2004), HIF-$1\alpha^{TE}$ (Depping et al., 2004) and an isoform with alternative exon 1 (I.3 isoform) (Lukashev and Sitkovsky,

2008) have also been reported. HIF-1β comprises of 774 amino acids (if exon 5 is excluded) or 789 amino acids (if exon 5 is included) (Wang et al., 1995). All HIF-1α splice variants dimerize with HIF-1β in human cells to form the transcriptionally active HIF-1 heterodimer (Dales et al., 2010).

HIF-1α and HIF-2α are regulated in response to hypoxia in a similar way (Hu et al., 2003) and exhibit 48% amino acid identity and high degree of homology in their bHLH (83%), PAS (70%), and ODDD (Hu et al., 2003) domains. In addition, their C–terminal domain, which is important for the binding of the transcriptional cofactor p300/CBP is highly conserved (Ebert and Bunn, 1998; Ema et al., 1999) implying that apart from the response to hypoxia the regulation of the transcriptional activity of both HIF-1α and HIF-2α is executed in a similar way. HIF-2α also dimerizes with HIF-1β and forms the transcriptionally active HIF-2 complex which binds to the HREs of hypoxia inducible genes regulating their expression (Ema et al., 1997). However, unlike HIF-1α which is ubiquitously expressed in most tissues, the distribution of HIF-2α is limited to various vascular structures (Jain et al., 1998) and brain, heart, lung, kidney and liver tissues (Wiesener et al., 2003).

Six splice variants of HIF-3α have been reported namely HIF-3α 1 to 6 (Maynard et al., 2003). Along with bHLH and PAS domains, HIF-3α also shares high homology with HIF-1α and HIF-2α in the N-terminal activation domain (N-TAD) and ODDD, but lacks C-terminal activation domain (C-TAD) (Gu et al., 1998) hence acts as a weak transcription factor compared to the other two members of the HIF-α family (Hara et al., 2001). Moreover, the human HIF-3α4 splice variant lacks ODD, N-TAD and C-TAD domains and functions as HIF-1α dominant negative repressing HIF-1 mediated transcription is downregulated in renal cell carcinoma cells demonstrating the role of HIF-3α4 in tumorigenesis (Maynard et al., 2005).

1.4.3 Functional domains of the HIF family members

All HIF family members contain N-terminal bHLH domains followed by PAS A and B motifs (Wang et al., 1995). The dimerization between HIFα and HIFβ subunits occurs through the HLH and PAS (A) domains whereas the DNA binding occurs through the basic and PAS (B) domains (Brahimi-Horn and Pouyssegur, 2009; Gradin et al., 1996; Jiang et al., 1996; Jiang et al., 1997b). Two nuclear localization signals (NLS) are found in HIF-1α; one in its N-terminal and the other in its C-terminal region (Figure 1.4.1) (Kallio et al., 1998; Luo and Shibuya, 2001). Upon stabilization, HIF-1α protein translocates into the nucleus and dimerizes with HIF-1β to form the HIF-1 transcription complex (Kallio et al., 1998).

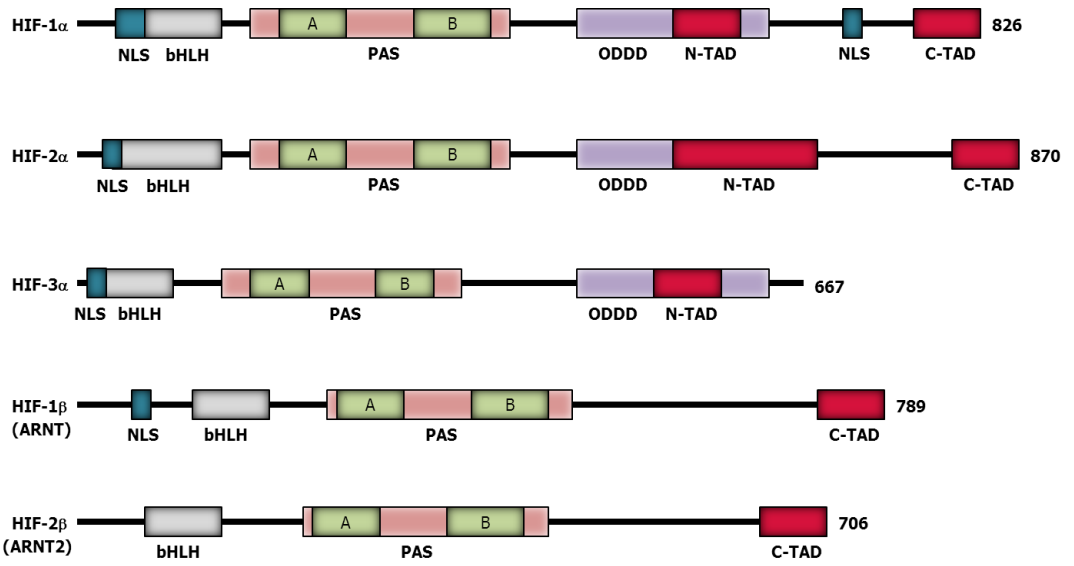

Figure 1.4.1: Domain structure of HIF family members

Schematic diagram indicating the domain structure of the HIF family members. Dimerization between the HIF-α and HIF-β subunits occurs through binding of the HLH and PAS (A) domains located in the N-terminal region of each subunit and the DNA binding occurs through the basic and PAS (B) domains (Brahimi-Horn and Pouyssegur, 2009). The different domains are represented in different colours. NLS: Nuclear localization signal; bHLH: basic helix loop helix; PAS: Per-ARNT-Sim; ODDD: Oxygen dependent degradation domain; N-TAD: N-terminal transactivation domain; C-TAD: C-terminal transactivation domain. ARNT: Aryl hydrocarbon nuclear translocator.

The oxygen dependent degradation domain (ODDD) plays an essential role in the stabilisation of HIF-α subunits (Huang et al., 1998). Under normoxic conditions prolyl hydroxylation occurring in their ODDD domain (Pro564 and Pro402) marks HIF-α proteins for proteasomal degradation by enhancing their interaction with the E3 ubiquitin ligase von Hippel-Lindau protein (pVHL). However, as PHD hydrodroxylases are inactive in hypoxic conditions proline hydroxylation does not occur, leading to stabilisation of the HIF-α subunits (Cockman et al., 2000; Maxwell et al., 1999; Ohh et al., 2000; Tanimoto et al., 2000).

HIF-1α and HIF-2α contain two transactivation domains, one N-terminal (N-TAD; amino acids 531 to 575 of HIF-1α) and one oxygen regulated C-terminal (C-TAD; amino acids 786 to 826) (Jiang et al., 1997b). Both N-TAD and C-TAD are involved in the recruitment of co-factors such as CBP/p300 (Arany et al., 1996; Ema et al., 1999), SRC-1 and TIF-1 (Carrero et al., 2000) and activate the transcription of HIF-1α and HIF-2α. In addition to hypoxia cobalt chloride and desferrioxamine can also induce HIF-α stabilisation and TAD functions (Jiang et al., 1997b; Pugh et al., 1997). The human inhibitory PAS (IPAS) protein orthologue HIF-3α4 lacks ODD and transactivation domains and acts as dominant negative regulator of both HIF-1α and HIF-2α (Maynard and Evans, 2007; Maynard et al., 2005). A schematic diagram indicating the functional domains of HIF proteins is shown in Figure 1.4.1.

1.4.4 Regulation of HIF stability and transcriptional activity

Although, both HIF-1α and HIF-1β subunits are constitutively expressed in normoxic and hypoxic conditions, HIF-1α protein stabilisation and enhanced DNA binding activity present only in hypoxic conditions. This indicated that HIF-1α subunit is responsive to low oxygen concentration (Kallio et al., 1997). Destruction of HIF-α subunits in normoxic conditions was found later to be mediated by the ubiquitin-proteasome pathway (Huang et al., 1998; Salceda and Caro, 1997; Sutter et al., 2000). In particular the constitutive stabilization of HIF-α subunits and the transcriptional activation of HIF-1 complex in cells deficient of the tumour suppressor protein pVHL established a role for this protein in regulating the function of HIF-α subunits in normoxic conditions (Cockman et al., 2000; Kamura et al., 2000; Maxwell et al., 1999;

Ohh et al., 2000; Tanimoto et al., 2000). The α-domain of pVHL forms a complex (VCBCR) with elongin B, elongin C, Cul-2 and Ring-H2 box protein (Rbx1) (Kamura et al., 1999), which has E3 ubiquitin ligase activity. Prolyl hydroxylated HIF-α protein binds to pVHL β domain resulting in HIF-1α poly ubiquitination (Ivan et al., 2001; Jaakkola et al., 2001; Masson et al., 2001) and degradation by the 26S proteasomes (Figure 1.4.2) (Kallio et al., 1999; Sutter et al., 2000).

The hydroxylation of proline residues at 564 (HIF-1α P564) (Ivan et al., 2001; Jaakkola et al., 2001) and 402 (HIF-1α P402) (Masson et al., 2001) within the ODD domain of HIF-α proteins is mediated by prolyl hydroxylase enzymes (PHDs 1-4) (Appelhoff et al., 2004; Bruick and McKnight, 2001; Epstein et al., 2001; Oehme et al., 2002).

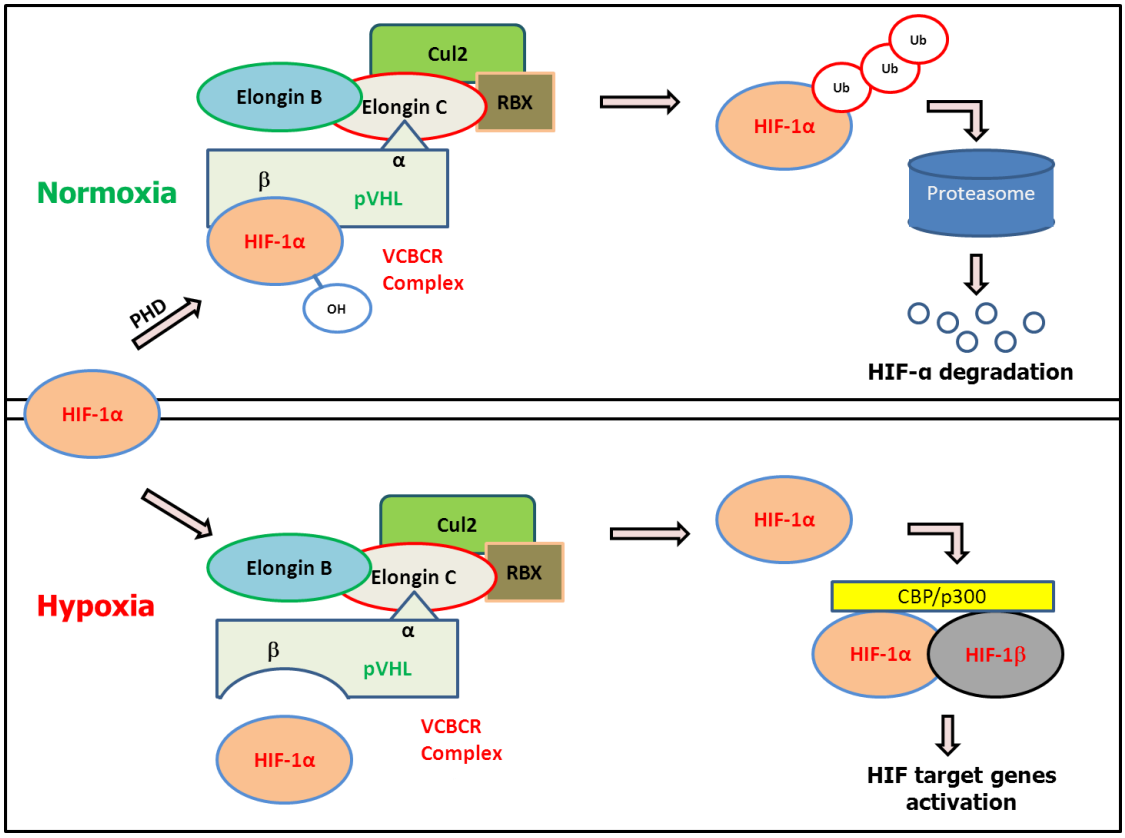

Figure 1.4.2: Oxygen dependent stabilization of HIF-1α

Prolyl hydroxylases (PHDs) hydroxylate HIF-1α in the presence of oxygen. The hydroxylated HIF-1α then binds to VCBCR complex which promotes HIF-1α ubiquitination followed by 26S proteasome dependent degradation (upper panel). Hypoxia prevents HIF-1α prolyl hydroxylation by PHDs, leading to its protein stabilization, and subsequent nuclear translocation, dimerization with HIF-1β and binding to transcription co-factors of the p300/CBP multi-protein complex becoming transcriptionally active (lower panel).

PHDs are non-heme Fe (II) and 2-oxoglutorate dependent dioxygenases (2-OG oxygenases) that utilize molecular oxygen as a co-substrate (Epstein et al., 2001) therefore their function is inhibited by iron chelators such as desferrioxamine (DSFX), transition metal ion salts such as cobalt chloride ($CoCl_2$) and small molecule inhibitors of 2-OG analogues.

The receptor activated protein kinase C (RACK1) (Liu et al., 2007) has also been shown to regulate HIF-1α protein stability interfering with the interaction between HIF-α PAS-A domain and HSP90 which protects HIF-α from degradation. In the case this interaction is inhibited, RACK1 binds to HIF-α and recruits components of E3 ubiquitin ligase such as Elongin-B and Elongin-C promoting HIF-α degradation (Liu et al., 2007). The E3 ubiquitin ligase hypoxia associated factor (HAF) has also been shown to mediate HIF-1α protein degradation (Koh et al., 2008).

Reactive oxygen species (ROS) production in mitochondria play important part in the regulation of cellular oxygen concentration and thus in the regulation of HIF-α protein stability. Although the precise role of mitochondria-derived ROS in the stabilization of HIF-1α has not been clearly elucidated, it has been hypothesised that ROS mediated inhibition of PHD enzymes is the mechanism by which HIF-1α is stabilised under these conditions (Chandel et al., 2000; Schroedl et al., 2002), though recent reports suggest that the stabilization of HIF-1α in hypoxic conditions is independent of mitochondrial ROS production (Chua et al., 2010). PHD activity is also affected by the function of the succinate dehydrogenase (SDH) which converts succinate to fumarate in the TCA cycle. Downregulation of SDH leads to increased accumulation of succinate in the cells, leading to the dissociation of pVHL from HIF-1α and subsequent stabilization of the transcription factor (Selak et al., 2005).

While oxygen concentration mainly mediates HIF-1α protein stability cell type specific stabilisation of HIF-1α in normoxic conditions by oxygen independent pathways have also been reported (Semenza, 2003). For example, genetic alterations including loss of function mutations in the tumour suppressor genes encoding p53, PTEN and pVHL (Maxwell et al., 1999; Ravi et al., 2000; Zundel et al., 2000), as well as gain of function

mutations of oncogenes that activate phosphatidyl-inositol 3-kinase (PI3K), SRC and mitogen-activated protein kinase (MAPK) pathways (Jiang et al., 1997a; Richard et al., 1999; Zhong et al., 2000) have also been shown to regulate HIF-1α protein stability.

Growth factors such as insulin (Zelzer et al., 1998), insulin like growth factor-2 (IGF-2) (Feldser et al., 1999), transforming growth factor-α (TGF-α) and interleukin-1β (Hellwig-Burgel et al., 1999) activate the phosphatidyl-inositol dependent kinase 1 which in turn phosphorylates and activates protein kinase B (PKB, also known as AKT) thereby stimulating the expression of HIF-1α in normoxic conditions (Zhong et al., 2000) in a series of reactions shown in Figure 1.4.3. Growth factors can also stimulate HIF-1α transcriptional activity by activating the Ras oncogene and eventually MAPK/ERK kinase (MEK1/2) and the extracellular signal-regulated kinase (ERK1/2) pathway as shown in Figure 1.4.3 (Richard et al., 1999; Sang et al., 2003).

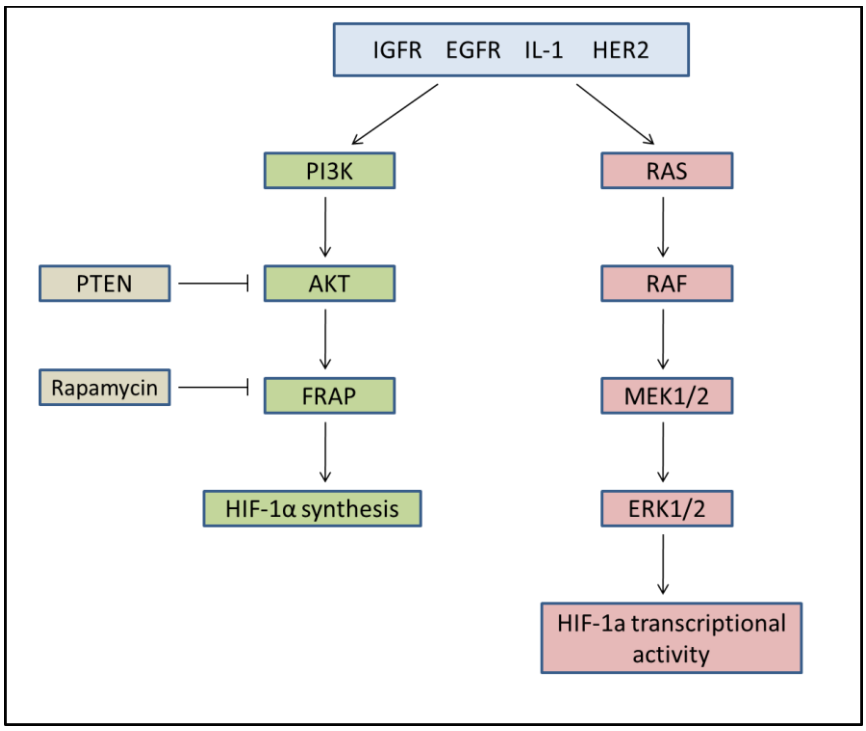

Figure 1.4.3: Signal transduction pathways of HIF-1α regulation

Schematic representation of signal transduction pathways promoting HIF-1α synthesis and transcriptional activity. HIF-1α can be induced under normoxic conditions by growth factors stimulating the PI3K/AKT/FRAP pathway. In hypoxic conditions, the RAS/RAF/MEK/ERK pathway induces HIF-1α transcriptional activity.

In addition to hydroxylation of proline residues, acetylation of lysine 532 within the ODD domain of HIF-1α by ARD1 also promotes the interaction of HIF-1α with pVHL and promotes its degradation (Jeong et al., 2002). Although the K532 acetylation is not affected in hypoxic conditions, endogenous ARD1 mRNA and protein levels are downregulated in hypoxia leading HIF-1α stabilization in hypoxia (Jeong et al., 2002; Xenaki et al., 2008). Recently Xenaki et al., have shown that PCAF interacts with and acetylates HIF-1α which enhances the stability of HIF-1α protein (Xenaki et al., 2008).

While prolyl hydroxylation of P564 and P402 and acetylation of K532 regulate HIF-1α protein stability, asparaginyl hydroxylation occurring at Asn803 in the C-TAD of the human HIF-1α by the factor inhibiting HIF (FIH) interferes with the binding of this transcription factor to p300/CBP co-activator complex and modulates its transcriptional activity (Hewitson et al., 2002; Lando et al., 2002a; Lando et al., 2002b; Mahon et al., 2001). Similar to PHDs, FIH is also a Fe (II) and 2-OG dependent oxygenase and utilizes molecular oxygen as a co-substrate (Dann et al., 2002). In-vitro experiments using HIF-1α polypeptides have shown that PHDs are inactivated as the severity of the hypoxia increases whereas FIH activity is lost in anoxic conditions. Recent reports though demonstrate that endogenous human HIF-1α hydroxylation is suppressed by hypoxia in the order of $Pro^{402} > Pro^{564} > Asn^{803}$ indicating that prolyl hydroxylation is more sensitive to hypoxia than asparaginyl hydroxylation (Tian et al., 2011). HIF-1α binding to the p300/CBP coactivator complex is also regulated by the HIF-1α transcription target CBP/p300 interacting transactivator with ED-rich tail 2 (CITED2; also known as Mrg1 and p35srj) in a negative feedback manner (Freedman et al., 2003).

Apart from prolyl hydroxylation and acetylation, sumoylation of HIF-1α at K391 and K477 also regulates its protein stability and transcriptional activity (Bae et al., 2004) possibly through modulation of other post translational modifications (Bae et al., 2004; Carbia-Nagashima et al., 2007).

1.4.5 HIF-1α and cancer metabolism

In hypoxic conditions, normal cells, in order to produce energy, switch from OXPHOS to glycolysis and when oxygen becomes again available, they revert back to OXPHOS. This is not the case for cancer cells which even in the presence of oxygen, adapt to glycolysis (Warburg, 1956). HIF-1 plays critical role in this metabolic adaptation since it activates the expression of genes encoding glucose transporters and glycolytic enzymes which convert glucose to pyruvate and subsequently to lactate (Seagroves et al., 2001).

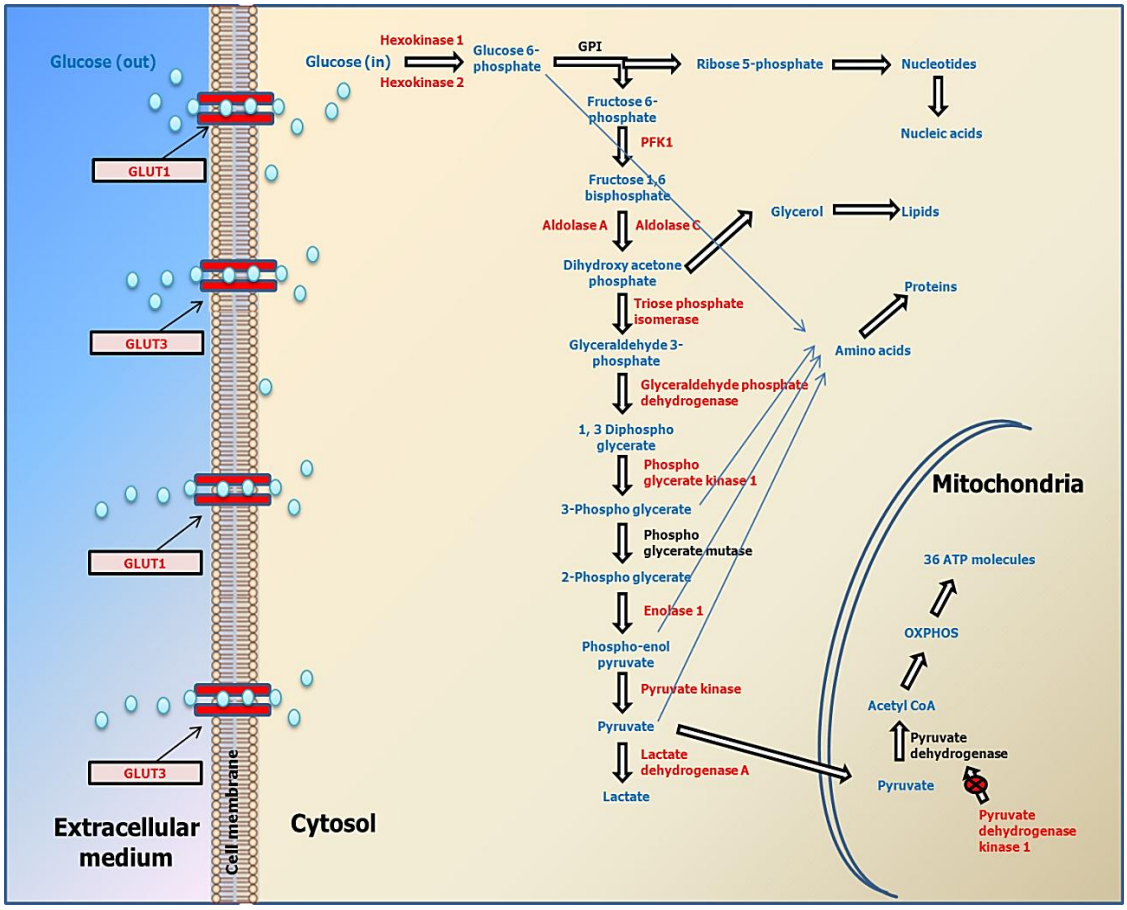

Figure 1.4.4: HIF-1α regulates cancer cell metabolism.

HIF-1α activates the glucose transporters GLUT1 and GLUT3 which promote the uptake of glucose by cells. In addition, HIF-1α promotes the rapid utilization of glucose by inducing the genes encoding glycolytic enzymes (indicated in red colour). HIF-1α also activates pyruvate dehydrogenase kinase 1 (PDK1) which phosphorylates and deactivates the pyruvate dehydrogenase (PDH) which converts pyruvate to Acetyl CoA, an important component for TCA cycle. The extracellular medium and cytosol are denoted in blue and pale orange respectively. Mitochondrion is drawn in blue colour.

HIF-1 stimulates *SLC2A1* and *SLC2A3* gene expression, genes that encode for the glucose transporters GLUT1 and GLUT3 respectively which promote the uptake of glucose by the cells (Iyer et al., 1998). Furthermore, the rapid utilization of glucose by cells is assisted by the HIF-1 mediated induction of several glycolytic enzymes including hexokinase, PFK1, aldolase, triose phosphate isomerase, glyceraldehyde phosphate dehydrogenase, phospho glycerate kinase enolase and lactate dehydrogenase (Dang and Semenza, 1999; Gess et al., 2004; Marín-Hernández et al., 2006; Minchenko et al., 2003; Semenza et al., 1994). Another HIF-1 transcription target gene named pyruvate dehydrogenase kinase 1 (PDK1) plays important role in cellular energy production. PDK1 phosphorylates and inhibits pyruvate dehydrogenase complex (PDH) (Kim et al., 2006; Papandreou et al., 2006), which catalyzes the conversion of pyruvate to Acetyl CoA. Inhibition of PDH activity limits the entry of glycolytic carbon into the TCA cycle and promotes the conversion of pyruvate to lactate. Also, by inducing the BH3 domain protein BNIP3, HIF-1 induces selective mitochondrial autophagy (Zhang et al., 2008). BNIP3 competes with Beclin 1 for binding to Bcl2 thereby freeing Beclin 1 to trigger autophagy.

HIF-1 regulates gene expression of several subunits of the mitochondrial cytochrome c oxidase (COX) complex thereby affecting oxidative phosphorylation and maintaining oxygen homeostasis in hypoxic cells (Fukuda et al., 2007). In particular, HIF-1α activates COX4-2 isoform gene expression and indirectly downregulates COX4-1 protein levels by inducing the expression of the mitochondrial protease that degrades COX4-1 called LON (Fukuda et al., 2007). In addition to regulating COX subunits, HIF-1 also regulates mitochondrial biogenesis as it has been indicated by ectopically expressing pVHL tumour suppressor in pVHL deficient cells, which exhibit increased mitochondrial mass, mitochondrial DNA and oxygen consumption (Hervouet et al., 2005).

1.4.6 Other functions of HIF-1

Hypoxia and nutrient deprivation result in reduced viability of cancer cells. HIF-1 as a master regulator of the cellular response to hypoxia contributes towards restoring oxygen homeostasis and supports cell survival in hypoxic conditions by stimulating gene expression of genes involved in angiogenesis, glycolysis, erythropoiesis and cell proliferation (Iyer et al., 1998).

1.4.6.1 Erythropoiesis

Erythropoiesis involves utilization of large amounts of iron by the bone marrow, which is used in the synthesis of haemoglobin. HIF-1 by regulating EPO, EPO receptor (EPOR), hepcidin, transferrin and transferrin receptor (TfR) controls erythropoiesis (Semenza, 2009). In the liver, HIF-1 stimulates iron uptake by repressing the gene encoding hepcidin, which is an inhibitor of ferroportin, the major protein responsible for intestinal iron uptake (Semenza, 2009). HIF-1 also activates hepatic synthesis of transferrin, the major plasma protein responsible for transporting iron from the intestine to the bone marrow via the transferrin receptor.

1.4.6.2 Angiogenesis

HIF-1 maintains oxygen homeostasis by promoting the growth of new blood vessels from the pre-existing blood vessels. HIF-1 mediates this effect by upregulating VEGF which increases the vascular density (Levy et al., 1995). In addition, HIF-1 controls the expression of genes involved in the maintenance of the vascular tone, including nitric oxide synthase (NOS2), heme oxygenease 1, endothelin 1 (ET1), adrenomedulin (ADM), and the a1B-adrenergic receptor (Ke and Costa, 2006).

1.4.6.3 Cell proliferation and survival

HIF-1 induces growth factors such as IGF-2, interleukin-1 and TNF-α (Section 0) and promotes the binding to their cognate receptors which lead to cell proliferation and survival. In addition these growth factors and cytokines activate the MAPK and PI3K signalling pathways upregulating HIF-1 activity thus forming a positive feed-back loop.

1.4.6.4 Apoptosis

In addition to promoting cell proliferation and cell survival in hypoxic conditions, HIF-1α has also effects on apoptosis in a cell type specific manner (Ke and Costa, 2006). Specifically, decreased apoptosis has been observed in embryonic stem cells with deleted HIF-1α (Carmeliet et al., 1998). Furthermore, HIF-1α induces apoptosis by activating caspase-3 and Apaf-1-mediated cleavage and activation of caspase-9 thus promoting the release of cytochrome-c (Ke and Costa, 2006). Also HIF-1α down-regulates anti-apoptotic Bcl-2 family members and up-regulates the pro apoptotic protein BNIP-3 (Ke and Costa, 2006). The cross talk between HIF-1α and the tumour suppressor p53 regulates apoptosis by determining the balance of the pro-apoptotic versus anti-apoptotic genes of the Bcl-2 family (Nakano and Vousden, 2001; Oda et al., 2000; Selvakumaran et al., 1994).

1.4.7 Targeting HIF-1α for cancer therapy.

The role of HIF-1α in angiogenesis, in the metabolic shift to glycolysis and survival and proliferation of tumour cells as well as its association with negative prognosis has been well documented. Hence silencing of HIF-1 activity has been considered in cancer therapy with positive initial indications. In mouse tumour xenografts for example, deletion of HIF-1 expression inhibited tumour growth (Brown and Wilson, 2004). Small molecule inhibitors such as echinomycin, which inhibits the DNA binding activity of HIF-1 (Cairns et al., 2007), chetomin which prevents HIF-1α binding to p300 (Kung et al., 2000) 2-methoxyestradiol, vincristine, 2-methoxyestradiol ($2ME_2$) and paclitaxel which inhibit the translation of HIF-1 mRNA have been reported to reduce tumour growth in mice (Mabjeesh et al., 2003; Yeo et al., 2003).

1.5 p53 tumour suppressor

1.5.1 Introduction to p53

Although identified as an oncogene in 1979, p53 attained its tumour suppressor status within a decade of its discovery (Soussi, 2010). The significance of p53 as a tumour suppressor is demonstrated by the fact that more than 70% of human cancers either have mutations within the p53 gene or defects in p53 regulatory pathways (Lozano and Elledge, 2000). p53 protein is a stress responsive transcription factor that is stabilized

and activated in response to numerous cellular stress types which include oncogenic activation, DNA-damage, hypoxia and nutrient deprivation (Lowe, 1999). Upon activation, p53 promotes cellular homeostasis by initiating a cascade of biological events which lead to cell cycle arrest, DNA repair, senescence and apoptosis (Toledo and Wahl, 2006). These regulatory roles of p53 are attributed to its well-known tumour suppressive functions by permitting the cells with mild damage to undergo cell cycle arrest and DNA repair whereas eliminating the cells with irreversible damage by apoptosis. The ability of p53 to monitor and maintain the integrity of the genome is well recognized. It has therefore been named "molecular policeman", "cellular gatekeeper" and "the guardian of the genome" (Lane, 1992; Müller et al., 2004). Recent studies have demonstrated that p53 is also involved in the regulation of glucose and glutathione metabolism, cellular redox homeostasis, autophagy, insulin resistance and longevity assurance (Bensaad et al., 2006; Bensaad and Vousden, 2007; Crighton et al., 2006; Donehower, 2006; Hu et al., 2010; Matoba et al., 2006; Minamino et al., 2009; Naito et al., 2010). These studies display that p53 plays broader roles not only in cancer but also in various other diseases such as myocardial infarction and diabetes.

1.5.2 Structure of p53

p53 is a nuclear phospho-protein encoded by a 20kb gene containing 11 exons and 10 introns that is located on the short arm of chromosome 17 (17p13) (Isobe et al., 1986; Lamb and Crawford, 1986). The wild type p53 protein is made up of 393 amino acids and composed of several structural and functional domains (Figure 1.5.1). The amino terminal end of p53 contains an acidic transactivation domain (NTAD1) which facilitates the recruitment of factors of the basal transcriptional machinery such as TBP, TAFs and TFIID (Lu and Levine, 1995). This domain binds also to proteins with transcriptional repression function such as MDM2 (Lin et al., 1994). In the amino terminal end there is also a proline rich transactivation domain (NTAD2) which is involved in the p53 mediated apoptosis (Sakamuro et al., 1997). The central domain of p53 contains the DNA binding domain which is the domain where more than 90% of p53 mutations occur in human cancers (Bensaad et al., 2003) rendering this transcription factor incapable to bind to the consensus sequences within the promoters of its target genes and demonstrating the importance of its transcriptional activity in executing its tumour suppressor functions (Benchimol, 2001).

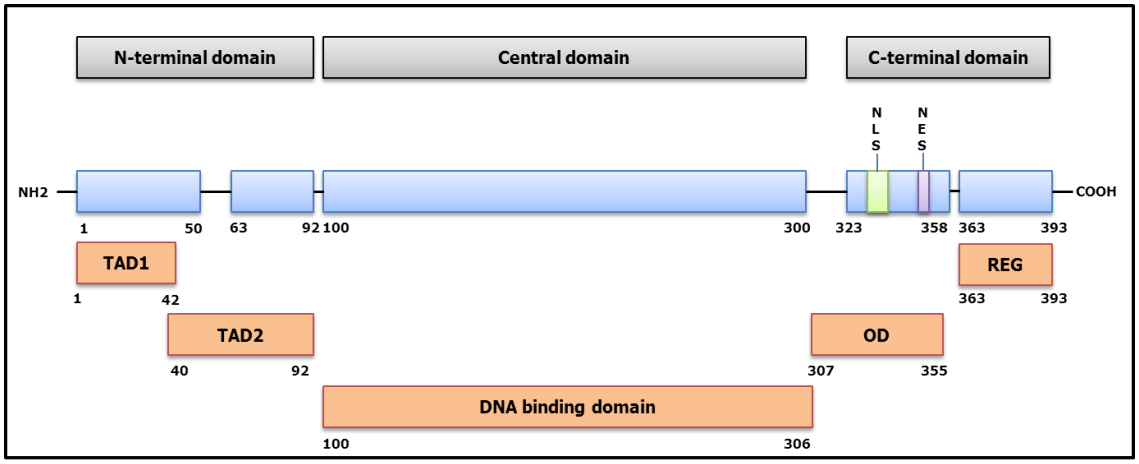

Figure 1.5.1: Domain structure of p53 protein

NLS – Nuclear localisation signal sequence; NES – Nuclear export signal sequence; TAD1 – Transactivation domain 1; TAD2 – Transactivation domain 2; OD – Oligomerization domain; REG – Regulatory domain.

The carboxy terminal end contains the oligomerization domain which facilitates the formation of p53 tetramer upon stabilization. Formation of p53 tetramer is essential for p53 dependent transactivation and p53 mediated growth suppression (Pietenpol et al., 1994). The carboxy terminal end also contains three nuclear export and a nuclear localization signal sequences and a strongly basic negative regulatory domain which is involved in the down regulation of DNA binding of the central DNA binding domain (Gu et al., 2001; Li et al., 2003) by locking this domain in a latent conformation. When the interaction between C-terminal regulatory region and the DNA binding domain is disrupted by post translational modifications such as phosphorylation and/or acetylation the DNA binding domain becomes active leading to enhanced p53 transcriptional activity (Ling and Wei-Guo, 2006).

1.5.3 Regulation of p53

p53 is a stress responsive transcription factor which modulates the expression of diverse sets of its target genes in a manner dependent on the type and severity of the stress. For example, under mild stress conditions p53 induces the expression of genes involved in cell cycle arrest (p21WAF-1/CIP-1) and DNA repair (GADD45) (Xiangbing, 1999) whereas after prolonged or irreversible cellular damage elevated levels of p53 and possibly combination of different post-translational modifications are required to activate genes involved in the initiation of apoptosis (bax, PUMA, NOXA, Apaf-1) and stimulation of senescence (p14ARF) that leads to cell death (Bensaad and

Vousden, 2007). Thus the levels of p53 as well as combination of its post-translational modifications orchestrate the balance between cell survival and death. Therefore it is extremely important to keep p53 levels at the appropriate level in non-stressed cells to avoid any unnecessary detrimental events directed by p53 (Gottifredi and Prives, 2001).

1.5.4 Post-translational modifications of p53

Post-translational modifications play important part in sensing and transmitting signalling effects in stress conditions. As stress responsive transcription factor the tumour suppressor protein p53 can be modified by a variety of stress conditions which are crucial for the regulation of p53 stability and transcriptional activity (Xu, 2003). Several post-translational modifications of p53 have been studied extensively including phosphorylation, acetylation, sumoylation, ubiquitination, etc., which affect the stability and transcriptional activity of p53.

1.5.4.1 Acetylation

The histone acetyl-transferases p300 and CBP act as transcriptional cofactors for numerous transcription factors including p53. CBP/p300 acetylate p53 at K305, K370, K372, K373, K381, K382 and K386 in its C-terminal region and K164 in its DNA binding domain, while PCAF and TIP-60 acetylate K320 and K120 respectively (Figure 1.5.2) (Gu and Roeder, 1997; Liu et al., 1999; Meek and Anderson, 2009; Sakaguchi et al., 1998; Tang et al., 2008; Wang et al., 2003). PCAF -mediated acetylation of the p53-K320 under DNA damage conditions such as UV irradiation results in the induction of the expression of the cyclin/CDK inhibitor p21WAF-1/CIP-1 leading to cell cycle arrest (Knights et al., 2006) an effect that has also been observed after acetylation of p53-K120 by TIP-60 (Tang et al., 2006). Similarly, in hypoxic conditions p53 is hypoacetylated in K320 and the limited amounts of acetylated p53K320 are preferentially recruited to the pro-survival gene $p21^{WAF\text{-}1/CIP\text{-}1}$ and not to the pro-apoptotic gene BID leading to cell survival (Xenaki et al., 2008). In addition PCAF dependent acetylation of p53 promotes p53 stability by decreasing its ubiquitination and degradation mediated by Mdm2 (Li et al., 2002b; Sakaguchi et al., 1997). Several reports have indicated that acetylation and phosphorylation occur simultaneously although a recently published report suggests that p53 transcriptional activation by acetylation is independent of p53 phosphorylation (Tang et al., 2008).

1.5.4.2 Phosphorylation

Human p53 is phosphorylated at multiple sites at the N and C-terminal regions by a number of kinases (Figure 1.5.2) (Xu, 2003). Following DNA damage, p53 is phosphorylated directly or indirectly by the phosphatidylinositol-3-kinase (PI3K) related kinases such as ataxia telangiectasia mutated (ATM) and ATM and Rad3-related (ATR). Following DNA single-strand break in which ATR is activated, and DNA double-strand break, in which many of these serine/threonine protein kinases are activated that regulate the activity of another group of kinases called the effector checkpoint kinases known as Chk1 and Chk2. Phosphorylation of p53 by ATM and ATR regulates the transcriptional activation of genes involved in DNA repair and apoptosis (reviewed in (Xu, 2003)). In hypoxic conditions, Chk2 kinase is phosphorylated by ATM but not by ATR and this phosphorylated Chk2 in turn phosphorylates p53 and stabilizes it. Chk2 mediated phosphorylation of p53 leads to cell cycle arrest and DNA repair (Gibson et al., 2005).

ATM and ATR phosphorylate p53 at Ser15 and Ser20 directly or indirectly by activating Chk1 and Chk2 (Lambert et al., 1998; Zhang and Xiong, 2001) which inhibit the interaction between p53 and MDM2 thereby stabilizing p53 protein (Unger et al., 1999). In addition to the stabilization and transactivation of p53, phosphorylation at various sites regulate its DNA binding activity and promote the recruitment of cofactors such as CBP/p300 and PCAF (Sakaguchi et al., 1998);(Xu, 2003).

1.5.4.3 Ubiquitination

Various post-translational modifications including ubiquitination, phosphorylation and acetylation are involved in the regulation of p53 protein stability. However, since p53 protein degradation is mainly carried out by the 26S proteasome, which recognises its target proteins when they are poly-ubiquitinated, this post-translational modification is of prime importance for p53 stability (Maki et al., 1996). Various ubiquitinase and deubiquitinase enzymes are involved in the degradation of p53 (Dai and Gu, 2010).

MDM2 (HDM2 in humans), is an oncoprotein with E3 ligase activity and the major negative regulator of p53. MDM2 gene expression is transcriptionally regulated by p53

in an auto regulatory feedback loop mode (Barak et al., 1993; Brooks and Gu, 2006). Overexpressed in various cancer types, MDM2 is shown to bind to the N-terminal transactivation domain of p53 inhibiting its phosphorylation at amino acid residues lay in this region (Chen et al., 1993). Since phosphorylation of amino acids in this domain is crucial for the stability and transcriptional activity of p53, binding of MDM2 to this domain inhibits both stabilisation and transactivation function of p53 (Oliner et al., 1993). MDM2 acts as an E3 ligase and ubiquitinates the lysine residues K101, K120, K132, K139, K370, K372, K373, K381, K382 and K386 (Coutts et al., 2009; Honda et al., 1997) (Figure 1.5.2). Mono-ubiquitination of p53 by low levels of MDM2 facilitates p53 cytoplasmic translocation (Dai and Gu, 2010; Li et al., 2003) whereas poly-ubiquitination by high levels of MDM2 aids 26S mediated p53 proteasomal degradation.

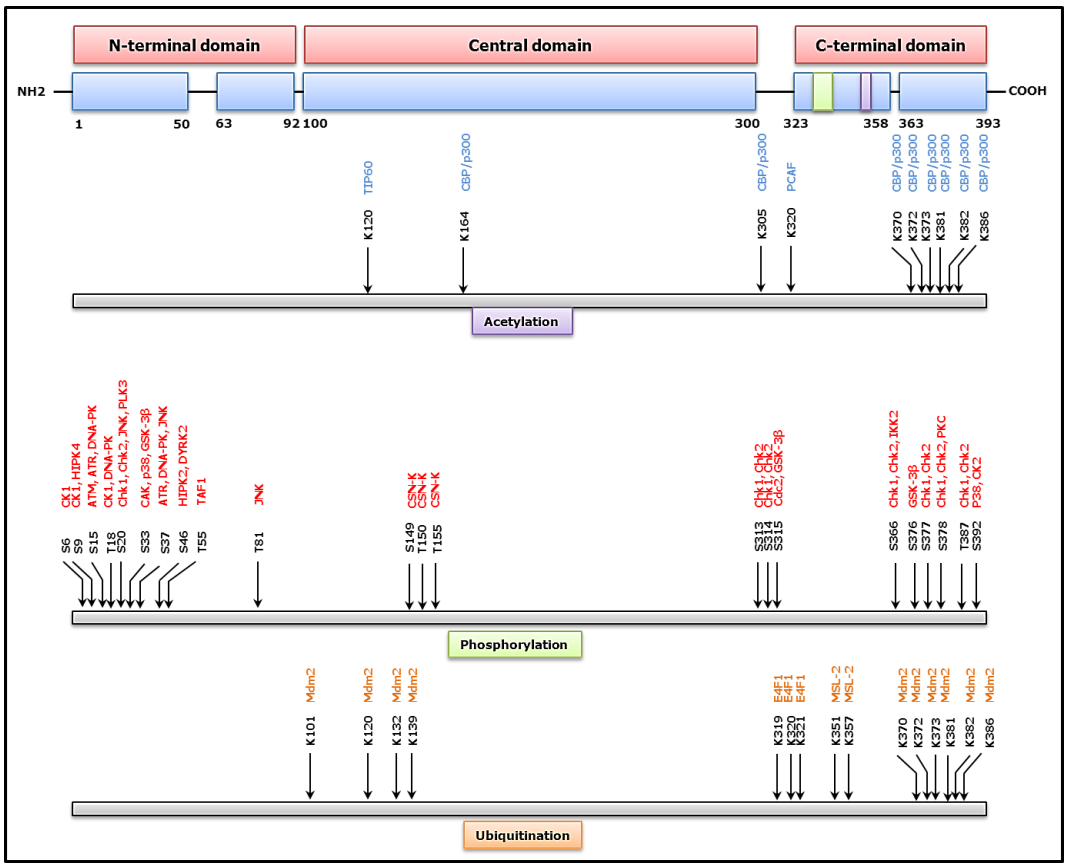

Figure 1.5.2: Major post translational modifications of p53

Schematic diagram showing the major post translational modifications of p53. The important sites of phosphorylation, acetylation and ubiquitination and the enzymes catalysing these modifications are shown. Figure modified from (Dai and Gu, 2010).

The feedback loop between p53 and MDM2 is affected by several enzymes including $p14^{ARF}$, MDMX and deubiquitinating enzymes such as HAUSP. Among these, $p14^{ARF}$ protects p53 by facilitating its translocation to subnuclear compartments such as the nucleoli thereby hindering p53 MDM2 interaction, or inhibiting MDM2 E3 ligase activity (Honda and Yasuda, 1999; Weber et al., 1999). MDMX (also known as MDM4) shares significant structural homology with MDM2 but unlike MDM2, MDMX does not seem to have E3 ligase function. Despite the lack of E3 ubiquitin ligase activity, MDMX forms a complex with p53 and both destabilises it, albeit with lower efficiency than that of MDM2, and inhibits its transcriptional activity (Shvarts et al., 1997; Shvarts et al., 1996). More recent studies have revealed more complex roles of MDMX demonstrating that ubiquitinated p53 is sequestered in the nucleus by MDMX and is stabilized (Stad et al., 2001).

Polyubiquitination of p53 is also mediated by other enzymes apart from MDM2 including RING domain containing p53 Induced protein with RING-H2 domain (PIRH2), Constitutively Photomorphogenic 1 (COP1) and HECT domain containing ARF Binding Protein 1 (ARF-BP1) (Honda et al., 1997; Moll and Petrenko, 2003; Oliner et al., 1992). Furthermore, the transcriptional cofactor p300 has been shown to exert E3 ligase activity and mediate p53 protein degradation (Grossman et al., 2003; Shi et al., 2009). Ubiquitination of p53 is counteracted by deubiquitinase enzymes (DUBs) which remove ubiquitin molecules from p53. Among the DUBs Herpesvirus-Associated Ubiquitin Specific Protease (HAUSP, also referred as USP7) deubiquitinates and stabilizes p53 mainly in the nucleus whilst USP10 functions mainly in the cytoplasm (Brooks et al., 2007; Dai and Gu, 2010; Li et al., 2002a; Yuan et al., 2010). Protein-protein interactions involved in the stabilization of p53 include interaction with the Heat Shock Protein – 90 (Hsp-90) and Simian Virus 40 (SV40) large T antigen (Müller et al., 2004).

1.5.5 Ubiquitin independent degradation of p53

Besides 26S proteasome, p53 protein degradation is also mediated by the 20S proteasome in an ubiquitin independent manner (Asher et al., 2002b). The 20S proteasomal degradation of p53 is regulated by NQO1 which binds to p53 in an NADH dependent manner (Asher et al., 2002a). NQO1 inhibitors such as dicoumarol compete

with NQO1 for NADH and the NQO1-p53 complex dissociates. Released p53 undergoes ubiquitination and MDM2 independent degradation (Tsvetkov et al., 2009). High NADH levels protect p53 from degradation by increasing its association with NQO1, whereas when NADH levels are low and the NQO1-p53 complex disrupted, p53 is subjected to degradation mediated by the 20S proteasome machinery (Tsvetkov et al., 2009). Also NQO1 has been shown to be associated with 20S proteasome which prevents the degradation of unstructured proteins such as p53 and p73 (Asher et al., 2005).

1.5.6 p53 and metabolism

1.5.6.1 p53 and metabolic stress

Cell signalling response under conditions of metabolic stress such as nutrient deprivation is mediated by p53 (Vousden and Ryan, 2009). AKT phosphorylates MDM2 and induces its translocation into the nucleus where it binds to p53 and marks it for 26S proteasomal degradation. p53 is activated in response to nutrient deprivation by the activation of AMP-activated protein kinase (AMPK) and by the inhibition of AKT. ATP and ADP exert opposing effects on the stability of p53-DNA complexes as ATP promotes and ADP represses the p53 binding to DNA (Okorokov and Milner, 1999). The nucleocytoplasmic enzyme malate dehydrogenase 1 (MDH1), which is involved in the TCA cycle, has been shown to act as a transcriptional co-activator for p53. Specifically, under conditions of glucose depletion, MDH1 translocates to the nucleus where it binds to p53 binding sites within the promoters of p53 transcription target genes (Lee et al., 2009) indicating that metabolic signals during starvation or low energy conditions induce p53 to exert its tumour suppressive effects (Vousden and Ryan, 2009).

1.5.6.2 p53 and energy production

Highly expressed glucose transporters such as various GLUT isoforms in many cancer cells provide to these cells the metabolic advantage. By repressing GLUT1 and GLUT4 gene expression, p53 reduces the pace of glucose uptake and slows down cancer cell proliferation (Schwartzenberg-Bar-Yoseph et al., 2004b). Another pathway by which p53 inhibits glycolysis is by stimulating the expression of genes exerting anti-glycolytic effects such as the Tp53 induced glycolysis and apoptosis regulator (TIGAR). TIGAR

shares structural and functional similarities with the phosphatase domain of the bi-functional (kinase and phosphatase activities) enzyme phospho fructo kinase 2/ fructose 2,6-bisphosphatase 2 (PFK2/FBPase2 or PFKFB). The PFK2 part of this enzyme with its kinase activity converts fructose 6-phosphate (F6-P) to fructose 2,6-bisphosphate (F2,6-BP) and promotes glycolysis, while the FBPase2 domain of this enzyme with its phosphatase activity reverses this reaction (Murray et al., 2003). The ratio of the kinase to phosphatase activity of the PFKFB3 enzyme in cancer cells has been shown to be 700:1 favouring the conversion of F2-P to F2,6-BP (which is an allosteric activator of the glycolysis rate limiting enzyme PFK-1) and hence induction of glycolysis (Minchenko et al., 2002). By stimulating TIGAR gene expression, p53 inhibits the intra-cellular levels of F2,6-BP, possibly by reducing the ratio of kinase to phosphatase activity of the PFKFB isoforms and hence inhibits glycolysis (Bensaad et al., 2006).

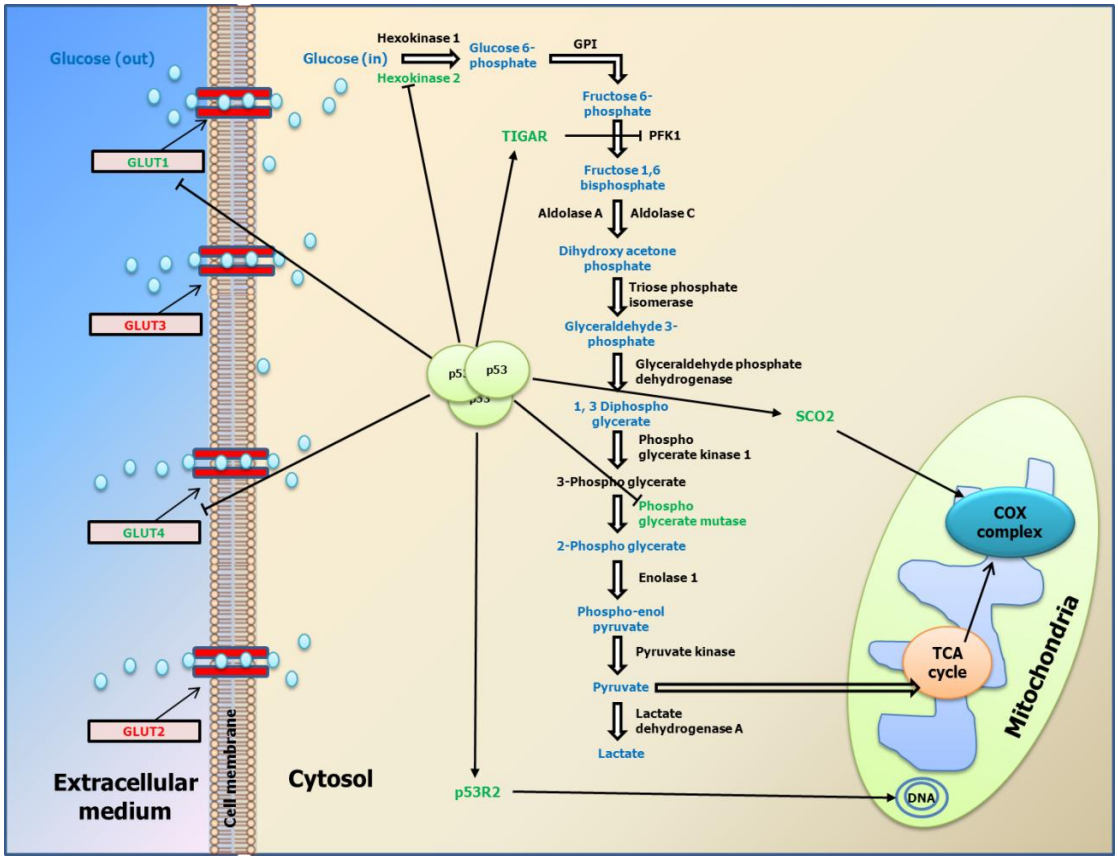

Figure 1.5.3: p53 regulates cellular energy metabolism

p53 inhibits glycolysis by modulating gene expression of GLUT1, GLUT4, HKII, PGM and TIGAR and promotes mitochondrial respiration by inducing SCO2 and p53R2. The extracellular medium and cytosol are denoted in blue and pale orange respectively. Mitochondrion is drawn in blue colour

Apart from TIGAR, p53 regulates the expression of other genes encoding for enzymes involved in glycolysis such as *phospho glycerol mutase* (*PGM*) which encodes for the phospho glycerate mutase (PGM) enzyme is downregulated by wild type p53 leading to inhibition of glycolysis and is upregulated by mutated p53 resulting in activation of glycolysis (Kondoh et al., 2005). Potential p53 DNA binding sites have been identified within the promoter of the gene encoding for the glycolytic enzyme hexokinase type II (HKII) (Mathupala et al., 1997). Figure 1.5.3 schematically demonstrates the involvement of p53 in cellular energy metabolism.

Except from glycolysis OXPHOS is also regulated by p53 through the effects this transcription factor exerts on gene expression of the Synthesis of cytochrome c oxidase 2 (SCO2). SCO2 is essential for the assembly of the subunit 2 of the cytochrome c oxidase (COX) complex, the major site of oxygen utilization in the eukaryotic cell (Matoba et al., 2006). In addition, mutation in Ribonuclotide reductase M2 B (*RRM2B)* gene which encodes for the p53 inducible ribonucleotide reductase (p53R2) has been shown to cause mitochondrial DNA depletion leading to the inhibition of OXPHOS indicating that p53 promotes OXPHOS by upregulating p53R2 (Bourdon et al., 2007).

1.5.6.3 p53 and ROS production

ROS mediated apoptosis is one of the mechanisms through which p53 exerts its tumour suppressive role. As explained in section 1.1 under mild or reversible stress conditions p53 allows the cells to undergo DNA repair and proceed to normal proliferation while under severe or irreversible stress conditions promotes apoptosis (Vousden and Ryan, 2009). In line with this model, under severe or irreversible stress conditions, p53 has been shown to upregulate pro-oxidant genes such as p53 inducible gene 3 (PIG3) (Ostrakhovitch and Cherian, 2005) and proline oxidase (Donald et al., 2001) and downregulates anti-oxidant genes such as PGM (Kondoh et al., 2005), superoxide dismutase 2 (SOD2) and NQO1 which promotes the ROS mediated apoptosis (Vousden and Ryan, 2009). The elevated ROS in turn cause DNA damage which activate p53 thus forms a feedback loop (Bensaad and Vousden, 2007). At the same time, in low stress conditions, p53 has been shown to induce anti-oxidant genes such as TIGAR (Bensaad et al., 2006) and Sestrins (Budanov et al., 2002) to protect the cells from ROS induced apoptosis.

1.6 PCAF

1.6.1 Acetylation and transcription

In human cells, about 3 billion base pairs of DNA are tightly packed in 23 pairs of chromosomes in roughly 3 micron diameter nucleus. This tight packaging of DNA is achieved by condensation of DNA into higher order chromatin structure. Nucleosomes are the basic functional packaging units of chromatin which consists of 147 base pairs of DNA wound around two copies of each of four histone proteins H2A, H2B, H3 and H4.

The regulation of gene transcription is a complex process which involves at least in part, the ATP dependent chromatin remodelling and post translational modifications of histone and non-histone proteins (Batta et al., 2007). Chromatin in its higher order compaction structure prevents whereas in its relaxed structure allows the access of the basal transcription machinery to the DNA which is essential for the initiation of gene expression. Various post translational modifications including methylation, acetylation, phosphorylation, ubiquitination, sumoylation, ADP-ribosylation, citrullination etc. determine the order of complexity of chromatin structure. Among many enzymes that change the structure of chromatin, the acetylating enzymes are the most extensively studied structurally and functionally.

Acetylation of histone tails reduces its net positive charge thereby reducing its affinity to DNA leading to the formation of relaxed DNA which now becomes accessible to general transcription factors (Verdin, 2006). Acetylation of histones is generally associated with activation while deacetylation with repression of gene expression. The enzymes which add and remove acetyl groups to and from the ε-amino group of lysine residues of histone tails are known as histone acetyl transferases (HATs) and histone deacetylases (HDACs) respectively. Known proteins with intrinsic HAT activity include p300, cAMP responsive element binding protein (CREB) binding protein (CBP), p300/CBP associated factor (PCAF) and steroid receptor coactivator 1 (SRC-1) (Verdin, 2006). HDACs are divided in four classes (class I-IV) on the basis of their structure and substrate specificity. The class III HDACs consists of the NAD^+ dependent deacetylases called Sirtuins (Bock and Goode, 2004; Ramkumar et al., 2011).

Later studies have provided evidence that apart from histones, HATs and HDACs have a large number of non-histone substrates including p53 (Gu and Roeder, 1997) and HIF-1α (Jeong et al., 2002; Lim et al., 2010; Xenaki et al., 2008)

1.6.2 Discovery and functional domains of PCAF

PCAF is a protein of 832 amino acids and the first identified mammalian cofactor with intrinsic histone acetyl transferase activity (Yang et al., 1996). PCAF belongs to GNAT (GCN-5 related N-acetyl transferases) superfamily of acetyl transferases (Dutnall et al., 1998). The PCAF splice variant PCAF-B/hGCN5-L (837 amino acids) is expressed in high levels in day 8 of mouse embryogenesis, whereas PCAF can be detected after day 12.5. PCAF-B null mice die in early stage of development, indicating that PCAF-B is essential for embryogenesis whereas PCAF plays a role in late development and differentiation. Moreover, increased PCAF-B levels observed in PCAF null mice suggest that PCAF-B compensates for the absence of PCAF (Yamauchi et al., 2000). While the C-terminal domain of PCAF is important for its intrinsic histone acetyl transferase activity, the N terminal domain has been shown to be essential for its interaction with p300/CBP complex (Yang et al., 1996) and stability (Herrera et al., 1997).

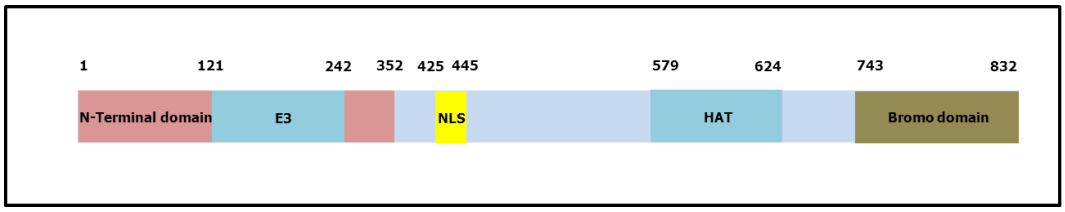

Figure 1.6.1: Domain structure of PCAF protein

Diagram indicating the functional domains of PCAF. The N-terminal region of the protein exerts E3 ligase activity. HAT and bromo domains lie in the C-terminal region of the protein. p53 is a target of PCAF E3 ligase which also auto-ubiquitinates PCAF.

PCAF functions as E3 ubiquitin ligase catalysing its own protein degradation and that of Hdm2 resulting in the stabilisation of p53 (Linares et al., 2007) and is auto-acetylated in its NLS domain indicating that acetylation plays an important role in the PCAF nuclear translocation (Santos Rosa et al., 2003). PCAF is auto-acetylated and acetylated by p300 in its N- terminal region and C- terminal region by intra and inter-molecular events respectively, which might be involved in the enhancement of its HAT activity

(Santos Rosa et al., 2003). Figure 1.6.1 demonstrates schematically the functional domains of PCAF.

1.6.3 Catalytic mechanism of PCAF

PCAF has a conserved glutamate residue within its central core domain that is hydrogen bonded with a very well-ordered water molecule which is located between the carbonyl oxygen of the glutamate and the Nε nitrogen of the target lysine. Thus, the water molecule mediates the de-protonation of the histone lysine by the enzyme glutamate (Figure 1.6.2). The conserved glutamate residue (Glu122 of tGcn5) is surrounded by several hydrophobic residues that possibly shield it from solvent water and help raise its pKa to facilitate proton extraction.

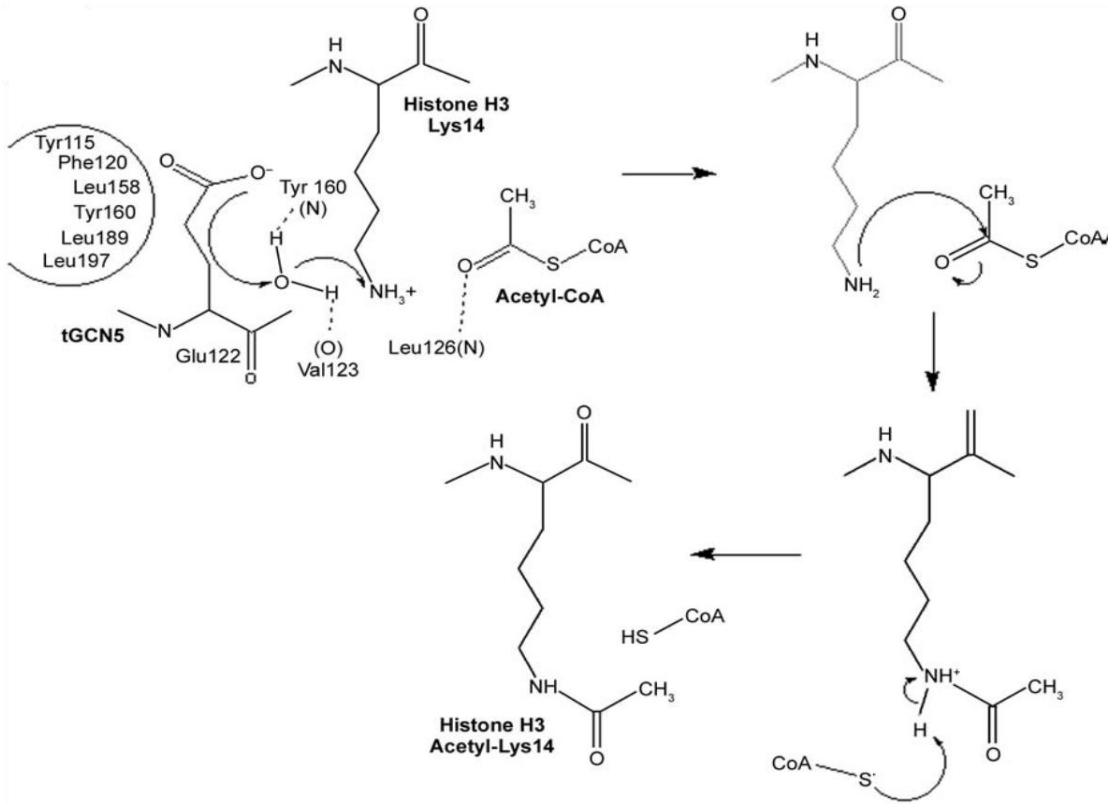

Figure 1.6.2: Catalytic mechanism of PCAF.

Proposed catalytic mechanism of GCN5/PCAF. The residue numbering is for tGcn5. The figure is modified from (Bock and Goode, 2004).

Once the lysine proton is extracted, the acetyl group of the acetyl-CoA, which is hydrogen bonded to the backbone NH of Leu126 (in the tGCN5/acetyl-CoA structure), is transferred to the reactive Lys14 side chain of the histone. The backbone NH of Leu126 probably functions to polarize the carbonyl group of the thio-ester prior to nucleophilic attack of the amino group and stabilize the negative charge that develops on the oxygen in the tetrahedral transition state (Bock and Goode, 2004).

1.6.4 PCAF complex and stability

PCAF forms complex with more than 20 distinct proteins ranging from 400 to 10 kDa. PCAF is a component of the PCAF associated factor 400 (PAF400) which belongs to the ATM superfamily of kinases indicating the complex network of general and DNA binding transcription factors, acetylases and kinases of which PCAF is an integral component (Vassilev et al., 1998).

PCAF is stable only in the presence of its co-enzyme acetyl-CoA which is required for its auto-acetylation in its N-terminal region (Herrera et al., 1997). PCAF was found to be in complex with p300/CBP and compete with E1A for binding to p300/CBP complex and antagonize E1A mediated cell proliferation (Yang et al., 1996). Later studies have shown that PCAF promotes cell survival by inducing E2F1 expression in cisplatin resistant cells (Hirano et al., 2010).

1.6.5 Non-histone targets of PCAF

While PCAF was identified initially as a histone acetylase, it is now clear that the substrate specificity of PCAF is not limited to histones. p53 is the first identified non-histone target of histone acetylases. The C- terminal DNA binding regulatory domain of p53 is acetylated at multiple lysine residues by p300/CBP (K305, 370, 372, 373, 381, 382) (Gu and Roeder, 1997; Wang et al., 2003). PCAF acetylates p53 at distinct sites from those acetylated by p300/CBP and particularly at K320 in response to stress (Liu et al., 1999). Acetylation of p53 is thought to increase its DNA binding affinity thereby enhancing its transcriptional activity (Liu et al., 1999). Acetylation of p53 possibly does not occur at multiple sites simultaneously but depends on the severity of cellular stress providing the means for amplification and target specificity of p53 transcriptional activity. In accord with this hypothesis recent reports have indicated that diverse types

of stress induce acetylation of p53 at different sites promoting either cell cycle arrest through induction of $p21^{WAF-1/CIP-1}$ gene expression or apoptosis by stimulating pro-apoptotic members of the Bcl-2 family (Knights et al., 2006; Xenaki et al., 2008)

Mdm2 interacts with PCAF and inhibits PCAF-mediated acetylation of p53 in vivo and in vitro, thus inhibiting p53 transcriptional activity (Jin et al., 2002). At the same time, the E3 ligase activity of both PCAF and Hdm2 exibit synergistic actions (Linares et al., 2007). PCAF mediated acetylation of p53 is also inhibited by the adenovirus encoding the E1B 55 kDa oncoprotein which interferes with the physical interaction between PCAF and p53 (Liu et al., 2000). Apart from p53 PCAF interacts with and acetylates HIF-1α at K674 (Lim et al., 2010) increasing its protein stability and transcription target selectivity in hypoxia (Lim et al., 2010; Xenaki et al., 2008) possibly facilitating the recruitment of p300 in the C-TAD domain of HIF-1α (Lim et al., 2010). Other transcription factors associated with PCAF include nuclear receptors such as RXR-RAR heterodimers, Estrogen receptor (ERα), androgen receptor (AR) and glucocorticoid receptor (GR) (Blanco et al., 1998).

1.6.6 PCAF and cancer

PCAF has been shown to interact with E2F transcription factors (Vassilev et al., 1998). Acetylation of E2F1 by PCAF increases its stability and transcriptional activity (Martínez-Balbas et al., 2000; Pillai et al., 2010) resulting in the promotion of cell cycle progression. Recently PCAF has been shown to interact with SIRT1 and control the E2F1 mediated apoptotic pathway (Pediconi et al., 2009). On the other hand PCAF dependent p53 acetylation induces $p21^{WAF-1/CIP-1}$ mediated cell cycle arrest (Knights et al., 2006; Xenaki et al., 2008). In response to growth factors PCAF acetylates the PTEN tumour suppressor at two lysine residues (K125 and K128) within the catalytic cleft, which compromise the ability of PTEN to regulate G1 arrest and inhibit cell proliferation induced by the PI3K/Akt pathway (Okumura et al., 2006). Therefore, PCAF has been shown to exert contrasting effects in the control of cell cycle progression in other words it promotes cell proliferation by acetylating E2F and PTEN and cell cycle arrest by acetylating p53.

1.6.7 The cross talk between p53 and HIF-1α

As p53 is stabilized in severe and prolonged hypoxia, hypoxia is considered to be one of the physiological inducers of p53 activity (Graeber et al., 1994; Halterman et al., 1999). The hypoxia mimicking agents DSFX and cobalt chloride induce p53 protein stabilisation in a HIF-1α dependent manner, however, stabilization of p53 under these conditions is not due to HIF-1α transcriptional activity, but rather a result of interaction between p53 and HIF-1α proteins (An et al., 1998). In-vitro studies have shown that the association between HIF-1α and p53 is indirectly mediated by MDM2 which interacts with both p53 and HIF-1α mediating ubiquitin dependent degradation of both transcription factors (Chen et al., 2003; Ravi et al., 2000).

In contrast to MDM2 the tumour suppressor pVHL negatively regulates HIF-1α protein stability in normoxic conditions whereas it functions as p53 co-activator and positive regulator of its protein stability preventing the p53-MDM2 interaction (Roe et al., 2006; Sermeus and Michiels, 2011). In addition the affinity for binding to p300 has been shown to be higher for p53 compared to HIF-1α. This enables p53 to exhibit its tumour suppressive activities in the presence of limited amount of p300, whereas HIF-1α under these conditions is transcriptionally inactive (Vleugel et al., 2006).

Although the molecular mechanisms involved have not been verified in details it is now clear that both p53 and HIF-1α regulate cellular energy production by modulating the gene expression of genes participating in the energy production pathways of glycolysis and OXPHOS. In particular, HIF-1α upregulates gene expression of the Glucose transporter Glut1 while p53 downregulates the expression of this gene (Chen et al., 2001; Schwartzenberg-Bar-Yoseph et al., 2004a). Similarly, p53 downregulates HK2 gene expression while HIF-1α upregulates it (Kim et al., 2007). In addition, p53 binding sites have identified in the regulatory promoter regions of the *TIGAR* and *SCO2* genes, which are involved in the regulation of glycolysis and OXPHOS respectively (Bensaad et al., 2006; Matoba et al., 2006) and has been shown to be differentially regulated in hypoxic cells (Kimata et al., 2010; Sung et al., 2010).

1.7 TIGAR

1.7.1 Discovery and structure

TIGAR was discovered by Bensaad et al., in a microarray analysis of gene expression following p53 induction (Bensaad et al., 2006). TIGAR is located on chromosome 12p13-3 and contains six potential coding exons and two possible p53 binding sites among which the one positioned within the first intron binds to p53 with higher affinity compared to that found upstream of the first exon (Figure 1.7.1). TIGAR mRNA expression was induced 6 hours after the activation of p53 following similar kinetics to that of the p53 anti-apoptotic target gene $p21^{WAF-1/CIP-1}$ and faster than that of its pro-apoptotic target gene BAX. Further studies have shown that TIGAR inhibits ROS mediated apoptosis (Bensaad et al., 2006).

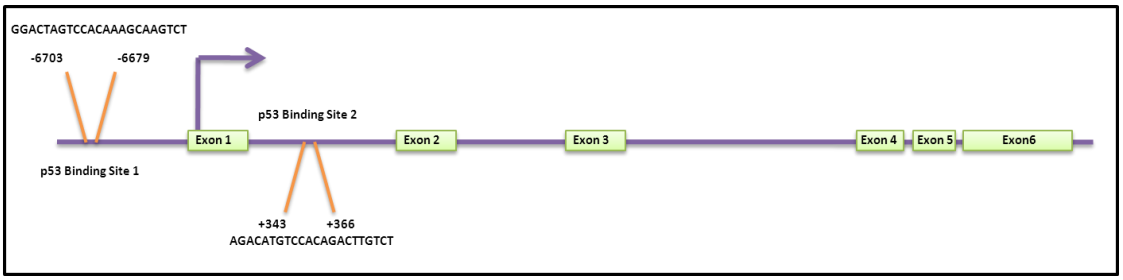

Figure 1.7.1: Structure of *TIGAR* gene

Schematic diagram showing the structure of TIGAR gene. The two p53 binding sites are located upstream of the first exon (-6703 to -6679) and within the first intron (-343 to -366). The predicted translation start site and the positions of the six exons are also indicated.

TIGAR belongs to the histidine phosphatase super-family of proteins which contain a strictly conserved catalytic core centred at the histidine residue and shares similarity with the catalytic regions of the PGM family of proteins (Bensaad et al., 2006; Li and Jogl, 2009). TIGAR shows highest similarity to the products of the pfkfb genes (pfkfb 1–4) which encode for the bifunctional enzymes PFK-2/FBPase-2 (1 to 4) (Figure 1.7.2) and has been found to catalyze the same phosphatase reaction as these enzymes, that is to convert F2,6-BP to F6-P (Lehninger et al., 2005) and is phosphorylated during the conversion of F2,6-BP to F6-P (Li and Jogl, 2009).

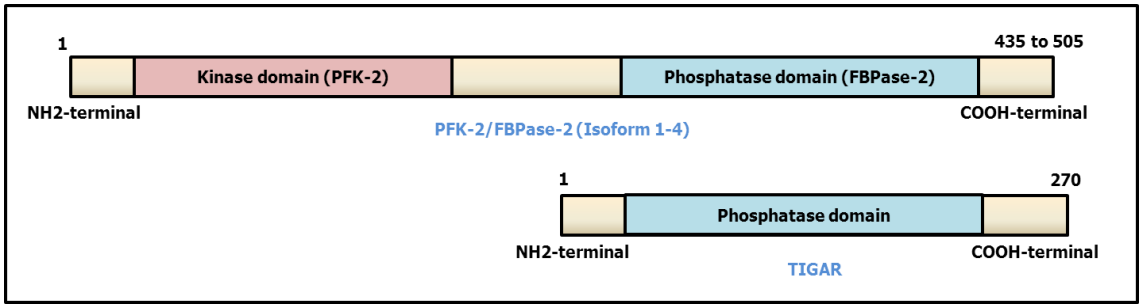

Figure 1.7.2: The phosphatise domain of the PFKFB (1-4) enzymes is similar to TIGAR

PFKFB bifunctional enzymes have a kinase domain in their amino terminal end and a phosphatase domain in their carboxy terminal end. TIGAR shares similarity with the phosphatase domain of PFKFB enzymes.

The crystal structure of TIGAR is most closely related to the bacterial broad specificity phosphatase PhoE followed by phosphoglycerate mutase and F2,6-BPase (Li and Jogl, 2009). Similar to F2,6-BPase, TIGAR catalyses the conversion of F2,6-BP to F6-P (Bensaad et al., 2006). However, the C-terminal region of FBPase-2 contains 25 additional residues that are not present in TIGAR. These additional residues form two external loop regions that enclose the active site of FBPase-2 and restrict the access to the active site contributing to the high specificity of FBPase-2 for F2,6-BP. On the other hand, TIGAR in addition to F2,6-BP catalyzes the breakdown of F1,6-BP (Li and Jogl, 2009). The broader TIGAR substrate specificity is currently under investigation.

1.7.2 Role of TIGAR in regulating glycolysis

F2,6-BP is a crucial regulator of glucose metabolism as it activates the rate limiting glycolytic enzyme PFK-1 and inhibits FBPase-1 an enzyme involved in gluconeogenesis (Pilkis et al., 1981; Uyeda et al., 1981). The level of intra-cellular concentration of F2,6-BP is regulated by a single bi-functional enzyme PFK-2/FBPase-2. The N-terminal kinase activity of PFK-2/FBPase-2 catalyzes the formation of F2,6-BP whereas the C-terminal phosphatase hydrolyses F2,6-BP to F6-P and inorganic phosphate (Figure 1.7.3). High levels of intracellular F2,6-BP activate PFK-1 by increasing its affinity for F6-P and diminishing the inhibitory effect of ATP on PFK-1 (Lehninger et al., 2005). F2,6-BP has antagonistic effects with glucokinase (GK) and glucose 6-phosphatase (G6Pase) enzyme. When levels of F2,6-BP are elevated in the

liver, GK gene expression is up-regulated while the G6Pase is down-regulated (Wu et al., 2006).

The molecular mechanism involved in the regulation of F2,6-BP intracellular levels by TIGAR has not been clearly delineated. However, since F2,6-BP is an allosteric activator of PFK-1, TIGAR mediated down-regulation of F2,6-BP levels render PFK-1 in inactive state (Bensaad et al., 2006). In addition, F2,6-BP by inducing glucokinase gene expression and inhibiting G6Pase enzymatic activity promotes glucose phosphorylation (Wu et al., 2006). Consistent with the above mentioned reports TIGAR dependent downregulation of F2,6-BP levels results in the accumulation of F6-P which is diverted to metabolize via the pentose phosphate pathway (PPP) through which it regulates the intracellular ROS levels (Bensaad et al., 2006; Wu et al., 2006).

1.7.3 Regulation of the intracellular ROS levels by TIGAR

TIGAR inhibits glycolysis by dephosphorylating F2,6-BP and contributing to the intracellular accumulation of F6P which is initially converted to G6P by glucose phosphate isomerise (GPI) and then metabolized to an alternate glucose metabolic pathway, PPP (Bensaad et al., 2006). PPP is the major source of NADPH which scavenges reactive oxygen species (ROS) by promoting the conversion of reduced glutathione to oxidised glutathione (Figure 1.7.4). By reducing the intracellular ROS levels TIGAR inhibits the ROS induced apoptosis in cancer cells which suggests that it is a pro-survival target of the p53 tumour suppressor (Bensaad et al., 2006).

The PFK-2/FBPase-2 isoform PFKFB3 has been shown to be induced in hypoxic conditions and exhibits kinase to phosphatase activity ratio of 700:1. (Minchenko et al., 2002). TIGAR, which shares structural and functional similarities with the phosphatase domain of PFK-2/FBPase-2, has also been found to be induced in hypoxic cardiac myocytes (Kimata et al., 2010) in a p53 dependent manner. Elevated TIGAR levels inhibit glycolysis and hypoxia induced apoptosis in these cells (Kimata et al., 2010) suggesting that TIGAR upregulation in hypoxic conditions might be a result of the crosstalk between HIF-1α, and p53 determining the cellular fate under these conditions.

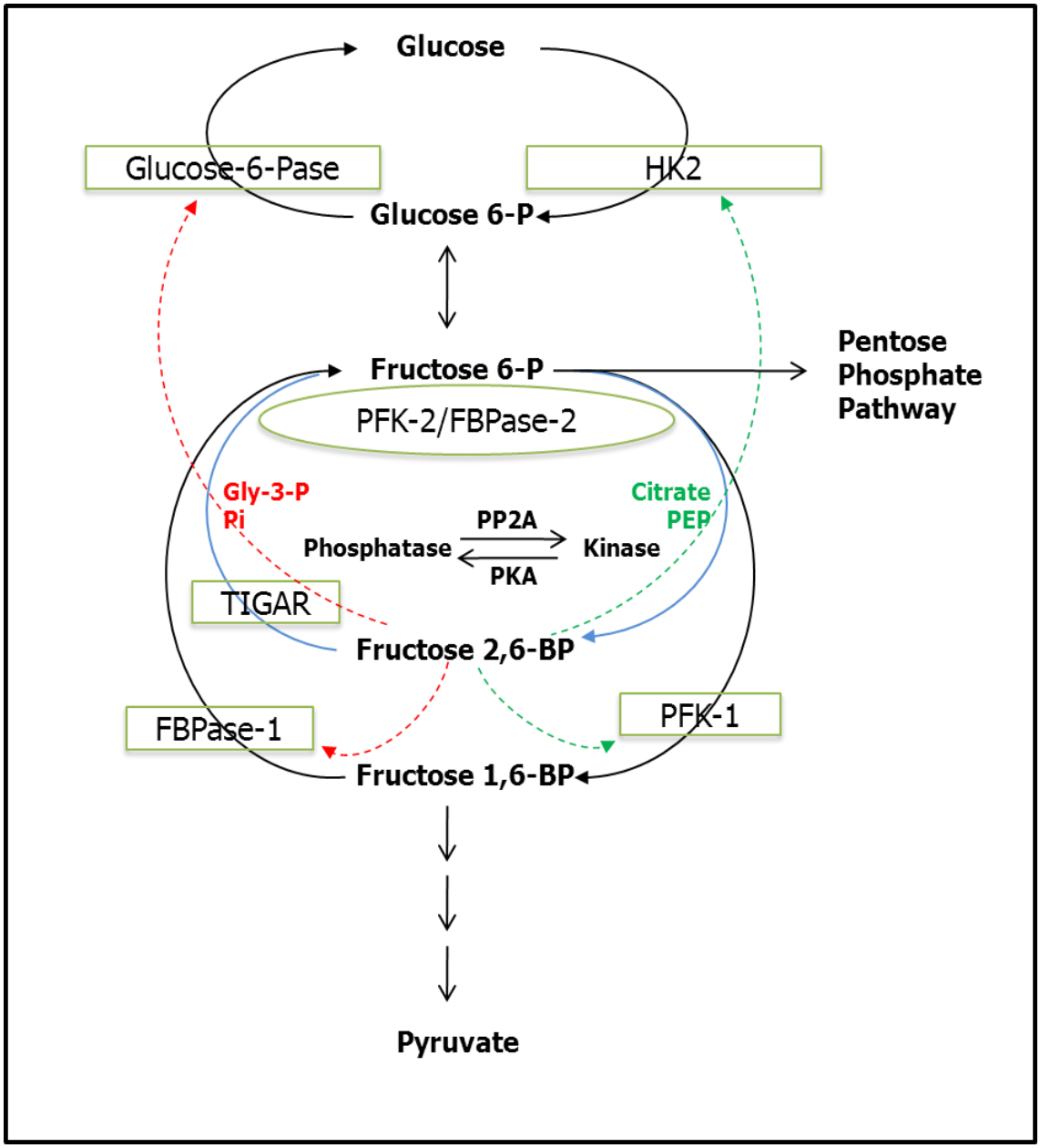

Figure 1.7.3: TIGAR regulates glucose metabolism

TIGAR catalyses F2,6-BP de-phosphorylation mimicking the enzymatic activity of the phosphatase domain of PFK-2/FBPase-2 with which it shares structural similarity. F2,6-BP is an allosteric activator of PFK-1, a rate limiting enzyme of glycolysis. Low F2,6-BP intracellular levels render PFK-1 inactive and glycolysis cannot proceed, thus explaining the mechanism by which TIGAR reduces the glycolytic rate.

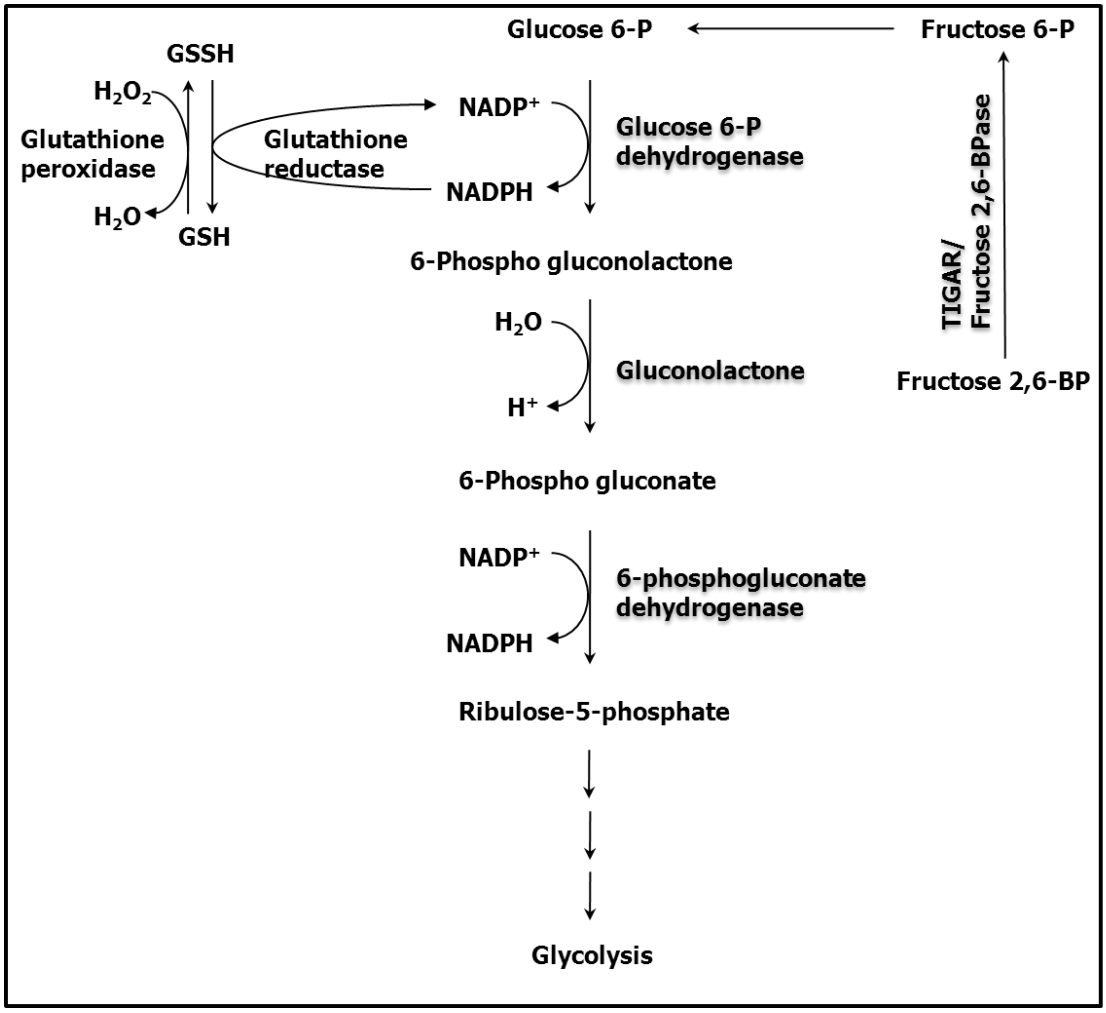

Figure 1.7.4: TIGAR inhibits intracellular ROS levels by promoting pentose phosphate pathway

TIGAR contributes to F6P accumulation, which diverts glycolysis to pentose phosphate pathway. In the presence of NADPH produced by PPP the reduced glutathione absorbs H_2O_2 and releases water becoming oxidised glutathione. GSH: Glutathione (reduced form); GSSH: Glutathione (oxidised form); NADP: Nicotinamide adenine dinucleotide phosphate; NADPH: Nicotinamide dinucleotide phosphate (reduced form)

In addition, since PFKFB3 and TIGAR are both induced in hypoxia and antagonise each other's function (PFKFB3 has positive effect on glycolysis whereas TIGAR inhibits it) the final outcome in terms of whether glycolysis will proceed or not in hypoxia might be a result of the balance of the intracellular levels of these two enzymes. This model however requires experimental evidence.

1.8 Synthesis of cytochrome c oxidase 2 (SCO2)

1.8.1 Introduction

The cytochrome c oxidase (COX) complex is the terminal enzyme of the energy transducing electron transport chain within the mitochondrial inner membrane. COX catalyzes the terminal step in electron transport chain reducing the molecular oxygen and coupling this reduction with proton translocation across the inner membrane. COX complex is composed of 13 polypeptide subunits three of which are encoded by mitochondrial DNA and form the catalytic core of the complex and the remaining ten are encoded by nuclear DNA. The catalytic cofactors of the COX complex include copper ions and heme moieties (Horng et al., 2005). COX I and II subunits contain copper centres Cu_B and Cu_A respectively. SCO2 was discovered in 1994 in an yeast sequencing project (Smits et al., 1994). COX17 delivers copper ions to SCO2 which subsequently transfers them to COX II subunit thus facilitating the assembly of the COX complex (Figure 1.8.1). SCO2 has also been shown to be involved in the maintenance of cellular copper homeostasis (Leary et al., 2007).

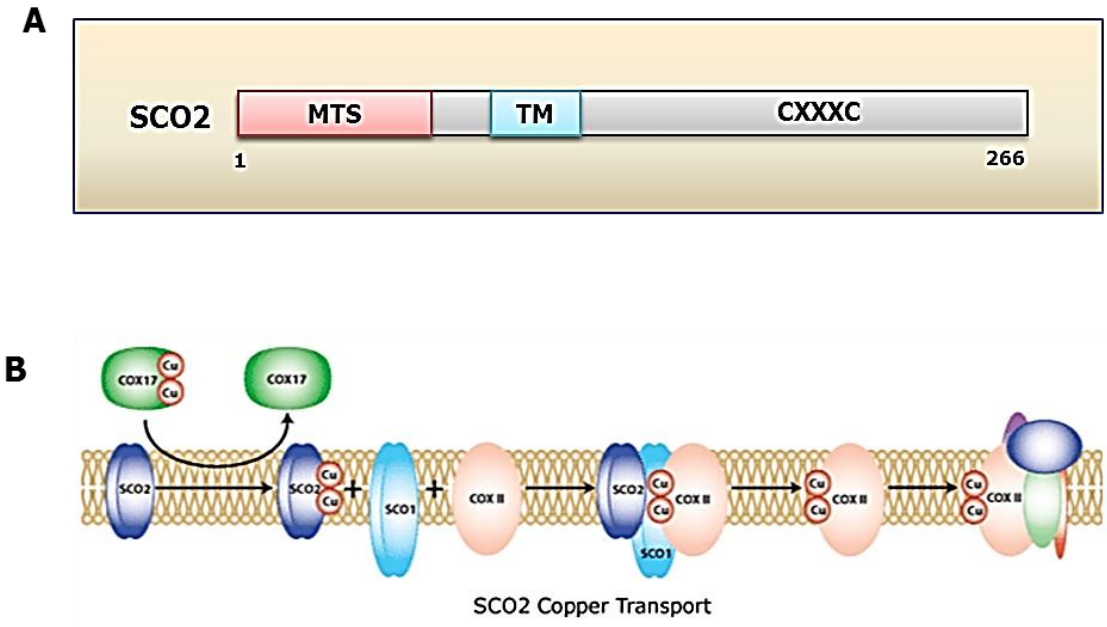

Figure 1.8.1: SCO2 is involved in the transport of copper ions to the COX 2 subunit

A. Domain structure of SCO2 protein. MTS- mitochondrial target sequences; TM- Trans membrane helics; CXXXC- Essential CXXXC motif. **B.** Copper ions are delivered to SCO2 by COX17. SCO2 transfers these copper ions to the COX II subunit. Figure adapted from Baylor college of Medicine website.

1.8.2 Regulation of SCO2 gene expression by p53

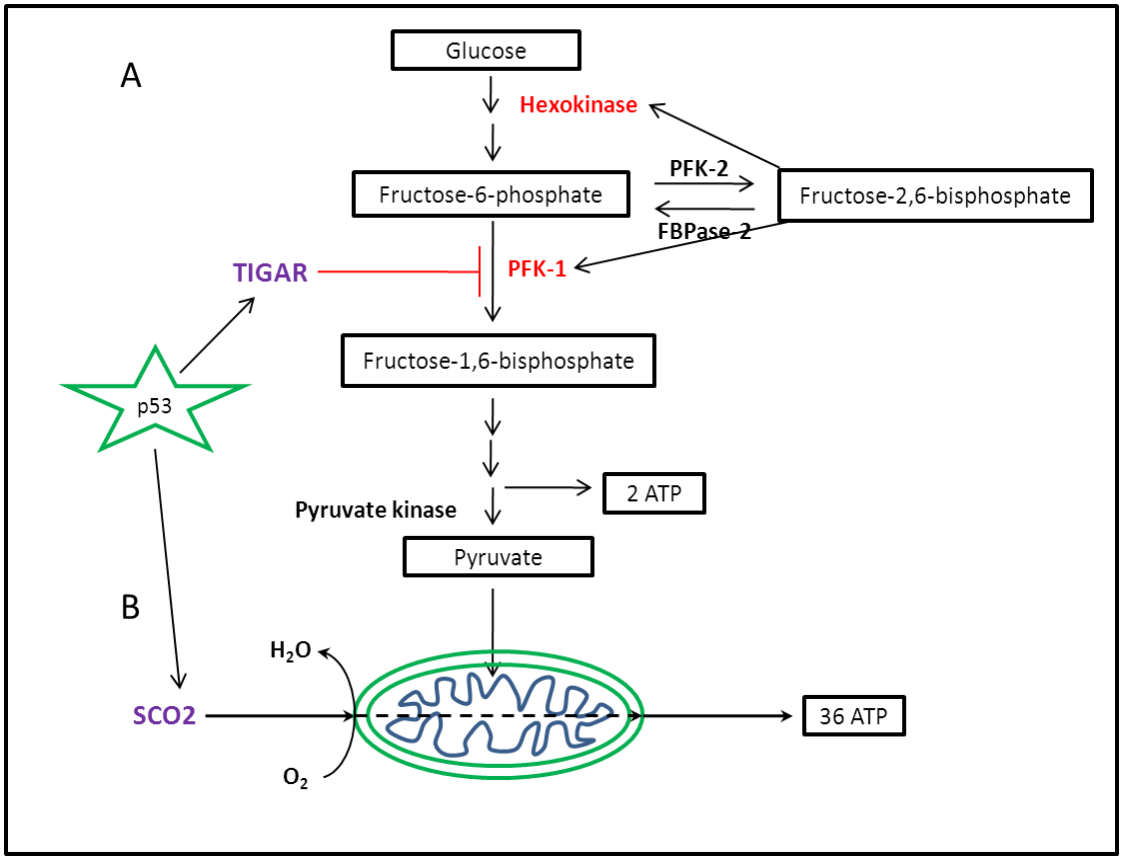

Figure 1.8.2: Regulation of cellular energy metabolism by p53

p53 modulates cellular energy metabolism by regulating its transcription target genes. p53 induces TIGAR gene expression inhibiting glycolysis (A) and SCO2 promoting mitochondrial respiration (B).

Cellular energy production is regulated by p53 through transcriptional regulation of its target genes involved in OXPHOS. Decreased OXPHOS has been observed in p53 deficient cell lines that could be rescued by the ectopic expression of SCO2 indicating that wild type p53 regulates OXPHOS by inducing SCO2 gene expression (Figure 1.8.2). Additional evidence supporting this notion has been lent by the observation that disruption of SCO2 gene expression in wild type p53 expressing cells recapitulates the phenotype of defective mitochondrial respiration (Matoba et al., 2006).

Furthermore, the fact that disruption of SCO2 gene expression did not affect the total ATP production suggested that the cells adapt to glycolysis as their primary source of energy production under these conditions. This view was confirmed by the increased lactate production observed in cell lines deficient in either SCO2 or p53 (Sung et al., 2010). Low SCO2 gene expression has shown to result in poor prognosis of breast cancers (Won et al., 2011). Although, it has been shown that both TIGAR and SCO2 gene expression are mediated by p53, the significant expression of these proteins in very low p53 expression and p53 null cell lines indicate that other factors are also involved in the regulation of TIGAR and SCO2 gene expression (Won et al., 2011).

2 Project aims and hypothesis

Transcriptional cofactors such as p300 and PCAF regulate the cross talk between HIF-1 and p53 by modulating protein stability and transcriptional activity of both transcription factors under diverse types of cellular stress (Arany et al., 1996; Liu et al., 1999; Schmid et al., 2004; Xenaki et al., 2008). We have recently reported that under hypoxic conditions PCAF orchestrates cellular survival or death by differentially recruiting p53 and HIF-1α to either the pro-survival gene $p21^{WAF-1/CIP-1}$ or the pro-apoptotic member of the Bcl-2 family BID (Xenaki et al., 2008). It is known that p53 and HIF-1 regulate the levels of enzymes involved in glucose metabolism and OXPHOS (Chen et al., 2001; Kim et al., 2007; Mathupala et al., 1997; Schwartzenberg-Bar-Yoseph et al., 2004a) thereby determining the pathway of cellular energy metabolism.

In particular p53 has been shown recently to inhibit glycolysis by inducing the inhibitor of glycolysis enzyme TIGAR and promote OXPHOS by upregulating the expression of the cytochrome c oxidase assembly gene SCO2. Since TIGAR has been shown recently to be upregulated in hypoxia (Kimata et al., 2010), and several cytochrome c oxidase subunits as well as mitochondrial biogenesis are under HIF-1α transcriptional control (Fukuda et al., 2007) we hypothesised that TIGAR and SCO2 might be transcriptionally regulated apart from p53 by hypoxia responsive transcription factors and PCAF could act as a coordinator in the decision of the pathway of cellular energy metabolism the same way as it has been shown for survival/death (Xenaki et al., 2008) in hypoxic conditions.

Thus the aim of this project is to investigate the role of HIF-1α in the regulation of gene expression of *TIGAR* and *SCO2* in hypoxic conditions and dissect the molecular mechanism(s) implicating the HAT activity of PCAF in the regulation of these genes by p53 and/or HIF-1α. In addition, this project aims to characterise the role of the HAT activity of PCAF in the regulation of *TIGAR* and *SCO2* gene expression and hence on the choice of the pathway of cellular energy metabolism and intracellular ROS generation. The hypothesis of the project and its aims are summarised in Figure 1.8.1.

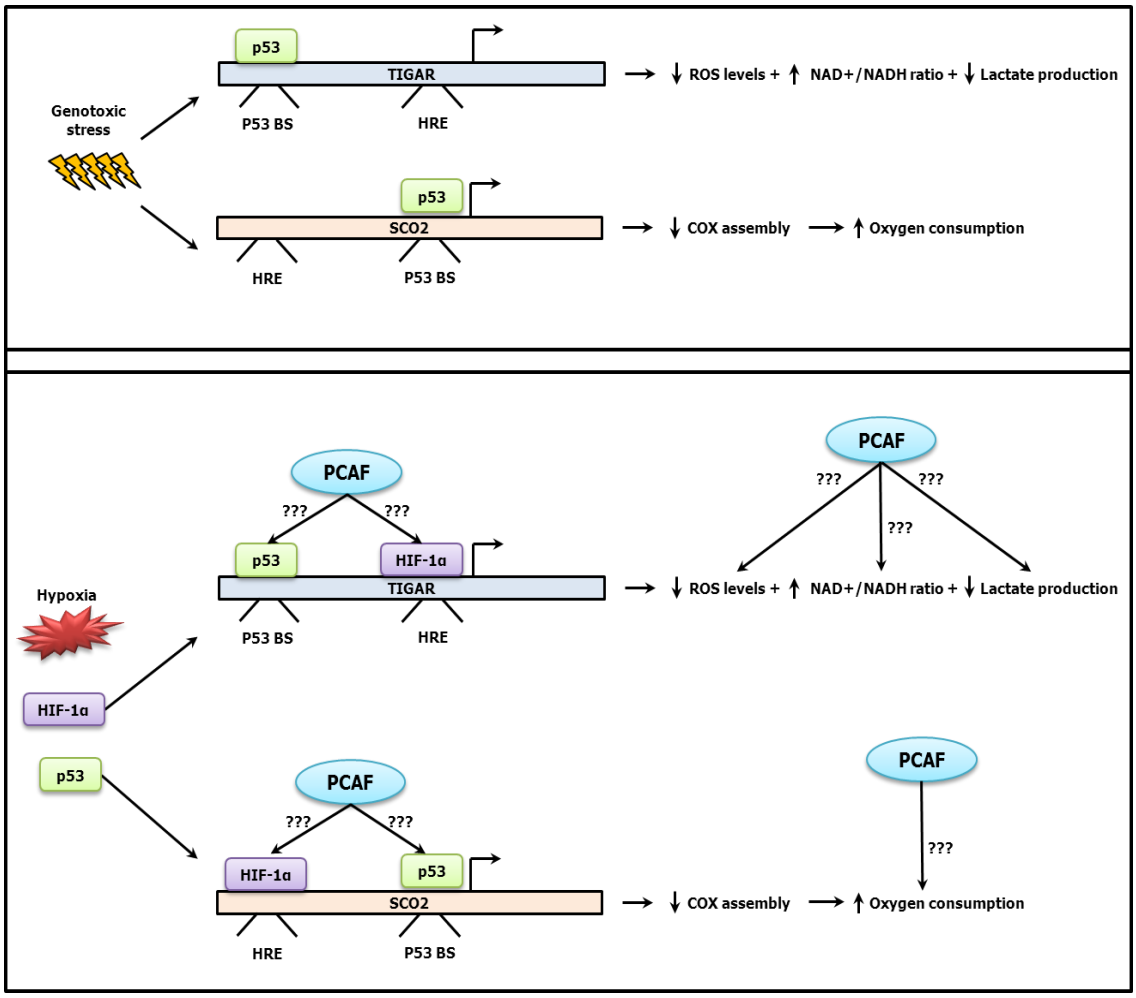

Figure 1.8.1: Hypothesis and aims of the project

In normoxia, in response to genotoxic stress, p53 is recruited to the regulatory region of the promoters of *TIGAR* and *SCO2* genes. Upregulation of *TIGAR* gene expression by p53 leads to decreased intracellular ROS levels, lactate production and increased NAD^+/NADH levels, whereas, upregulation of *SCO2* gene expression by p53 leads to increased oxygen consumption as a consequence of efficient assembly of the COX complex in the mitochondria (upper panel). Given the crosstalk between p53 and HIF-1 we hypothesised that under hypoxia the HIF-1 transcription factor might be recruited to *TIGAR* and *SCO2* promoters and regulate their gene expression. Since PCAF is a common cofactor for both p53 and HIF-1α, we also hypothesised that PCAF might play an important role in facilitating p53 and/or HIF-1 to selectivity modulate *TIGAR* and *SCO2* gene expression under diverse types of stress. We propose that differential regulation of TIGAR and/or SCO2 in hypoxia mimicking conditions determine the pathway by which cells produce energy (OXPHOS or glycolysis) (lower panel).

To study whether the *TIGAR* and *SCO2* gene expression were under HIF-1 transcriptional control in hypoxia mimicking conditions we followed protein and mRNA levels of these genes in DSFX treated cells bearing wild type or mutant p53. The involvement of HIF-1 transcriptional activity in the regulation of *TIGAR* and *SCO2* gene expression was followed with chromatin immunoprecipitation and luciferase reporter assays.

The protein and mRNA levels of TIGAR and SCO2 were also monitored in cells overexpressing PCAFwt or PCAFΔHAT to investigate the role that PCAF plays in the regulation of the cellular levels of those genes. The functional consequences of the differential regulation of TIGAR and SCO2 gene expression was assessed by assays measuring lactate production, NAD^+/NADH ratio, intracellular ROS levels and cellular oxygen consumption in PCAF wild type and PCAFΔHAT overexpressing cells.

3 Materials and Methods

3.1 Materials

3.1.1 Chemicals

All the chemicals and general reagents used in this study and their supplier details are listed in Table 3.1.1

Serial No	Materials	Supplier	Product code
1	2-Mercaptoethanol	Sigma, UK	M3148
2	Acetic acid glacial	Fisher, UK	A/0400/PB15
3	Acrylamide/Bis-acrylamide (37.5:1)	Sigma, UK	A6050
4	Agarose low melting	Melford, UK	A1201
5	Ammonium per sulphate (APS)	Flowgen, UK	H17423
6	Calcium chloride	VWR Prolabo, UK	1.02379.1000
7	Chemiluminescent substrate (ECL reagent)	Chembio Ltd, UK	16031
8	Cryovials	Scientific laboratory supplies, UK	G122263
9	Cyclohexamide	Sigma, UK	C4859
10	Desferrioxamine (DSFX)	Sigma, UK	D9533
11	Dimethylsulphoxide (DMSO)	Sigma, UK	D8418
12	Di sodium hydrogen phosphate	Fisher, UK	S/P525/53
13	dNTPs	Bioline, UK	Bio-39025
14	Dithiothreitol (DTT)	Sigma, UK	D0632
15	Magnetic beads (Dynabeads)	Invitrogen, UK	100-01D
16	Ethylene diamine tetra acetatic acid	Sigma, UK	EDS
17	Ethanol absolute	Fisher	E/0600/05
18	Ethidium bromide	Mo Bio, USA	15006-10
19	Etoposide	Sigma, UK	E1383
20	Formaldehyde (36-38%)	Sigma, UK	F8775
21	Gel loading tips	Star labs, UK.	I1010-3000
22	Glucose	Sigma, UK	158968
23	Glycerol	VWR BDH Prolabo, UK	24387.361
24	Glycine	Fisher, UK	BPE381-1
25	HEPES	Sigma, UK	54457
26	Isopropanol	Fisher, UK	P/7490/15
27	Magnesium chloride 6 hydrate	VWR BDH Prolabo, UK	436994U
28	Methanol	Fisher, UK	BPE1105-1

Serial No	Materials	Supplier	Product code
29	Nicotinamide	Sigma, UK	72340
30	Nonidet P40	VWR BDH Prolabo, UK	A2239.0100
31	Ortho boric acid	VWR BDH Prolabo, UK	443905T
32	PageRuler Prestained protein ladder	Fermentas, UK	SM0672
33	Phenylmethylsulphonylfluoride (PMSF)	Sigma, UK	P7626
34	Potassium chloride	VWR BDH Prolabo, UK	26759.291
35	PVDF membrane	Millipore, UK	IPVH00010
36	Rotenone	Sigma, UK	R8875
37	Sodium acetate 3 hydrate	VWR BDH Prolabo, UK	27652.298
38	Sodium butyrate	Sigma, UK	B5887
39	Sodium carbonate	VWR BDH Prolabo, UK	27766.292
40	Sodium chloride	Fisher, UK	BPE358-1
41	Sodium dihydrogen phosphate	Fisher, UK	S/4480/60
42	Sodium dodecyl sulphate (SDS)	Fisher, UK	S/P530/48
43	Sodium hydroxide	VWR BDH Prolabo, UK	28244.262
44	Sodium hydrogen carbonate	VWR BDH Prolabo, UK	27778.293
45	Sodium ortho vandate	Sigma, UK	S6508
46	Sodium pyrophosphate	Sigma, UK	221368
47	SYBR Green I	Sigma, UK	S9430
48	Tetra methyl ethylene diamine (TEMED)	VWR BDH Prolabo, UK	443083G
49	Trichostatin A	Sigma, UK	T8552
50	Tris base	Fisher, UK	BPE152-1
51	Triton X100	Sigma, UK	T8787
52	Tween 20	Sigma, UK	P9416
53	X-Ray film	Fuji Films, UK	Super Rx

Table 3.1.1: Suppliers of chemicals and general laboratory reagents.

3.1.2 Media and other biological materials

Cell culture media, other biological materials used in this study and their sources are listed in Table 3.1.2

Sl No	Materials	Supplier	Product code
1	Ampicillin	Sigma, UK	A1593
2	Bovine serum albumin	Roche, UK	10711454001
3	Dissociation buffer	Gibco, UK	13151014
4	Dulbecco's Modified Eagle's Medium (DMEM)	Lonza, UK	BE12-604F
5	Foetal calf serum (FCS)	Lonza, UK	14-416F
6	HyperLadder 1 (DNA ladder)	Bioline, UK	BIO-33025
7	Kanamycin	Sigma, UK	K1876
8	LB agar	Sigma, UK	L2897
9	LB broth	Invitrogen, UK	12780029
10	Penicillin/Streptomycin	Lonza, UK	DE17-602E
11	Polyfect transfection reagent	Qiagen (UK)	301107
12	Reporter lysis buffer 5X	Promega, UK	E3971
13	Salmon sperm DNA	Sigma, UK	D7656
14	SOC media	Invitrogen, UK	15544034
15	Trypsin with EDTA	Lonza, UK	BE17-161E

Table 3.1.2: Suppliers of media and other biological materials

3.1.3 Enzymes, antibodies and kits

All the enzymes, antibodies and ready-made kits used in this study and their supplier details are listed in Table 3.1.3

Sl No	Product	Catalog number	Supplier
1	Anti-Flag M2	F3165	Sigma (UK)
2	Anti HIF-1α (H1α)67	400080	Calbiochem
3	Anti HIF-1α	(AB2185)	Abcam, UK
4	Anti p53 (DO1)	SC-126	Santa Cruz Biotechnology
5	Anti PCAF (E8)	SC-13124	Santa Cruz Biotechnology
6	Anti SCO2 (CT)	4045	ProSci Incorporated
7	Anti TIGAR (IN1)	4049	ProSci Incorporated
8	β-actin antibody	ab8227	Abcam (UK)
9	Bio-Rad protein assay kit	500-0001	Bio-Rad (UK)
10	CD-20 (APC-H7)	641396	BD Biosciences
11	ECL mouse IgG	NA931	Amersham Biosciences (UK)
12	ECL Rabbit IgG	NXA931	Amersham Biosciences (UK)

Sl No	Product	Catalog number	Supplier
13	GFX genomic Blood DNA purification kit	N/A	GE healthcare (UK)
14	HA antibody	MMS-101P	Covance (New Jersey)
15	Kpn1	10 899 186 001	Roche Diagnostics (Germany)
16	Lactate reagent	73510-10x10mls	Trinity Biotech (Ireland)
17	NAD	N0632	Sigma (UK)
18	NADH	N4505	Sigma (UK)
19	PCAF (E-8) antibody	Sc-13124	Santa Cruz (Santa Cruz)
20	PFKFB3 antibody	AP8145a	Abgent (San Diego)
21	Proteinase K	03115879001	Roche (UK)
22	Reverse Transcriptase (Bioscript)	BIO-27036	Bioline
23	Sac1	10 669 792 001	Roche Diagnostics (Germany)
24	T4 DNA ligase	481 220	Roche Diagnostics (Germany)
25	Taq DNA polymerase	M0273S	New England Biolabs (UK)
26	Xho1	10 899 194 001	Roche Diagnostics (Germany)

Table 3.1.3: Suppliers of antibodies and enzymes.

3.1.4 Buffers and general solutions

All the solutions and general buffers used in this study and their compositions are listed in Table 3.1.4

Sl No	Buffer	Composition
1	2X HBS	25mM HEPES, 0.75mM $Na_2HPO_4.12H_2O$, 140mM NaCl pH: 7.1
2	3X SDS sample buffer	187mM Tris, 30% Glycerol, 6% SDS, 15% 2-mercapto ethanol, 0.01% bromophenolblue.
3	β-gal buffer	200mM Sodium phosphate pH: 7.3, 2mM MgCl2, 100mM β-mercaptoethanol, 4.5mM ONPG.
4	Blocking solution (ChIP)	0.5% BSA w/v in PBS.
5	Blocking solution (western)	5% Milk in PBS 0.1% Tween-20
6	ChIP buffer 1	50mM Hepes-KOH; pH: 7.5, 140mM NaCl,

Sl No	Buffer	Composition
		1mM EDTA, 10% glycerol, 0.5% Igepal CA-630, 0.25% Triton X-100.
7	ChIP buffer 2	10mM Tris-HCl; pH: 8.0, 200mM NaCl, 1mM EDTA, 0.5mM EGTA.
8	ChIP buffer 3	10mM Tris-HCl; pH: 8.0, 100mM NaCl, 1mM EDTA, 0.5mM EGTA, 0.1% Na-Deoxycholate, 0.5% N-lauroylsarcosine.
9	Cycling buffer	100mM Tris-HCl (pH:8), 5mM EDTA and 0.5mM MTT
10	Elution buffer (ChIP)	50mM Tris-HCl; pH:8, 100mM EDTA and 1% SDS w/v.
11	Elution buffer (Maxiprep)	100mM Tris-HCl; pH: 8.5, 125mM NaCl.
12	Extraction buffer (NAD+/NADH)	20mM Sodium bicarbonate, 100mM Sodium carbonate, 10mM Nicotinamide and 0.05% Triton-X-100.
13	Formaldehyde solution	50mM Hepes-KOH, 100mM NaCl, 1mM EDTA, 0.5mM EGTA and 11% formaldehyde
14	Lysis buffer (Miniprep and Maxiprep)	200mM NaOH, 1% w/v SDS.
15	PBS Tween	PBS + 0.1% Tween-20
16	Phosphate buffered saline (PBS)	170mM NaCl, 3.3 mM KCl, 1.8 mM Na2HPO4, 10.6 mM KH2PO4; pH 7.4.
17	Precipitation buffer	3.1M Potassium acetate pH 5.5.
18	Resuspension buffer	50 mM Tris HCl pH 8.0, 10 nM EDTA.
19	RIPA buffer	50mM Hepes-KOH; pH: 7.5, 500mM LiCl, 1mM EDTA, 1% Igepal CA-630, 0.7% Na-Deoxycholate.
20	Stripping buffer	100 mM 2-Mercaptoethanol, 2% SDS, 62.5 mM Tris-HCl pH 6.7.
21	TAE buffer	40 mM Tris-acetate, 1 mM EDTA.
22	TE buffer	10 mM Tris-HCl pH 7.5, 1 mM EDTA.
23	TNN buffer 120 mM	50 mM Tris-HCl pH 7.4, 120 mM NaCl, 5 mM EDTA, 0.5% NP-40.
24	TNN buffer 240mM	50 mM Tris-HCl pH 7.4, 240 mM NaCl, 5 mM EDTA, 0.5% NP-40.
25	Tris buffered saline (TBS)	20mM Tris-HCl; pH: 7.6, 150mM NaCl.
26	Western transfer buffer	150 mM Glycine, 25 mM Tris-HCl pH 8.3, 20% Methanol.

Table 3.1.4: Composition of buffers and general solutions.

3.2 Cell culture and maintenance

3.2.1 Cell lines and culturing medium

Dulbecco's Modified Eagle's medium (DMEM) supplemented with 10% (v/v) heat inactivated fetal bovine serum (FBS), 1% 10,000 U/ml penicillin and streptomycin (P/S) and 2 mM L-Glutamine was used to maintain the human osteosarcoma cell lines U2OS ($p53^{+/+}$), SaOS2 ($p53^{-/-}$) and breast cancer cell lines MCF- 7 ($p53^{+/+}$) and MDA-MB-231 ($p53^{mutated}$). The variations in the p53 status of these cell lines provides a suitable system to study gene expression in the presence (fully or partially) or absence of p53 and also to study the crosstalk between p53 and other transcription factors such as HIF-1α.

3.2.2 Cell maintenance

Cells were maintained in 75 cm^2 vented tissue culture flasks and subcultured every 2-3 days when they were 70 - 80% confluent. Cell culture work was carried out in class II microbiological safety cabinets to provide safe and sterile environment. During subculture, the cells were rinsed briefly with 3ml of Trypsin-EDTA and incubated with 1ml Trypsin-EDTA for 3min in 37°C to detach cells from the flask. Fresh DMEM medium with FBS and P/S was added to dilute trypsin and the cells were passaged at a ratio of 1:5. Cells were incubated at 37°C in a humidified atmosphere of 21% O_2, 5% CO_2 and 74% N_2. Cells were seeded into 12 well plates for luciferase assays, 6 well plates for immuno-blotting and RNA extraction and 100mm plates for Chromatin immuno-precipitation assays and oxygen consumption measurement.

3.2.3 Cell counting

Cell counting was performed under a light microscope using a ruled haemocytometer (Bright-line, Hausser scientific, USA). The cells were detached from the flask and suspended well in order to avoid cell clumps. 100µl of cell suspension was mixed with 100µl of trypan blue solution. 10µl of cell suspension was loaded into the haemocytometer and the cell count was performed according to manufacturer's instructions.

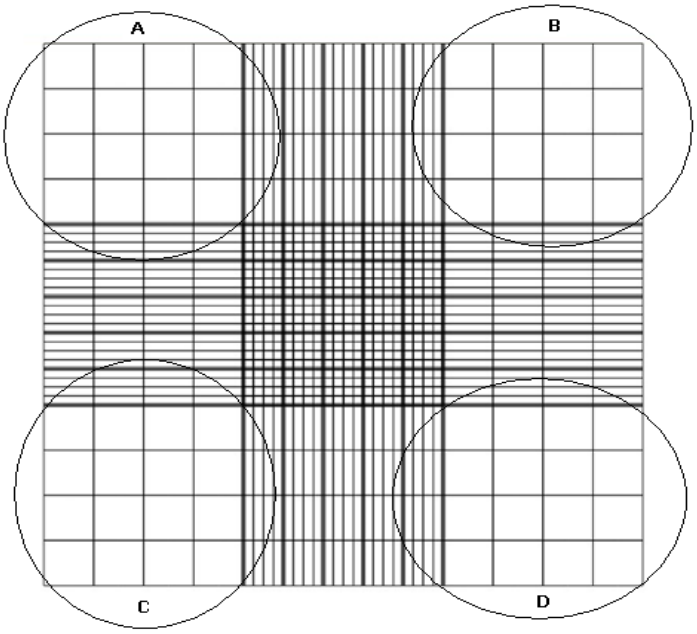

Figure 3.2.1: Haemocytometer Figure adapted from Sigma website.

The cells in areas A, B, C and D were counted and the total number of cells was calculated according to the formula mentioned in the text.

The number of cells was calculated from

$$C = N \times 10^4$$

where C is cells per ml, N is average cells counted and 10^4 is the volume conversion factor for $1mm^2$. The total number of cells is calculated from

$$\text{Total number of cells} = C \times V$$

where C is cells per ml and V is the total volume of cells. The cell counting was carried out before the experiments in order to use the appropriate number of cells (Figure 3.2.1).

3.2.4 Freezing the cells

To freeze the cells, first they were pelleted by centrifugation at 1,200 rpm for 4 minutes (Centaur-2, Sanyo, UK) and resuspended in 1ml of FBS and 1ml of 20% DMSO in FBS. DMSO prevents the formation of intracellular ice crystals. FBS + DMSO was added drop-wise through the wall of the tube to avoid the osmotic shock to the cells and to minimize the heating that occurs when DMSO is added. The cell suspension was then

aliquoted into cryovials, transferred to a cryofreeze container (Nalgene) and stored at -80°C overnight, before transferred for storage in liquid nitrogen (-196^{0}C).

3.2.5 Thawing the cells

To restore the cell culture, the frozen cells were thawed rapidly by the addition of 1ml warm DMEM media. This rapid thawing reduces or prevents the formation of damaging ice crystals within the cells during rehydration (Ryan, 2004). 9 ml of warm DMEM media was added slowly to the cells and transferred to a sterile 25 cm^2 culture flask and the cells were incubated for 3-4 hours. After the cells were attached to the surface of the flask the media was changed to fresh media containing 10% FBS and 1% penicillin/streptomycin. After they reach 70 - 80% confluency, the cells were transferred to 75cm^2 flasks.

3.2.6 Cell treatments

HIF-1α protein is hydroxylated by prolyl hydroxylase enzymes (PHDs 1-4). PHDs are non-heme Fe (II) and 2-oxoglutorate dependent dioxygenases (2-OG oxygenases) that utilize molecular oxygen as a co-substrate (Epstein et al., 2001) therefore their function is inhibited by iron chelators such as desferrioxamine (DSFX) and creates a hypoxia mimicking condition (Wang and Semenza, 1993b). 250μM final concentration of desferrioxamine (DSFX) was used to mimic hypoxia, a condition in which HIF-1α is stabilized. Etoposide is a topoisomerase II inhibitor, induces DNA strand breaks by trapping the enzyme in a complex with cleaved DNA (Zhou et al., 1999). As DNA damage conditions induce p53, 10μM final concentration of etoposide was used to induce p53. The cells were treated with DSFX or etoposide 16 hours before harvesting.

3.3 Molecular Biology

3.3.1 Extraction of genomic DNA

Genomic DNA from U2OS and SaOS2 cells was extracted using GFX genomic blood DNA purification kit (Amersham Biosciences). The cells were grown in a 75cm^2 flask and collected by trypsinization and resuspended in the residual fluid by vigorous vortexing. 500ml of the extraction solution (buffered solution containing a chaotropic agent and detergent) was added and incubated for 5 minutes at room temperature. The mixture was transferred to a micro spin column (Amersham Biosciences) and

centrifuged at 5,000g. The chaotropic agent used in the extraction buffer facilitated the lysis of nucleated cells and the binding of genomic DNA to a glass fibre prepacked in the micro spin column. The column was then washed once with 500µl of extraction buffer and 500µl of wash buffer (TE buffer with ethanol). The DNA retained on the micro spin column was eluted with 200µl of distilled water.

3.3.2 Measurement of DNA concentration

Determination of nucleic acid concentration is achieved by following the absorption of UV light by nucleicacids. UV light analysis may be utilised not only to quantify the nucleic acid content of a sample, but also used to measure its purity. DNA yield determination is based on its ability to absorb light maximally at 260nm. The DNA concentration was calculated by the following formulae

$$[\text{DNA}]\ \text{mg/ml} = A^{260} \times \text{dilution} \times 50,$$

Where A^{260} = absorbance at 260 nm, dilution = dilution factor, 50 = the DNA extinction coefficient. Although this calculation provides information about the amount of DNA yield, it does not determine the quality and purity of the sample, which can be affected by the presence of excess salt, contaminating proteins and/or organic solvents. To provide an estimation of the sample purity, the ratio of the absorbance at 260nm divided with the absorbance at 280nm (A^{260}/A^{280}) is calculated. For the DNA sample to be considered pure the A^{260}/A^{280} ratio should be close to 1.8±0.05.

The DNA concentration and purity was determined using NanoDrop ND-1000 UV visible spectrophotometer. The calibration of the instrument was performed using 1.0µl of distilled water. To determine DNA concentration, 1.0 µl of the sample was pipetted onto the end of a fibre optic cable (the receiving fibre). To determine DNA concentration, a second fibre optic cable (the source fibre) is brought into contact with the liquid sample and the gap between the fibre optic ends is then bridged through the sample. A light emitted by a pulsed xenon lamp passes through the sample, which is then analyzed by the spectrometer utilizing a linear charge coupled device (CCD) array. The PC software displays the sample concentration in ng/µl based on the absorbance at 260nm. The ratio of absorbance at 260nm and 280nm to assess nucleic acid purity is also calculated.

3.3.3 Polymerase chain reaction

Polymerase chain reaction (PCR) allows the enzymatic amplification of a double-stranded DNA region flanked by two known sequences. These two short oligonucleotide sequences (primers) can hybridise to their complementary sequence. In the first step of the reaction (denaturation) the DNA is heated at 95ºC for 5 minutes which separates the two strands of the DNA into single strands. In the second step of the reaction (primer annealing) the PCR mixture is cooled down to an optimum temperature which is known as the melting temperature in which the primers hybridise with their complementary DNA sequence to form a double-stranded region. In the third step (primer extension), DNA polymerase enzyme is used to extend the primer region to synthesize full-length complementary DNA strands. This step requires the presence of deoxynucleoside triphosphates (dNTPs), which serve as substrates for the polymerase. The process of denaturation, primer annealing, and primer extension (known as a cycle) is repeated with the new double strands since they also contain the primer binding sites. This cycle is repeated for 30 to 35 times to obtain an exponential amplification of the DNA sequence between the forward and the reverse primers (Figure 3.3.1)

Genomic DNA of U2OS cells was extracted using GFX genomic DNA purification kit (Section 3.3.1). To amplify the TIGAR and SCO2 promoter regions, suitable primers (Table 3.3.1) were designed using Primer 3 software which amplify a specific region containing the HRE 5, 6 and p53 binding site 2 within the TIGAR promoter or HRE 1 to 5 and p53 binding site in the SCO2 promoter (Figure 4.2.4 and Figure 4.2.5) Polymerase chain reaction (PCR) was performed using Phusion high fidelity DNA polymerase (Finnzymes, Finland) which synthesizes blunt end PCR product.

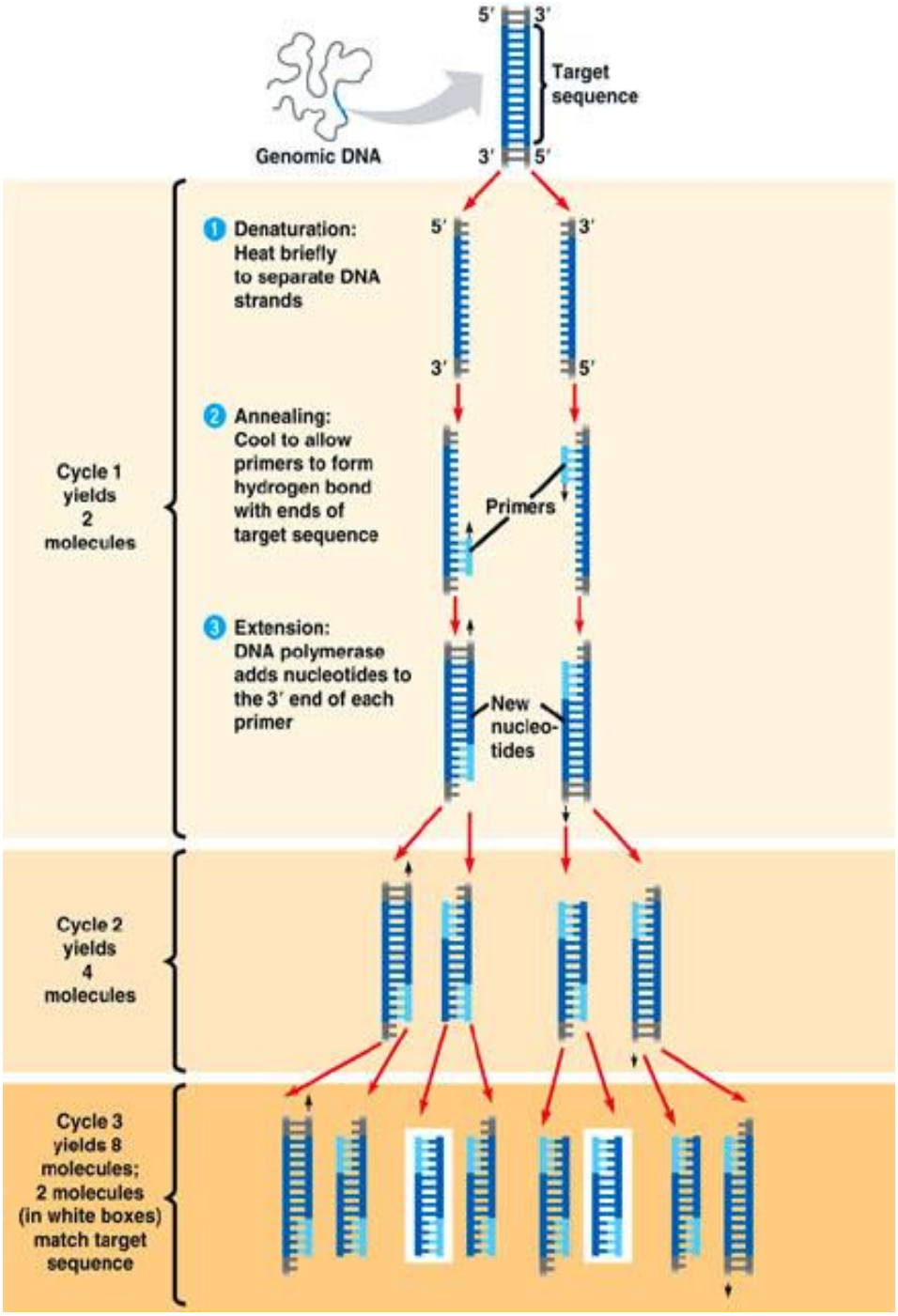

Figure 3.3.1: Principle of PCR reaction.

Schematic diagram demonstrating the principle of PCR reaction. The DNA undergoes denaturation, primer annealing and primer extension processes to produce an amplified target region of DNA. The figure is adapted from (Mullis, 1983)

Gene name	Forward primer	Reverse primer
TIGAR	5'-CTCGAGGGGTGGGTGGGTCTAAGTCT -3'	5'-GAGCTCGGACGAGCAATTCTGCAAAC -3'
SCO2	5'- ACCGTGGAGCTGGTCC -3'	5'- CAGCAAGGTGAACCTCT -3'

Table 3.3.1: Luciferase primer sequences

The following mixture was prepared in the tissue culture hood in order to avoid contamination.

Component	Volume (50µl)	Final concentration
5X Phusion HF buffer	10µl	1X
10mM dNTPs	1µl	200µM each
Forward primer (20µM)	1µl	100nM
Reverse primer	1µl	100nM
DNA template (100ng/1µl)	1µl	-
Phusion DNA polymerase	0.5µl	0.02U/µl
Distilled water	35.5µl	-

Table 3.3.2: Composition of PCR mixture

The following PCR set-up was employed to amplify TIGAR and SCO2 promoter regions

Segment	Number of cycles	Temperature	Duration
1	1	95°C	5 minutes
2	35	95°C	1 minute
3		55-66°C	1 minute
4		72°C	1 minute
5	1	72°C	10 minutes

Table 3.3.3: PCR set-up for the amplification of genomic DNA

The PCR products synthesized using different annealing temperatures ran in a 1% agarose gel and purified using QIAquick Gel extraction Kit (Qiagen, UK) (Figure 3.3.3 A and Figure 3.3.4 A).

3.3.4 Construction of luciferase vectors

The purified DNA was ligated to pCR-Blunt II-TOPO vector using Blunt TOPO PCR Cloning Kit (Invitrogen, UK). TOPO cloning is based on DNA TOPO isomerase 1 enzyme which functions both as a restriction enzyme and as a ligase. TOPO vectors are linearized with DNA TOPO isomerase 1 enzyme attached to it. While it cleaves the DNA strand and enables DNA unwinding it religates the ends of cleaved stands. When incubated with PCR product, the enzyme ligates the compatible ends of PCR product and TOPO vector (Invitrogen, 2007). Figure 1.5.2 schematically explains the principle of TOPO cloning.

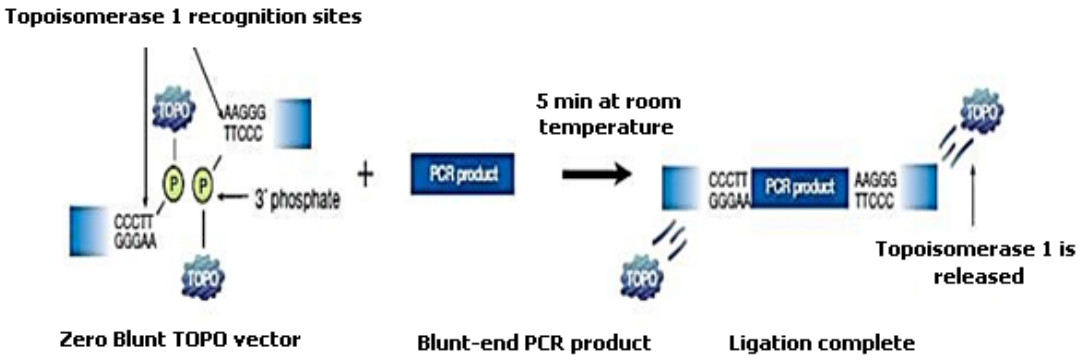

Figure 3.3.2: Principle of TOPO cloning.

Schematic diagram explain the principle involved in TOPO cloning. The figure is adapted from (Invitrogen, 2007).

The ligated TIGAR-HRE5,6-p53BS2-TOPO vector was then transformed into chemically competent DH5α and plated on agar plates containing 50µg/ml final concentration of kanamycin and incubated for 16 hours in 37°C. Eight individual colonies from the agar-kanamycin plates were picked up and inoculated into 2ml of LB broth containing 50 µg/ml final concentration of kanamycin and incubated in a shaker at 37ºC for 16 hours as the bacteria reach the stationary phase of their growth at 16 hours.

The DNA from the cultured bacterial cells was extracted by alkaline lysis miniprep method (Section 3.4.3.1) and digested using Kpn1 restriction enzyme and ran in a 1% agarose gel (Figure 3.3.3 B and Figure 3.3.4 B). The linear DNA fragment then ligated into pre-digested pGL3 promoter vector (Promega, UK) using T4 DNA ligase (New England Biolabs, UK). The ligated vector was then transformed into chemically

competent DH5α cells and plated on agar plate containing 50µg/ml final concentration of ampicillin and incubated at 37°C for 16 hours.

Four individual colonies were selected and inoculated in 2ml of LB broth containing 50µg/ml final concentration of ampicillin and incubated in a shaker at 37ºC for 16 hours. After alkaline miniprep the DNAs from different colonies digested with Kpn1 restriction enzyme and ran in 1% agarose gel (Figure 3.3.3 C and Figure 3.3.4 C). The glycerol stock was inoculated in 200ml LB broth with ampicillin and the DNA was extracted using PureLink HiPure Plasmid Maxiprep Kit (Invitrogen, UK).

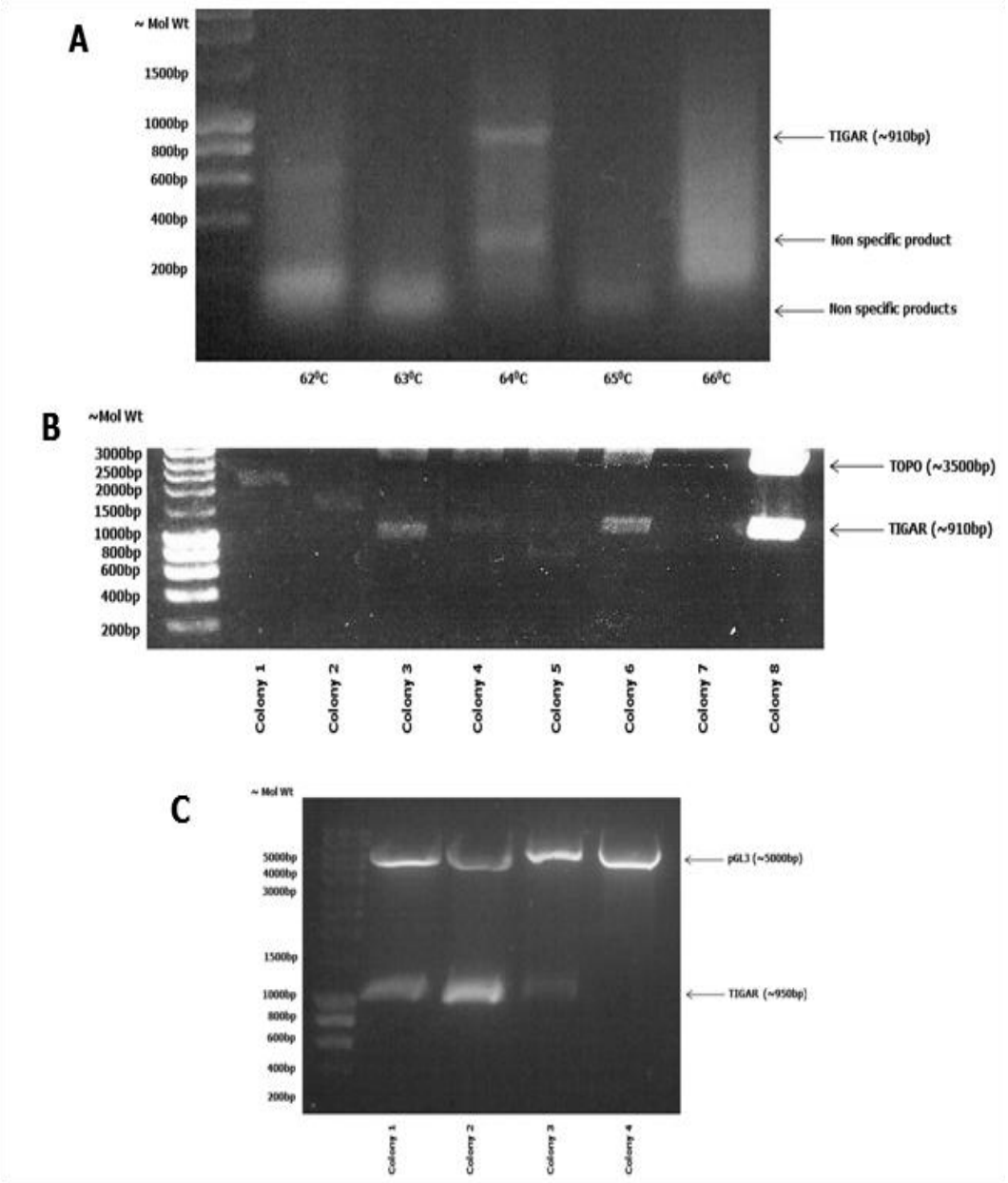

Figure 3.3.3: Construction of TIGAR-HRE5,6-p53BS2-luc vector

A. Genomic DNA from U2OS cells was used in the PCR reaction to amplify the region of the TIGAR promoter containing HREs 5, 6 and p53 binding site 2 (approximate molecular weight 910bp). **B.** The amplified DNA was cloned into pCR-Blunt II-TOPO vector. The cloned vector was digested using Kpn1 restriction enzyme and ran in a 1% agarose gel. **C.** The PCR product extracted from TOPO vector was ligated into pGL3 vector (pre-digested with Kpn1) and the ligated vector was digested using Kpn1 and ran in a 1% agarose gel.

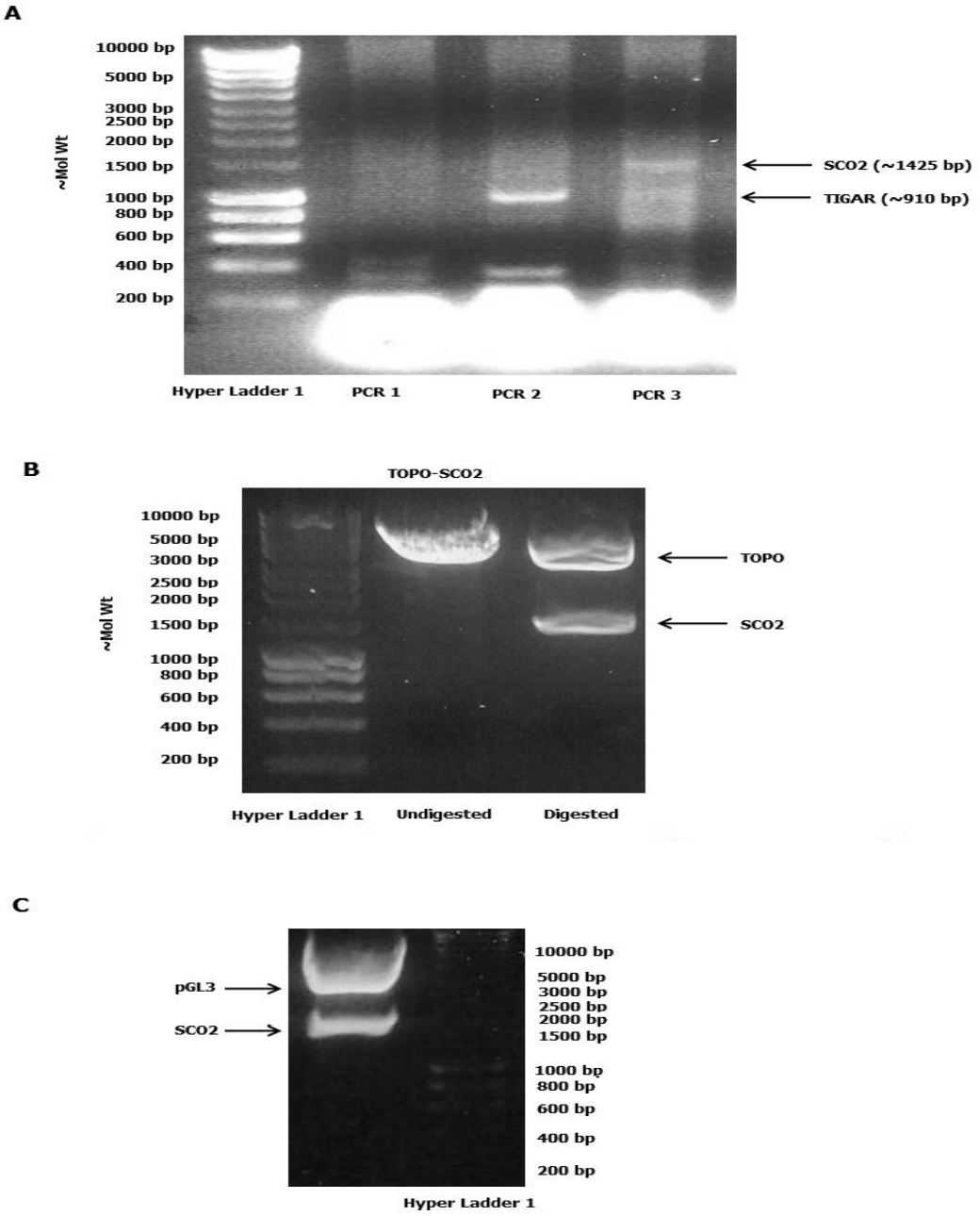

Figure 3.3.4: Construction of SCO2-HRE1-5,p53-luc vector

A. Genomic DNA from U2OS cells were used in the PCR reaction to amplify the region of the SCO2 promoter containing HREs 5, 6 and p53 binding site 2 (approximate molecular weight 1425 base pairs). **B.** The amplified DNA was cloned into pCR-Blunt II-TOPO vector. The cloned vector was digested using Kpn1 restriction enzyme and ran in a 1% agarose gel. **C.**The PCR product extracted from TOPO vector was ligated into pGL3 vector (pre-digested with Kpn1) and the ligated vector was digested using Kpn1 and ran in a 1% agarose gel.

3.4 Microbiology

3.4.1 Preparation of LB broth and LB agar plates

LB broth was prepared by dissolving 20 grams of Luria Bertani (LB) powder in one litre of distilled water which was then autoclaved at 15psi and 121°C for 15 minutes. After the solution was cooled down to room temperature, ampicillin (100µg/ml) or kanamycin (50µg/ml) was added under aseptic conditions.

LB agar plates were prepared by dissolving 20 grams of LB agar in one litre of distilled water which was then autoclaved at 15psi and 121°C. After the solution was cooled down to 50°C, under aseptic condition, ampicillin (100µg/ml) or kanamycin (50µg/ml) was added. Approximately 10ml of the mixture was poured in sterile 90cm petri dishes and stored at 4°C.

3.4.2 Preparation of competent bacteria and transformation

Transformation is the process by which the bacterial cells take up the naked DNA molecules. Since the bacterial genome is made up of circular DNAs and plasmids, the bacteria will replicate the foreign DNA along with their own DNA if the foreign plasmid DNA has an origin of replication recognized by the host cell DNA polymerases. In order for the bacteria to be able to uptake foreign DNA they should first be submitted to a process that transforms them to competent bacteria. To prepare competent bacteria, DH5α (non-competent bacteria) were grown in LB broth. The cells were collected by centrifuging at 5000 rpm for 10 minutes at 4°C and resuspended in 500ml of ice cold 100mM calcium chloride and incubated on ice for 30 minutes with occasional swirling. The cells were pelleted again by centrifuging at 5000rpm for 10 minutes at 4°C. The pellet was resuspended in 40ml of ice cold 100mM calcium chloride with 15% glycerol. The bacterial suspension was aliquoted into 600µl in sterile eppendorf tubes and kept in 4°C for 12 hours. The cells were frozen down rapidly in liquid nitrogen and immediately transferred to -80°C.

The bacterial cell membrane is permeable to chloride ions, but not to calcium ions. When the chloride ions enter the cell, it will be accompanied by water molecules which cause the cells to swell which facilitate the cells to uptake the DNA. The calcium

chloride treatment is followed by heat shock at 42°C for 45 seconds during which a set of genes aiding the bacteria to survive in high temperatures are expressed. These so called heat shock genes are believed to be involved in the uptake of foreign DNA by the bacteria.

Briefly, 200µl of chemically competent DH5α bacterial suspension was thawed on ice and approximately 100ng of plasmid DNA was added to it and mixed well. This mixture was kept on ice for 30 minutes and then heat shocked at 42°C for 45 seconds and placed on ice for 2 minutes. 500µl of SOC medium was added to bacterial mixture and incubated in a shaker at 37°C for 1 hour. 200µl of the resultant mixture was streaked on an LB agar plate containing the appropriate antibiotics. The plate was incubated at 37°C for 16 hours.

3.4.3 Preparation of plasmid DNA

3.4.3.1 Miniprep

A single colony from the LB agar plate was inoculated in 2ml of LB broth with appropriate antibiotic and allowed to grow overnight in a shaking incubator at 200 rpm and 37°C for 16 hours. The bacterial cell pellet was collected by centrifuging the cells at 6,000g for 15 minutes and resuspended in 100µl of ice cold resuspension buffer (containing 20µg/µl RNAse A) by vortexing. 200µl of miniprep lysis buffer was added and mixed well by inverting the tube rapidly five times (to ensure proper lysis of the cells) and kept on ice for 2 minutes. 150µl of ice cold precipitation buffer was added and vortexed gently for 10 seconds to disperse precipitation buffer through the viscous bacterial lysate. This mixture was incubated on ice for 5 minutes and centrifuged at 12,000g for 5 minutes at 4^0C and the supernatant was transferred to a fresh Eppendorf tube. 400µl of phenol:chloroform was added and mixed by vortexing. The mixture was centrifuged at 12,000g for 5 minutes at 4^0C and the supernatant was transferred to a fresh Eppendorf tube. The DNA dissolved in the aquatic phase was then precipitated with 800µl of absolute ethanol, and washed with 70% ethanol. The remaining ethanol was removed carefully and the precipitated double stranded DNA was dissolved in 50µl of TE buffer and stored at -20^0C for future use. In some occasions, the miniprep was carried out using Qiagen Miniprep Kit following the manufacturer's instructions.

3.4.3.2 Maxiprep

To isolate high quality plasmid DNA which was used for transfection of mammalian cells, PCR reactions and cloning, the PureLink HiPure Plasmid Filter Purification Kit (Invitrogen) was used. This kit contains columns which have an anion-exchange resin, which selectively binds plasmid DNA and enzymes that remove endotoxins. A single colony was picked up from a transformation plate and inoculated into a sterilised conical flask containing 150 ml of sterile LB broth supplemented with the appropriate antibiotic. Bacteria were incubated for 16 hours at 37°C with shaking (200 rpm), harvested by centrifugation for 10 min at 4,000g, resuspended, lysed, precipitated and the precipitated mixture was loaded on the HiPure Filter Columns that contain filtration cartridges. During this process, the negatively charged phosphates of the DNA backbone are bound to the positively-charged surface of the resin and while DNA is retained on the resin, RNA, proteins, carbohydrates and other impurities are washed with the wash buffer. The plasmid DNA was then eluted in high salt concentration by applying the elution buffer. The DNA was precipitated with isopropanol by centrifugation (12,000g, 30min, 4°C) and the DNA pellet was washed with 70% ethanol and resuspended in 250-400 µl of TE buffer.

3.5 Transfection Studies

3.5.1 Plasmids

The details of the plasmids used in this study are listed in Table 3.5.1

Sl No	Plasmid	Source
1	CA-IX-HRE Luc	(Wykoff et al., 2000)
2	CMV-p53	T Halazonetis, University of Geneva
3	CMV-β-Gal	(Zamanian and La Thangue, 1992)
4	Flag-PCAF	(Barbacci et al., 2004)
5	Flag-PCAFΔHAT	(Barbacci et al., 2004)
6	HA-HIF-1α	(Huang et al., 1998)
7	HA-HIF-1αK389R	(Xenaki et al., 2008)
8	HA-HIF-1αK532R	(Xenaki et al., 2008)
9	HA-p53K320R	T Halazonetis, University of Geneva
10	pcDNA3	Invitrogen
11	RNAi-HIF-1α	(Xenaki et al., 2008)
12	pcDNA3-SCO2	(Matoba et al., 2006)
13	SCO2-p53-HRE-Luc	Part of promoter region of *SCO2* gene

Sl No	Plasmid	Source
		cloned into pGL3 promoter vector
14	pcDNA3-Flag-TIGAR	(Bensaad et al., 2006)
15	TIGAR-p53-HRE5,6-Luc	Part of promoter region of *TIGAR* gene cloned into pGL3 promoter vector

Table 3.5.1: List of plasmids used in this study and their sources

3.5.2 Transfection methods

3.5.2.1 Calcium phosphate method

The principle of calcium phosphate transfection involves the slow mixing of HEPES buffered saline containing sodium phosphate with a calcium chloride solution containing the DNA. The resulting calcium-phosphate DNA complex adheres to the cell membrane and enters the cytoplasm possibly by endocytosis. Briefly, the cells were subcultured in 100mm culture plates at least 24 hours before transfection. A fresh media was added to the cells just before transfection. A total of 10µg of plasmids listed in Table 3.5.1 (also as described in the Figure legends), were diluted to 360µl with sterile distilled water. 120µl of 1M calcium chloride was added to the diluted DNA and vortexed for 15 secs. This mixture was incubated at room temperature for 10 minutes. 480µl of 2X HBS was added to the mixture and immediately vortexed for 15 seconds. The mixture was incubated in room temperature for 20 minutes (at the end of 20 minutes a faint precipitate formed by calcium phosphate was visible). The whole mixture was added drop wise to the cells with swirling. The cells were incubated in 37°C incubator for 16 hours and then washed twice with sterile PBS and changed to fresh media. The cells were harvested 36-48 hours after transfection.

3.5.2.2 Polyfect transfection method

For luciferase reporter assays, mRNA analysis and estimation of lactate production, oxygen consumption, NAD^+/NADH ratio and intra-cellular ROS levels the cells were transfected using Polyfect transfection reagent. A recommended amount of plasmid DNA was diluted in DMEM without serum and antibiotics as the presence of serum, proteins and antibiotics in this step would interfere with the complex formation and significantly reduce the transfection efficiency. A specified amount of Polyfect transfection reagent was added to the DNA solution and the mixture was vortexed for 10 seconds (Polyfect reagent possesses a specific spherical structure, with branches

radiating a central core and terminating at charged amino groups. Polyfect reagent assembles DNA into compact structures, facilitating the entry of DNA into the cells (Qiagen, 2000)). The mixture was then incubated at room temperature for 5-10 minutes to allow Polyfect-DNA complex formation. Meanwhile, the cells were washed once with PBS and the fresh media containing FBS and P/S was added. DMEM with FBS and P/S was added to the Polyfect-DNA complex and mixed well and the mixture was added to the cells with swirling to ensure the uniform distribution of the complexes (Polyfect-DNA complex possesses a net positive charge, which allows them to bind to negatively charged receptors on the surface of the eukaryotic cells. Inside the cells, Polyfect reagent buffers the lysosome after it has fused with the endosome, leading to the pH inhibition of lysosomal nuclease. This ensures the stability of Polyfect-DNA complexes and the transport of intact DNA into the nucleus (Qiagen, 2000)). The cells with the complexes were incubated at 37°C and 5% CO2 and harvested after 24 - 48 hours.

3.6 Luciferase assay

This assay is based on the principle that luciferase enzyme catalyzes the transformation of D-luciferin into oxyluciferin in an oxygen and ATP dependent process, leading to the emission of photons which can be detected at 500 to 620nm wavelength (Figure 3.6.1 A) (Baert, 2008). The luciferase reporter vectors have been designed to report the binding activity of an individual transcription factor. The pGL3 Luciferase Reporter Vectors provide a basis for the quantitative analysis of factors that potentially regulate mammalian gene expression. These factors may be cis-acting, such as promoters and enhancers, or trans-acting, such as various DNA-binding factors (Figure 3.6.1 B) (Baert, 2008).

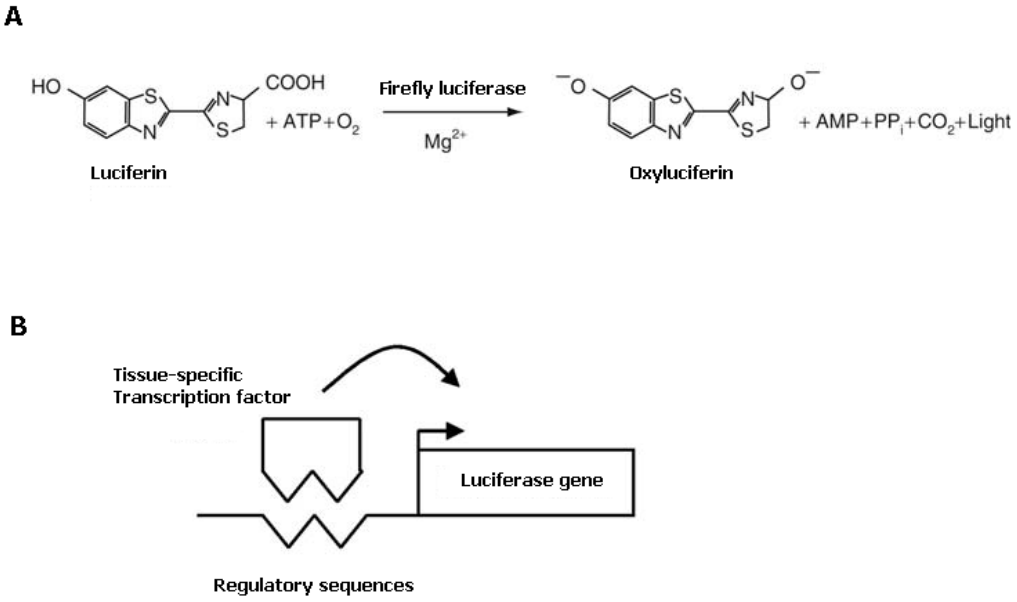

Figure 3.6.1: Principle of luciferase assay

A. In the presence of oxygen, ATP and Mg^{2+} ions luciferase enzyme converts luciferin into oxyluciferin and produces light. B. Transcription factors bind to regulatory sequences cloned directly adjacent to the luciferase gene, and the expression of luciferase which can be measured by the conversion of luciferin into oxyluciferin and light (Baert, 2008)..

The cells were grown in 6 well plates and transfected with PCDNA3 or PCAF or PCAFΔHAT using Polyfect transfection reagent. 24 hours after transfection the cells were left untreated or treated with DSFX for 16 hours. The cells were harvested using Reporter lysis buffer (Promega, UK) and centrifuged at 13,000 rpm for 15 minutes at 4°C. 10µl of this cleared lysate was added to 100µl of luciferin reagent (Promega, UK) and briefly vortexed and the luminescence produced was immediately measured in a luminometer at 560nm.

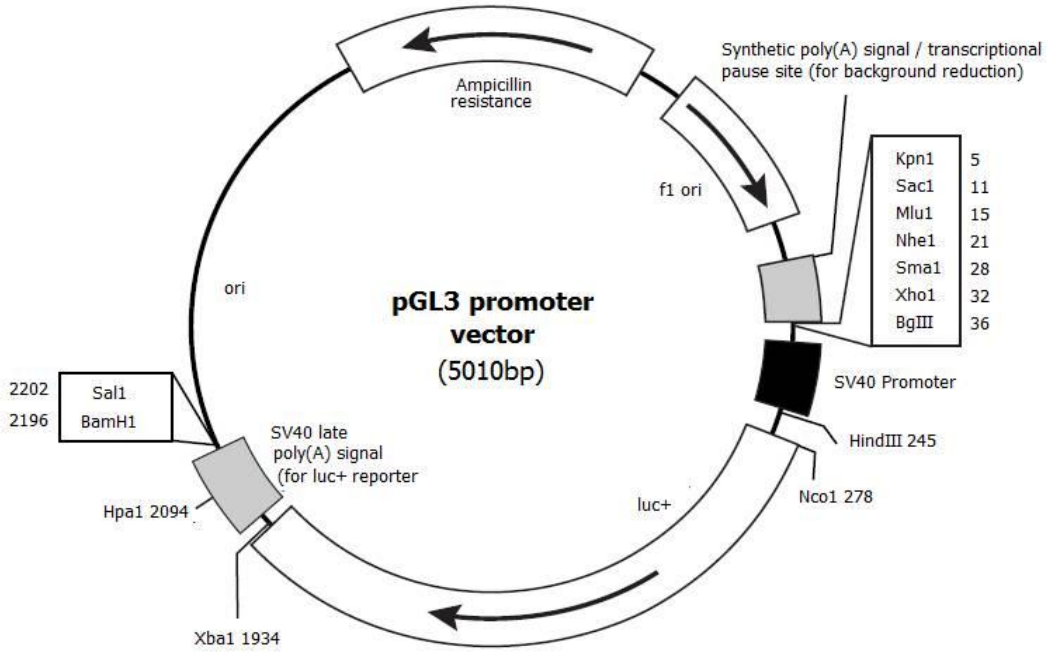

Figure 3.6.2: pGL3 promoter vector circle map (Promega, 2007)

Schematic diagram showing the vector map of pGL3 promoter vector.

3.6.1 β-galactosidase assay

β-galactosidase assay was performed to measure the transfection efficiency of the cells. β-galactosidase is an enzyme encoded by the *lacZ* gene of the *lac* operon in *E.Coli*. β-galactosidase cleaves lactose to glucose and galactose. The synthetic compound o-nitrophenyl-β-D-galactoside (ONPG) is also recognized as a substrate and cleaved to yield galactose and o-nitrophenol which has a yellow colour whose absorbance can be measured at 420nm. The conversion of ONPG to o-nitrophenol is proportional to the concentration of β-galactosidase enzyme.

The cells were grown in 6 well plates and transfected with PCDNA3 or PCAF or PCAFΔHAT using Polyfect transfection reagent. 24 hours after transfection the cells were left untreated or treated with DSFX for 16 hours. The cells were harvested using Reporter lysis buffer (Promega, UK) and centrifuged at 13,000 rpm for 15 minutes at 4°C. 30µl of this supernatant was added to 300µl of β-gal buffer (Table 3.1.4) and incubated at 37°C for 1 hour. 500µl of distilled water was added to the mixture and the absorbance was measured at 420nm.

3.7 Immunoblotting

3.7.1 Preparation of whole cell extract

For western blotting, the cells were seeded at 60 - 70% confluency in 100mm culture plates and were incubated overnight in 37°C incubator. Wherever necessary the cells were transfected with calcium phosphate method or with Polyfect transfection reagent. Fresh media was added to the cells after 16 hours of transfection and the cells were treated with appropriate chemicals for the periods mentioned in each experiment. Then the media was removed and the cells were washed twice with 1X cold PBS. 250µl of 240 mM TNN buffer (Table 3.1.4) (with freshly added protease and phosphatase inhibitors) was added to the cells and the cells were scraped in the cold room using a rubber policeman.

The extracts were collected in 1.5ml centrifuge tubes and rotated for 20 minutes at 4^0C followed by centrifugation at 4^0C for 30 minutes at 13,000rpm. The pellets were discarded and the supernatants were carefully transferred to a fresh centrifuge tube kept on ice.

3.7.2 Determination of protein concentration

The concentration of proteins present in the whole cell extract was measured using Bio-Rad Protein Assay reagent. This assay is based on the Bradford method for protein quantification (Bradford, 1976). The Bradford's assay relies on a colour change of the dye Coomassie Brilliant Blue G-250 after binding to different concentrations of protein. The Coomassie Blue dye readily binds to arginyl and lysyl residues of the protein. In acidic conditions, binding of the dye to the protein results in shifting of the maximum absorbance of the dye from 465 nm to 595 nm. The concentration of the protein is then determined by measuring the absorbance at 595 nm.

The Bio-Rad working solution was prepared by 1 part of the dye with 4 parts of distilled and de-ionized water in a 1.6 ml, 1 cm path visible cuvette. 2µl of distilled and de-ionised water was used to calibrate the spectrophotometer that was set at 595 nm and was used as blank. To normalise the protein concentrations of samples used for Western Blotting or co-immunoprecipitation, 2µl of sample was added to the diluted dye, mixed

well and incubated for five minutes at room temperature before the absorbance of the resultant solution was measured. After determining the protein concentration equal amount of proteins were mixed with 3X SDS sample buffer (Table 1.1.4) and subjected to SDS PAGE.

3.7.3 SDS-PAGE

Electrophoresis is a process in which the macromolecules are separated in an electric field. A common method for separating proteins by electrophoresis uses a poly acrylamide gel as a supporting medium and SDS to denature the proteins. This method is called SDS-poly acrylamide gel electrophoresis (SDS-PAGE).

Polypeptides are amphoteric and their net charge is determined by the pH of the suspension they are in. SDS is an anionic detergent and in solution form it possesses negative charge in a wide pH range. When added to the proteins, the amount of SDS binds with the polypeptide chain is directly proportional to the molecular mass of the polypeptide. The SDS denatures the proteins by wrapping around the polypeptide backbone and binds to proteins fairly specifically in a mass ratio of 1.4:1 thus conferring negative charge to the polypeptide in proportion to its length which leads them to move towards the positively charged electrode in an electric field.

Poly acrylamide gels have pores which allow the smaller molecules to move faster and restrain the larger molecules from moving as fast as the smaller molecules. In an electric field, when the charge to mass ratio is nearly the same among SDS denatured polypeptides, the movement of the proteins are almost entirely dependent on the molecular mass of the polypeptides. To ensure that the proteins are fully denatured and attain a random-coil configuration which is necessary for separation by size, a disulphide reducing agent, 2-mercapto ethanol is used.

SDS-PAGE was performed using 7.5% and 10% gels according to the size of the proteins of interest. The compositions of the gels are listed in Table 3.7.1.

Solutions	**7.5%**		**10%**	
	Resolving	**Stacking**	**Resolving**	**Stacking**
Distilled water	13.3 ml	6.73 ml	10.94 ml	6.73 ml
Acrylamide	7 ml	1.67 ml	9.33 ml	1.67 ml
1.5M Tris pH 8.95	7 ml	-	7 ml	-
1M Tris pH 6.95	-	1.25 ml	-	1.25 ml
0.2M EDTA	280µl	100µl	280µl	100µl
10% SDS	280µl	100µl	280µl	100µl
10% APS	157µl	100µl	157µl	100µl
TEMED	17µl	10µl	17µl	10µl

Table 3.7.1: Composition of poly acrylamide gels

The gel casting apparatus (Mini-PROTEAN 3 - Bio-Rad, UK) was set-up according to the manufacturer's guidelines. The components mentioned in Table 3.7.1 were mixed together and TEMED and APS were added at the end before pouring the mixture between the plates. Once the resolving gel was poured into the gel casting apparatus, 500 µl of isopropanol was added on top of it to ensure that the gel was evenly flat on top and to remove any air bubbles. Once the resolving gel was set isopropanol was removed and the stacking gel was poured and 1.5 mm wide well combs were inserted into the stacking gel solution. The stacking gel was used to get the optimal resolution of the proteins. It has lower percentage of acrylamide and pH compared to the resolving gel, which allows the proteins to be stacked before they enter the resolving gel. After the stacking gel was set, the gels were fitted into the electrophoresis mini buffer tank (Bio-Rad) and the tank was filled with SDS-PAGE running buffer (Table 3.1.4) and the combs were removed.

The protein samples were boiled at 95ºC for 5 minutes, centrifuged at 13,000 rpm for 1 minute and loaded into the wells using gel loading tips (Star Labs, UK). 5µl of PageRuler Prestained protein ladder (Fermentas, UK) was loaded in every gel and the samples were run at 80V until they enter the resolving gel and then at 110V.

3.7.4 Western transfer and detection of proteins

The proteins resolved on the gels were transferred to a polyvinylidene fluoride PVDF membrane (Millipore, UK) using western transfer method. Electroblotting is a commonly used method that uses an electric current and a transfer buffer solution to transfer proteins from the gel onto the membrane. Western transfer apparatus (Bio-Rad, UK) was set-up according to manufacturer's guidelines and filled with western transfer buffer (Table 3.1.4). The transfer was carried out in 0.4amps for 90 minutes with the ice pack changed at 45 minutes. After the proteins were transferred, the PVDF membranes were blocked in 5% dried milk powder in PBS for 1 hour. The membrane was then incubated with specific primary antibody (Table 3.1.3) in 2.5% milk/PBS/0.1% Tween solution on a rocking platform overnight at 4ºC.

Membranes were washed 3 times with PBS/0.1% Tween for 10 minutes and incubated for 1 hour with relevant anti-rabbit or anti-mouse IgG horseradish peroxidise conjugated secondary antibody (Table 3.1.3) in 2.5% milk/PBS/0.1% tween. The membranes were washed 3 times with PBS/0.1% Tween for 10 minutes. 500µl of One Step ECL (Chembio, UK) was sprayed on each membrane and the proteins were visualised on medical X-ray films (Fujifilm, UK) developed using the Compact X4, Xograph imaging system according to the manufacturer's guidelines.

3.7.5 Densitometric analysis

To quantify blots, densitometric scanning was performed using the Image J 1.38e software. Three readings of each band were recorded and then each band was normalised to its correspondent Actin band intensity. The average of the three readings were calculated, and presented as chart bars. The final average and standard deviation readings were measured by taking the values of three sets of independent experiments.

3.7.6 Stripping the membrane

After detecting the first protein, the membranes were subjected to antibody striping, wherever necessary, to detect the second protein whose molecular weight is close to the first protein. To remove the antibody, the membranes were incubated in stripping buffer (Table 3.1.4) for 30 minutes at 55ºC and washed three times in 10ml of PBS with 0.1% tween-20 for 10 minutes. After stripping the membranes were blocked with the desired primary antibody.

3.8 Measurement of mRNA level

3.8.1 RNA isolation

The total RNA was extracted using RNeasy plus mini kit (Qiagen, UK). This kit is specially designed to extract all RNA molecules which are longer than 200 nucleotides. The procedure offers enrichment for mRNA as most RNAs less than 200 nucleotides such as rRNA and tRNA are selectively excluded. Briefly, the cells were lysed and homogenised in a highly denaturing guanidine-isothiocyanate containing buffer which immediately inactivates RNase to ensure the isolation of intact RNA. Since numerous disulfide bonds make ribonucleases very stable enzymes 2-mercaptoethanol was added to the lysis buffer to reduce these disulfide bonds and denature the enzymes. A high salt buffer along with a spin column eliminates the gDNA from the sample. The binding capacity of RNA is improved by the addition of ethanol. Then the solution was passed through a specially designed column which retains only the RNA and the retained RNA is then eluted in distilled water.

U2OS and SaOS2 cells were grown in 6 well plates, transfected and treated as described in the figure legends. The cells were lysed using RLT plus buffer containing 1% β mercaptoethanol. The lysates were homogenised using Qia-shredder spin column and centrifugation. The gDNA eliminator was used to remove the genomic DNA and one volume of 70% ethanol was added to the flow through. RNA was recovered from the solution with the RNeasy column, which was washed once with RW1 buffer and once with the RPE buffer. The RNA captured on the column was eluted with 30µl of RNase-free water and its concentration was determined using NanoDrop ND-1000 UV-Vis spectrophotometer.

3.8.2 Reverse transcription

The cDNA was generated from the isolated RNA by a process called reverse transcription. In eukaryotic mRNA, poly-A tail is present at the 3' ends, therefore a poly-T oligonucleotide (anchored oligo) is used as a primer to anneal to the 3' end of the mRNA. This primer is then extended with the reverse transcriptase using mRNA strand as a template.

500ng of anchored oligo dT was added to 1µg of the isolated total RNA (section 3.8.1) and the total volume of the mixture was made up to 12µl using RNase free water. This mixture was incubated at 70°C for 5 minutes to remove any secondary structure and then chilled on ice. dNTPs and reverse transcriptase enzyme were added along with the reaction buffer to this mixture. This mixture was incubated at 37°C for 1 hour and heated at 75°C for 10 minutes to stop the reaction. The cDNA synthesised in this process was used in qRT-PCR to measure gene expression using specific primers that amplify the genes of interest.

3.8.3 Quantitative Real Time PCR (qRT-PCR)

cDNA levels corresponding to mRNA content of specific genes were determined by quantitative real-time PCR. qRT-PCR is a method that allows continuous data logging with plate read-outs at each DNA amplification cycle throughout the assay. RT-PCR was first described by Higuchi and colleagues (Higuchi et al., 1992) and was developed to quantify the levels of amplified DNA which represent the transcribed RNA. The SYBR Green I double-stranded binding dye (Sigma, UK) intercalates only to double stranded PCR products, so that the fluorescence signal is proportional to the number of amplified copies. SYBR Green I has an excitation and emission maxima of 494 nm and 521 nm, respectively. It binds to all double stranded DNA so there is no need for adaptation to individual samples and it is a very sensitive method as multiple molecules of the dye bind to a single amplification product. Primers listed in Table 3.8.1 were used to amplify cDNA and the cycling parameters are described in Table 3.3.3. A melting curve is calculated from 72°C to 95°C with 1°C increase in every 30 secs.

Gene	Orientation	Primer sequence	Product size
TIGAR	Forward	5'- ATGGAATTTTGGAGAGAA-3'	84
	Reverse	5'-CCATGGCCCTCAGCTCAC-3'	
SCO2	Forward	5'-TCACTCACTGCCCTGACATC-3'	149
	Reverse	5'-CGGTCAGACCCAACAGTCTT-3'	
Rpl19	Forward	5'-ATGTATCACAGCCTGTACCTG-3'	122
	Reverse	5'-TTCTTGGTCTCTTCCTCCTTG-3'	

Table 3.8.1: qPCR primer sequences

The components used for qRT-PCR reactions are listed in table 2.6.

Component	Amount per reaction
Nuclease free water	11.93µl
10X Thermopol buffer (NEB, UK)	2µl
$MgCl_2$ 50mM	0.4µl
dNTPs (10mM)	0.6µl
SYBR Green I (1X)	0.75µl
Forward primer (100µM)	0.06µl
Reverse primer	0.06µl
Taq polymerase (NEB, UK)	0.2µl
cDNA template	4µl
Total reaction volume	**20µl**

Table 3.8.2: Components of qPCR reaction

Opticon Monitor 2 System (MJ Research) was used for qRT-PCR assay. Data was analysed with Opticon Monitor Analysis Software, version 2.02. The principle of qPCR analysis is demonstrated in Figure 3.8.1

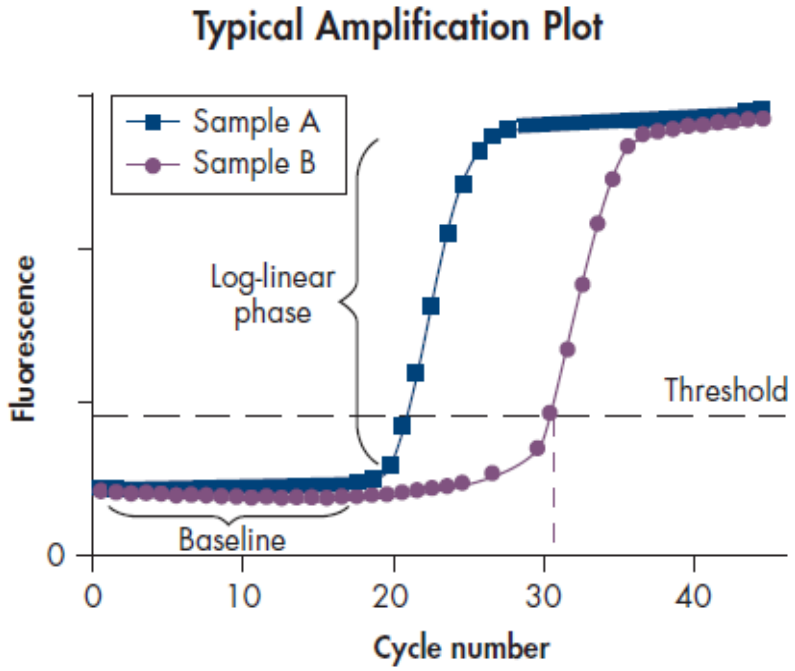

Figure 3.8.1: Principle involved in qPCR assay

The threshold cycle (Ct value) determines the cycle at which there is a significant increase in fluorescence. On the contrary, the baseline area represents the noise level in early cycles and therefore at this stage there is no significant fluorescence. The log- linear phase is the linear portion of the amplification plot that represents the exponential phase of amplification. The intensity of the intercalated SYBR green fluorescence is measured at the end of every cycle and this determines the copy number of the amplified DNA. In this case, sample A reaches the Ct value at 21 cycles, whereas sample B at 31 cycles. Figure adapted from (Qiagen, 2006).

3.9 Chromatin immuno-precipitation (ChIP) assay

DNA-protein interactions mediate critical nuclear and cellular functions. Chromatin immunoprecipitation is a powerful tool for studying protein/DNA interactions hence very useful to study the transcription factors that are bound to specific DNA regions. In this method the cells are fixed with formaldehyde which facilitates the formation of covalent bond between DNA and specific protein located on it and preserves the protein/DNA interactions. The DNA is then sheared to small fragments and the specific protein/DNA complex is pulled down using an antibody directed against the DNA binding protein of interest. Following pull down, the cross link between DNA and protein is reversed, and the DNA is recovered. The DNA is then analysed to determine which fragments of the DNA were bound by the protein of interest (Motif, 2009). A schematic diagram of the ChIP protocol is shown Figure 3.9.1.

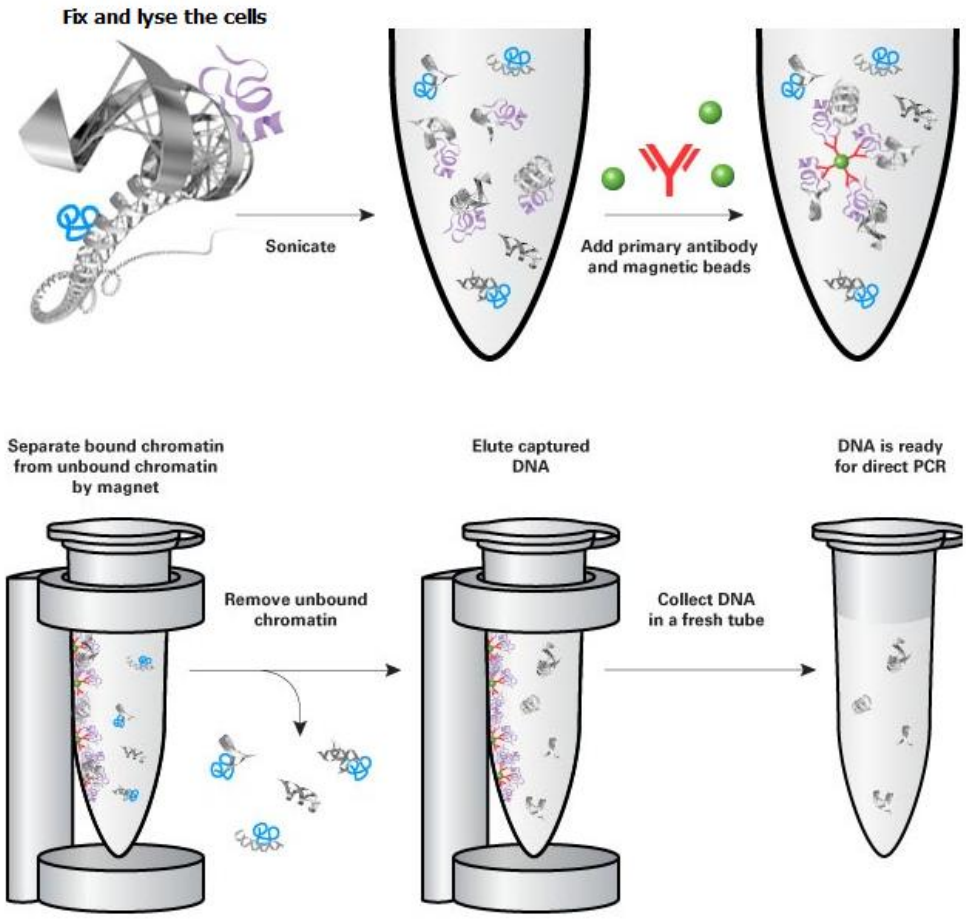

Figure 3.9.1: Principle of Chromatin immunoprecipitation (ChIP).

DNA and binding proteins are cross-linked and the chromatin-DNA complex is immuno-precipitated using a primary antibody specific for the protein of interest, and magnetic beads for easy separation. The protein-DNA cross-links are then reversed, to release DNA fragments that are ready for direct PCR. Figure adapted from Clontech website.

Approximately 10 million cells were grown for each treatment point. The cells were left untreated or treated with 250µM DSFX for 16 hours. The chromatin was cross-linked to DNA by the addition of 1ml of formaldehyde solution Table 3.1.4. After incubating at room temperature for 10 minutes, the effect of formaldehyde was quenched by incubating the cells with 125mM final concentration of glycine for 5 minutes at room temperature. The cells were washed twice with 10mls of ice-cold PBS and harvested with 2mls of ice cold ChIP buffer 1 containing 100µM PMSF and 1X protease inhibitor cocktail (PIC). The cell pellet was obtained by centrifuging at 4,700 rpm for 5 minutes at 4°C. The supernatant was discarded and the cell pellet was washed once with 10ml of ChIP buffer 2 which was supplemented with 100µM PMSF, 1X protease inhibitor

complex. After centrifugation at 4700 rpm for 5 minutes the cells were resuspended in 3ml of ChIP buffer 3. The cell suspension was aliquoted as 500µls into fresh eppendorf tubes, and subjected to sonication in Bio-ruptor UCD 200, set 30 seconds ON/OFF pulse for 5 minutes. This setup will produce 0.5kb to 1kb size of DNA fragments (Figure 3.9.2). The sonicated lysate was cleared by centrifugation at 11,400 rpm for 10 minutes at 4°C and the supernatant was transferred to fresh sterile eppendorf tubes. 100µl of this whole cell lysate was taken for input and 1ml of lysate was used for immuno-precipitation.

Meanwhile, 100µl of magnetic beads were washed three times in 1ml of blocking solution and resuspended in 250µl of blocking solution. 2µg of mouse IgG or anti-HIF-1α antibody was added and rotated in the cold room for 16 hours. The magnetic beads were washed three times in 1ml blocking solution and resuspended in 100µl of blocking solution 1 ml of whole cell extract was added to the beads and rotated overnight in the cold room.

The magnetic beads were collected and washed 5 times in 1ml of RIPA buffer (Table 3.1.4) and once in 1ml of Tris buffered saline (TBS). The residual TBS was removed after brief centrifugation and the beads were resuspended in 200µl of elution buffer (Table 3.1.4) and incubated at 65°C for 16 hours. 200µl of the supernatant was transferred to new tubes. 200µl of TE buffer was added to IP and input samples along with 8µl of 1mg/ml of RNase A and incubated at 37°C for 30 minutes. 4µl of 20mg/ml of Proteinase K was added and the mixture was incubated at 55°C for 2 hours. 400µl of phenol-chloroform-isoamyl alcohol (25:24:1) was added and vortexed. The aqueous phase was separated after centrifugation at 13,000 rpm for 5 minutes at 4°C and transferred to fresh tube. 16µl of 5M NaCl (200mM final concentration) and 1µl of 20mg/ml of glycogen was added to the mixture along with 800µl of 100% ethanol and incubated at -80°C for 30 minutes. The DNA pellet was collected after centrifugation at 13,000rpm for 30 minutes at 4°C. The pellets were washed with 500µl of 70% ethanol and air dried for 10 minutes at 45°C and finally resuspended in 50µl of distilled water and isolated DNA fragments were submitted to PCR using the TIGAR and SCO2 primers flanking the HREs within their promoter regions (Table 3.9.1 and Table 3.9.2).

The equal shearing of DNA is necessary for all samples as it affects the immunoprecipitation efficiency. The shearing efficiency was checked by 2% agarose gel electrophoresis of 10µl of the input samples (Figure 3.9.2)

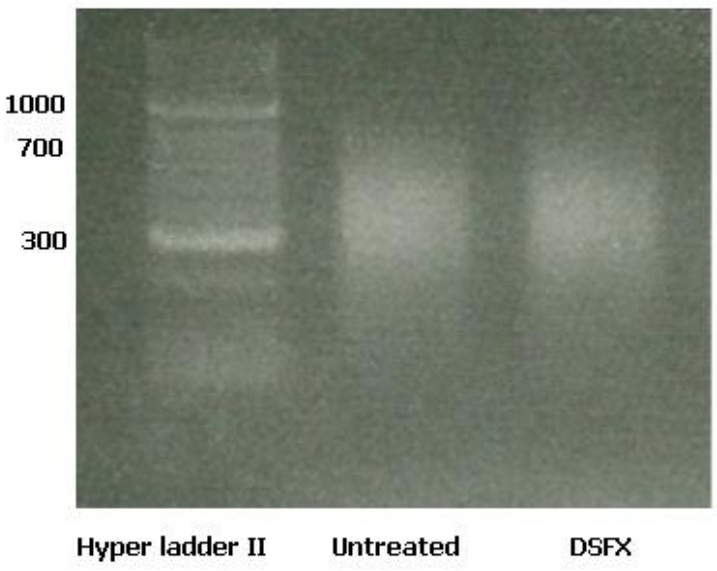

Figure 3.9.2: Equal shearing of DNA in all samples.

The untreated and DSFX treated samples were sheared equally to produce DNA fragment sized between 200 and 700 base pairs.

The sequences of the primers used to enrich the region of TIGAR and SCO2 promoters which contain HREs are listed in Table 3.9.1 and Table 3.9.2

TIGAR	Forward	Reverse
HRE 1	GTGTTGGAATCTCGGCTCAC	CAAGGCAGGTCAGGAGAATC
HRE 2	CCGTGTTAGCCAAAATGGTC	CACATTTGGCCTTCTGAACA
HRE 3 and E2F1	CTATAGAAGGGTGCGTCCTT	TGACTCCTTCCCATTACCTA
HRE 4	ACACGGTGAAACCCTGTCTC	AGTGCAGTGGTGTGATCTCG
HRE 5	CACAGTCTGTTGGTCGCTG	GATTCCTTCCCTCGATAGCC
HRE 6	AGGAATCCTACCGCGGACT	CTACCTCCCCCACACCACT

Table 3.9.1: Sequences of the TIGAR primers used in ChIP assay.

SCO2	Forward	Reverse
HRE 1	TGGTGCTGCACGAGCTCGG	CTCACCACGGCGCAGCCTC
HRE 2	CTCTGCAGGGACCCCCTGGC	GCGGTCGGAGAGTACGAGCG
HRE 3	CAGGAGGCGCTCGTACTCT	GACAGGCTCTCAGCGCGTGC
HRE 4	CATGCGCAGCTCCGGGGAC	ACGAGAGGAAGCGCCGACCT
HRE 5 and p53	GCCAGAGAGTTACCCACCTCC TTTTAA	CTGTCACCGCACCCTGCCC
HRE 6	GTGTGGTTGCCCAGGTGTGGA	GGCTGCCCCTGCGACTTGAG

Table 3.9.2: Sequences of the SCO2 primers used in ChIP assay.

3.10 Glycolysis OXPHOS and ROS generation analysis

3.10.1 Lactate measurement

Lactic acid is a by-product of carbohydrate metabolism under hypoxic conditions. Lactic acid is converted to pyruvate and hydrogen peroxide (H_2O_2) by lactate oxidase. In the presence of the H_2O_2 formed, peroxidase catalyzes the oxidative condensation of chromogen precursors present in lactate reagent (Trinity Biotech, Ireland) to produce a coloured dye with an absorption maximum at 540 nm. The increase in absorbance at 540 nm is directly proportional to the lactate concentration in the sample.

U2OS and SaOS2 cells were seeded at 60-70% confluency in 6 well plates and transfected with appropriate plasmids using Polyfect transfection reagent. Fresh media without phenol red pH indicator (Sigma, UK) was added to the cells after 16 hours of transfection and the cells were treated with 250µM DSFX for 16 hours. 300µl of the media was collected in a 96 well plate before and 16 hours after treating with DSFX. 2µl of this media was mixed with 200µl of lactate reagent and incubated at room temperature for 5 to 10 minutes and the absorbance was recorded at 540nm. Lactic acid standard solutions (Trinity Biotech, Ireland) were used to plot the standard curve and the concentration of lactic acid present in the media was calculated accordingly.

3.10.2 NAD^+/NADH measurement

The NAD^+/NADH ratio is an indication of the metabolic and redox state of a cell. The NAD^+/NADH measurement assay utilizes a cycling mixture composed of MTT (3- (4, 5-Dimethylthiazol-2-yl)-2, 5-diphenyltetrazolium bromide), phenazine ethosulfate (PES), ethanol and alcohol dehydrogenase. When NAD^+ is added to a suitably buffered mixture of PES, MTT, alcohol dehydrogenase and its substrate ethanol an enzymatic cycling is initiated (Nisselbaum and Green, 1969). The rate of reduction of MTT (from a yellow tetrazole to purple formazan) is proportional to the concentration of the co-enzyme NAD^+. Since NAD^+ is not thermo stable the NAD^+ and NADH amounts were determined from the heated and unheated samples. NADt (NAD and NADH) or NADH can be quantified by comparison with the amount of standard NADH.

U2OS and SaOS2 cells were seeded at 60-70% confluency in 100mm plates and transfected with appropriate plasmids using Polyfect transfection reagent and treated with 250µM DSFX for 16 hours. The cells were washed twice with PBS and 1 ml of extraction buffer (Table 3.1.4) was added. The plates were swirled until the cells were lysed and the jelly like lysate was transferred to 15ml universal tubes and sonicated briefly on ice. 200µl of these lysates was transferred to fresh eppendorf tubes and incubated at 60ºC for 30 minutes. 5µl of both the heated and unheated samples were mixed with 83µl cycling buffer (Table 3.1.4) 1µl of 200mM phenazine ethosulfate (PES) and 1µl of 20mg/ml alcohol dehydrogenase enzyme. This mixture was incubated at 25ºC for 5 minutes. 20µl of 6M ethanol was added and the absorbance was measured at 570nm for 2 minutes (7 cycling points). The standard curves for NAD^+ and NADH were plotted using the NAD^+ and NADH standards (Sigma, UK).

3.10.3 Measurement of oxygen consumption

The amount of oxygen consumed by U2OS and SaOS2 cells under normoxic and hypoxic conditions were measured using the Clark-type polarographic electrodes. A Clark type oxygen electrode consists of a platinum electrode (cathode) and a silver electrode (anode). To maintain the chamber temperature stable at 37°C, there is an additional surrounding chamber filled with water and connected with a water circulation system. The electrode is located at the bottom of the chamber. The platinum cathode is

located on top of a dome-like centre which is surrounded by the silver anode. These two electrodes are connected with each other by a thin layer of 50% saturated KCl electrolyte. The dome is covered by an oxygen permeable Teflon membrane which is attached by an O-ring that surrounds the electrodes. When current is given to the electrodes, the platinum electrode is negatively charged while the silver electrode is positively charged. Oxygen diffuses through the Teflon membrane to the platinum electrode and is reduced there while the silver electrode is oxidised and accumulates silver chloride. The oxygen monitor holds a constant voltage difference across the two electrodes so that the platinum electrode is negatively charged with respect to the silver electrode. The current which is produced by the electrode is proportional to the oxygen tension in the solution. The Clark-type electrode is diagrammatically presented in Figure 3.10.1. The chemical reaction that occurs at the electrodes is shown below (Heimburg et al., 2005)

At the anode (positive electrode)

$$4Ag + 4Cl^- \longleftrightarrow 4AgCl + 4e^-$$

At the cathode (Negative electrode)

$$4H^+ + 4e^- + O_2 \longleftrightarrow 2H_2O$$

Overall

$$4Ag + 4Cl^- + 4H^+ + O2 \longleftrightarrow 4AgCl + 2H_2O$$

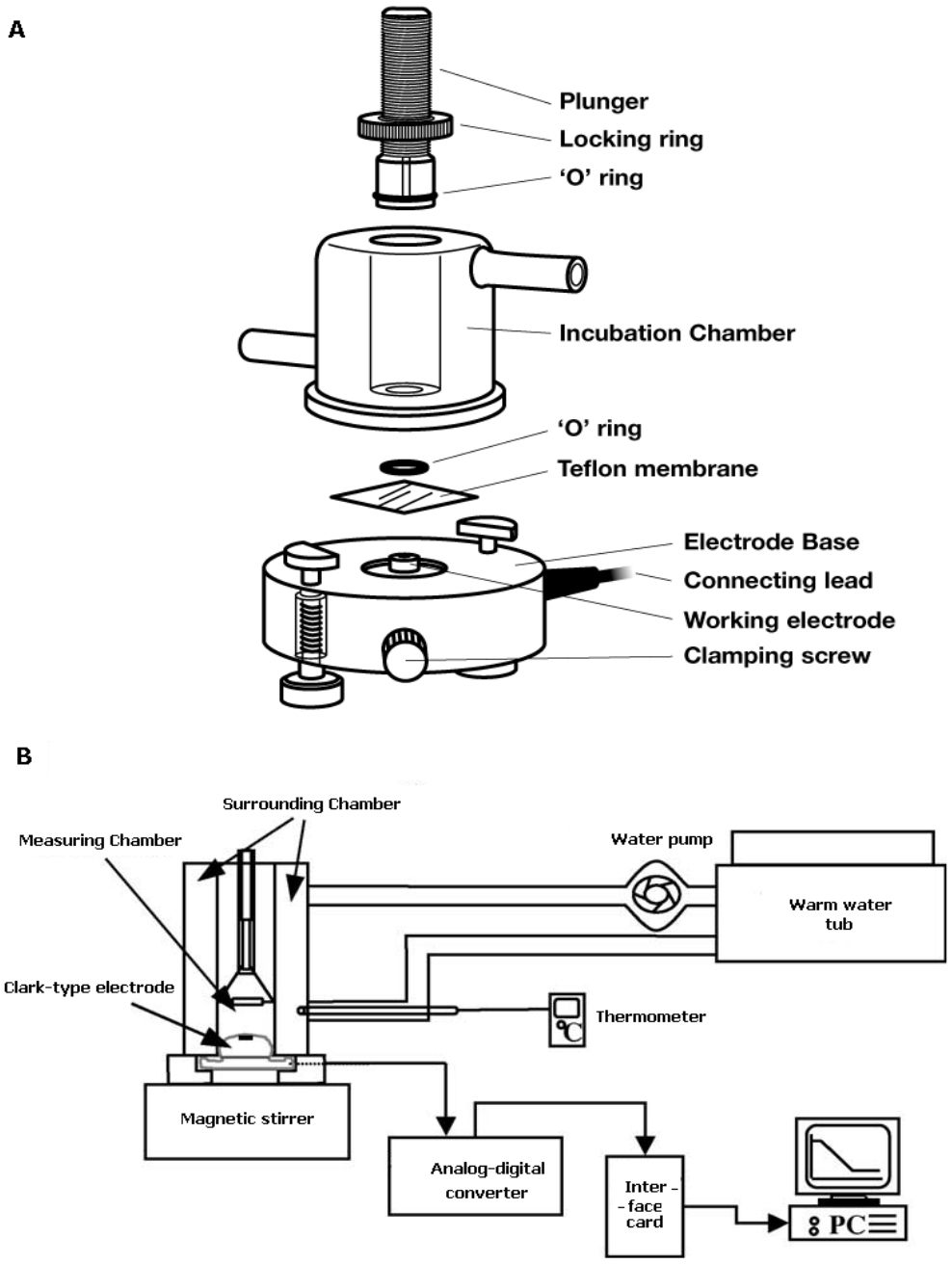

Figure 3.10.1: Clark type electrode system.

A. Schematic diagram of Clark-type electrode system. **B.** The electrode is located at the bottom of the chamber. The platinum cathode is located on top of a dome-like centre which is surrounded by the silver anode. These two electrodes are connected with each other by a thin layer of 50% saturated KCl electrolyte. The dome is covered by an oxygen permeable Teflon membrane. When current is given to the electrodes, the platinum electrode is negatively charged while the silver electrode is positively charged. Oxygen diffuses through the Teflon membrane to the platinum electrode and is reduced there while the silver electrode is oxidised and accumulates silver chloride. The current which is produced by the electrode is proportional to the oxygen tension in the solution. The figure is adapted from Rank Brothers company website.

U2OS and SaOS2 cells were grown in 100mm plates and transfected with PCDNA3, or PCAF, or PCAFΔHAT along with PCDNA3 or SCO2 expression vector and left untreated or treated with DSFX for 16 hours. The Clark-type electrode system was set up and calibrated using 1ml of air saturated PBS and sodium dithionite which completely reduced the oxygen in the measuring solution. The cells were counted after collection and 2 million cells were loaded into the measuring chamber. A magnetic stirrer was positioned at the bottom of the measuring chamber. Using a 1ml pipette, the cell suspension was saturated with air and the chamber was closed using a plastic nob. The amount of oxygen consumed by the cells was calculated from the measurable units displayed in the computer monitor.

3.10.4 ROS measurement

The mixed isomers of 5-(and-6)-chloromethyl-2',7' dichlorodihydrofluorescein diacetate (H_2-DCFDA) are probes for intracellular oxidants (Macey, 2007).

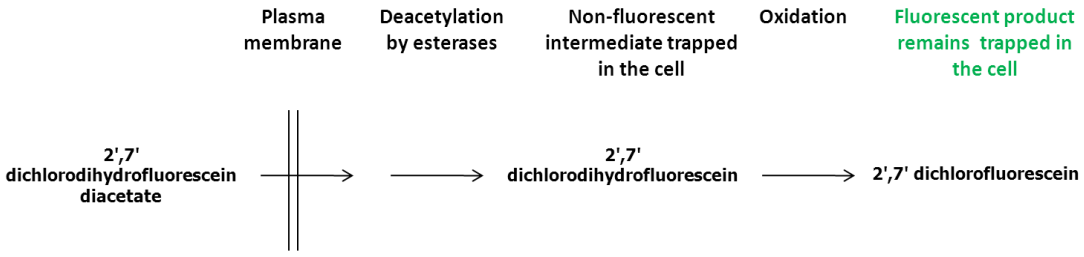

Figure 3.10.2: Principle of ROS measurement by H2-DCFDA (Macey, 2007)

The uptake and conversion of 2',7' dichlorodihydrofluorescein diacetate (He-DCFDA) to the fluorescent product 2',7' dichlorofluorescein (DCF) this is retained within the cell.

H_2-DCFDA is a cell permeant non-fluorescent precursor that on oxidation is converted to a cell impermeable fluorescent form (Chen et al., 2010). Esterases first convert H2DCFH-DA to a non-fluorescent intermediate, 2',7'-dichlorofluorescin (DCFH), that is retained in the cell. Then during the respiratory burst, the intermediate is further converted by H_2O_2 and superoxide (O^-2) together with peroxidase action to fluorescent 2',7'-dichlorofluorescein (DCF), which is also well retained in cells (Figure 3.10.2).

U2OS and SaOS2 cells were transfected with appropriate plasmids and left untreated or treated with DSFX for 16 hours. The cells were collected in a 15 ml universal tube using dissociation buffer (Invitrogen, UK) washed twice with sterile PBS and resuspended in 10ml DMEM media with FBS and penicillin /streptomycin and incubated in 37°C incubator with 5% CO_2 for 30 minutes. 100µM final concentration of H_2-DCFDA was added to the cells and incubated in 37°C with 5% CO2 for 30 minutes. The cells were washed twice in PBS and resuspended in 500µl of PBS and subjected to FACS analysis. The excitation and emission of the H_2-DCFDA fluorescence was measured at 488nm and 530 nm respectively.

4 Results

4.1 HIF-1α regulates TIGAR gene expression

Given that cellular energy metabolism plays important role in tumour growth and survival both oncogenes and tumour suppressors antagonistically regulate the pathways involved in energy production such as glycolysis and oxidative phosphorylation (OXPHOS) to exert their pro- survival and pro-apoptotic functions on tumour cells. Increase in glycolysis has been shown to be beneficial for the proliferation and survival of the tumour cells (Gatenby and Gillies, 2004). Among the transcription factors that regulate cellular energy metabolism, the tumour suppressor p53 inhibits glycolysis and facilitates OXPHOS by transcriptionally regulating *TIGAR* and *SCO2* gene expression, which have prominent roles in glycolysis and OXPHOS respectively (Bensaad et al., 2006; Matoba et al., 2006). Apart from p53, other transcription factors have also been reported to exert important functions in the regulation of cellular energy metabolism. In particular, the HIF-1α transcription factor increases glycolysis in tumour cells by inducing several of its target genes encoding enzymes involved in glycolysis including HK2, PFK-1 and PFKFB (Sakakibara et al., 1997). In addition, HIF-1α inhibits mitochondrial respiration by upregulating the gene expression of the enzyme PDK1 which inactivates the enzyme PDH which is involved in the oxidative decarboxylation of pyruvate (the end product of glycolysis) to produce acetyl-coA (an essential component of TCA cycle) (Kim et al., 2006; Papandreou et al., 2006).

Regulation of the F2,6-BP level is of critical importance for the glycolytic pathway to proceed further, owing to the fact that F2,6-BP is an allosteric activator of the glycolytic rate limiting enzyme PFK-1. The F2,6-BP levels are regulated by the bifunctional PFKFB enzyme, whose amino terminal kinase domain increases whereas the carboxy terminal bisphosphatase domain decreases the F2,6-BP intracellular levels. Phosphorylation of the serine 32 residue (Ser^{32}) in the amino terminal domain of PFKFB1 (an isozyme of PFKFB found in liver) by cAMP-dependent kinase (PKA) has been shown to inhibit the kinase activity of the enzyme thereby decreasing the ratio of the kinase to phosphatase activity of this enzyme (El-Maghrabi and Pilkis, 1984). In

contrast, PFKFB3 (another isozyme of PFKFB overexpressed in many tumour cell lines) lacks the critical serine residue corresponding to Ser^{32} in PFKFB1 (Sakakibara et al., 1997). As a consequence, the kinase activity of this PFKFB isozyme is constitutively high thus explaining the high ratio of kinase to phosphatase activity (700 to 1) in the tumour cells bearing high levels of PFKFB3 (Sakakibara et al., 1997). Interestingly, PFKFB3 has been shown to be upregulated in hypoxic cells in an HIF-1α dependent manner (Obach et al., 2004)

TIGAR protein on the other hand, encoded by *TIGAR* gene, has been shown to bear structural and functional similarities with the bisphosphatase domain of PFKFB enzyme, hence lowering the F2,6-BP level and as a consequence inhibiting the glycolytic flux (Bensaad et al., 2006). TIGAR exhibits significantly high basal protein levels in many tumour cell lines including U2OS and MCF-7 which increase further upon DNA damage in these cell lines (Bensaad et al., 2006). Taken together, these results raise the questions whether high levels of TIGAR in tumour cells play any role in the regulation of F2,6-BP in hypoxia thereby modulating glycolysis under these conditions, and if that was the case, whether this TIGAR regulatory effect on glycolysis was related to the PFKFB3 phosphatase activity. In other words, we hypothesised that TIGAR overexpression in hypoxic cells might result in the enhancement of the PFKFB3 phosphatase and concomitant decrease of its kinase activity, reducing the kinase to phosphatase ratio of the enzyme and by doing so inhibits glycolysis.

Functional cross talk between p53 and HIF-1α at several levels including protein stability (Ravi et al., 2000), and effects of one transcription factors on the transcriptional activity of the other have been reported (Blagosklonny et al., 1998; Chen et al., 2003). However, the crosstalk between p53 and HIF-1α in metabolic pathways has not been well documented. In this respect, we sought to investigate the involvement of HIF-1α in the regulation of the glycolytic pathway through possible effects that this transcription factor might exert on the p53 metabolic target TIGAR.

4.1.1 TIGAR protein levels in cells exposed to hypoxia mimicking conditions

PFK-1 is a rate limiting enzyme of glycolysis which is regulated by the level of the allosteric activator F2,6-BP which is in turn determined by the function of PFKFB and TIGAR (Bensaad et al., 2006; Van Schaftingen et al., 1980). Although TIGAR has been identified as a p53 transcriptional target, the significantly high TIGAR basal protein levels identified in various tumour cell lines (H1299, U2OS and RKO cells) indicate the existence of additional p53-independent mechanisms regulating *TIGAR* gene expression (Bensaad et al., 2006). Taking into account that F2,6-BP level is primarily regulated by the function of the PFKFB 1 - 4 isozymes and that these isozymes are under the control of HIF-1α in hypoxic conditions (Minchenko et al., 2002; Minchenko et al., 2003; Minchenko et al., 2004). we hypothesised that *TIGAR* could be a common p53 and HIF-1α transcriptional target in the glycolytic pathway the same way as it has been shown for *Noxa* (Kim et al., 2004b; Nardinocchi et al., 2011), and *Bid* (Xenaki et al., 2008) in the apoptotic pathway.

To investigate the involvement of hypoxia inducible transcription factors in the regulation of TIGAR, we initially followed TIGAR protein levels in untreated, DSFX or etoposide (Section 3.2.6; page 71) treated cell lines with different p53 status such as U2OS and MCF-7 cells which express wild type p53 ($p53^{+/+}$), MDA-MB-231 cells in which p53 is expressed by one allele ($p53^{mutant}$) and the p53 deficient ($p53^{-/-}$) SaOS2 cells using western blot analysis.

Accumulation of p53 protein was observed in etoposide treated wild type p53 expressing U2OS and MCF-7 cells (Figure 4.1.1 A and B., compare lanes 3 and 1; Figure 4.1.2 A and B., compare black bar 3 with black bar 1) whereas no significant change in p53 levels was found between etoposide treated and untreated MDA-MB-231 cells which express mutated p53 (Figure 4.1.1 C., compare lane 3 with lane 1; Figure 4.1.2 C., compare black bar 3 with black bar 1). In the p53 null cell line SaOS2 p53 was not detected (Figure 4.1.1 D).

The interaction between HIF-1α and its ubiquitin E3 ligase pVHL depends on the hydroxylation of Pro^{402} and Pro^{564} residues of HIF-1α in which iron plays important role

(Yu et al., 2001). In cells treated with the iron chelator DSFX iron is not available, the hydroxylation reaction is inhibited and as a consequence HIF-1α is stabilised (Figure 4.1.1 A, B, C and D., lane 2) (Maxwell et al., 1999). Consistently with the published reports p53 is also stabilized in DSFX treated cells in a HIF-1α dependent manner (Figure 4.1.1 A and B., lane 2) (An et al., 1998).

Densitometric analysis of the TIGAR and p53 protein levels using ImageJ 1.43 software (Figure 4.1.2) indicated that TIGAR was upregulated in all four cell lines treated with etoposide compared to non-treated cells (Figure 4.1.1 A, B, C and D, compare lanes 3 with lanes 1 and Figure 4.1.2 A, B, C and D, white bar 3 with white bar 1).

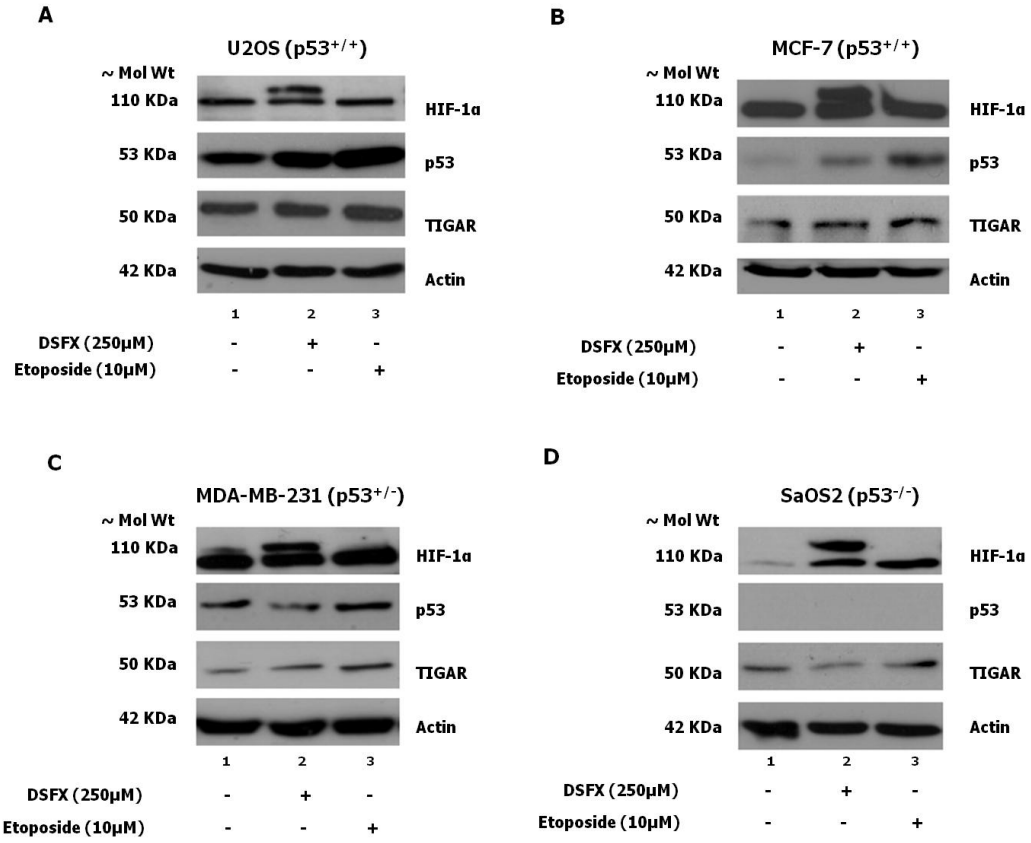

Figure 4.1.1: TIGAR protein levels in hypoxia mimicking and DNA damaged cell lines

U2OS **(A)**, MCF-7 **(B)**, MDA-MB-231 **(C)** and SaOS2 **(D)** cells were left untreated or treated with either DSFX or etoposide as indicated and subjected to western blot analysis. Actin was used as loading control. Data are representative of three independent experiments.

On the other hand, in DSFX treated cells, the pattern of TIGAR protein levels followed that of p53 only in the p53 wild type cell lines U2OS and MCF-7 (Figure 4.1.1 A and B, compare lanes 2 with lane 1 and Figure 4.1.2 A and B, compare bars 2 with bars 1). In contrast, in MDA-MB-231 and SaOS2 cells treated with DSFX, TIGAR protein levels followed different pattern from that of p53.

In particular TIGAR protein levels were upregulated in MDA-MB-231 cells (Figure 4.1.1 C, compare lane 2 with lane 1 and Figure 4.1.2 C, white bar 2 with white bar 1) even though p53 protein levels were downregulated under these conditions (Figure 4.1.1 C, compare lane 2 with lane 1 and Figure 4.1.2 C, black bar 2 with black bar 1). In addition, in the DSFX treated p53 deficient SaOS2 cells TIGAR was downregulated (Figure 4.1.1 D, compare lane 2 with lane 1 and Figure 4.1.2 D, white bar 2 with white bar 1). These results indicated that TIGAR protein levels in hypoxia mimicking conditions were regulated by other factors apart from p53.

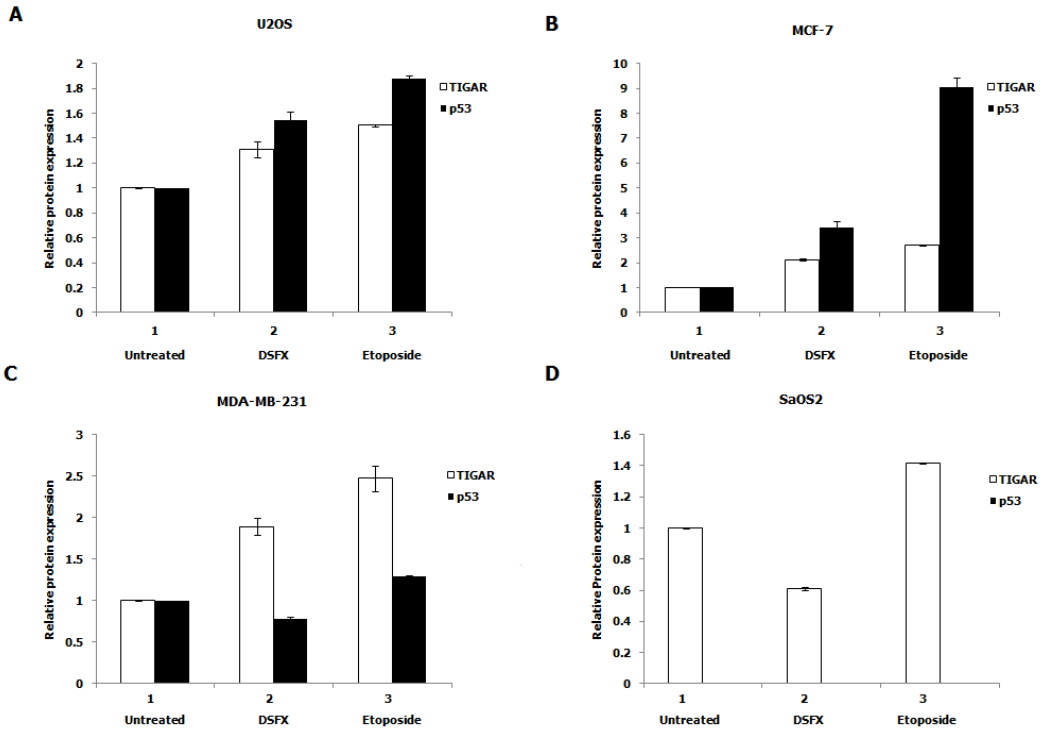

Figure 4.1.2: Densitometric analysis of Figure 4.1.1

ImageJ 1.43 was used to perform the densitometric measurements of Figure 4.1.1. The band intensity of TIGAR protein was normalized to the band intensity of Actin. The values of

untreated samples were considered 1 and the values from DSFX and etoposide treated cells calculated accordingly.

4.1.2 Regulation of TIGAR gene expression in hypoxia mimicking conditions occurs at the transcriptional level

The pattern of TIGAR protein levels in DSFX treated p53 deficient cells did not follow that of p53 protein levels (Figure 4.1.1). This led us to investigate the factors that are involved in the regulation of TIGAR expression in hypoxia mimicking conditions. For this purpose, the TIGAR mRNA levels were determined in cells treated with either DSFX or etoposide employing qRT-PCR. Briefly, total mRNA from all four cell lines (U2OS, MCF-7, MDA-MB-231 and SaOS2) was extracted and subsequently reverse transcribed to cDNA and qRT-PCR reactions were performed as described in the Materials and Methods section 3.8.3 (Page 92). TIGAR mRNA levels were measured using Opticon Monitor 3 software.

In etoposide treated U2OS, MCF-7 and MDA-MB-231 cells, increased TIGAR mRNA levels were observed (Figure 4.1.3 A, B and C, compare bars 3 to bars 1), a pattern similar to that observed for TIGAR protein levels (Figure 4.1.1, B and C and Figure 4.1.2 A, B and C compare white bars 3 to bars 1). However, in etoposide treated SaOS2 cells, decreased TIGAR mRNA level compared to the non-treated cells was evident (Figure 4.1.3 D, compare bar 3 with bar 1). This downregulation might be attributable to the recruitment of repressive transcription complexes in the *TIGAR* promoter by other p53 family members such as p73 or other transcription factors such as E2F1 and NF-κB, which are responsive to etoposide treatment in SaOs2 cells (Lin et al., 2001; Morotti et al., 2006). This notion was supported by the fact that putative binding sites for E2F1 and NF-κB were identified within the regulatory region of *TIGAR* gene promoter (Figure 4.1.5) (page 113).

In line with TIGAR protein expression pattern, TIGAR mRNA levels also increased in DSFX treated p53 wild type U2OS and MCF-7 cell lines and a slight increase was also evident in the $p53^{mutant}$ MDA-MB-231 cell line (Figure 4.1.3 A, B and C, compare bars 2 with bars 1). Slightly decreased TIGAR mRNA levels were observed in DSFX treated SaOS2 cells (Figure 4.1.3 D, compare bar 2 with bar 1).

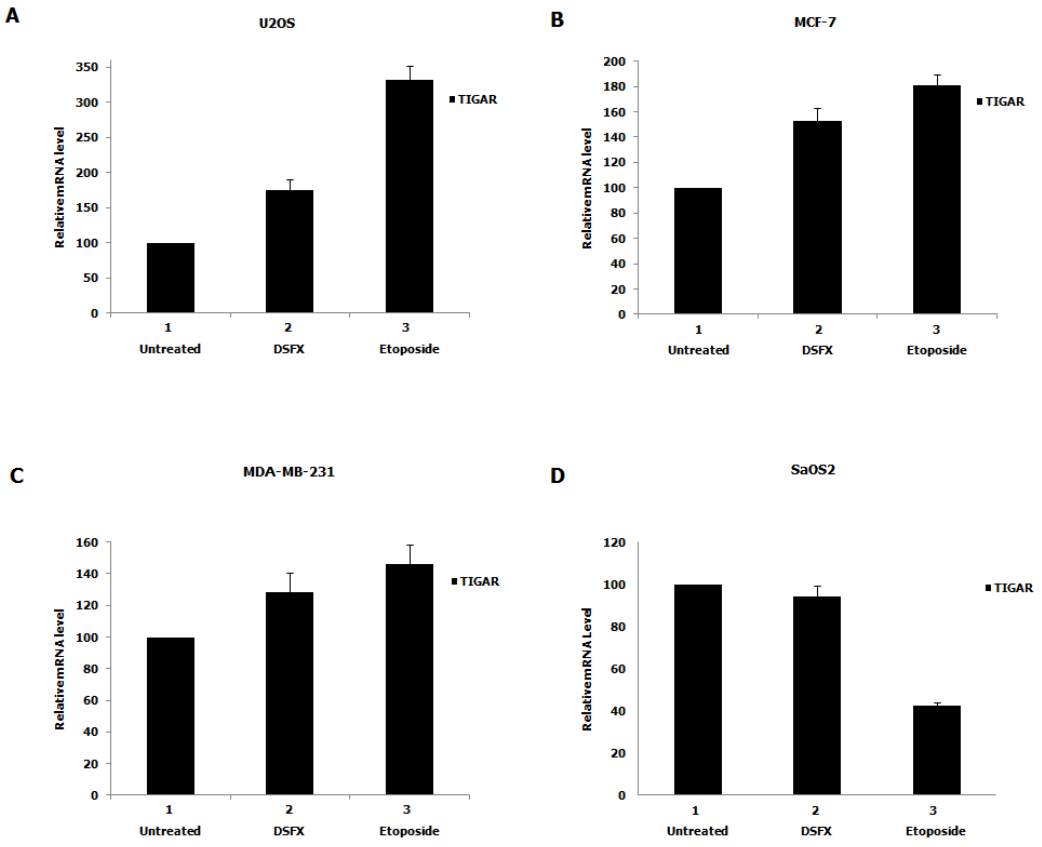

Figure 4.1.3: TIGAR mRNA levels in hypoxia mimicking and DNA damaged cell lines

Total mRNA from U2OS **(A),** MCF-7 **(B),** MDA-MB-231 **(C)** and SaOS2 **(D)** cells untreated or treated with either DSFX or etoposide was extracted and reverse transcribed. The cDNAs were then subjected to qRTPCR using specific primers amplifying TIGAR mRNA. Rpl19 was used as an internal control. The data was analyzed by Opticon Monitor 3 software. The data are representative of three independent experiments each performed in duplicates.

The difference in the TIGAR mRNA levels in DSFX versus etoposide treated U2OS, MCF-7 and MDA-MB231 cells (Figure 4.1.3 A, B and C, compare bars 2 to 3) as well as the upregulation of TIGAR mRNA levels in DSFX compared to etoposide treated SaOS2 cells (Figure 4.1.3 D, compare bar 2 to 3) indicated that other factors, apart from p53 are involved in the transcriptional regulation of TIGAR gene expression in hypoxia mimicking conditions. Since DSFX treatment has been shown to stabilize and induce HIF-1α transcriptional activity (Wang and Semenza, 1993a), we hypothesised that the differential regulation of *TIGAR* gene expression in DSFX treated cells might indicate

the potential involvement of HIF-1α in the modulation of TIGAR gene expression in hypoxia under these conditions. (Wang and Semenza, 1993a)

4.1.3 HIF-1α regulates TIGAR cellular levels

To investigate the potential involvement of HIF-1α in the regulation of TIGAR gene expression in hypoxia mimicking conditions, we followed TIGAR mRNA (Figure 4.1.4 A) and protein levels (Figure 4.1.4 B) in DSFX treated U2OS cells in the presence or absence of HIF-1α. RNAi-HIF-1α (Table 3.5.1) was used to silence the HIF-1α expression and scrambled RNAi was used as a negative control.

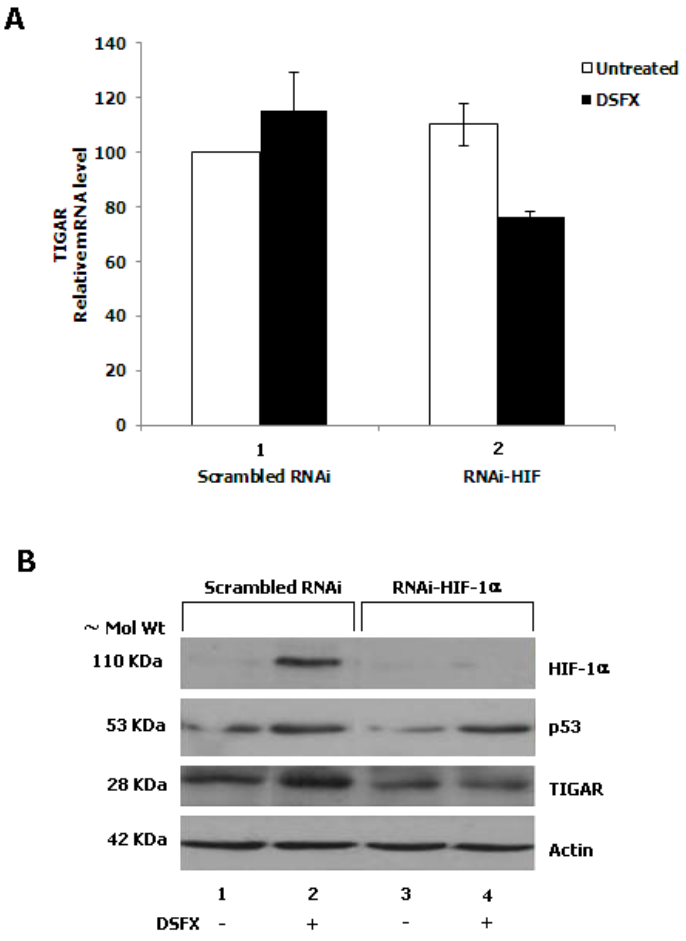

Figure 4.1.4: TIGAR cellular levels are regulated by HIF-1α in U2OS cells

A. U2OS cells were transfected either with scrambled RNAi or with RNAi for HIF-1α and treated with DSFX (black bars) or left untreated (white bars). Total mRNA was extracted, reverse transcribed and the cDNA was then subjected to qRT-PCR using specific primers for TIGAR. Rpl19 was used as an internal control. The data were analysed by Realplex software (Eppendorf, UK) and are representative of three independent experiments performed in duplicates. **B.** U2OS cells were transfected with scrambled RNAi (lanes 1 and 2) or RNAi for

HIF-1α (lanes 3 and 4) and left untreated (lanes 1 and 3) or treated with DSFX (lanes 2 and 4). Cell lysates were prepared and subjected to PAGE and western transfer. Actin was used as loading control. Data shown are representative of 2 independent experiments

Decreased TIGAR mRNA levels in U2OS cells transfected with RNAi for HIF-1α compared to those in cells transfected with scrambled RNAi (Figure 4.1.4 A., compare black bar 2 with black bar 1) suggested that in DSFX treated U2OS cells, *TIGAR* gene expression was downregulated in the absence of HIF-1α. In other words, HIF-1α upregulated TIGAR mRNA levels in hypoxia mimicking conditions. To investigate whether this HIF-1α effect was reflected in the TIGAR protein levels, cellular extracts from untreated or DSFX treated U2OS cells transfected with either scrambled RNAi or RNAi for HIF-1α were subjected to western blot analysis.

Efficient silencing of HIF-1α protein was observed in cells transfected with RNAi for HIF-1α (Figure 4.1.4 B, compare lane 4 to lane 2). In addition, stabilization of p53 was also observed in DSFX treated U2OS cells transfected with either the scrambled RNAi or the RNAi for HIF-1α (Figure 4.1.4 B., compare lanes 2 and 4 with lanes 1 and 3 respectively). TIGAR protein expression was downregulated in U2OS cells in which HIF-1α was silenced compared to those in which HIF-1α was expressed (Figure 4.1.4 B, compare lane 4 with lane 2). These results indicated that HIF-1α upregulated TIGAR gene expression, both at mRNA and protein levels in DSFX treated U2OS cells.

4.1.4 Identification of HREs in the regulatory region of the TIGAR gene promoter

Results shown in sections 4.1.1 and 4.1.2 indicated the potential involvement of transcription factors induced in hypoxia mimicking conditions, although it is known that TIGAR gene expression is primarily regulated by p53. Upregulation of TIGAR protein levels in DSFX treated cells (Figure 4.1.1 A, B and C) in combination with the downregulation of TIGAR mRNA and protein levels in DSFX treated U2OS cells in which HIF-1α had been silenced (Figure 4.1.4 A and B) indicated the potential involvement of HIF-1α in the modulation of TIGAR gene expression in hypoxia mimicking conditions. In order to exert its transcriptional effects, HIF-1α dimerizes with HIF-1β and this complex then is recruited to the hypoxia responsive element (HRE) present within the regulatory regions of the promoters of HIF target genes.

Figure 4.1.5: Promoter region of TIGAR gene showing the binding sites for various transcription factors

The regulatory region of the promoter of *TIGAR* gene was analyzed for the presence of hypoxia responsive elements. The 5'-CGTG-3' sequences present within the *TIGAR* promoter region are marked and numbered. The translation start site is marked in green. The previously reported p53 (Bensaad et al., 2006) as well as the NF-κB and the E2F1 binding sites are also indicated.

To gain further insight in the HIF mediated *TIGAR* gene expression the nucleotide sequence of the promoter of *TIGAR* gene was analyzed for the presence of putative binding sites for HIF-1α. Six putative HREs (5'-CGTG-3') were identified within 2600 nucleotides upstream of the translation start site (Figure 4.1.5). In addition NF-κB (-

2569 to -2578 upstream of translation start site) and E2F-1 binding sites (-1509 to -1516 upstream of translation start site) were also detected within this region (Figure 4.1.5). Figure 4.1.6 A., schematically demonstrates the presence of putative binding sites for various transcription factors in the regulatory region of the promoter of *TIGAR* gene. The presence of multiple binding sites for different transcription factors within the close proximity of the previously published p53 binding sites (p53bs1: -6680 to -6702 upstream and p53bs2: +344 to +365 downstream of translation start site) (Bensaad et al., 2006) imply that *TIGAR* gene expression is under control of several transcription factors.

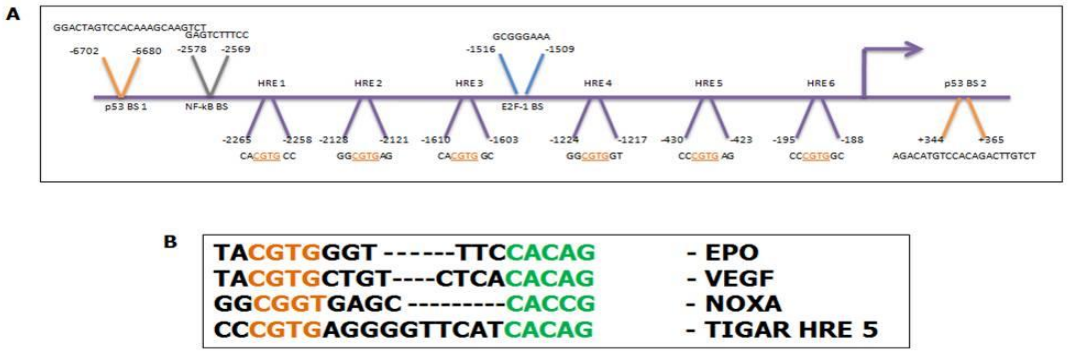

Figure 4.1.6: HREs in the regulatory region of the promoter of TIGAR gene.

(A) Schematic diagram of the *TIGAR* promoter showing the binding sites for various transcription factors. The regulatory region of the promoter of TIGAR gene was analyzed for the presence of putative binding sites for various transcription factors. The numbers shown in the figure are the position of the first and last nucleotide of the sequences of the putative binding sites calculated upstream or downstream from the translation start site. **(B)** *TIGAR* HRE 5 followed by 5'-CACAG-3' region after 10 nucleotides is similar to the known HIF-1α transcriptional target genes EPO, VEGF and NOXA.

Interestingly, the bio-informatics studies indicated that after 10 nucleotides of the *TIGAR* HRE 5 a consensus 5'-CACAG-3' sequence followed which has been shown to be present in many of the promoters of HIF-1α transcriptional target genes including VEGF, EPO, NOXA (Fukuda et al., 2007; Kim et al., 2004b; Semenza and Wang, 1992; Shima et al., 1996). The nucleotide sequences of known HIF-1α transcriptional target genes and the position of 5'-CACAG-3' region following the HRE are shown in Figure 4.1.6 B.

4.1.5 TIGAR HRE-5 is functional HIF-1α binding site

The transcription factor HIF-1α is upregulated in hypoxia or hypoxia mimicking conditions, dimerizes with HIF-1β (Aryl hydrocarbon receptor nuclear translocator – ARNT) to form the HIF-1 complex and this hetero-dimeric complex recognizes and binds to the HREs present in the promoter of HIF-1α target genes modulating their transcription. To investigate the functionality of the HREs present within the *TIGAR* gene promoter untreated or DSFX treated U2OS cells were subjected to chromatin immuno-precipitation (ChIP) assay using a specific anti-HIF-1α ChIP grade antibody to precipitate HIF-1α chromatin immuno-complexes (Abcam, UK).

Briefly, chromatin in DSFX treated or untreated U2OS cells was cross-linked with transcription factors using formaldehyde as described in Materials and Methods and the formed chromatin complexes were immuno- precipitated using specific antibody for HIF-1α or Rabbit IGG.

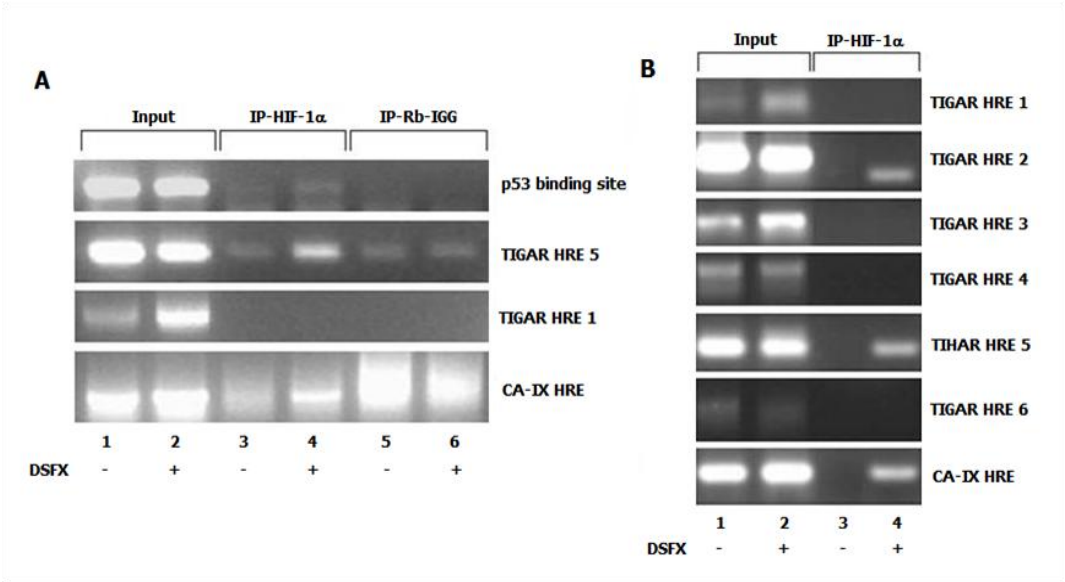

Figure 4.1.7: HIF-1α binds to TIGAR HRE-5

A. Chromatin immuno-complexes were precipitated using a specific HIF-1α (lanes 3 and 4) or Rabbit IGG (lanes 5 and 6) as negative controls. The pulled down DNA was amplified with specific primers flanking the regions containing various HREs and p53 binding sites present in *TIGAR* promoter. The resultant PCR product was then submitted to 2% agarose gel electrophoresis. CA-IX was used as a positive control (lane 4). Lanes 1 and 2 are 10% of the input. **B.** ChIP assay was performed with all 6 HREs present within the *TIGAR* promoter. Only the *TIGAR* HRE-5 produced a specific product. Lanes 1 and 2 represent 10% of the input.

The precipitated DNA was sonicated, ethanol precipitated and the purified DNA was then amplified using specific primers flanking the region containing the different HREs present in the *TIGAR* promoter. The sequences of the primers used in ChIP assays are listed in Table 3.9.1 (Page 97). 10% of the input samples were used as control. Also the input was used as a positive control for the primers and the product size. Rabbit IgG which does not bind to any specific protein was used as a negative control. Since CA-IX is a known transcriptional target gene of HIF-1α, only in DSFX treated cells but not in non-treated cells, the binding of HIF-1α to the specific region of the promoter of CA-IX flanking the HRE sequence was observed indicating that DSFX stabilized and induced the transcriptional activity of HIF-1α as expected (Figure 4.1.7 A and B., lanes 4 and 3). HIF-1α was pulled down only with the promoter region of TIGAR which contains the HRE 5. This indicated that HIF-1 complex binds with HRE 5 present in the regulatory region of promoter of TIGAR gene (Figure 4.1.7 A and B., compare lanes 4 and 3). Although other HREs contain 5'-CGTG-3' sequence, HIF-1α did not bind with them.

The ChIP results have indicated that the HIF-1 complex is recruited to the TIGAR gene promoter. To investigate whether HIF-1α was involved in the transcriptional regulation of TIGAR gene expression, a luciferase reporter assay was performed. For luciferase experiment, a specific region of TIGAR promoter consists of 908 base pairs of nucleotides (+400 to -508 from translation start site) contains HRE 5 which has been shown to bind to HIF-1α, (-423 to -430 upstream of translation start site) (Figure 4.1.7), HRE 6 and a p53 binding site (p53 BS2) (-188 to -195 upstream and +344 to +365 downstream of translation start site respectively) was cloned in pGL3 promoter vector (Promega, UK) as described in the Materials and Methods section. It is important to note that the p53 binding site included in this vector is shown to be less efficient in binding with p53 protein compared to the other binding site for p53 (p53 BS 1; -6680 to -6702 upstream of translation start site) (Bensaad et al., 2006).

To confirm that the TIGAR HRE-5 was functional a luciferase assay was performed in U2OS and SaOS2 cells as they are p53 wild type and p53 null cell lines respectively. Briefly, U2OS or SaOS2 cells were grown in 6 well plates and after reaching 60% confluency, they were transfected with TIGAR-HRE5,6-p53BS2-luc vector along with

β-galactosidase and HIF-1α expression vector. 24 hours after transfection the cells were either left untreated or treated with 250μM DSFX and incubated for 16 hours at 37°C. The cell lysates were subjected to luciferase reporter assay. β-galactosidase expression was used as a transfection efficiency control.

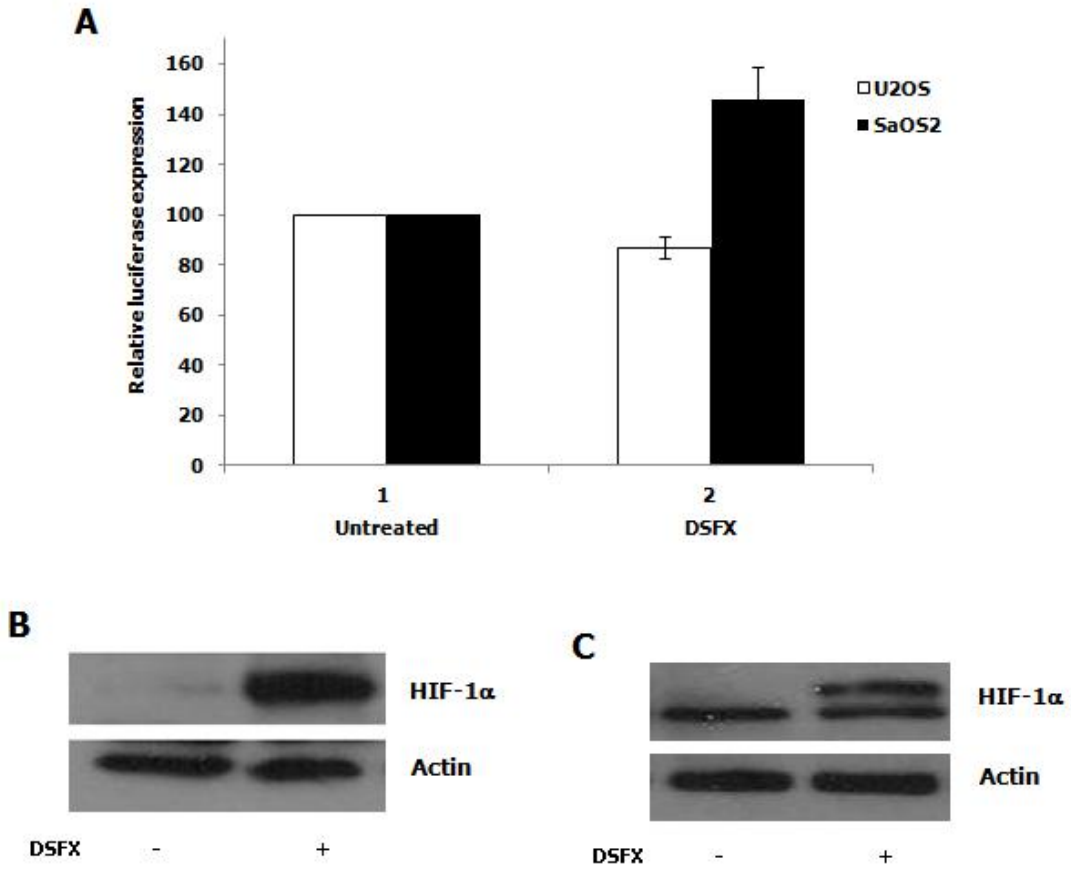

Figure 4.1.8: HIF-1α regulates the transcription of TIGAR gene in DSFX condition

A. U2OS and B. SaOS2 cells were transfected either with TIGAR-HRE5,6-p53BS2-Luc vector along with β-galactosidase and HIF-1α expression vectors using Polyfect transfection reagent (Qiagen, UK). 24 hours after transfection, the cells were left untreated or treated with 250μM DSFX and incubated in 37°C for 16 hours. The cell lysates were prepared using Promega luciferase lysis buffer (Promega, UK) and subjected to luciferase assay. 30μl of the lysate was used to measure β-galactosidase expression. The values from the luciferase assay were normalized to the values from β-galactosidase experiment. C. and D. Western blots showing the expression level of HIF-1α protein in untreated and DSFX treated U2OS and SaOS2 cells respectively. Data shown are representative of three individual experiments.

The western blotting with U2OS and SaOS2 cells treated with DSFX showed that HIF-1α was stabilized in DSFX treated cells (Figure 4.1.8 B and C). In contrast to the protein and mRNA expression pattern, in which the TIGAR expression was upregulated in DSFX treated U2OS cells, the luciferase experiment showed a downregulation of TIGAR gene transcription (approx. 13%) in DSFX treated U2OS cells (Figure 4.1.8 A). Although the TIGAR-HRE5,6-p53BS2-luc vector contains the HRE 5 which has been shown to be a binding site for HIF-1α (Figure 4.1.7), it does not contain the full length TIGAR promoter region which also contain binding sites for other transcription factors such as NF-κB and E2F1 which might interact with HIF-1α in the regulation of TIGAR gene expression.

Also, it is possible that the region which is necessary for the transcription cofactors might have not been included in the vector which might have affected the transcriptional activity of HIF-1α. In addition, p53 protein is also shown to be stabilized in DSFX treated U2OS cells (Figure 4.1.1 A, lane 2), hence the presence of p53 binding site 2 (Figure 4.1.5 and Figure 4.1.6 A) in the TIGAR-HRE5,6-p53BS2-luc vector might have facilitated p53 to exert its transcription regulatory functions in DSFX treated conditions. Since both p53 and HIF-1α proteins were stabilized in DSFX treated U2OS cells, the cross talk between these two transcription factors might have affected the gene expression of TIGAR.

However, the upregulation of TIGAR transcription in DSFX treated p53 null SaOS2 cells, indicate that HIF-1α upregulate TIGAR gene expression in the absence of p53 (Figure 4.1.8 B). Together, these results suggest that HIF-1α regulate TIGAR gene expression both in the presence and absence of p53 in hypoxia mimicking conditions. Since both p53 and HIF-1α proteins were stabilized in DSFX treated U2OS cells, the cross talk between these two transcription factors might have affected the gene expression of TIGAR.

4.2 HIF-1α regulates SCO2 gene expression

Maintaining the proton gradient across the inner mitochondrial membrane is necessary for the mitochondrial ATP synthase enzyme to drive ATP production (Sone et al., 1977; Yoshida et al., 2001). This proton gradient is maintained by the mitochondrial respiratory enzyme complex IV, also known as cytochrome c oxidase (COX), a multimeric protein complex that catalyzes the transfer of electrons from cytochrome c to molecular oxygen and pumps protons across the inner mitochondrial membrane (Fetter et al., 1995). Human COX complex is made up of 13 protein subunits of which 3 subunits that form the catalytic core of the enzyme are encoded by mitochondrial DNA and the remaining 10 subunits are encoded by nuclear DNA (Kadenbach et al., 1983). The human COX complex requires several assembly components including SCO2 protein (encoded by *SCO2* gene) which transports copper to the Cu_A site on the cytochrome c oxidase subunit II (COX II) (Leary et al., 2004), a process which is essential for the biogenesis of COX II (Horn and Barrientos, 2008).

While attenuating glycolysis by modulating the *TIGAR* gene expression, tumour suppressor p53 regulates mitochondrial respiration by fine-tuning the *SCO2* gene expression (Bensaad et al., 2006; Matoba et al., 2006). The disruption of *SCO2* gene in p53 wild type cell line HCT-116 has been associated with defective OXPHOS and increased lactate production which resembles the metabolic phenotype observed in p53 mutant cells (HCT-116 $p53^{-/-}$) (Matoba et al., 2006; Sung et al., 2010). In addition HCT-116 cells lacking *SCO2* gene expression ($SCO2^{-/-}$) has been shown to have increased ROS and oxidative DNA damage (Sung et al., 2010). Together these results indicate that by regulating SCO2 gene expression, p53 not only controls mitochondrial respiration but also protects the cells from ROS mediated genotoxic stress. Although *SCO2* gene expression has been shown to be regulated by p53, the significant level of SCO2 protein expression detected in $p53^{-/-}$ mice and human p53 mutant cell line (HCT-116 $p53^{-/-}$) suggests that p53 independent pathways exist in the regulation of *SCO2* gene expression (Matoba et al., 2006).

Apart from upregulating glycolysis, HIF-1α has been shown to inhibit both TCA cycle and OXPHOS by inducing PDK1 enzyme in tumour cells which inhibits the activity of PDH enzyme thereby attenuates the oxidative decarboxylation of pyruvate and inhibits the synthesis of acetyl-CoA which is essential for the TCA cycle to proceed (Kim et al., 2006; Papandreou et al., 2006). In addition, prolonged hypoxia is reported to attenuate the mitochondrial respiration by inhibiting COX activity in intact cells and in isolated mitochondria (Chandel et al., 1995). Recently, Fukuda et al., demonstrated that HIF-1α regulate several of the mitochondrial COX complex subunits in hypoxia (Fukuda et al., 2007). These results indicate the role of HIF-1α in the regulation of cellular mitochondrial respiration. However, the involvement of HIF-1α in the regulation of the COX complex subunit II assembly factor *SCO2* gene expression has not been documented. Since SCO2 protein is involved in the assembly of COX complex subunit II and many subunits of the COX complex are regulated by HIF-1α in hypoxic conditions, we asked a question, whether *SCO2* gene expression is modulated by HIF-1α in hypoxic condition. Along this line, the involvement of HIF-1α in the regulation of SCO2 gene expression was investigated.

4.2.1 SCO2 protein levels in hypoxic cells

Inhibition of COX activity has been reported in hypoxic conditions (Chandel et al., 1995). Also, recent reports provide evidence that many subunits of COX complex are regulated by HIF-1α in hypoxic conditions (Fukuda et al., 2007). An important assembly component of the subunit II of COX complex, SCO2 (encoded by *SCO2* gene) which has been shown to be regulated transcriptionally by p53, shows a high basal level protein expression in $p53^{-/-}$ tumour cells (HCT-116 cells) (Matoba et al., 2006). Together, by these results we were intrigued to investigate whether *SCO2* gene expression is controlled by HIF-1α in hypoxic conditions.

In order to study the involvement of transcription factors induced in hypoxic conditions in the regulation of *SCO2*, the SCO2 protein levels were followed in untreated or DSFX treated or etoposide treated cell lines with different p53 status such as U2OS and MCF-7 cells which express wild type p53 ($p53^{+/+}$), MDA-MB-231 cells in which p53 is expressed by one allele ($p53^{mutant}$) and the p53 deficient ($p53^{-/-}$) SaOS2 cells (Soussi, 2007) using western blot analysis.

The p53 and HIF-1α protein levels in untreated, DSFX treated and etoposide treated conditions are the same as in Section 4.1.1. The densitometric analysis of the p53 and SCO2 protein levels indicated that except MCF-7 cells, the SCO2 protein expression was upregulated in all the three cell lines in etoposide treated conditions (Figure 4.2.1 A, B, C and D compare lane 3 with lane 1 and Figure 4.2.2 A, B, C and D compare white bar 3 with white bar 1). As putative binding site for NF-κB were found on the *SCO2* gene promoter (Result 4.2.3), the downregulation of SCO2 protein expression in MCF-7 cells in etoposide treated condition might attribute to the induction of NF-κB transcriptional activity in these conditions (Morotti et al., 2006).

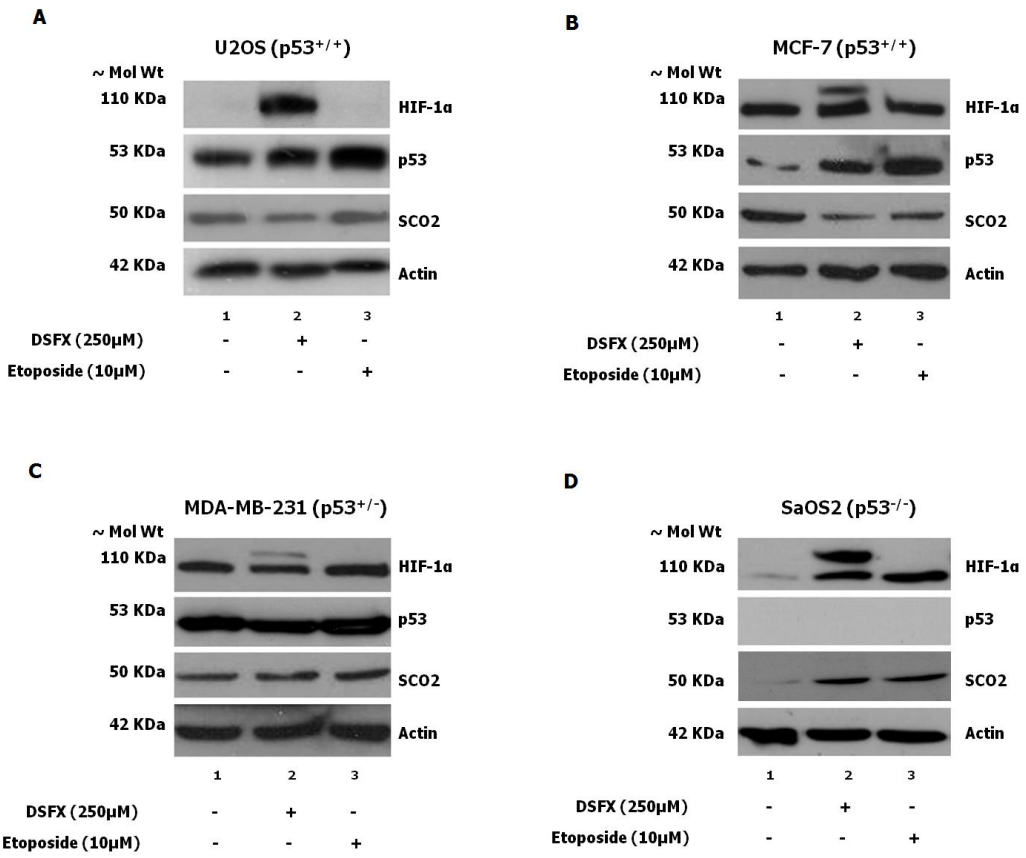

Figure 4.2.1: SCO2 protein is differentially regulated in hypoxia mimicking and etoposide treated conditions.

U2OS (A), MCF-7 (B), MDA-MB-231 (C) and SaOS2 (D) cells were left untreated or treated either with DSFX or with etoposide for 16 hours before harvested using TNN buffer (contains 240mM NaCl) and the lysates were subjected to western blotting. Actin was used as loading control and the data are representative of three independent experiments.

In contrast to etoposide treated conditions, the DSFX treated wild type p53 expressing U2OS cells showed a downregulation of SCO2 protein expression (Figure 4.2.1 A., compare lane 2 with lane 1; Figure 4.2.2 A., compare white bar 2 with white bar 1) indicating the antagonistic effect of the hypoxia induced transcription factor against p53 in the regulation of SCO2 protein expression.

However, the SCO2 protein expression was downregulated in DSFX treated MCF-7 cells (Figure 4.2.1 B., compare lane 2 with lane 1; Figure 4.2.2 B., compare white bar 2 with white bar 1) which is similar to etoposide treated conditions (Figure 4.2.1 B., lane 3; Figure 4.2.2 B., white bar 3) indicating that in hypoxia mimicking conditions p53 is not the only regulator of SCO2 protein expression.

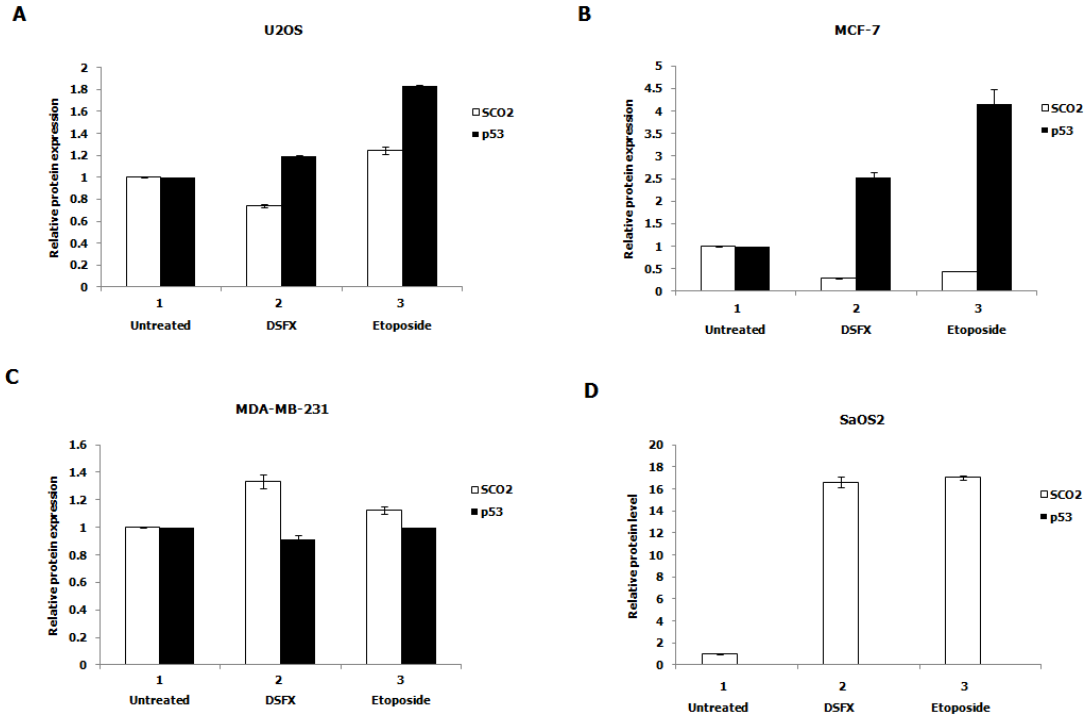

Figure 4.2.2: Densitometric analysis of Figure 4.2.1

ImageJ 1.43 was used to perform the densitometric measurements of Figure 4.2.1. The band intensity of SCO2 protein was normalized to the band intensity of Actin. The values of untreated samples of each cell line were considered as 1 and the values of treated samples were calculated accordingly. Measurements were made in duplicates and the standard deviations were used in the error bars.

This notion was strengthened by the upregulation of SCO2 protein expression in DSFX treated mutant p53 expressing MDA-MB-231 cells (Figure 4.2.1 C., compare lane 2 with lane 1; Figure 4.2.2 C., compare white bar 2 with white bar 1) in which p53 protein expression was downregulated in these conditions (Figure 4.2.1 C., compare lane 2 with lane 1; Figure 4.2.2 C., compare black bar 2 with black bar 1). p53 null SaOS2 cells showed upregulation of SCO2 protein expression (Figure 4.2.1 D., compare lane 2 with lane 1 and Figure 4.2.2 D., compare white bar 2 with white bar 1). Together these results indicate that apart from p53 other transcription factors are also involved in the SCO2 protein expression in hypoxia mimicking conditions.

4.2.2 Regulation of SCO2 gene expression in hypoxia occurs at the transcriptional level

SCO2 protein expression studies in p53 mutant and null cell lines (Result 4.2.1) indicated that factors other than p53 are involved in the regulation of *SCO2* gene expression in hypoxia mimicking conditions (Result 4.2.1). To investigate whether the modulation of SCO2 gene expression is under the transcriptional control of these factors, qRT-PCR reactions were performed in U2OS, MCF-7, MDA-MB-231 and SaOS2 cells treated with DSFX or etoposide to follow the SCO2 mRNA levels.

In line with published reports (Matoba et al., 2006), SCO2 mRNA levels were increased in etoposide treated wild type p53 expressing U2OS cells (A, compare bar 3 with bar 1). A slight decrease in SCO2 mRNA levels was observed in etoposide treated wild type p53 expressing MCF7 cells (Figure 4.2.3 B, compare bar 3 with bar 1). In etoposide treated mutant p53 expressing MDA-MB-231 cells and p53 null cell line SaOS2 showed increased SCO2 mRNA levels (Figure 4.2.3 C and D., compare bar 3 with bar 1). The increase in SCO2 mRNA levels in etoposide treated MDA-MB-231 and SaOS2 cell lines indicated the potential role of transcription factors other than p53 involved in the regulation of *SCO2* gene expression. Since NF-κB is induced in etoposide treated cells (Morotti et al., 2006), the NF-κB consensus binding site which was found in the regulatory region of the promoter of *SCO2* gene (Figure 4.2.4) allowed the hypothesis for a potential role of NF-κB in the modulation of *SCO2* gene expression.

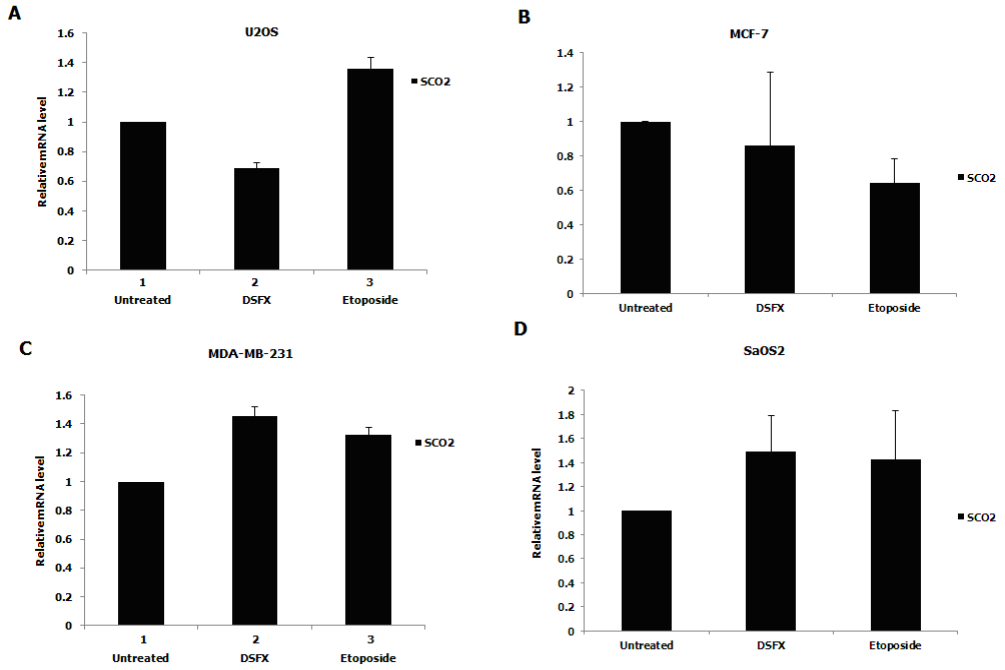

Figure 4.2.3: SCO2 mRNA levels are regulated by factors other than p53 in DSFX treated cells

U2OS **(A),** MCF-7 **(B),** MDA-MB-231 **(C)** and SaOS2 **(D)** cells were left untreated or treated with either DSFX or etoposide for 16 hours before the total mRNA was extracted and reverse transcribed to cDNA. The cDNAs were then subjected to qRTPCR using specific primers amplifying SCO2 mRNA. Rpl19 was used as an internal control. The data was analyzed by Opticon Monitor 3 or Realplex 2.2.4. software. The data is representative of three independent experiments.

In DSFX treated conditions, in line with the pattern of SCO2 protein levels (Figure 4.2.1 and Figure 4.2.2) the SCO2 mRNA levels decreased in p53 wild type expressing U2OS and MCF-7 cell lines (Figure 4.2.3 A and B., compare bar 2 with bar 1) and increased in p53 mutant cell line MDA-MB-231 and p53 null cell line SaOS2 (Figure 4.2.3 C and D., compare bar 2 with bar1). This indicated that in hypoxia mimicking conditions, the regulation of *SCO2* gene expression is under the transcriptional control of factors other than p53. In view of the fact that HIF-1α is the major transcription factor activated in DSFX treated cells (Wang and Semenza, 1993a), the increase in SCO2 mRNA levels in SaOS2 and MDA-MB-231 cells might be an indication of the potential role of HIF-1α in the regulation of SCO2 gene expression.

4.2.3 Identification of HREs in the regulatory region of the promoter of SCO2 gene

Although *SCO2* gene expression has been shown to be regulated by p53, the SCO2 protein and mRNA levels in DSFX treated cells (Result 4.2.1 and 4.2.2) indicated the potential involvement of other transcription factors induced in hypoxia in the regulation of SCO2 gene expression. Since HIF-1α is transcriptionally activated in DSFX treated cells, to explore the possibility that *SCO2* gene expression is regulated by HIF-1α, the regulatory region of the promoter of *SCO2* gene was subjected to bio-informatics analysis to find the putative binding sites for HIF-1α and other transcription factors induced in hypoxia mimicking conditions.

Figure 4.2.4: Presence of putative binding sites for various transcription factors in the promoter of SCO2 gene

The regulatory region of the promoter of *SCO2* gene was analyzed for the presence of putative binding sites for transcription factors induced in hypoxia mimicking conditions. The putative binding sites for HIF-1α are marked and numbered as HRE 1 -6 along with p53 binding site (Matoba et al., 2006) and putative NF-κB binding site. The translation start site is marked in green.

The presence of multiple binding sites for different transcription factors within 1700 base pairs from the translation start site and within the close proximity of the previously published p53 binding site (Matoba et al., 2006) imply that SCO2 gene expression is under control of multiple transcription factors. Figure 4.2.5 schematically demonstrates the putative binding sites for various transcription factors present in the SCO2 promoter region.

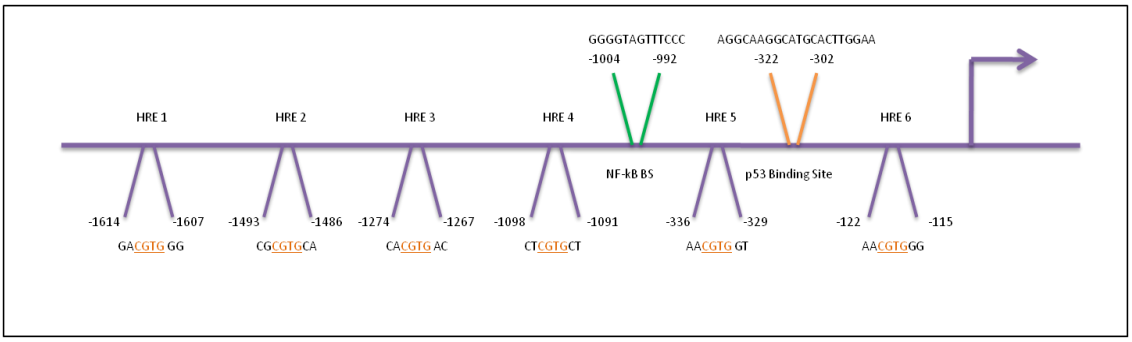

Figure 4.2.5: Schematic diagram showing the putative binding sites for various transcription factors in the SCO2 promoter region.

Cartoon showing the putative binding sites for various transcription factors found in the regulatory region of the promoter of SCO2 gene. The translation start site was marked with the arrow.

4.2.4 Potential role of HIF-1α in SCO2 gene expression

The bio-informatics studies indicated the presence of 8 putative binding sites for HIF-1α in the regulatory region of the promoter of SCO2 gene. To investigate the involvement of HIF-1α in the transcriptional regulation of SCO2 gene expression, a luciferase reporter assay was performed. A specific region of SCO2 promoter which contain the putative HREs 1 to 5 (Figure 4.2.4 and Figure 4.2.5) and the previously published p53 binding site (Matoba et al., 2006) was cloned into pGL3 promoter vector (Promega, UK) as described in the Materials and Methods.

Briefly, in luciferase assay, U2OS and SaOS2 cells were grown in 6 well plates and after reaching 60% confluency, they were transfected either with SCO2-HRE(1-5)-p53-luc vector or with CA-IX(HRE)3 along with β-galactosidase and HIF-1α expression vectors. 24 hours after transfection the cells were either left untreated or treated with 250µM DSFX and incubated for 16 hours at 37°C. The cell lysates were subjected to luciferase reporter assay. β-galactosidase expression was used as a transfection efficiency control.

Since CA-IX(HRE)3 has three HREs inserted into the pGL3 promoter vector, it has been transcribed efficiently in DSFX treated U2OS and SaOS2 cells (Figure 4.2.6 A and B, compare black bar 2 with white bar 2). A western blot was performed to confirm the stabilization of HIF-1α in DSFX treated cell (Figure 4.2.6 C and D). Together, these

experiments have confirmed that HIF-1α is stabilized and transcriptionally active in DSFX treated U2OS and SaOS2 cells.

In line with the protein and mRNA levels, SCO2 gene expression was downregulated in wild type p53 expressing U2OS cells (Figure 4.2.6 A., compare black bar 1 with white bar 1) while upregulated in p53 null SaOS2 cell line in hypoxia mimicking conditions (Figure 4.2.6 B., compare black bar 1 with white bar 1). The increase in SCO2-HRE(1-5)-p53-luc expression in SaOS2 cells indicate that HIF-1α increases SCO2 transcription in the absence of p53.

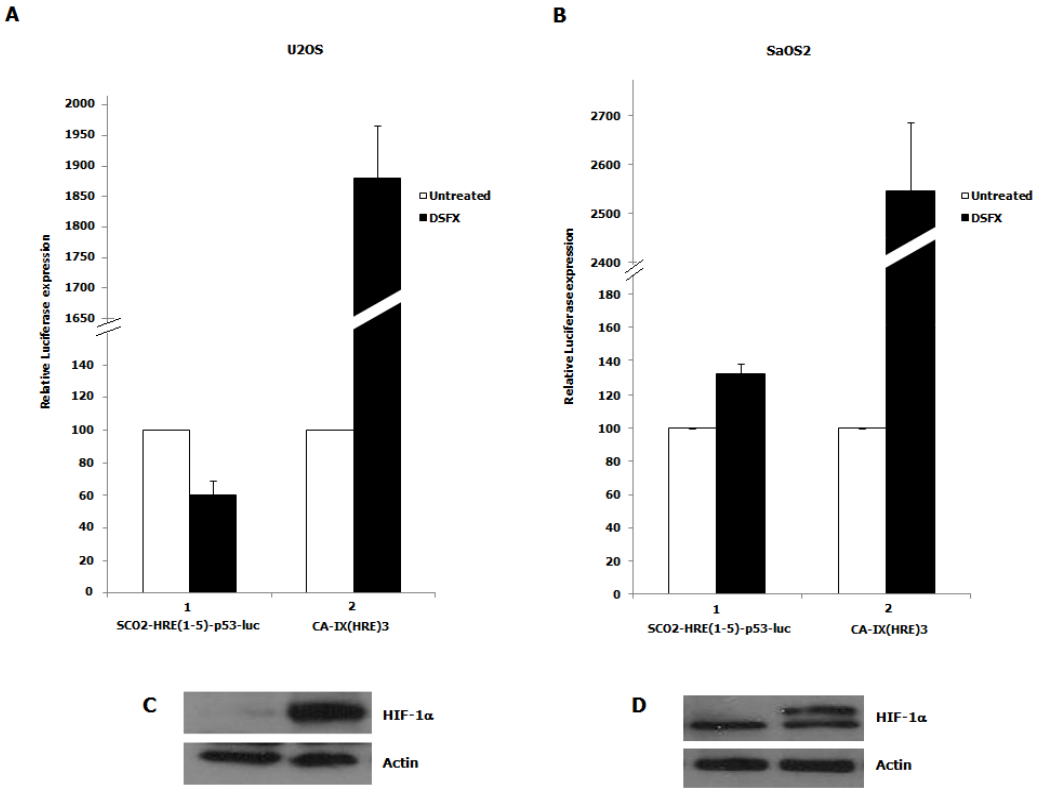

Figure 4.2.6: Role of HIF-1α in SCO2 gene expression

A. U2OS and B. SaOS2 cells were transfected either with SCO2-HRE(1-5)-p53-Luc vector or CA-IX(HRE)3 along with β-galactosidase and HIF-1α expression vectors using Polyfect transfection reagent (Qiagen, UK). 24 hours after transfection, the cells were left untreated or treated with 250μM DSFX and incubated in 37°C for 16 hours. The cell lysates were prepared using Promega luciferase lysis buffer (Promega, UK) and subjected to luciferase assay. 30μl of the lysate was used to measure β-galactosidase expression. The values from the luciferase assay were normalized to the values from β-galactosidase experiment. C. and D. Western blots showing the expression level of HIF-1α protein in untreated and DSFX treated U2OS and SaOS2 cells respectively. Data shown are representative of three individual experiments

The decrease in the SCO2-HRE(1-5)-p53-luc expression in U2OS cells indicated the possible involvement of interaction between p53 and HIF-1α in the regulation of SCO2 gene expression in hypoxia mimicking conditions. However, the huge increase in the induction of CA-IX(HRE)3-luc expression in both U2OS (~19 fold) and SaOS2 (~25 fold) in DSFX treated conditions raised a question that the changes observed in SCO2-HRE(1-5)-p53-luc transfected DSFX treated U2OS and SaOS2 cells (~1.4 fold induction) whether reflecting the transcriptional activity of HIF-1α or not.

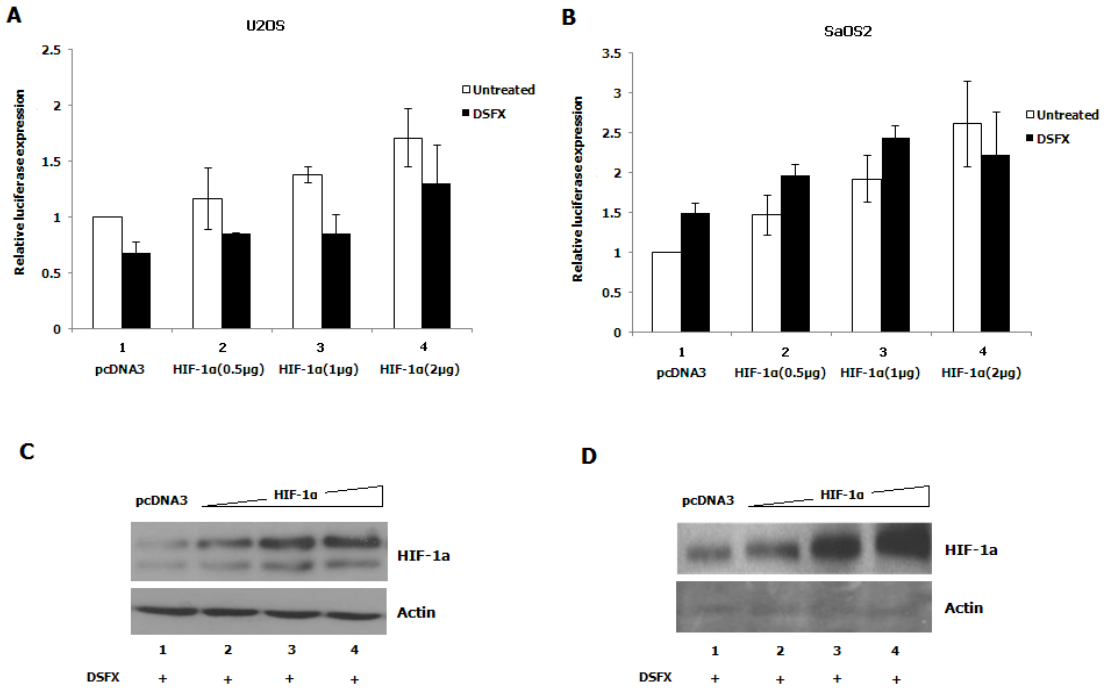

Figure 4.2.7: SCO2 gene expression in DSFX treated condition is HIF-1α independent

A. U2OS and B. SaOS2 cells were transfected with pcDNA3 or increasing amounts of HIF-1α expression vector along with SCO2-HRE(1-5)-p53-luc vector and β-galactosidase vector using Polyfect transfection reagent. 24 hours after transfection, the cells were treated with DSFX and incubated at 37° C for 16 hours. The cells were lysed using Promega luciferase lysis buffer (Promega., UK) and subjected to luciferase assay. 30μl of cell lysate was used to measure β-galactosidase expression. The values from the luciferase assay were normalized to the values from β-galactosidase experiment. C. and D. Western blots showing the expression level of HIF-1α protein in pcDNA or increasing amount of HIF-1α transfected and DSFX treated U2OS and SaOS2 cells respectively. Data shown are representative of three independent experiments.

To verify that the changes observed in the luciferase reporter assay is due to the transcriptional activity of HIF-1α, we performed a luciferase reporter assay with increased amounts of ectopically expressed HIF-1α expecting to magnify the changes observed in Figure 4.2.6. The transfection efficiency of the increased amounts of ectopically transfected HIF-1α in U2OS and SaOS2 cells were observed in the increased accumulation of HIF-1α protein in the western blotting of DSFX treated U2OS and SaOS2 cells (Figure 4.2.7 C and D).

Although the SCO2-HRE(1-5)-p53-luc expression has been increased with the increased accumulation of HIF-1α in DSFX treated U2OS and SaOS2 cells (Figure 4.2.7 A and B., compare black bars 4, 3 2 and 1), no significant changes in luciferase expression were observed between the DSFX treated and untreated cells (Figure 4.2.7 A and B., compare black bar with white bar in all the 4 lanes). This indicated that the increase in SCO2-HRE(1-5)-p53-luc expression was not due to the increased transcriptional activity of HIF-1α but could be due to the regulation of SCO2 transcription by other factors such as p53 and NF-κB whose binding sites are present in the luciferase vector (Figure 4.2.4 and Figure 4.2.5). However this notion needs further investigation of the HREs present in the SCO2 promoter region

4.2.5 Functional analysis of SCO2 HREs

In order to exhibit the transcriptional activation functions, HIF-1α needs to form a complex with HIF-β and the complex should be recruited to the HREs present in the regulatory region of the promoter of its target genes (Semenza, 1998). To investigate the functionality of the HREs present within the *SCO2* gene promoter untreated or DSFX treated U2OS cells were subjected to chromatin immuno-precipitation (ChIP) assay as mentioned in Materials and Methods, using a specific anti-HIF-1α ChIP grade antibody to precipitate HIF-1α chromatin immuno-complexes (Abcam, UK). The sequence of the primers used in this assay are listed in Table 3.9.2.

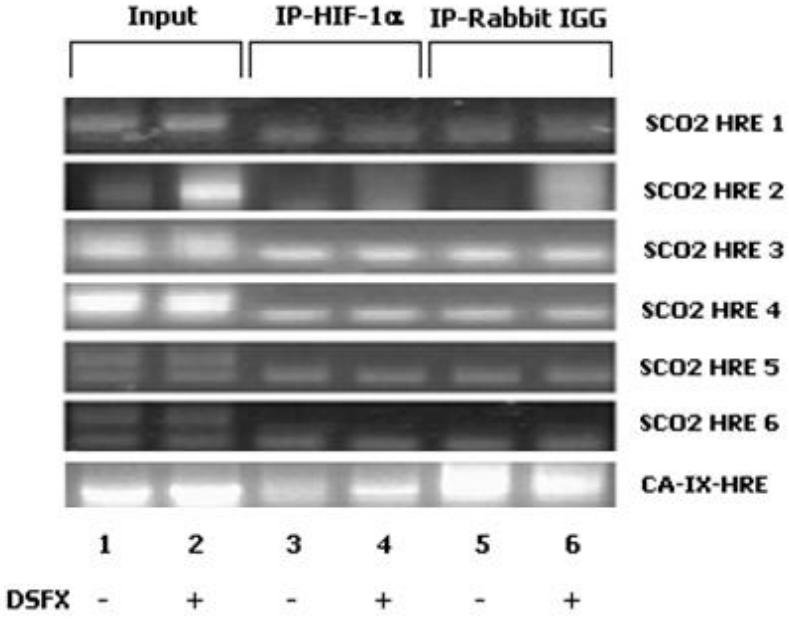

Figure 4.2.8: Functional analysis of HREs present in SCO2 promoter

Chromatin immuno-complexes were precipitated using a specific HIF-1α (lanes 3 and 4) or Rabbit IGG (lanes 5 and 6) as negative controls. The pulled down DNA was amplified with specific primers flanking the regions containing various HREs present in *SCO2* promoter. The resultant PCR product was then submitted to 2% agarose gel electrophoresis. CA-IX was used as a positive control (lane 4). Lanes 1 and 2 are 10% of the input.

10% of the input samples were used as control. Also the input was used as a positive control for the primers and the product size. Rabbit IGG which does not bind to any specific protein was used as a negative control and CA-IX was used as a positive control for the binding ability of HIF-1α to its target gene promoter in hypoxia mimicking conditions. As expected the binding of HIF-1α to the specific promoter of CA-IX flanking the HRE sequence was observed only in the DSFX treated cells but not in the untreated cells (Figure 4.2.8, compare lane 4 with lane 3). This indicated that HIF-1α was stabilized and the transcriptionally activity was induced in hypoxia mimicking conditions.

However, HIF-1α did not bind to any of the 6 tested HREs present in the SCO2 promoter region in hypoxia mimicking conditions (Figure 4.2.8., compare lane 4 and 3 with lane 2 and 1) indicated that HIF-1α might have not involved directly in the regulation of SCO2 gene expression. However, HIF-1α has been shown to interact with other transcription factors such as p53 and NF-κB and modulate their stability and

transcriptional functions (An et al., 1998; BelAiba et al., 2007; Bendinelli et al., 2009; Chen et al., 2003). In addition, HIF-1α has been reported to compete for transcription cofactors with p53 and NF-κB in hypoxic conditions (Arany et al., 1996; Mendonça et al., 2011; Schmid et al., 2004; Xenaki et al., 2008). Since p53 and NF-κB binding sites are found in the SCO2 promoter (Figure 4.2.4 and Figure 4.2.5) HIF-1α could potentially interact with these transcription factors and indirectly regulate the SCO2 gene expression.

4.3 Role of transcriptional co-factors in the regulation of TIGAR and SCO2 gene expression

While the contribution of the p53 tumour suppressor in the regulation of TIGAR gene expression under conditions of genotoxic stress has been shown (Bensaad et al., 2006), the transcriptional network modulating TIGAR gene expression in hypoxia has not been elucidated. The determination of the TIGAR protein and mRNA levels (Results presented in Section 1) indicated that factors other than p53 might be involved in the regulation of TIGAR gene expression in hypoxia mimicking conditions (Results 4.1.1, 4.1.2). Furthermore, experiments in cells where HIF-1α had been silenced by RNAi, supported the view that HIF-1α might be a potential candidate regulating TIGAR gene expression in hypoxia mimicking conditions (Result 4.1.3). This notion was strengthened by bio-informatics studies revealing the existence of putative HREs in the regulatory region of *TIGAR* gene promoter (Result 4.1.4). In addition, ChIP and luciferase experiments identified the HRE5 as a functional HIF-1α binding site and under hypoxia mimicking conditions HIF-1 binds to *TIGAR* gene promoter and regulates its gene expression (Result 4.1.5).

Results described in sections 4.1.1, 4.1.2 and 4.1.3 indicated that TIGAR protein and mRNA levels were differentially regulated in U2OS and SaOS2 cells treated with DSFX. In particular, upregulation of TIGAR gene expression was evident only in the presence of p53 (U2OS cells), whereas in its absence (SaOS2 cells) TIGAR gene expression was downregulated in hypoxia mimicking conditions. Furthermore, there was a difference in the TIGAR induction pattern when it was assessed in DSFX treated U2OS cells, using the TIGAR-HRE5,6-p53-luc luciferase reporter (Figure 4.1.8) compared to that observed in protein and mRNA levels (Figure 4.1.1, 4.1.2 and 4.1.3),

implying that the second p53 binding site (that was not included in the TIGAR-HRE5,6-p53-luc reporter) might be essential for p53 to exert its transcriptional activity on TIGAR gene expression. Another explanation for this difference could be provided by the fact that the fragment of the TIGAR promoter that was included in the TIGAR-HRE5,6-p53-luc reporter contained a putative binding site for E2F1 (Figure 4.1.6 A). It is known that while U2OS express wild type pRb tumour suppressor, SaOS2 cells express a non-functional form of pRb (p95) (Shew et al., 1990). Given the fact that pRb represses E2F1 transcriptional activity by preventing its binding to the promoters of its transcriptional targets (Trimarchi and Lees, 2002) the difference observed in the TIGAR-HRE5,6-p53-luc reporter activity in DSFX treated U2OS and SaOS2 cells could be due to the diverse E2F1 transcriptional activity in the two cell lines. In addition, the potential role of common p53, HIF-1α and E2F1 transcriptional co-factors in the regulation of TIGAR gene expression in DSFX treated U2OS and SaOS2 cells cannot be excluded.

On the other hand, SCO2 gene expression has been shown to be regulated by p53 (Matoba et al., 2006). However, the SCO2 protein (Figure 4.2.1 and Figure 4.2.1) and mRNA levels (Figure 4.2.3) in hypoxia mimicking conditions indicated the possible involvement of factors other than p53 in the regulation of SCO2 gene expression. Although bio-informatics studies revealed the presence of putative binding sites for HIF-1α and NF-κB in the regulatory region of the SCO2 gene promoter (Figure 4.2.4 and Figure 4.2.5), the luciferase experiments indicated that the regulation of SCO2 gene expression in hypoxia mimicking conditions is independent of the HIF-1α transcriptional activity. This conclusion is supported by ChIP assays showing that HIF-1α did not bind to the SCO2 promoter under hypoxia mimicking conditions (Figure 4.2.8). Nevertheless, the significant difference in the SCO2 luciferase expression between DSFX treated U2OS and SaOS2 cells suggested that HIF-1α was indirectly involved in the regulation of SCO2 gene expression potentially either through interaction with other transcription factors such as p53 (An et al., 1998; Blagosklonny et al., 1998; Schmid et al., 2004), NF-κB (Mendonça et al., 2011), or competition for p53 and HIF-1α common transcriptional co-factors such as p300/CBP and PCAF (Blagosklonny et al., 1998; Xenaki et al., 2008).

Under diverse stress conditions, both p53 and HIF-1α undergo post-translational modifications that alter their protein stability and transcriptional activity (Arany et al., 1996; Xenaki et al., 2008). Transcriptional co-factors such as p300/CBP (Arany et al., 1996; Gu and Roeder, 1997; Kallio et al., 1998; Liu et al., 1999), SRC-1 (Carrero et al., 2000; Lee et al., 1999) and PCAF (Liu et al., 1999; Xenaki et al., 2008) are among the co-factors shared between p53, p73, NF-κB and HIF-1α and modify their protein stability and transcriptional activity under diverse stress conditions. The role of PCAF as common transcriptional co-factor for p53 and HIF-1α in the regulation of genes involved in cell cycle arrest and apoptosis has been reported in the past (Xenaki et al., 2008). Since TIGAR and SCO2 genes are p53 transcription targets (Bensaad et al., 2006; Matoba et al., 2006) and HIF-1α is directly involved in the regulation of TIGAR gene expression and indirectly in the case of SCO2 (Results described in Chapters 1 and 2), we were interested to test the hypothesis whether PCAF determined the cellular energy production pathway by selectively acetylating p53 and HIF-1α, thereby differentially regulating TIGAR and SCO2 gene expression and hence the balance between glycolysis and OXPHOS.

4.3.1 TIGAR and SCO2 protein levels are affected by the HAT activity of PCAF

To investigate the involvement of PCAF in the regulation of TIGAR and SCO2 gene expression, the TIGAR and SCO2 protein levels were followed in U2OS cells transfected with PCDNA3, Flag-PCAFwt or Flag-PCAF-ΔHAT expression vectors. The Flag-PCAF-ΔHAT expresses a HAT defective mutant of PCAF which lacks histone acetyl transferase activity (Barbacci et al., 2004).

Accumulation of p53 protein was observed in etoposide treated U2OS cells (Figure 4.3.1 A and Figure 4.3.2 A., compare lanes 3, 6 and 9 with lanes 1, 4 and 7 respectively). Also, HIF-1α was stabilized in DSFX treated conditions (Figure 4.3.1 A and Figure 4.3.2 A., compare lanes 2, 5 and 8 with lanes 1, 4 and 7 respectively). The anti-flag antibody was used to show the transfection efficiency of PCAF and PCAFΔHAT in U2OS and SaOS2 cells (Figure 4.3.1 A and Figure 4.3.2 A). Densitometric analysis of the TIGAR and SCO2 proteins was carried out using ImageJ 1.43 software (Figure 4.3.1 B and Figure 4.3.2 B).

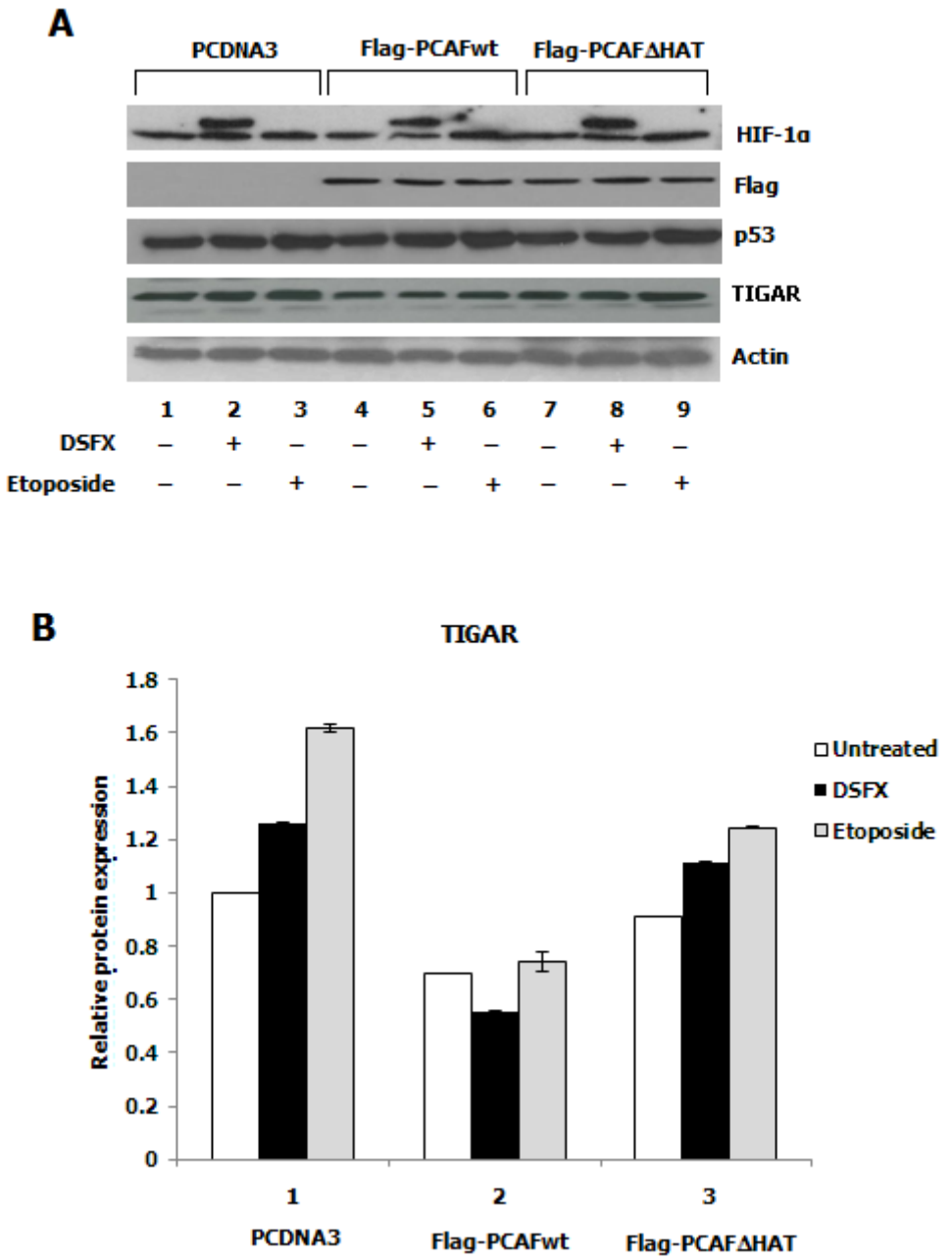

Figure 4.3.1: Role of PCAF in TIGAR protein expression

A. U2OS cells were transfected with either PCDNA3 (lanes 1 to 3) or Flag-PCAFwt (lanes 4 to 6) or Flag-PCAF-ΔHAT (lanes 7 to 9). 24 hours after transfection the cells were left untreated or treated with either DSFX or etoposide. 16 hours after treatment the cells were harvested and subjected to western blotting. B. Densitometric analysis of the TIGAR protein from Figure 4.3.1 A., was carried out using ImageJ 1.43. The data are representative of two independent experiments.

Downregulation of TIGAR protein expression in DSFX treated U2OS cells ectopically expressing PCAFwt was reversed in cells transfected with PCAF-ΔHAT (Figure 4.3.1 A., compare lanes 5 and 8 with lanes 4 and 7 respectively; Figure 4.3.1 B., compare black bar 2 and 3 with white bars 2 and 3 respectively). This indicated the repressive effect of the HAT activity of PCAF in TIGAR protein levels in hypoxia mimicking conditions. At the same time, in etoposide treated cells overexpression of PCAFwt did not downregulate TIGAR protein level (Figure 4.3.1 A., compare lane 6 with lane 4; Figure 4.3.1 B., compare grey bar 2 with white bar 2). TIGAR protein level was upregulated in etoposide treated U2OS cells transfected with PCAF-ΔHAT (Figure 4.3.1 A., compare lane 9 with lane 6; Figure 4.3.1 B., compare gray bar 3 with white bar 3). While PCAFwt downregulated the TIGAR protein level only in DSFX treated cells, PCAF-ΔHAT upregulated TIGAR protein level in cells treated with either DSFX or etoposide. Given that HIF-1α and p53 are recruited to TIGAR promoter in DSFX and etoposide treated cells ((Bensaad et al., 2006) and Figure 4.1.7) the results presented in Figure 4.3.1 imply that the HAT activity of PCAF might facilitate the selective recruitment of HIF-1α and/or p53 in the TIGAR promoter in DSFX and etoposide treated cells. This observation is in line with our previous finding indicating that p53 and HIF-1α compete for PCAF in the regulation of anti and pro-apoptotic gene expression (Xenaki et al., 2008).

SCO2 protein levels, on the other hand, were downregulated in DSFX treated U2OS cells ectopically expressing PCAFwt, which was reversed in cells transfected with PCAF-ΔHAT mutant vector (Figure 4.3.2 A., compare lanes 5 and 8 with lanes 4 and 7 respectively; Figure 4.3.2 B., compare black bars 2 and 3 with white bars 2 and 3 respectively). Downregulation of SCO2 protein levels was also observed in etoposide treated cells transfected with PCAFwt (Figure 4.3.2 A., compare lane 3 to lane 6 and Figure 4.3.2 B., compare gray bar 2 to grey bar 1). This downregulation was reversed when PCAF-ΔHAT was transfected in etoposide treated U2OS cells (Figure 4.3.2 A., compare lane 3 to lane 9 and Figure 4.3.2 B., compare gray bar 3 to grey bar 1).

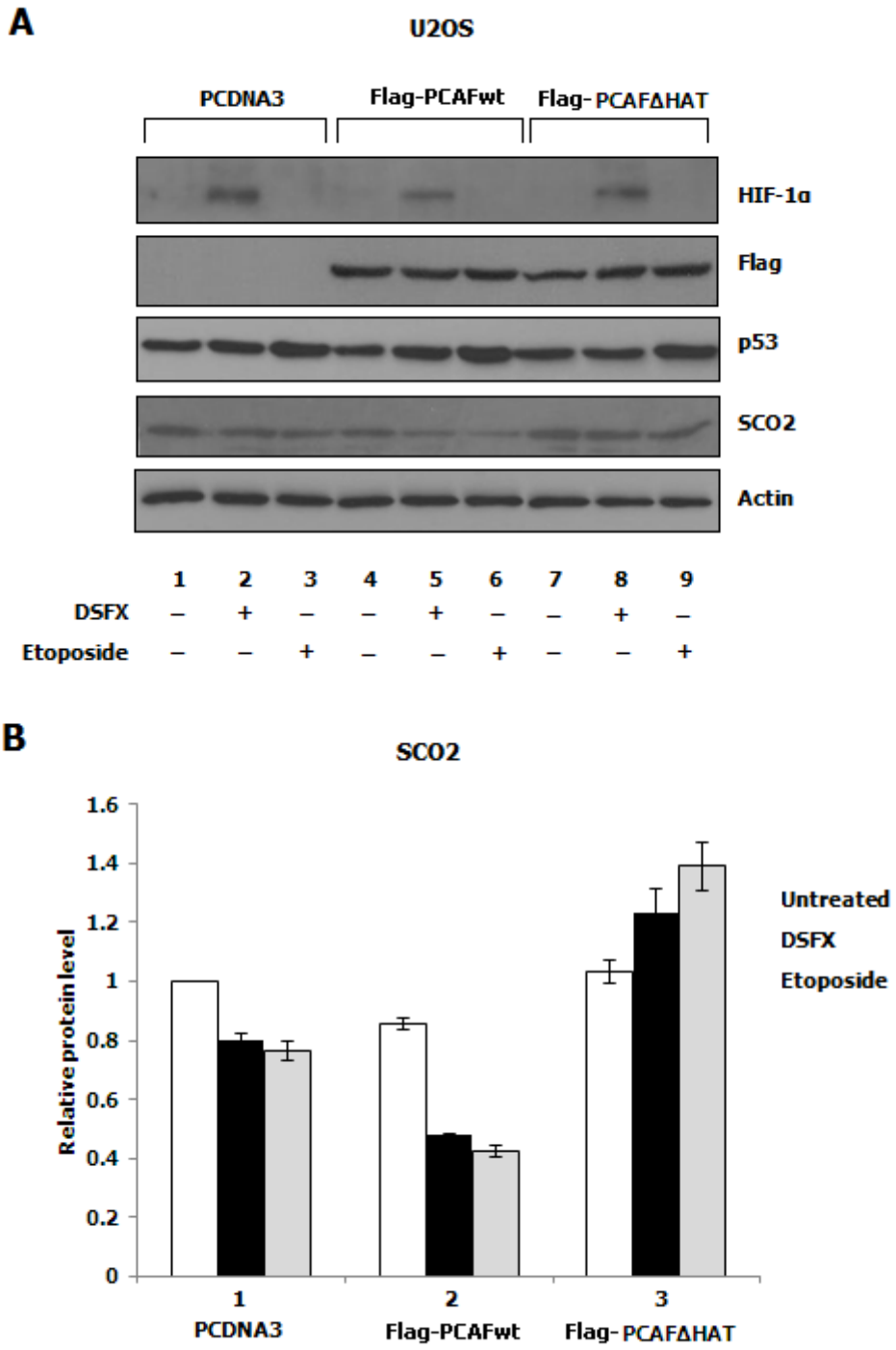

Figure 4.3.2: Role of PCAF in SCO2 protein expression

A. U2OS cells were transfected with either PCDNA3 (lanes 1 to 3) or Flag-PCAFwt (lanes 4 to 6) or Flag-PCAF-ΔHAT (lanes 7 to 9). 24 hours after transfection the cells were left untreated or treated with either DSFX or etoposide. 16 hours after treatment the cells were harvested and subjected to western blotting. **B.** Densitometric analysis of the SCO2 protein from Figure 4.3.2 A., was carried out using ImageJ 1.43. The data are representative of two independent experiments.

This result implies that the HAT activity of PCAF plays a role in the modulation of SCO2 protein levels in U2OS cells treated with either DSFX or etoposide. Results shown in Figure 4.2.8 indicated that HIF-1α was not recruited to the regulatory region of the SCO2 promoter in DSFX treated U2OS cells conditions while p53 has been shown to bind SCO2 promoter under DNA damage conditions (Matoba et al., 2006). Taken together these observations indicate that the HAT activity of PCAF plays an important role in the regulation of SCO2 gene expression under DSFX and etoposide treated conditions. However, this conclusion requires further experimental support since the half-life of the SCO2 protein could be affected by various factors under different stress conditions. To investigate whether the fluctuation of the SCO2 protein levels under different stress conditions was due to transcriptional regulation of its gene expression, the SCO2 mRNA levels were investigated in cells after DSFX and etoposide treatment.

4.3.2 Role of PCAF HAT activity in the regulation of TIGAR and SCO2 mRNA levels

To investigate whether PCAF mediated regulation of TIGAR and SCO2 gene expression occurs at the transcriptional level, TIGAR and SCO2 mRNA levels were followed in U2OS cells transfected with PCDNA3 empty, PCAFwt or PCAF-ΔHAT expression vectors and treated with DSFX or etoposide or left untreated for 16 hours. Total mRNA from these cells was extracted and reverse transcribed to cDNA, which was then subjected to qRT-PCR to estimate TIGAR and SCO2 mRNA levels.

The low level of TIGAR mRNA expressed in PCAFwt transfected and DSFX treated cells (Figure 4.3.3 A., compare black bar 2 with black bar 1) comply with the protein expression pattern observed in U2OS cells (Figure 4.3.1 A and B). Similar to TIGAR protein levels (Figure 4.3.1), transfection of the PCAF-ΔHAT mutant which lacks acetylation activity, resulted in the reversion of the repressive effect exerted by the PCAFwt ectopic expression in DSFX treated cells (Figure 4.3.3 A., compare black bar 3 with black bar 2). These results indicated that the HAT activity of PCAF exerted suppressive effect on the regulation of TIGAR gene expression in hypoxia mimicking conditions.

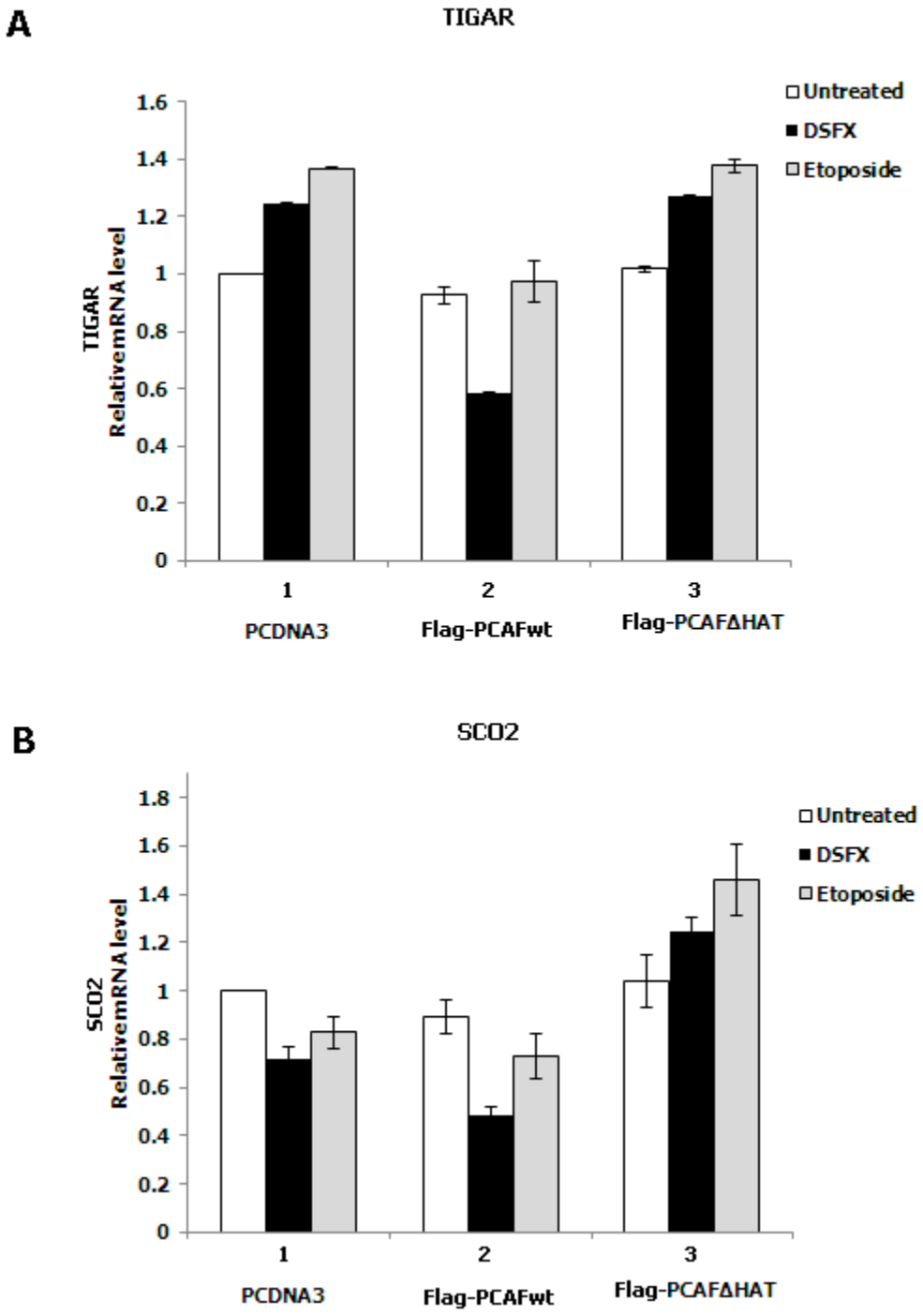

Figure 4.3.3: Regulation of TIGAR gene expression by PCAF, occurs at the transcriptional level

U2OS cells were transfected with either PCDNA3 (bars 1) or PCAF (bars 2) or PCAFΔHAT (bars 3). 24 hours after transfection the cells were left untreated or treated with either DSFX or etoposide. 16 hours after treatment the total mRNA from the cells were extracted and subsequently reverse transcribed. The resultant cDNA was then subjected to qRT-PCR using specific primers flanking TIGAR **(A)** or SCO2 **(B)** mRNA sequences. The equal expression of PCAF and PCAFΔHAT in U2OS under DSFX and etoposide treated conditions are shown in Figure 4.3.1 A and Figure 4.3.2 A. The data are representative of three independent experiments.

On the other hand, in line with the pattern of protein levels in DSFX treated conditions (Figure 4.3.1 A lanes 2, 5, 6 and Figure 4.3.1 B, black bars), PCAFwt transfection had repressive effect on SCO2 mRNA in DSFX treated U2OS cells (Figure 4.3.3 B., compare black bar 2 with black bar 1), which was reversed in cells transfected with PCAF-ΔHAT (Figure 4.3.3 B., compare black bar 3 with black bar 2) indicating that SCO2 gene expression was suppressed by the HAT activity of PCAF in hypoxia mimicking conditions. Although this suppressive effect was not observed in PCAFwt transfected cells in etoposide treated conditions, the high mRNA levels observed in PCAF-ΔHAT transfected cells (Figure 4.3.3 B., compare gray bar 3 with gray bar 2) implied potential involvement of the HAT activity of PCAF in the regulation of SCO2 gene expression in etoposide treated conditions.

4.3.3 Role of PCAF in the transcriptional regulation of TIGAR and SCO2 gene expression

To further explore the role of PCAF in the transcriptional regulation of TIGAR and SCO2 gene expression, luciferase reporter assays were performed using TIGAR-HRE5,6-p53-luc and SCO2-HRE(1-5)-p53-luc reporter vectors containing specific HREs and p53 binding sites identified within the regulatory region of the promoter of TIGAR and SCO2 genes respectively. U2OS and SaOS2 cells were transfected with TIGAR or SCO2 luciferase reporter vector, β-galactosidase, and HIF-1α along with PCDNA3 or increasing amounts of PCAFwt or PCAF-ΔHAT (Figure 4.3.4 and Figure 4.3.5). 24 hours after transfection the cells were treated with DSFX for further 16 hours at 37°C. The cell lysates were subjected to luciferase reporter assay. β-galactosidase expression was used as a transfection efficiency control.

TIGAR-HRE5,6-p53-luc reporter activity was progressively downregulated in response to increasing amounts of PCAFwt transfected cells (Figure 4.3.4 A., compare bars 2 and 3 to bar 1). This trend was gradually reversed in cells overexpressing increasing amounts of PCAF-ΔHAT in a dose dependent manner (Figure 4.3.4 A., compare bars 4 and 5 to bars 2, and 3 respectively).

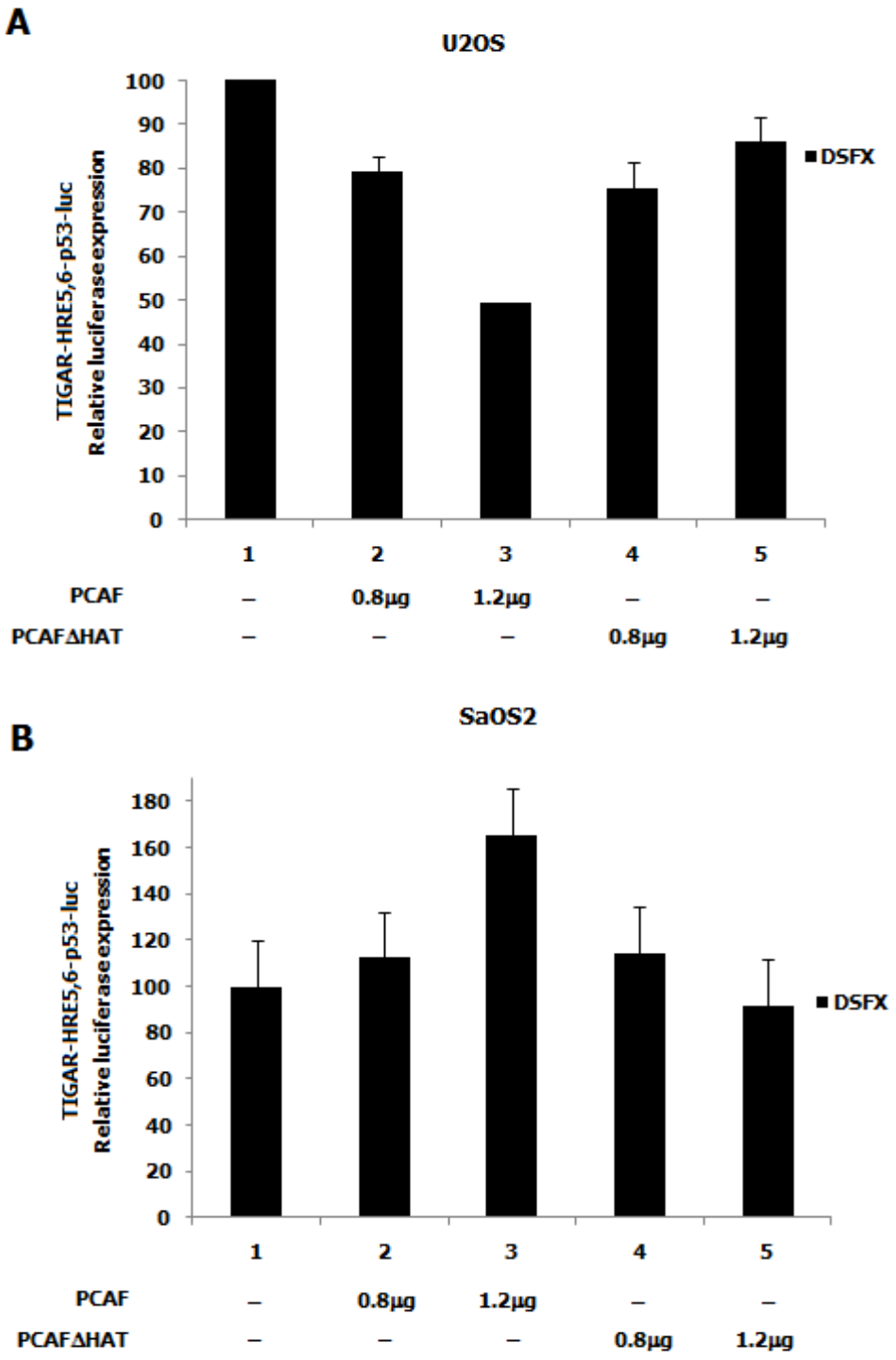

Figure 4.3.4: The involvement of PCAF HAT activity in the regulation of TIGAR gene expression

A. U2OS and B. SaOS2 cells were co-transfected with TIGAR-HRE5,6-p53BS2-Luc, β-galactosidase and HIF-1α expression vector along with either PCDNA3 or increasing amounts of PCAFwt or PCAF-ΔHAT and treated with DSFX as shown in the Figure 4.3.6 A and Figure 4.3.6 B respectively. Data shown are representative of two independent experiments in duplicates.

These results support the conclusions presented in Result sections 4.3.1 and 4.3.2 demonstrating that the HAT activity of PCAF exhibits repressive role in the regulation of TIGAR gene expression in hypoxia mimicking conditions. In DSFX treated SaOS2 cells transfection of increasing amounts of PCAFwt resulted in the gradual increase of the TIGAR-HRE5,6-p53-luc reporter activity (Figure 4.3.4 B., compare bars 2 and 3 to bar 1) whereas transfection of gradually increasing amounts of PCAF-ΔHAT exhibited the opposite trend (Figure 4.3.4 B., compare bars 4 and 5 to bars 2, and 3 respectively). The effect of the HAT activity of PCAF in SaOS2 cells was the opposite of that observed in U2OS cells (compare Figure 4.3.4 B., to Figure 4.3.4 A).

Luciferase reporter assays performed in U2OS (Figure 4.3.5 A and SaOS2 cells (Figure 4.3.5 B) using the SCO2-HRE(1-5)-p53-luc reporter in hypoxia mimicking conditions showed that increasing amounts of PCAFwt gradually downregulated the activity of this reporter in U2OS cells (Figure 4.3.5 A., compare bars 2 and 3 to bar 1) whereas the opposite was the case for the SaOS2 cells under the same conditions where gradually increasing quantities of PCAFwt transfection upregulated the activity of the SCO2-HRE(1-5)-p53-luc reporter (Figure 4.3.5 B., compare bars 2 and 3 to bar 1). In DSFX treated U2OS cells transfected with increasing amounts of PCAF-ΔHAT a slight reversion of the repressive effect of the PCAFwt was evident (Figure 4.3.5 A, compare bars 4 and 5 to bars 2, and 3 respectively). Reversion of the upregulating effect of PCAFwt in the luciferase activity of the SCO2-HRE(1-5)-p53-luc reporter was observed in DSFX treated SaOs2 cells transfected with increasing amounts of PCAF-ΔHAT (Figure 4.3.5 B, compare bars 4 and 5 to bars 2, and 3 respectively). Taken together these results provided evidence for the involvement of the HAT activity of PCAF in the regulation of TIGAR and SCO2 gene expression.

Furthermore the fact that the suppressive role of PCAFwt in TIGAR and SCO2 gene expression was observed only in U2OS cells and not in SaOS2 cells suggests that this cofactor mediates a complex regulatory effect on the activity of both HIF-1α and p53 transcription factors.

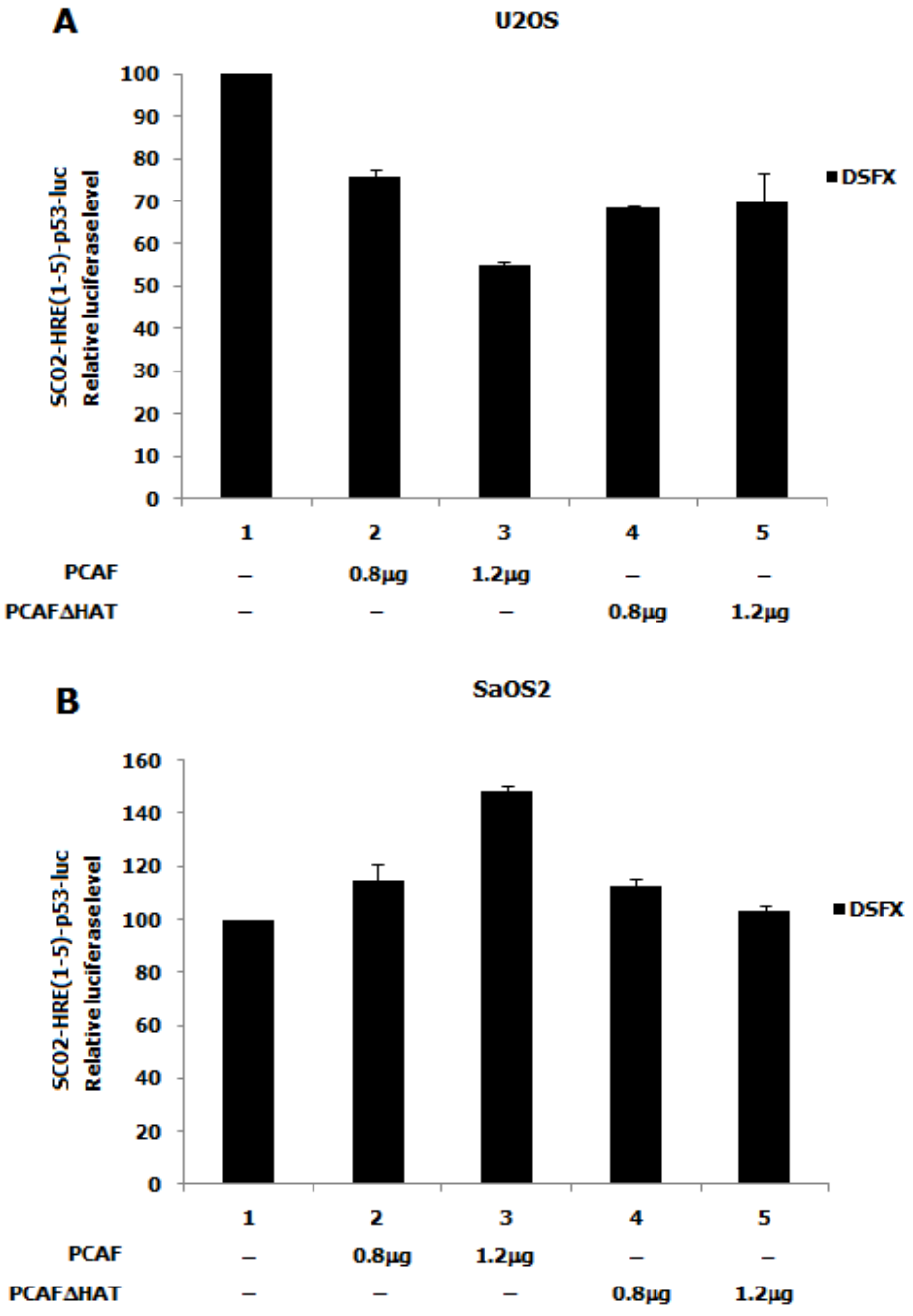

Figure 4.3.5: Role of PCAF in the transcriptional regulation of SCO2 gene expression

A. U2OS and B. SaOS2 cells were transfected with TIGAR-HRE5,6-p53BS2-Luc vector, β-galactosidase and HIF-1α expression vector along with either PCDNA3 or increasing amounts of PCAF or PCAFΔHAT expression vectors. 24 hours after transfection, the cells were treated with DSFX and incubated in 37°C for 16 hours. The cell lysates were subjected to luciferase assay. 30µl of the lysate was used to measure β-galactosidase expression. The values from the luciferase assay were normalized to the values from β-galactosidase experiment. Data shown are representative of two independent experiments in duplicates.

The differential effects of the HAT activity of PCAF in the presence or absence of p53 in hypoxic conditions on the TIGAR and SCO2 gene expression could be exemplified by competition events occurring between the two transcription factors for the limiting amounts of PCAF in U2OS cells which results in preferential co-activation between HIF-1α and p53 (Xenaki et al., 2008). This notion is supported by the upregulation of TIGAR and SCO2 gene expression in SaOS2 cells (Figure 4.3.4 B and Figure 4.3.5 B) where there is no competition between p53 and HIF-1α due to the absence of p53 in SaOS2 cell. This could have led to more acetylation of HIF-1α by PCAF in SaOS2 cells compared to U2OS cells. However, PCAF is a common co-factor for HIF-1α and p53, in DSFX treated U2OS cells where both HIF-1α and p53 are stabilized, the expression of luciferase reporters which include binding sites for both HIF-1α and p53 did not give clear indication that whether PCAF binds to HIF-1α or p53 in order to recruit them to their binding sites in TIGAR and SCO2 gene promoters. Further experiments such as ChIP, co-immunoprecipitation are required to find out whether PCAF recruits HIF-1α or p53 to the promoters of TIGAR and SCO2 genes.

To investigate whether this suppressive role of PCAF was reflected at the protein level, we followed the TIGAR and SCO2 protein expression in DSFX treated U2OS and SaOS2 cells, transfected with PCDNA3 or Flag-PCAF or Flag-PCAF-ΔHAT expression vectors and treated with DSFX for 16 hours. Anti-Flag antibody was used to estimate the transfection efficiency of these plasmids in U2OS and SaOS2 cells. Actin was used as a loading control.

As seen in the luciferase expression, the TIGAR protein expression was also downregulated gradually in DSFX treated U2OS cells in response to the increasing amount of PCAF (Figure 4.3.6 A., compare lanes 2, 3 and 4 with lane 1) which was reversed gradually in a dose dependent manner as ectopic expression of PCAF-ΔHAT increases (Figure 4.3.6 A., compare lanes 5, 6 and 7 with lane 1) indicated the repressive role of PCAF HAT activity in the regulation of TIGAR protein expression in hypoxia mimicking conditions.

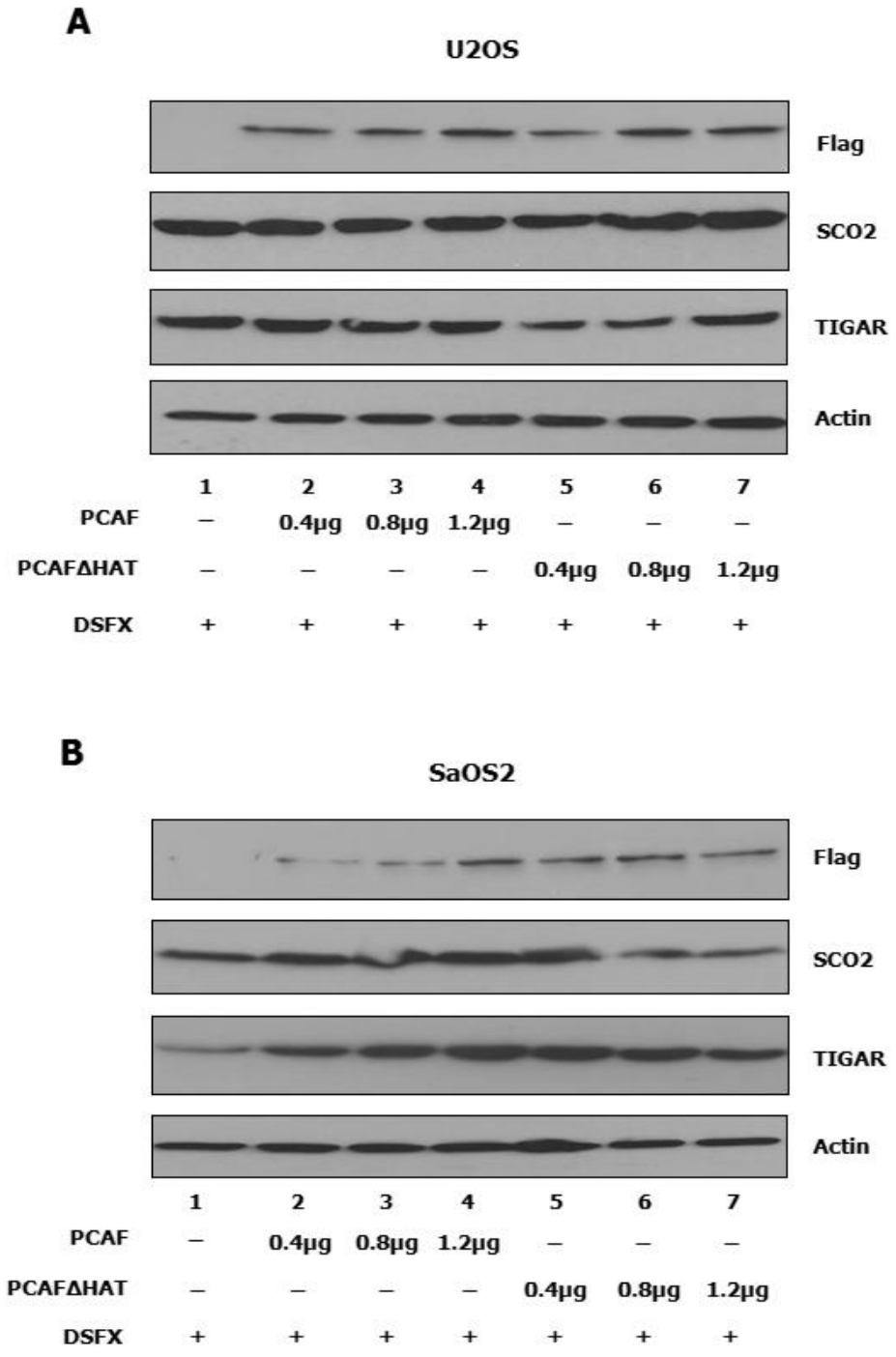

Figure 4.3.6: Role of PCAf in the regulation of TIGAR and SCO2 protein expression

A. U2OS and B. SaOS2 cells were transfected with PCDNA3 or Flag-PCAF or Flag-PCAFΔHAT and 24 hours after transfection treated with DSFX. 16 hours after treatment the cell lysates were subjected to western blot analysis. Anti-flag antibody was used to measure the amounts of PCAF and PCAFΔHAT transfection. Actin was used as a loading control. The data are representative of two independent experiments.

Also in line with the luciferase expression pattern, in DSFX treated p53 null SaOS2 cells showed gradual upregulation of TIGAR protein expression as the ectopic expression of PCAF went up (Figure 4.3.6 B., compare bars 2, 3 and 4 with bar 1) which was reversed gradually in response to increasing amount of PCAF-ΔHAT transfection (Figure 4.3.6 B., compare lanes 5, 6 and 7 with bar 1) indicated the inductive role of PCAF HAT activity in the TIGAR protein expression in the absence of p53 in hypoxia mimicking conditions.

Together, these experiments suggest that PCAF HAT activity plays an important role in the regulation of TIGAR and SCO2 gene expression in hypoxia mimicking conditions. PCAF downregulates *TIGAR* and *SCO2* gene expression when it acetylates both HIF-1α and p53 and it upregulates TIGAR and SCO2 gene expression when it acetylates HIF-1α alone (in the absence of p53).

As evidenced in previous reports (Xenaki et al., 2008), both HIF-1α and p53 might compete for PCAF in hypoxia mimicking conditions, in U2OS cells where both HIF-1α and p53 are present, only limited amount of PCAF will be available for HIF-1α acetylation. On the other hand, since p53 is absent in SaOS2 cells, more PCAF will be available for HIF-1α acetylation. In SaOS2 cells, the more acetylated HIF-1α might upregulate the TIGAR gene expression and in U2OS cells, the less acetylated HIF-1α might downregulate the TIGAR gene expression.

Similarly, the acetylated p53 in U2OS cells, might down-regulate the SCO2 gene expression. Also, in SaOS2S which express non-functional form of pRb thus having increased E2F1 transcriptional activity (Shew et al., 1990), and PCAF is the major acetyl transferase involved in E2F1 acetylation (Pillai et al., 2010), the upregulation of SCO2 gene expression in SaOS2 cells in hypoxia mimicking conditions might involve a complex network of transcriptional regulation by HIF-1α and E2F1 mediated by PCAF HAT activity.

4.4 Functional consequences of PCAF mediated TIGAR and SCO2 gene expression

Recent reports have demonstrated that the regulation of *TIGAR* gene expression is under the transcriptional control of p53 (Bensaad et al., 2006). Our results described in Section 4.1 indicated that under hypoxia mimicking conditions, HIF-1α plays an important regulatory role in *TIGAR* gene expression. Results presented in Section 4.3 showed that the regulation of *TIGAR* gene expression in hypoxia is controlled by a complex network of transcription factors involving HIF-1α and p53 and implicating the HAT activity of PCAF as a crucial regulatory factor. Results shown in Section 4.3 also pointed out that in PCAF-ΔHAT ectopically expressing and DSFX treated U2OS cells, TIGAR is downregulated at both protein and mRNA levels. Moreover, results in Section 4.3 demonstrated that in DSFX treated SaOS2 cells, PCAFΔHAT overexpression resulted in the upregulation of TIGAR gene expression. The differential regulation of *TIGAR* gene expression in the presence or absence of p53 in hypoxia mimicking conditions coordinated by the HAT activity of PCAF implied that PCAF mediated acetylation of p53 and/or HIF-1α allows selective recruitment of one or the other transcription factor to the *TIGAR* promoter in a manner dependent on the environmental conditions.

Results shown in Section 4.2 revealed that the gene expression of the known p53 transcriptional target *SCO2* (Matoba et al., 2006), in hypoxia mimicking conditions is regulated independently of the p53 status. This suggested that, a hypoxia responsive transcription factor might be involved in the regulation of *SCO2* gene expression in hypoxia. However, further studies demonstrated that HIF-1α was not directly involved in the regulation of *SCO2* gene expression (Section 4.2.4 and 4.2.5). Nevertheless, the differential SCO2 protein and mRNA levels in cells bearing wild type or defective p53 in hypoxia mimicking conditions, indicated that HIF-1α might be involved in the regulation of *SCO2* gene expression indirectly by other transcription factors such as E2F1 or NF-κB associated with HIF-1α and for which DNA binding sites have been identified within the *SCO2* promoter, or could be a result of competition for binding with transcriptional co-factors such as p300/CBP or PCAF, which are common for HIF-1α (Lim et al., 2010), E2F1 (Pediconi et al., 2009) and NF-κB (Zhong et al., 1998).

Support to the latter is provided by the observations described in Section 5.3 indicating that the HAT activity of PCAF plays a major role in the regulation of *SCO2* gene expression by acetylating p53 and/or HIF-1α thereby regulating their transcriptional activity and selectively targeting these transcription factors to a specific subset of their promoters.

TIGAR and SCO2 are involved in the regulation of cellular energy metabolism by modulating glycolysis (Bensaad et al., 2006) and OXPHOS (Bensaad et al., 2006; Matoba et al., 2006) respectively. In particular TIGAR has been shown to inhibit glycolysis -therefore lactic acid production as well- whereas SCO2 to increase OXPHOS and hence oxygen consumption. Given that PCAF plays important role in the regulation of *TIGAR* and *SCO2* gene expression in hypoxia mimicking conditions as demonstrated in Section 4.3 we were intrigued to assess its role in the regulation of TIGAR and SCO2 mediated glycolysis and OXPHOS.

4.4.1 Lactate Production

HIF-1α has been shown to increase the lactate production by inducing the expression of genes encoding glycolytic enzymes such as aldolase-A, phosphoglycerate kinase-1, pyruvate kinase M, lactate dehydrogenase A, phosphofructokinase (PFK), and glucose transporter-1 (Glut-1) which are induced in hypoxic conditions (Firth et al., 1994; Firth et al., 1995; Minchenko et al., 2002; Semenza et al., 1994). To confirm that lactate production was affected in our experimental conditions we silenced the expression of HIF-1α in DSFX treated U2OS cells using specific RNAi against HIF-1α and determined the lactate production in the media the cells were cultured collected at 0 minutes and 16 hours after treatment. 10µl of the media was then added to 60µl of lactate reagent (Trinity Biotech, Dublin) and the absorbance of the resultant mixture was measured at 540nM. A standard curve was prepared using lactate standard solutions (Trinity Biotech, Dublin).

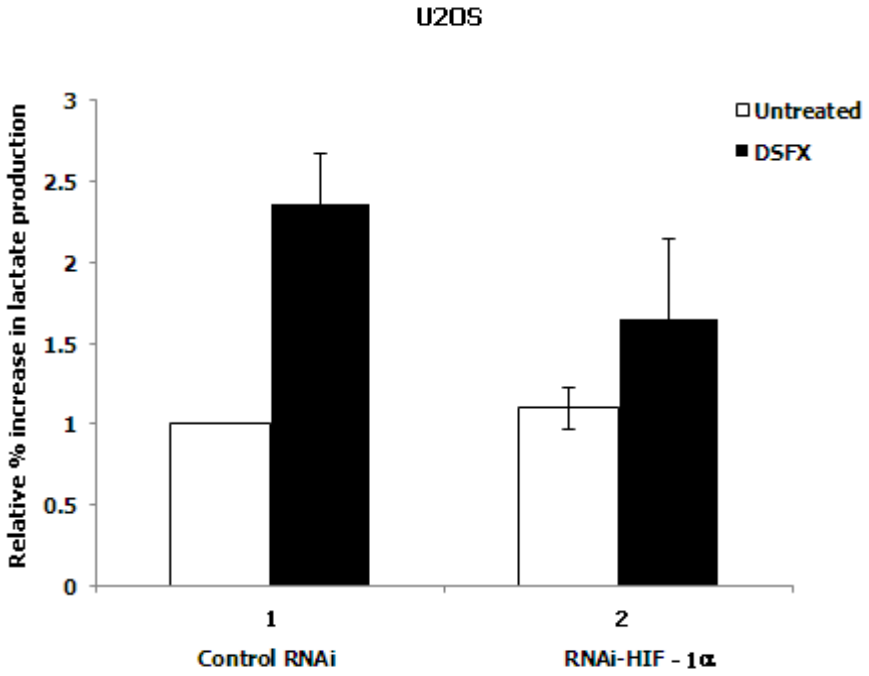

Figure 4.4.1: HIF-1α regulates lactate production

U2OS cells were transfected with scrambled RNAi (Control RNAi) or RNAi-HIF-1α and left untreated or treated with DSFX for 16 hours. Media from these cells was collected before, 0 min and 16 hours after the addition of DSFX. Lactate reagent (Trinity Biotech, Dublin) was added to the media and the absorbance at 540nm was measured. A standard curve was prepared using lactate standards (Trinity Biotech, Dublin). The efficiency of HIF-1α silencing is shown in Figure 4.1.4. Data shown are representative of three independent experiments.

The involvement of HIF-1α in the regulation of lactate production was evident as DSFX treated U2OS cells transfected with scramble RNAi exhibited increased lactate production compared to those transfected with RNAi against HIF-1α under the same conditions (Figure 4.4.1, compare black bar 2 with black bar 1). Still, even in the absence of HIF-1α, DSFX treated cells produced higher lactate levels compared to the untreated cells (Figure 4.4.1, compare black bar 2 with white bar 2).

TIGAR has been shown to inhibit glycolysis and reduce lactate production (Bensaad et al., 2006). Results shown in Figure 4.1.1 and Figure 4.1.3 indicated that in hypoxia mimicking conditions, TIGAR protein levels were differentially regulated in DSFX treated cells in the presence or in the absence of HIF-1α. Since decrease in glycolysis is one of the major consequences of TIGAR induction (Bensaad et al., 2006) we were

intrigued to investigate whether TIGAR overexpression reduces lactate production in DSFX treated U2OS cells. To this direction we analysed lactate production in DSFX treated U2OS cells transfected with either empty vector (PCDNA3) or a TIGAR expressing construct. In accord with previously published observations (Kimata et al., 2010), TIGAR overexpression in DSFX treated cells, reduced the lactate production compared to PCDNA3 transfected cells (Figure 4.4.2.), compare black bar 2 with black bar 1) signifying the ability of TIGAR to inhibit glycolysis and hence lactate production (Bensaad et al., 2006).

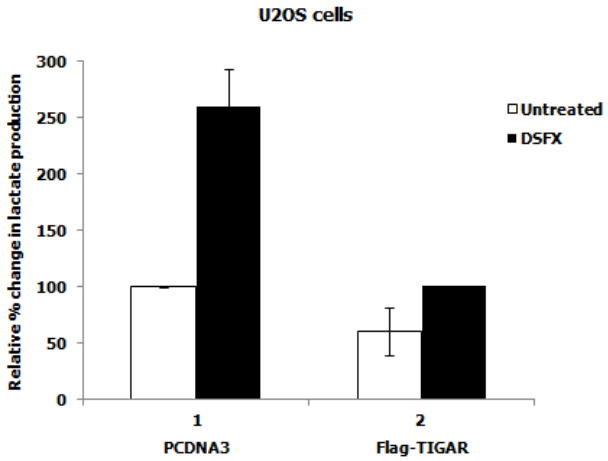

Figure 4.4.2: TIGAR overexpression reduces lactate production in hypoxic conditions

U2OS cells were transfected with either PCDNA3 or Flag-TIGAR expressing vector and left untreated or treated with DSFX for 16 hours. The media was collected at 0 minute and 16 hours after treatment and lactate production was measured. The data is representative of 3 independent experiments.

To investigate the role of the HAT activity of PCAF in the regulation of lactate production, lactate levels were determined in DSFX treated or untreated cells transfected with either empty (PCDNA3) or PCAFwt, or PCAF-ΔHAT expression vectors. Consistently with TIGAR cellular levels increased lactate production was observed in PCAFwt transfected cells and decreased in those ectopically expressing PCAF-ΔHAT (Figure 4.4.3 A, compare black bar 2 with black bars 1 and 3) indicating that the HAT activity of PCAF promoted upregulation of glycolysis in hypoxia mimicking conditions.

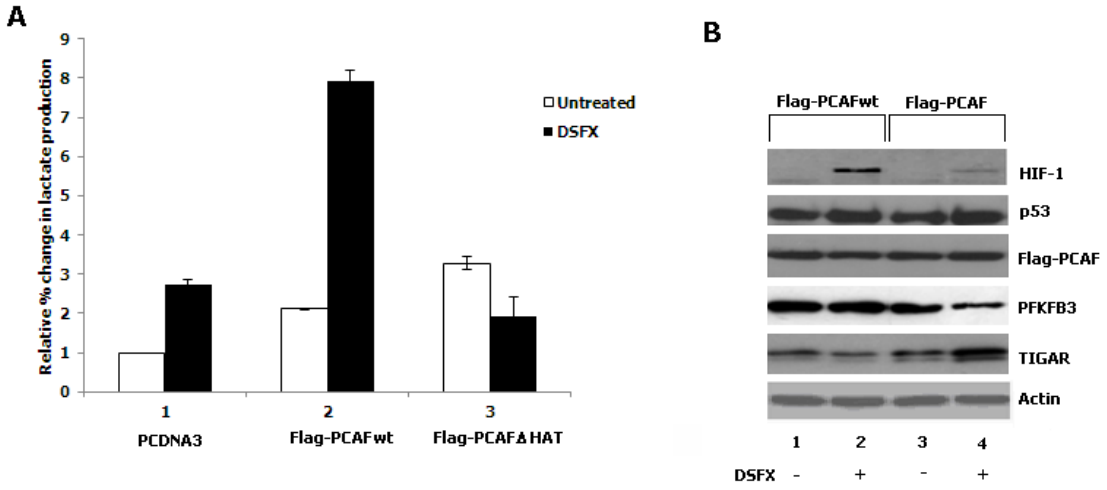

Figure 4.4.3: Role of PCAF in the regulation of lactate production mediated by TIGAR

A. U2OS cells were transfected with either PCDNA3 or PCAFwt or PCAFΔHAT expression vectors and left untreated or treated with DSFX. Media was collected immediately and 16 hours after treatment and lactate production was determined as described in Materials and Methods. Lactate production values normalized to the number of cells. The data are representative of three independent experiments. B. U2OS cells transfected with either PCAFwt or PCAFΔHAT and untreated or treated with DSFX as indicated, were subjected to western blot analysis. Actin was used as a loading control. Equal PCAFwt and PCAF-ΔHAT transfection was confirmed blotting with the anti-Flag antibody. Data shown are representative of two independent experiments.

The results shown in Figure 4.4.3 might be a consequence of PCAF mediated acetylation of HIF-1α and subsequent prevention of the recruitment of the acetylated transcription factor to the *TIGAR* promoter Figure 4.1.7 and subsequent inhibitory effect on *TIGAR* gene expression and promotion of glycolysis.

TIGAR has been shown to share structural and functional similarities with the phosphatase domain of the bi-functional enzyme PFK2/FBPase-2 (Bensaad et al., 2006). PFKFB3, an isozyme of PFK2/FBPase-2 has 700 times higher kinase compared to its phosphatase activity (Obach et al., 2004; Sakakibara et al., 1997). Given that PFKFB3 is a HIF-1α transcription target and its expression is induced in hypoxic conditions the formation of F2,6-BP is induced under these conditions leading to increased glycolytic rate (Lehninger et al., 2005; Obach et al., 2004). As the inhibitory effect of PCAF on TIGAR gene expression resulted in the upregulation of glycolysis, we explored the possibility that PCAF mediated acetylation of HIF-1α selectively

targets this transcription factor to the promoter of the glycolytic *PFKFB3* and concurrently prevents the recruitment of this transcription factor to the glycolytic inhibitor *TIGAR*. This assumption was tested in not treated or DSFX treated U2OS cells over expressing PCAFwt or PCAF-ΔHAT. Decreased PFKFB3 and concomitant increased TIGAR protein levels were observed in DSFX treated U2OS cells overexpressing PCAF-ΔHAT (Figure 4.4.3 B, compare lane 4 with lane 2). These findings might support the notion that the HAT activity of PCAF is crucial in the regulation of glycolysis in hypoxia mimicking conditions by regulating *TIGAR* and *PFKFB3* gene expression, but further experiments in other cell lines are required to confirm this assumption.

4.4.2 Oxygen consumption

SCO2 plays an important role in the assembly of the COX complex, the major site of oxygen utilization in eukaryotic cells (Matoba et al., 2006). The disruption of *SCO2* gene expression in wild type p53 expressing cells leads to down-regulation of oxygen consumption which resembles the metabolic phenotype observed in $p53^{-/-}$ cells (Matoba et al., 2006). However, the total ATP production in SCO2wt and SCO2 defective cells did not change implying that cells bearing mutant SCO2 compensate their energy requirements by upregulating the glycolytic pathway. Support to this view was provided by observations indicating elevated lactate production in these cells (Kimata et al., 2010; Matoba et al., 2006).

Results presented in Section 4.3 allowed the hypothesis that the HAT activity of PCAF might be involved in the regulation of *SCO2* gene expression in hypoxia mimicking conditions (Figure 4.3.6). These results triggered our interest to study the role of PCAF in oxygen consumption and OXPHOS regulation in hypoxic cells. To this direction oxygen consumption was monitored in untreated and DSFX treated U2OS cells transfected with PCDNA3, TIGAR or SCO2 along with PCDNA3, PCAFwt or PCAF-ΔHAT expression vectors.

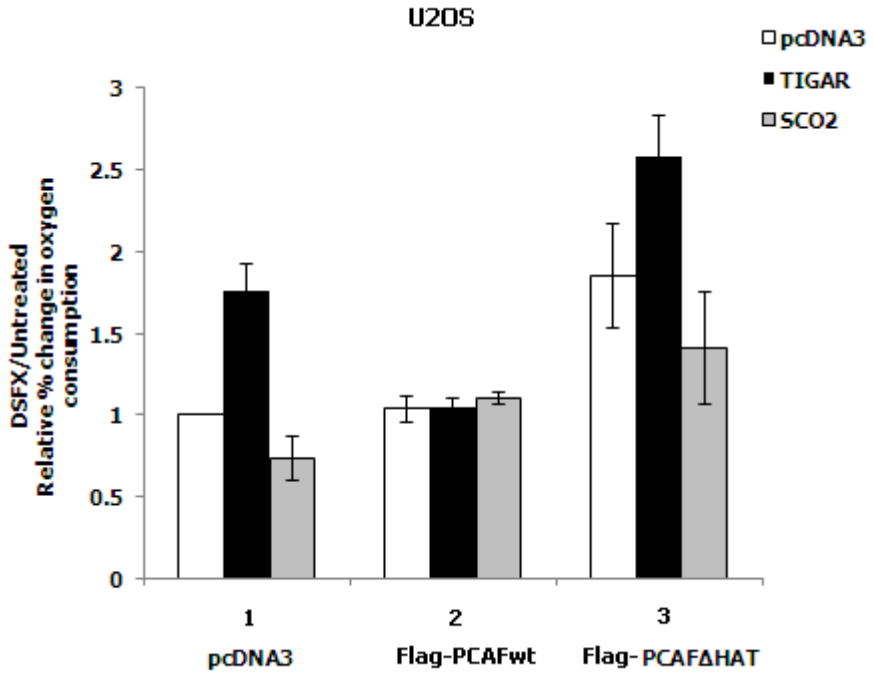

Figure 4.4.4: Role of PCAF in the regulation of oxygen consumption

U2OS cells were transfected with PCDNA3 (white bars), TIGAR (black bars) or SCO2 (grey bars) expression vectors along with PCDNA3 (1), PCAFwt (2) and PCAF-ΔHAT (3) and left untreated or treated with DSFX for 16 hours. Oxygen consumption was monitored in these cells using a Clark-type polarographic oxygen electrode instrument as described in Materials and Methods.

No significant changes were observed in the DSFX treated versus the untreated cells overexpressing PCAFwt (Figure 4.4.4 , compare white bar 2 to white bar 1) whereas increased oxygen consumption was exhibited by DSFX treated compared to untreated cells ectopically expressing PCAF-ΔHAT (Figure 4.4.4), compare white bar 3 to white bars 1 and 2) suggesting that the HAT activity of PCAF decreased oxygen consumption in hypoxia mimicking conditions.

The potential combinatory effect of the HAT activity of PCAF with TIGAR and SCO2 overexpression on oxygen consumption was investigated in untreated or DSFX treated U2OS cells cotransfected with PCAFwt or PCAF-ΔHAT together with TIGAR or SCO2 expressing constructs. Reduced oxygen consumption was detected in DSFX treated versus untreated cells overxpressing PCAFwt together with TIGAR (Figure 4.4.4., compare black bar 2 to black bar 1). On the contrary increased oxygen

consumption was measured in DSFX treated versus untreated cells overxpressing PCAF-ΔHAT together with TIGAR (Figure 4.4.4., compare black bar 3 with black bars 1 and 2). Although TIGAR has been shown to inhibit glycolysis, its involvement in the regulation of OXPHOS has not been documented and in order to reach firm conclusions further investigation is required.

Increased oxygen consumption was demonstrated by DSFX treated versus untreated U2OS cells overexpressing SCO2 together with PCAFwt and PCAF-ΔHAT (Figure 4.4.4., compare grey bar 2 to grey bar 1 and grey bar 3 to grey bar 1) suggesting that overexpressing SCO2 cells promote oxygen uptake in hypoxic conditions. Taken together, results shown in Figure 4.4.3 and Figure 4.4.4., supported the view that the HAT activity of PCAF promoted glycolysis and inhibited OXPHOS in hypoxic cells possibly by coordinating the transcriptional activity of HIF-1α and/or other hypoxia responsive transcription factors.

4.4.3 NAD+/NADH ratio

Nicotinamide adenine dinucleotide (NAD^+) participates in many biological processes including the regulation of energy metabolism. In particular, during glycolysis and citric acid cycle energy from nutrients is transferred to NAD^+ which is reduced to NADH. NADH is then oxidized back to NAD^+ by transferring its reducing electrons to electron acceptors and ultimately to oxygen and the energy released during this process is coupled to ATP generation through OXPHOS (Murray et al., 2003). The NAD^+/NADH ratio is an indicator of intracellular redox and metabolic state as the NAD^+/NADH ratio fluctuates in response to changes in metabolism (Schwartz et al., 1974); (Lin and Guarente, 2003) (MacDonald and Marshall, 2000; Mongan et al., 2002; Ramasamy et al., 1998; Sanni et al., 2001). Therefore, the NAD^+/NADH ratio plays an important role in the regulation of intracellular redox state. Also, NAD^+/NADH ratio has been shown to affect cellular energy metabolism by regulating enzymes such as glyceraldehyde 3-phosphate dehydrogenase and pyruvate dehydrogenase complex (Lin and Guarente, 2003).

To investigate the possibility that the HAT activity of PCAF is involved in the regulation of NAD^+/NADH ratio, the amounts of NAD^+ and NADH were estimated in

untreated and DSFX treated U2OS and SaOS2 cells transfected with PCDNA3, PCAFwt or PCAF-ΔHAT as described in the Materials and Methods section. The standard curves for NAD^+ and NADH were prepared using the standard solutions provided by the supplier (Sigma, UK).

Reduced NAD+/NADH ratio was observed in the DSFX treated versus untreated U2OS cells transfected with PCAFwt (Figure 4.4.5, compare black bar 2 with black bar 1). In other words there was higher NADH production in the DSFX treated cells compared to the untreated ones. Considering that the glycolytic pathway utilizes NAD+ and produces NADH which is re-oxidized to NAD^+ in ETC and when pyruvate is converted to lactate (Lehninger et al., 2005), the low NAD+ and high NADH levels observed in PCAFwt transfected cells compared to the untransfected cells could be explained by increased glycolytic rate, which is in agreement with the lactate production results (Figure 4.4.3 A., compare black bar 2 with black bar 1). In contrast decreased NAD+/NADH ratio was observed in the NAD+/NADH ratio in DSFX treated versus untreated U2OS cells ectopically expressing PCAF-ΔHAT (Figure 4.4.5, compare black bar 3 with black bar 1).

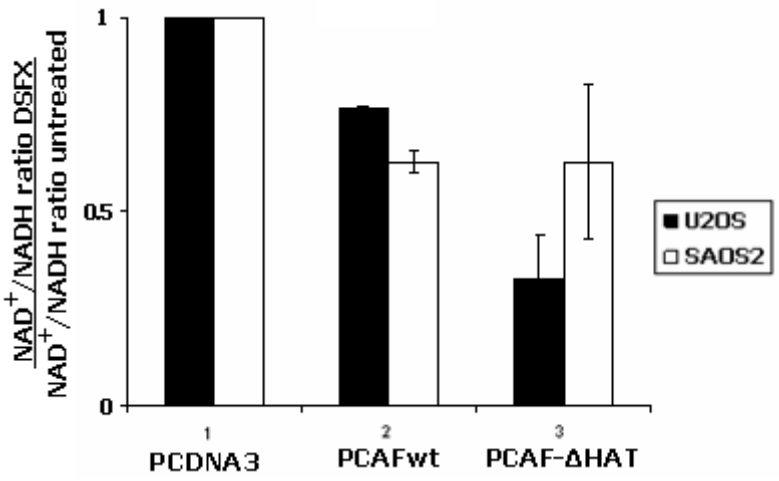

Figure 4.4.5: Role of PCAF in the regulation of NAD+/NADH ratio

The NAD^+ and NADH levels were estimated in untreated or DSFX treated U2OS and SaOS2 cells transfected with PCDNA3, PCAFwt or PCAF-ΔHAT. A standard curve was prepared using NAD^+ and NADH standards (Sigma, UK). The data are representive of three independent experiments.

In the p53 null SaOS2 cells on the other hand, slightly downregulated NAD^+/NADH ratio was observed in DSFX treated versus untreated PCAFwt and PCAF-ΔHAT transfected cells (Figure 4.4.5, compare white bars 2 and 3 with white bar 1). Results shown in Figure 4.4.5 implied that the PCAF mediated regulation of the NAD^+/NADH ratio depends on the presence of p53.

4.4.4 ROS production

TIGAR has been shown to inhibit intracellular ROS levels by diverting fructose 6-phosphate from glycolysis into pentose phosphate pathway that leads to increased NADPH production, which contributes to the scavenging of ROS by reduced glutathione (Bensaad et al., 2009; Bensaad et al., 2006). To investigate whether the inhibitory role of HAT activity of PCAF on TIGAR gene expression played any role in the regulation of intracellular ROS levels mediated by TIGAR, we followed intracellular ROS levels in untreated or DSFX treated U2OS cells transfected with PCDNA3, PCAFwt and PCAFΔHAT. The intracellular ROS levels were estimated by FACS analysis as described in the Materials and Methods section.

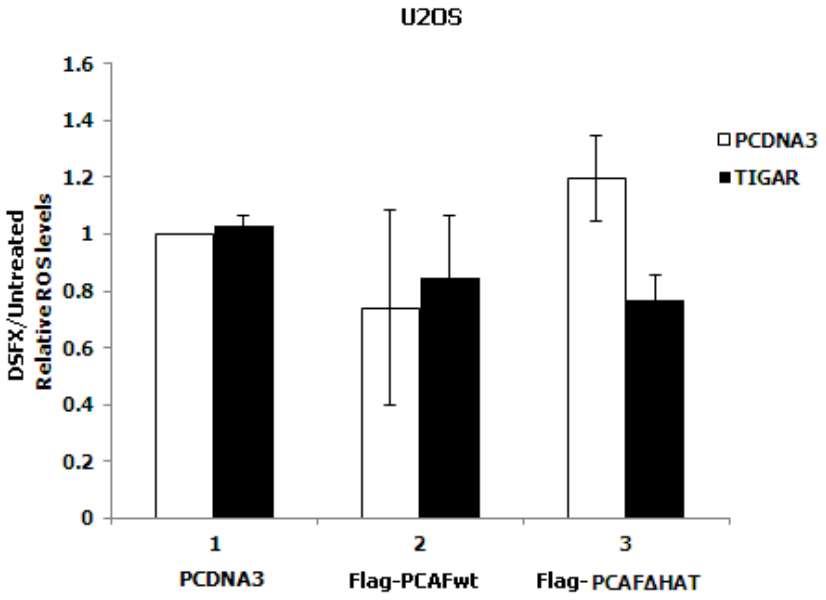

Figure 4.4.6: Role of PCAF in the regulation of intracellular ROS levels

U2OS cells were transfected with PCDNA3 or TIGAR expression vectors along with PCDNA3 or PCAFwt or PCAFΔHAT vectors and left untreated or treated with DSFX for 16 hours. The cells were treated with H2DCF-DA for 30 minutes and subjected to FACS analysis for the measurement of intracellular ROS levels. The data represents two independent experiments.

Under hypoxia mimicking conditions, PCAF exerted a suppressive role in the regulation of TIGAR gene expression at protein and mRNA levels (Section 4.3). The suppression of TIGAR gene expression should result in increased intracellular ROS levels (Bensaad et al., 2006). However, the suppressive effect of PCAF on TIGAR gene expression was not reflected in intracellular ROS levels (Figure 4.4.6 compare white bar 2 with white bar 1). At the same time, the difference in intracellular ROS levels between PCAF and PCAFΔHAT transfected cells (Figure 4.4.6 compare white bar 2 with white bar 3) indicated that the HAT activity of PCAF might regulate intracellular ROS levels.

However, when TIGAR was overexpressed in U2OS cells, both PCAF and PCAFΔHAT transfected cells showed a slight reduction in intracellular ROS levels (Figure 4.4.6 compare black bar 2 and 3 with black bar 1) indicating that TIGAR overexpression abolished the effects of the HAT activity of PCAF on intracellular ROS generation. Together these results indicate the potential role of PCAF in the regulation of intracellular ROS levels and oxidative stress.

5 Discussion

5.1 Significance and key findings

Otto Warburg has discovered that cancer cells prefer to produce energy through the low energy yielding glycolysis pathway irrespectively of the presence of oxygen supply, whereas in the presence of oxygen, their normal counterparts produce energy preferentially through OXPHOS which is a highly efficient energy producing pathway (Warburg et al., 1924). Although it is now clear that the so called Warburg effect provides tumour cells survival and proliferative advantages, the molecular mechanism involved in this metabolic shift is not clear. However, numerous oncogenes and tumour suppressors have been shown to act as inducers or inhibitors of this metabolic shift. The oncogenes HIF-1α, AKT and MYC, for example, have been shown to promote glycolysis and inhibit OXPHOS by differentially regulating the gene expression of genes encoding enzymes that are involved in glycolysis and OXPHOS (Elstrom et al., 2004; Kim et al., 2004a; Papandreou et al., 2006; Semenza et al., 1994). Conversely, the tumour suppressor p53 inhibits glycolysis and promotes mitochondrial respiration by transcriptionally modulating its target genes involved in these metabolic pathways to prevent proliferation of transformed cells (Bensaad et al., 2006; Matoba et al., 2006; Yeung et al., 2008). Reversing Warburg Effect (decreased glycolysis and elevated OXPHOS) might selectively kill tumour cells as these cells rely mainly on glycolysis for their energy production, survival and proliferation. Since the metabolic phenotype is the Achilles' heel of cancer, this model has been proposed by many researchers as a potential therapy for cancer (Chen et al., 2007; Jones and Thompson, 2009; Kroemer and Pouyssegur, 2008).

The role of transcriptional cofactors such as p300 and PCAF in the regulation of the functional cross talk between HIF-1α and p53 has been investigated in the past and it is known that p300 and PCAF modulate the stability and transcriptional activity of both transcription factors (Arany et al., 1996; Liu et al., 1999; Schmid et al., 2004; Xenaki et al., 2008). Under hypoxic conditions p300 and PCAF orchestrate cellular homeostasis by differentially recruiting p53 and HIF-1α to their target genes (Xenaki et al., 2008). Both transcription factors intervene in the determination of the pathway of cellular

energy production regulating the levels of enzymes involved in glucose metabolism such as GLUT-1 and HK2 which are modulated by both p53 and HIF-1α (Chen et al., 2001; Kim et al., 2007; Mathupala et al., 1997; Schwartzenberg-Bar-Yoseph et al., 2004a). In addition, TIGAR and SCO2 gene expression has been shown to be under p53 transcriptional control whereby p53 regulates glycolysis and OXPHOS (Bensaad et al., 2006; Matoba et al., 2006).

TIGAR has been shown recently to be upregulated in hypoxic myocytes and inhibits glycolysis (Kimata et al., 2010), however the molecular mechanism involved in the regulation of TIGAR in hypoxic conditions has not yet been elucidated. Given the important role of HIF-1α in the regulation of cellular energy metabolism, we were interested to test whether TIGAR and SCO2 gene expression was HIF-1α dependent under hypoxic conditions. To this direction we followed TIGAR and SCO2 protein and mRNA levels in cell lines with variable p53 status treated with the hypoxia mimicking agent DSFX. We found evidence to suggest that under hypoxic conditions HIF-1α is recruited to one of the HREs identified within the TIGAR promoter using bioinformatic tools thereby regulating its cellular levels. On the other side although SCO2 was observed to be differentially regulated in hypoxic conditions and the presence of HREs within its regulatory region was identified there was no evidence for direct involvement of HIF-1α in the regulation of its gene expression. Next we studied the role of the acetyl transferase activity of PCAF in the regulation of TIGAR and SCO2 gene expression knowing that PCAF dependent acetylation of p53 and HIF-1α plays important role in their protein stability as well as in targeting these transcription factors to a specific subset of their transcription target genes. Our results suggested that the HAT activity of PCAF was important in determining the pathway of cellular energy production in hypoxic conditions by regulating the cellular levels of both TIGAR and SCO2 which are to be involved in the regulation of glycolysis and OXPHOS respectively (Bensaad et al., 2006; Matoba et al., 2006). To verify this assumption we followed lactate production, oxygen consumption, NAD/NADH ratio and ROS generation in cells treated with the hypoxia mimicking agent DSFX and ectopically overexpressing wild type PCAF or PCAF-ΔHAT mutant.

5.2 Detailed analysis of the results

5.2.1 TIGAR protein and mRNA levels are upregulated in DSFX treated cells

To study whether TIGAR was differentially regulated in hypoxia mimicking conditions, we followed both its protein and mRNA levels in DSFX treated cell lines with different p53 status. TIGAR protein and mRNA levels increased in hypoxia mimicking conditions in wild type p53 expressing U2OS and MCF-7 as well as in MDA-MB-231 cells expressing mutated p53 which was not stabilized in hypoxic conditions (Figure 4.1.1 A, B, and C, Figure 4.1.2 A, B, and C and Figure 4.1.3 A, B, and C). Furthermore in DSFX treated p53 null SaOS2 cells, TIGAR protein and mRNA levels were downregulated compared to untreated cells (Figure 4.1.1 D, Figure 4.1.2 D and Figure 4.1.3 D). As expected in etoposide treated U2OS and MCF-7 cells TIGAR protein and mRNA levels were elevated compared to untreated and DSFX treated cells. Interestingly etoposide treatment of MDA-MB-231 and SaOS2 cells resulted in upregulation of TIGAR protein levels compared to non-treated and DSFX treated cells (Figure 4.1.1 C and D, Figure 4.1.2 C and D and Figure 4.1.3) whereas TIGAR mRNA levels increased slightly in etoposide treated MDA-MB-231 and downregulated significantly in SaOS2 cells under the same conditions (Figure 4.1.1 D, Figure 4.1.2 D and Figure 4.1.3 D).

These results are in agreement with previously published observations indicating that p53 upregulates TIGAR in response to DNA damage (Bensaad et al., 2006) and in addition they implied that TIGAR was regulated in a similar manner in hypoxia mimicking conditions. Although, in p53 wild type cells the increase of TIGAR protein and mRNA levels after DSFX treatment can be explained by the stabilisation of p53 in these conditions, the results obtained in p53 defective cell lines indicated that TIGAR expression in hypoxia mimicking conditions was independent of p53 activation and other hypoxia responsive transcription factors such as MYC (Knies-Bamforth et al., 2004), NF-κB (Koong et al., 1994) and FOXO-3a (Bakker et al., 2007) possibly determine TIGAR levels under these conditions.

5.2.2 TIGAR gene expression is regulated by HIF-1α

HIF-1α is the master regulator of cellular response to hypoxia (Semenza, 1998) and has been shown to regulate most of the glycolytic enzymes (Obach et al., 2004; Semenza et al., 1994). To study whether HIF-1α was involved in the regulation of TIGAR gene expression in hypoxic conditions, we followed TIGAR protein and mRNA levels in U2OS cells in the presence and absence of HIF-1α. In the latter case RNAi against HIF-1α was used to silence its expression in U2OS cells. Decreased TIGAR mRNA and protein levels were evident in DSFX treated U2OS cells in which HIF-1α had been silenced compared to those in DSFX treated cells that had been transfected with scrambled RNAi (Figure 4.1.4 A and B) indicating potential involvement of HIF-1α in the regulation TIGAR gene expression.

HIF-1α exhibits its transcriptional activity by binding to the cis- responsive elements present in the promoters of its target genes. To investigate, whether HIF-1α binding sites existed within the regulatory region of the TIGAR promoter, we used bioinformatics tools which identified the presence of six putative HREs numbered from 1 to 6 (HRE 1-6) where the HRE-6 is the closer one to the translation start site (Figure 4.1.5 and Figure 4.1.6 A). The DNA sequence of the consensus HRE is 5'-RCGTG-3' (where R is A or G) (Wenger et al., 2005), although the sequence 5'-CCGTG-3' has also been found in some of the HIF-1α transcription target genes. In addition the sequence 5'-CACAG-3' has been detected in the HIF-1α includible genes EPO, VEGF and NOXA (Figure 4.1.6 B) (Fukuda et al., 2007). The functionality of the TIGAR HREs was assessed using chromatin immunoprecipitation assays, which indicated that HIF-1α was recruited to the HRE5 of the TIGAR promoter (Figure 4.1.7) implying that this transcription factor regulates TIGAR gene expression.

Luciferase reporter assays using the pGL3 reporter constructs containing the HRE5 alongside the p53 binding site (Materials and methods 3.3.4) were employed to verify the results observed with ChIP assays. No significant changes in luciferase expression were observed in DSFX treated versus non-treated U2OS cells whereas an approximate 1.5 fold upregulation was observed in DSFX treated versus untreated SaOS2 cells (Figure 4.1.8 A).

The luciferase assay results could be explained by the fact that the luciferase reporter used in these assays contained only a short fragment of the TIGAR promoter region bearing the p53 and HIF-1α binding sites. Apart from p53 and HIF-1α, binding sites for other transcription factors such as NF-κB and E2F1 have been identified within the TIGAR promoter, which were not included in the luciferase reporter construct and might play crucial role in the modulation of TIGAR gene expression. The induction of the TIGAR luciferase reporter in SaOS2 cells however indicated that HIF-1α contributes to the modulation of TIGAR gene expression in hypoxia mimicking conditions. Taken together these results provide evidence that HIF-1α is recruited to the TIGAR promoter and transcriptionally regulates its gene expression.

5.2.3 SCO2 protein and mRNA levels are regulated in a p53 independent mode in hypoxia mimicking conditions

SCO2 plays important role in the mitochondrial respiration by facilitating the assembly of the subunit II of the complex IV of the COX holoenzyme (Figure 1.8.1). p53 regulates mitochondrial respiration by modulating SCO2 gene expression (Matoba et al., 2006). Mitochondrial respiration is also affected by HIF-1α which regulates gene expression of several COX subunits in many different types of cancer (Fukuda et al., 2007). To investigate the possibility that SCO2 was transcriptional target of both p53 and HIF-1α, protein and mRNA levels of this enzyme were followed in four cell lines with different p53 status treated with either the hypoxia mimicking agent DSFX or etoposide.

Upregulation of SCO2 protein and mRNA levels was observed in etoposide treated U2OS, MDA-MB-231 and SaOS2 cells, whereas in MCF-7 cells SCO2 was downregulated under the same conditions (Figure 4.2.1, Figure 4.2.2 and Figure 4.2.3). This downregulation could be due to factors other than p53 that are induced in etoposide treated MCF-7 cells such as NF-κB (Morotti et al., 2006) for which consensus binding sites have been identified within the regulatory region of the SCO2 promoter (Figure 4.2.4).

In contrast to etoposide treated cells, SCO2 gene expression was upregulated in DSFX treated p53 mutant MDA-MB-231 and p53 null SaOS2 cells and downregulated in wild type p53 expressing U2OS and MCF-7 cells (Figure 4.2.1, Figure 4.2.2, Figure 4.2.3). These cell type dependent differences could be due to the involvement of hypoxia responsive transcription factors other than p53 in the regulation of SCO2 gene expression. Moreover, the difference in SCO2 gene expression between etoposide and DSFX treated U2OS cells indicate the possible participation of hypoxia responsive factors affecting p53 transcriptional activity. In addition results presented in Figure 4.2.1, Figure 4.2.2, Figure 4.2.3 implied that SCO2 gene expression in hypoxia mimicking conditions is independent of p53.

5.2.4 SCO2 gene expression in hypoxia mimicking conditions is not regulated by HIF-1α

Results indicating that HIF-1α regulates many subunits of the COX complex (Fukuda et al., 2007) together with the observations described above presenting evidence that SCO2 protein and mRNA levels in hypoxia mimicking conditions were regulated in a p53 independent manner, triggered our interest to investigate whether HIF-1α was involved in the regulation of SCO2 gene expression in hypoxic conditions. To that end, we used bioinformatic tools to analyse the regulatory region of the SCO2 promoter to identify putative binding sites for HIF-1α. Six putative HREs were detected within 1700 base pairs upstream of the translational start site (Figure 4.2.4 and Figure 4.2.5) implying that HIF-1α might play a role in SCO2 gene expression. To this end, a luciferase reporter containing 5 of the identified putative HREs, one p53 and one NF-κB binding sites was constructed (Materials and methods - Figure 3.3.4)

Luciferase reporter assay performed with this reporter in hypoxia mimicking conditions, showed that SCO2 reporter was downregulated in SaOS2 cells and moderately upregulated in U2OS cells (Figure 4.2.6). The same experiment performed with gradually increasing amounts of transfected HIF-1α indicated that although there was a slight increase in luciferase activity following the increase of HIF-1α no significant changes were observed between untreated and DSFX treated cells (Figure 4.2.8 A and B) implying that the differences in SCO2 luciferase activity monitored in U2OS and

SaOS2 cells were not due to HIF-1α but to other factors such as p53 and NF-κB for which binding sites were included in the luciferase reporter construct.

ChIP assays carried out to investigate whether HIF-1α was recruited to any of the putative HREs present within the SCO2 promoter confirmed this conclusion as HIF-1α was not recruited to any of the identified putative HREs within the SCO2 promoter (Figure 4.2.8). Together these results indicated that HIF-1α does not regulate SCO2 gene expression.

5.2.5 PCAF regulates TIGAR and SCO2 gene expression in hypoxic conditions

We have recently demonstrated that PCAF is a common cofactor for both p53 and HIF-1α playing important role in the regulation of the stability and transcriptional activity of both transcription factors thereby determining cellular life and death in hypoxic conditions (Xenaki et al., 2008). In particular we have shown that in hypoxic conditions the PCAF mediated acetylation of p53 at K320 (Liu et al., 1999) is compromised and the limited amount of acetylated p53 at K320 is preferentially recruited to the prosurvival $p21^{WAF-1/CIP-1}$ promoter and not to the proapoptotic BID promoter leading to cell cycle arrest in the G1 phase and hence cell survival (Xenaki et al., 2008). Along with published reports the results presented in sections 4.1.1and 4.1.2 have shown that TIGAR gene expression is regulated by both p53 and HIF-1α (Bensaad et al., 2006). On the other hand, although evidence for HIF-1α direct involvement in the regulation of SCO2 gene expression has not been found in sections 4.2.1and 4.2.2 it has been shown that SCO2 gene expression is modulated in hypoxic conditions in a p53 independent manner (Matoba et al., 2006).

To test whether the HAT activity of PCAF was involved in the regulation of TIGAR and SCO2 gene expression, we monitored protein and mRNA levels of these two enzymes in DSFX treated U2OS cells transfected with wild type PCAF or the HAT defective mutant PCAFΔHAT. TIGAR protein levels were downregulated in PCAFwt transfected cells in hypoxia mimicking conditions, whereas no significant changes were observed in etoposide treated cells (Figure 4.1.1). In contrast increased TIGAR protein levels were detected in both DSFX and etoposide treated cells transfected with PCDNA3 and PCAFΔHAT (Figure 4.1.1) suggesting that the HAT activity of PCAF

exerts negative effect on TIGAR protein levels in hypoxia mimicking conditions. Although it is evident from this experiment that the HAT activity of PCAF is involved in the regulation of TIGAR protein levels, the molecular mechanisms engaged in the execution of these events is not clear. Binding sites for transcription factors for which PCAF serves as a cofactor have been identified within the regulatory region of the TIGAR promoter such as HIF-1α (Xenaki et al., 2008), p53 (Bensaad et al., 2006), NF-κB (Sheppard et al., 1999) and E2F1 (Frolov and Dyson, 2004).

On the other hand, SCO2 protein levels were downregulated in etoposide and DSFX treated U2OS cells over-expressing PCAFwt whereas PCAFΔHAT overexpression resulted in a slight upregulation of SCO2 protein levels in hypoxia mimicking and DNA damage conditions (Figure 4.2.1 A and B). Taken together these results indicated that the HAT activity of PCAF negatively regulated SCO2 protein levels in hypoxia mimicking and DNA damage conditions. The downregulation of SCO2 protein levels in DSFX and etoposide treated U2OS cells is in disagreement with published reports indicating that p53 is recruited to the SCO2 promoter in DNA damage conditions (Matoba et al., 2006). Since the ChIP assays described in section 4.2.5 indicated that HIF-1α was not recruited in SCO2 promoter under hypoxia mimicking conditions this discrepancy could be explained by the fact that hypoacetylated HIF-1α might have higher affinity for binding with the HREs present within the SCO2 promoter or is more effective in recruiting p53 in the promoter of this gene in hypoxia mimicking conditions. Further experiments are required to verify this hypothesis.

To study whether PCAF mediated regulation of TIGAR and SCO2 gene expression occurred at the transcriptional level, TIGAR and SCO2 mRNA levels were analysed in U2OS cells overexpressing either PCAFwt or PCAFΔHAT. In line with the protein expression patterns, TIGAR mRNA levels were down regulated in PCAFwt expressing cells in hypoxia mimicking conditions, whereas this inhibition was abolished in PCAFΔHAT transfected cells under the same conditions (Figure 4.3.3 A). In etoposide treated PCAFwt expressing cells a slight downregulation of TIGAR mRNA levels was evident that was again abolished in PCAFΔHAT transfected cells under the same conditions (Figure 4.3.3 A). The greater extent of TIGAR mRNA downregulation in

hypoxia mimicking conditions compared to that in etoposide treated cells might be an indication that PCAF recruited different transcription factors in hypoxia mimicking than in DNA damage conditions which comply with our previously published data demonstrating that PCAF under diverse stress conditions differentially acetylates p53 and HIF-1α directing them to different subsets of their transcription target genes (Xenaki et al., 2008).

In similar way to that observed for TIGAR, SCO2 mRNA levels were downregulated in PCAFwt over expressing U2OS cells in hypoxia mimicking conditions (Figure 4.3.3 B). However, increased SCO2 mRNA levels in PCAFΔHAT transfected cells in both DSFX and etoposide treated cells were evident (Figure 4.3.5 B) in accord with the pattern of SCO2 protein levels (Figure 4.3.2 A and B). To shed light in the role of the HAT activity of PCAF in the transcriptional regulation of TIGAR and SCO2 gene expression, luciferase reporter assays were performed using the TIGAR and SCO2 luciferase reporter constructs described in Materials and methods section. Gradually increasing amounts of PCAFwt transfected in DSFX treated U2OS cells decreased both TIGAR and SCO2 luciferase activity whereas the opposite trend was apparent in the cells transfected with gradually increasing amounts of PCAFΔHAT under the same conditions (Figure 4.3.4 A and Figure 4.3.5 A) supporting the view that the HAT activity of PCAF exerts negative effects on the transcriptional regulation of both TIGAR and SCO2 gene expression in U2OS cells under hypoxia mimicking conditions. In contrast to U2OS in the DSFX treated p53 null SaOS2 cells, the HAT activity of PCAF wielded a positive effect on both TIGAR and SCO2 gene expression (Figure 4.3.4 B and Figure 4.3.5 B). This result could be an indication that PCAF mediated acetylation of p53 hindered the recruitment of this transcription factor to the TIGAR and SCO2 promoter in the DSFX treated U2OS cells. In addition PCAF mediated acetylation of HIF-1α or another hypoxia responsive transcription factor relieved this repression in DSFX treated SaOS2 cells. In other words, the absence of p53 enables PCAF to recruit hypoxia responsive transcription factor(s) to the regulatory region of the promoter of TIGAR and SCO2 genes inducing their expression.

In conclusion our results shown in Figure 4.3.6 A and B support the view that the HAT activity of PCAF exerts a suppressive effect on TIGAR and SCO2 gene expression in the presence of p53 and induces gene expression of these two enzymes in the absence of p53 in hypoxia mimicking conditions.

5.2.6 The HAT activity of PCAF regulates energy production pathways and ROS generation

TIGAR has been shown to inhibit glycolysis and hence reduce lactate production (Bensaad et al., 2006). Taking into account our results suggesting the involvement of HIF-1α and the HAT activity of PCAF in the regulation of TIGAR gene expression in hypoxia mimicking conditions we were interested to investigate whether the HAT activity of PCAF played any role in the TIGAR mediated repression of glycolysis in hypoxic conditions. To this direction, we initially confirmed the role of HIF-1α in the regulation of lactate production by silencing HIF-1α expression using RNAi in U2OS cells. In accord with published data (Semenza et al., 1994) HIF-1α over expressing cells exhibited elevated lactic acid levels compared to cells in which HIF-1α expression had been silenced in hypoxia mimicking conditions (Figure 4.4.1). Furthermore TIGAR overexpression in DSFX treated U2OS cells reduced the lactate levels (Figure 4.4.2) in agreement with previously published reports showing that TIGAR is an inhibitor of glycolysis (Bensaad et al., 2006).

The role of the HAT activity of PCAF in the regulation of glycolysis was assessed by recording the lactate production in U2OS cells transfected with PCAFwt or PCAFΔHAT in normal and hypoxia mimicking conditions. In line with our results presented in Figure 4.3.1, Figure 4.3.3 A indicating reduced TIGAR protein and mRNA levels in U2OS cells overexpressing PCAFwt, elevated lactate levels were observed in U2OS cells overexpressing PCAFwt and reduced in those cells transfected with PCAFΔHAT in hypoxia mimicking conditions (Figure 4.4.3 A). Moreover the upregulation of TIGAR coincided with reduced protein levels of the bi-functional enzyme PFKFB3 (Obach et al., 2004) in PCAFΔHAT transfected U2OS cells in hypoxia mimicking conditions (Figure 4.4.3 B) suggesting that the lactic acid downregulation in these cells might be the outcome of both TIGAR upregulation and PFKFB3 downregulation, however, this concept requires further experimental support.

Given the inhibitory role of TIGAR in glycolysis we next were interested to investigate whether cells overexpressing TIGAR could cover their energy needs by producing ATP through increased OXPHOS. To address this question we assessed the ability of U2OS cells ectopically expressing TIGAR or SCO2 together with PCAFwt or PCAFΔHAT to uptake oxygen as a measure of their capability to produce ATP through OXPHOS. Oxygen consumption in DSFX treated PCAFΔHAT transfected U2OS cells was upregulated compared to PCDNA3 or PCAFwt transfected cells (Figure 4.4.4) indicating that the HAT activity of PCAF exhibited a repressive role in oxygen consumption in hypoxia mimicking conditions. Consistent with this conclusion was the observation that PCAFwt transfected cells co-expressing TIGAR exhibited low oxygen consumption in hypoxia mimicking conditions (Figure 4.4.4). On the other hand, overexpression of SCO2 increased OXPHOS in hypoxia mimicking conditions irrespectively of the presence of either PCAFwt or PCAFΔHAT, suggesting that overexpression of SCO2 abolishes the effects of the HAT activity of PCAF on the ability of the cells to uptake oxygen (Figure 4.4.4).

To further investigate whether the HAT activity of PCAF played any role in the regulation of energy metabolism as well as in determining the cellular redox state we followed the NAD^+/NADH ratio in U2OS and SaOS2 cells transfected with either PCAFwt or PCAFΔHAT. In PCAFΔHAT transfected and DSFX treated U2OS cells high NAD^+ and low NADH levels were observed (Figure 4.4.5) indicating low glycolytic rate under these conditions. In contrast to U2OS cells in p53 null SaOS2 cells low NAD^+/NADH ratio was observed in those cells transfected with PCAFΔHAT and treated with DSFX (Figure 4.4.5) implying that the HAT activity of PCAF regulated the NAD^+/NADH ratio in a p53 dependent mode.

The effect of the HAT activity of PCAF in the regulation of intracellular ROS generation was assessed in U2OS cells transfected with PCAFwt or PCAFΔHAT. Slightly increased intracellular ROS levels were observed in DSFX treated and PCAFΔHAT transfected cells compared to PCDNA3 transfected and untreated cells (Figure 4.4.6) which returned to the basal levels after TIGAR was ectopically

expressed. No significant changes in intracellular ROS levels were observed in the cells overexpressing PCAFwt although the variability between two experiments did not allow firm conclusions to be reached. Taken together, these results indicated that the HAT activity of PCAF is involved in the determination of the pathway of cellular energy production and the intracellular ROS generation.

5.3 Conclusions

5.3.1 HIF-1 is involved in the regulation of TIGAR and SCO2 gene expression in hypoxia mimicking conditions

The tumour suppressor p53 modulates cellular energy metabolism by upregulating *TIGAR* and *SCO2* gene expression. The HIF-1 transcription factor, on the other hand induces the expression of genes encoding for enzymes involved in cellular metabolism in hypoxic conditions thereby facilitating the production of sufficient energy to promote survival and confer proliferative advantage to cancer cells. Our study attempted to dissect the molecular mechanisms which fine tune *TIGAR* and *SCO2* gene expression under hypoxia mimicking conditions.

The results shown in chapter 1 suggest that HIF-1 is involved in the regulation of TIGAR gene expression in hypoxia mimicking conditions. Our observations (Section 4.1.1, 4.1.2) indicated that *TIGAR* gene expression, was differentially regulated in hypoxia mimicking conditions as evidenced at both TIGAR protein and mRNA levels. This notion complies with published data suggesting that apart from p53, other factors are possibly involved in the regulation of *TIGAR* gene expression (Bensaad et al., 2006). Bio-informatic analysis revealed the presence of putative HREs in the regulatory region of *TIGAR* promoter (Section 4.1.4). Further experiments using luciferase reporter and ChIP assays (Section 4.1.3 and Section 4.1.5) suggested that *TIGAR* gene expression is potentially under HIF-1 transcriptional control in hypoxia mimicking conditions.

Similar to *TIGAR*, *SCO2* gene expression was also differentially regulated in hypoxia mimicking conditions both at protein and mRNA levels (Section 4.2.1 and Section 4.2.2). However, the lack of experimental evidence verifying the recruitment of HIF-1 within the *SCO2* promoter suggested that HIF-1 may not be directly involved in the regulation of *SCO2* gene expression. Nevertheless, the upregulation of *SCO2* gene expression recorded in luciferase reporter assays implied that HIF-1 might be involved in the regulation of *SCO2* gene expression indirectly but this issue requires further investigation.

Taken together results presented in Chapters 4.1 and 4.2 indicated that HIF-1α might be involved in the regulation of *TIGAR* and *SCO2* gene expression in hypoxia mimicking conditions either directly or indirectly.

5.3.2 PCAF plays an important role in the regulation of *TIGAR* and *SCO2* gene expression

Previous work in our laboratory has reviled the important role of the transcriptional co-factor PCAF as a common co-factor for both p53 and HIF-1α in determining their transcription target selectivity thereby regulating cell cycle arrest and apoptosis (Xenaki et al., 2008). Given that *TIGAR* and *SCO2* are common p53 and HIF-1 targets (Chapters 4.1 and 4.2), in this study we investigated whether PCAF exerted similar effects on cellular energy metabolism by selectively targeting p53 and/or HIF-1 to either *TIGAR* or *SCO2*.

Results shown in Chapter 4.3 indicated that in hypoxia mimicking conditions, PCAF played crucial role in the regulation of *TIGAR* and *SCO2* gene expression under hypoxia mimicking conditions. In particular, ectopic expression of PCAFwt downregulated both TIGAR and SCO2 protein and mRNA levels whereas PCAFΔHAT did not have any significant effect on the expression of these genes (Sections 4.3.1 and 4.3.2). Moreover, luciferase reporter assays confirmed the involvement of PCAF in the regulation of *TIGAR* and *SCO2* gene expression under hypoxia mimicking conditions (Section 4.3.3). In conclusion, results shown in Chapter 4.3 indicated that PCAF played an important role in the regulation of *TIGAR* and *SCO2* gene expression in hypoxia mimicking conditions.

5.3.3 PCAF affects cellular energy metabolism and ROS generation by regulating *TIGAR* and *SCO2* gene expression.

The functional consequences of PCAF mediated regulation of *TIGAR* and *SCO2* gene expression in hypoxia mimicking conditions, were investigated in cells overexpressing PCAFwt and PCAFΔHAT in the presence or absence of p53 (Chapter 4.4). Results shown in Chapter 4.4 suggested that PCAF HAT activity regulates cellular lactate production (Section 4.4.1), oxygen consumption (Section 4.4.2), and NAD^+/NADH

levels (Section 4.4.3) under hypoxia mimicking conditions. The role of PCAF in the regulation of intracellular ROS levels needs further experimental evidence (Section 4.4.4).

5.4 Future work

Further investigation is required to address the following issues which will take this project forward.

Investigate the involvement of the other HREs identified within the *TIGAR* regulatory region of the promoter apart from the HRE5. Explore the possibility for the requirement of other transcription factors or cofactors required for HIF-1 to bind efficiently to these sites. In addition, confirm the functionality of the HREs within the *TIGAR* promoter by engineering mutated HIF-1 binding sites (5'-CGTG-3') and perform luciferase reporter assays.

Although *SCO2* gene expression has been shown to be modulated differentially in hypoxic conditions (Section 4.2.1 and 4.2.2), the evidence for the direct involvement of HIF-1 in the regulation of *SCO2* gene expression requires more experimental support. ChIP assays with different exposure times to hypoxia (2 hours, 4 hours, 10 hours and 16 hours), or different levels of hypoxia (0.5%, 1% and 5% oxygen) or anoxia (0.01% oxygen) should be performed to study the involvement of HIF-1 in the regulation of *SCO2* gene expression.

The role of PCAF in the regulation of *TIGAR* and *SCO2* gene expression in hypoxia mimicking conditions has been shown in Section 4.3. The role of PCAF should be further investigated in cells in which PCAF expression has been silenced using shRNA or RNAi targeting PCAF. Oxygen consumption, lactate production NAD^+/NADH ratio and oxidative stress should be followed in these cells.

The role of the NAD^+ dependent histone deacetylases sirtuins need to be investigated under the light of the interaction between PCAF and SIRT1 (Yeung et al., 2004) and the fact that both p53 and HIF-1α are targeted by this HDAC.

The investigation of the role of other common transcriptional cofactors for p53 and HIF-1 such as p300/CBP and SRC-1 in the regulation of *TIGAR* and *SCO2* gene expression might answer the question whether, *TIGAR* and *SCO2* gene expression is regulated by different network of transcription factors and coactivators/corepressors under diverse stress conditions.

Given that PFKFB3 is overexpressed in hypoxic conditions, and PCAF is shown to regulate the cellular lactate levels (in other words, glycolysis) it would be interesting to follow the role of PCAF in the modulation of kinase/phosphatase ratio of PFKFB3 enzyme. This will shed light in the modulating process of two enzymes that exert opposing effects in glycolysis (PFKFB3 and TIGAR) and might provide some insight in possible ways to reverse the Warburg Effect in cancer cells. In addition, the possibility that the regulation of cellular ROS and autophagy by TIGAR (Bensaad et al., 2009), is mediated by PCAF could be further explored.

In order to investigate the net effect of the HAT activity of PCAF on ROS generation transfected cells with either PCAFwt or PCAFΔHAT expression vectors need to be sorted using a surface marker (CD20) and ROS measurement cell cycle analysis be performed using FACs.

Reference list

Alberts B, Johnson A, Lewis J, Raff M, Roberts K and Walter P (2002) *Molecular biology of the cell*. Garland Science.

An WG, Kanekal M, Simon MC, Maltepe E, Blagosklonny MV and Neckers LM (1998) Stabilization of wild-type p53 by hypoxia-inducible factor 1[alpha]. *Nature* **392**(6674):405-408.

Appelhoff RJ, Tian Y-M, Raval RR, Turley H, Harris AL, Pugh CW, Ratcliffe PJ and Gleadle JM (2004) Differential Function of the Prolyl Hydroxylases PHD1, PHD2, and PHD3 in the Regulation of Hypoxia-inducible Factor. *Journal of Biological Chemistry* **279**(37):38458-38465.

Arany Z, Huang LE, Eckner R, Bhattacharya S, Jiang C, Goldberg MA, Bunn HF and Livingston DM (1996) An essential role for p300/CBP in the cellular response to hypoxia. *Proceedings of the National Academy of Sciences of the United States of America* **93**(23):12969.

Asher G, Lotem J, Kama R, Sachs L and Shaul Y (2002a) NQO1 stabilizes p53 through a distinct pathway. *Proceedings of the National Academy of Sciences* **99**(5):3099-3104.

Asher G, Lotem J, Sachs L, Kahana C and Shaul Y (2002b) Mdm-2 and ubiquitin-independent p53 proteasomal degradation regulated by NQO1. *Proceedings of the National Academy of Sciences* **99**(20):13125-13130.

Asher G, Tsvetkov P, Kahana C and Shaul Y (2005) A mechanism of ubiquitin-independent proteasomal degradation of the tumor suppressors p53 and p73. *Genes & Development* **19**(3):316-321.

Bae S-H, Jeong J-W, Park JA, Kim S-H, Bae M-K, Choi S-J and Kim K-W (2004) Sumoylation increases HIF-1[alpha] stability and its transcriptional activity. *Biochemical and Biophysical Research Communications* **324**(1):394-400.

Baert AL (2008) *Encyclopedia of Diagnostic Imaging*.

Bakker WJ, Harris IS and Mak TW (2007) FOXO3a Is Activated in Response to Hypoxic Stress and Inhibits HIF1-Induced Apoptosis via Regulation of CITED2. *Molecular Cell* **28**(6):941-953.

Barak Y, Juven T, Haffner R and Oren M (1993) mdm2 expression is induced by wild type p53 activity. *EMBO J* **12**(2):461-468.

Barbacci E, Chalkiadaki A, Masdeu C, Haumaitre C, Lokmane L, Loirat C, Cloarec S, Talianidis I, Bellanne-Chantelot C and Cereghini S (2004) HNF1β/TCF2 mutations impair transactivation potential through altered co-regulator recruitment. *Human Molecular Genetics* **13**(24):3139-3149.

Batta K, Das C, Gadad S, Shandilya J and Kundu TK (2007) Reversible acetylation of non histone proteins: role in cellular function and disease. *Sub-cellular biochemistry* **41**:193.

Bayley J-P and Devilee P (2010) Warburg tumours and the mechanisms of mitochondrial tumour suppressor genes. Barking up the right tree? *Current Opinion in Genetics & Development* **20**(3):324-329.

Baysal BE, Ferrell RE, Willett-Brozick JE, Lawrence EC, Myssiorek D, Bosch A, Mey Avd, Taschner PEM, Rubinstein WS, Myers EN, Richard CW, Cornelisse CJ, Devilee P and Devlin B (2000) Mutations in SDHD, a Mitochondrial Complex II Gene, in Hereditary Paraganglioma. *Science* **287**(5454):848-851.

Beck I, Ramirez S, Weinmann R and Caro J (1991) Enhancer element at the 3'-flanking region controls transcriptional response to hypoxia in the human erythropoietin gene. *Journal of Biological Chemistry* **266**(24):15563-15566.

BelAiba RS, Bonello S, Zahringer C, Schmidt S, Hess J, Kietzmann T and Gorlach A (2007) Hypoxia Up-Regulates Hypoxia-Inducible Factor-1{alpha} Transcription by Involving Phosphatidylinositol 3-Kinase and Nuclear Factor {kappa}B in Pulmonary Artery Smooth Muscle Cells. *Mol Biol Cell* **18**(12):4691-4697.

Benchimol S (2001) p53-dependent pathways of apoptosis. *Cell Death and Differentiation* **8**(11):1049-1051.

Bendinelli P, Matteucci E, Maroni P and Desiderio MA (2009) NF-κB Activation, Dependent on Acetylation/Deacetylation, Contributes to HIF-1 Activity and Migration of Bone Metastatic Breast Carcinoma Cells. *Molecular Cancer Research* **7**(8):1328-1341.

Bensaad K, Cheung EC and Vousden KH (2009) Modulation of intracellular ROS levels by TIGAR controls autophagy. *EMBO J* **28**(19):3015-3026.

Bensaad K, Le Bras M, Unsal K, Strano S, Blandino G, Tominaga O, Rouillard D and Soussi T (2003) Change of Conformation of the DNA-binding Domain of p53 Is the Only Key Element for Binding of and Interference with p73. *Journal of Biological Chemistry* **278**(12):10546-10555.

Bensaad K, Tsuruta A, Selak MA, Vidal MN, Nakano K, Bartrons R, Gottlieb E and Vousden KH (2006) TIGAR, a p53-inducible regulator of glycolysis and apoptosis. *Cell* **126**(1):107-120.

Bensaad K and Vousden KH (2007) p53: new roles in metabolism. *Trends in Cell Biology* **17**(6):286-291.

Blagosklonny M, An W, Romanova L, Trepel J, Fojo T and Neckers L (1998) p53 inhibits hypoxia-inducible factor-stimulated transcription. *Journal of Biological Chemistry* **273**(20):11995.

Blanco JCG, Minucci S, Lu J, Yang X-J, Walker KK, Chen H, Evans RM, Nakatani Y and Ozato K (1998) The histone acetylase PCAF is a nuclear receptorâ€‰coactivator. *Genes & Development* **12**(11):1638-1651.

Bock G and Goode J (2004) *Reversible protein acetylation*. John Wiley & Sons.

Bone and Cooper (2000) In vitro inhibition of rat cauda epididymal sperm glycolytic enzymes by ornidazole, α-chlorohydrin and 1-chloro-3-hydroxypropanone. *International Journal of Andrology* **23**(5):284-293.

Bourdon A, Minai L, Serre V, Jais J-P, Sarzi E, Aubert S, Chretien D, de Lonlay P, Paquis-Flucklinger V, Arakawa H, Nakamura Y, Munnich A and Rotig A (2007) Mutation of RRM2B, encoding p53-controlled ribonucleotide reductase (p53R2), causes severe mitochondrial DNA depletion. *Nat Genet* **39**(6):776-780.

Bradford MM (1976) A rapid and sensitive method for the quantitation of microgram quantities of protein utilizing the principle of protein-dye binding. *Analytical Biochemistry* **72**(1-2):248-254.

Brahimi-Horn MC and Pouyssegur J (2009) HIF at a glance. *J Cell Sci* **122**(8):1055-1057.

Brooks CL and Gu W (2006) p53 Ubiquitination: Mdm2 and Beyond. *Molecular Cell* **21**(3):307-315.

Brooks CL, Li M, Hu M, Shi Y and Gu W (2007) The p53-Mdm2-HAUSP complex is involved in p53 stabilization by HAUSP. *Oncogene* **26**(51):7262-7266.

Brown JM and Wilson WR (2004) Exploiting tumour hypoxia in cancer treatment. *Nature Reviews Cancer* **4**(6):437-447.

Bruick RK and McKnight SL (2001) A Conserved Family of Prolyl-4-Hydroxylases That Modify HIF. *Science* **294**(5545):1337-1340.

Budanov AV, Sablina AA, Feinstein E, Koonin EV and Chumakov PM (2004) Regeneration of Peroxiredoxins by p53-Regulated Sestrins, Homologs of Bacterial AhpD. *Science* **304**(5670):596-600.

Budanov AV, Shoshani T, Faerman A, Zelin E, Kamer I, Kalinski H, Gorodin S, Fishman A, Chajut A and Einat P (2002) Identification of a novel stress-responsive gene Hi95 involved in regulation of cell viability. *Oncogene* **21**(39):6017.

Cairns RA, Papandreou I, Sutphin PD and Denko NC (2007) Metabolic targeting of hypoxia and HIF1 in solid tumors can enhance cytotoxic chemotherapy. *Proceedings of the National Academy of Sciences* **104**(22):9445-9450.

Carbia-Nagashima A, Gerez J, Perez-Castro C, Paez-Pereda M, Silberstein S, Stalla GK, Holsboer F and Arzt E (2007) RSUME, a Small RWD-Containing Protein, Enhances SUMO Conjugation and Stabilizes HIF-1[alpha] during Hypoxia. *Cell* **131**(2):309-323.

Carmeliet P, Dor Y, Herbert J-M, Fukumura D, Brusselmans K, Dewerchin M, Neeman M, Bono F, Abramovitch R, Maxwell P, Koch CJ, Ratcliffe P, Moons L, Jain RK, Collen D and Keshet E (1998) Role of HIF-1[alpha] in hypoxia-mediated apoptosis, cell proliferation and tumour angiogenesis. *Nature* **394**(6692):485-490.

Carrero P, Okamoto K, Coumailleau P, O'Brien S, Tanaka H and Poellinger L (2000) Redox-Regulated Recruitment of the Transcriptional Coactivators CREB-Binding Protein and SRC-1 to Hypoxia-Inducible Factor 1alpha. *Mol Cell Biol* **20**(1):402-415.

Chandel N, Budinger GR, Kemp RA and Schumacker PT (1995) Inhibition of cytochrome-c oxidase activity during prolonged hypoxia. *American Journal of Physiology - Lung Cellular and Molecular Physiology* **268**(6):L918-L925.

Chandel NS, McClintock DS, Feliciano CE, Wood TM, Melendez JA, Rodriguez AM and Schumacker PT (2000) Reactive Oxygen Species Generated at Mitochondrial Complex III Stabilize Hypoxia-inducible Factor-1α during Hypoxia. *Journal of Biological Chemistry* **275**(33):25130-25138.

Chen C, Pore N, Behrooz A, Ismail-Beigi F and Maity A (2001) Regulation of glut1 mRNA by Hypoxia-inducible Factor-1. *Journal of Biological Chemistry* **276**(12):9519.

Chen D, Li M, Luo J and Gu W (2003) Direct Interactions between HIF-1α and Mdm2 Modulate p53 Function. *Journal of Biological Chemistry* **278**(16):13595-13598.

Chen J, Marechal V and Levine AJ (1993) Mapping of the p53 and mdm-2 interaction domains. *Mol Cell Biol* **13**(7):4107-4114.

Chen X, Zhong Z, Xu Z, Chen L and Wang Y (2010) 2', 7'-Dichlorodihydrofluorescein as a fluorescent probe for reactive oxygen species measurement: Forty years of application and controversy. *Free radical research* **44**(6):587-604.

Chen Z, Lu W, Garcia-Prieto C and Huang P (2007) The Warburg effect and its cancer therapeutic implications. *Journal of Bioenergetics and Biomembranes* **39**(3):267-274.

Chua YL, Dufour E, Dassa EP, Rustin P, Jacobs HT, Taylor CT and Hagen T (2010) Stabilization of HIF-1α protein in hypoxia occurs independently of mitochondrial reactive oxygen species production. *Journal of Biological Chemistry*.

Chun Y-S, Choi E, Kim T-Y, Kim M-S and Park J-W (2002) A dominant-negative isoform lacking exons 11 and 12 of the human hypoxia-inducible factor-1alpha gene. *Biochem J* **362**(1):71-79.

Chun Y-S, Choi E, Yeo E-J, Lee JH, Kim M-S and Park J-W (2001) A new HIF-1 alpha variant induced by zinc ion suppresses HIF-1-mediated hypoxic responses. *J Cell Sci* **114**(22):4051-4061.

Chun Y-S, Lee K-H, Choi E, Bae S-Y, Yeo E-J, Huang LE, Kim M-S and Park J-W (2003) Phorbol Ester Stimulates the Nonhypoxic Induction of a Novel Hypoxia-Inducible Factor 1α Isoform. *Cancer Research* **63**(24):8700-8707.

Cockman ME, Masson N, Mole DR, Jaakkola P, Chang G-W, Clifford SC, Maher ER, Pugh CW, Ratcliffe PJ and Maxwell PH (2000) Hypoxia Inducible Factor-α Binding and Ubiquitylation by the von Hippel-Lindau Tumor Suppressor Protein. *Journal of Biological Chemistry* **275**(33):25733-25741.

Coutts AS, Adams CJ and La Thangue NB (2009) p53 ubiquitination by Mdm2: A never ending tail? *DNA Repair* **8**(4):483-490.

Crighton D, Wilkinson S, O'Prey J, Syed N, Smith P, Harrison PR, Gasco M, Garrone O, Crook T and Ryan KM (2006) DRAM, a p53-Induced Modulator of Autophagy, Is Critical for Apoptosis. *Cell* **126**(1):121-134.

Dai C and Gu W (2010) p53 post-translational modification: deregulated in tumorigenesis. *Trends in Molecular Medicine* **16**(11):528-536.

Dales J-P, Beaufils N, Silvy M, Picard C, Pauly V, Pradel V, Formisano-Treziny C, Bonnier P, Giusiano S, Charpin C and Gabert J (2010) Hypoxia inducible factor 1alpha gene (HIF-1alpha) splice variants: potential prognostic biomarkers in breast cancer. *BMC Medicine* **8**(1):44.

Dang CV and Semenza GL (1999) Oncogenic alterations of metabolism. *Trends in biochemical sciences* **24**(2):68-72.

Dann CE, Bruick RK and Deisenhofer J (2002) Structure of factor-inhibiting hypoxia-inducible factor 1: An asparaginyl hydroxylase involved in the hypoxic response pathway. *Proceedings of the National Academy of Sciences* **99**(24):15351-15356.

DeBerardinis RJ, Lum JJ, Hatzivassiliou G and Thompson CB (2008) The Biology of Cancer: Metabolic Reprogramming Fuels Cell Growth and Proliferation. *Cell Metabolism* **7**(1):11-20.

Depping R, Hägele S, Wagner KF, Wiesner RJ, Camenisch G, Wenger RH and Katschinski DM (2004) A Dominant-Negative Isoform of Hypoxia-Inducible Factor-1α Specifically Expressed in Human Testis1. *Biology of Reproduction* **71**(1):331-339.

Donald SP, Sun X-Y, Hu C-AA, Yu J, Mei JM, Valle D and Phang JM (2001) Proline Oxidase, Encoded by p53-induced Gene-6, Catalyzes the Generation of Proline-dependent Reactive Oxygen Species. *Cancer Research* **61**(5):1810-1815.

Donehower LA (2006) p53, longevity assurance and longevity suppression. *Drug Discovery Today: Disease Mechanisms* **3**(1):33-39.

Dutnall RN, Tafrov ST, Sternglanz R and Ramakrishnan V (1998) Structure of the Histone Acetyltransferase Hat1: A Paradigm for the GCN5-Related N-acetyltransferase Superfamily. *Cell* **94**(4):427-438.

Ebert BL and Bunn HF (1998) Regulation of Transcription by Hypoxia Requires a Multiprotein Complex That Includes Hypoxia-Inducible Factor 1, an Adjacent Transcription Factor, and p300/CREB Binding Protein. *Mol Cell Biol* **18**(7):4089-4096.

Ebert BL, Firth JD and Ratcliffe PJ (1995) Hypoxia and Mitochondrial Inhibitors Regulate Expression of Glucose Transporter-1 via Distinct Cis-acting Sequences. *Journal of Biological Chemistry* **270**(49):29083-29089.

El-Maghrabi MR and Pilkis SJ (1984) Rat liver 6-phosphofructo 2-kinase/ fructose 2,6-bisphosphatase: A review of relationships between the two activities of the enzyme. *Journal of Cellular Biochemistry* **26**(1):1-17.

Elstrom RL, Bauer DE, Buzzai M, Karnauskas R, Harris MH, Plas DR, Zhuang H, Cinalli RM, Alavi A, Rudin CM and Thompson CB (2004) Akt Stimulates Aerobic Glycolysis in Cancer Cells. *Cancer Research* **64**(11):3892-3899.

Ema M, Hirota K, Mimura J, Abe H, Yodoi J, Sogawa K, Poellinger L and Fujii-Kuriyama Y (1999) Molecular mechanisms of transcription activation by HLF and HIF1[alpha] in response to hypoxia: their stabilization and redox signal-induced interaction with CBP/p300. *EMBO J* **18**(7):1905-1914.

Ema M, Taya S, Yokotani N, Sogawa K, Matsuda Y and Fujii-Kuriyama Y (1997) A novel bHLH-PAS factor with close sequence similarity to hypoxia-inducible factor 1 regulates the VEGF expression and is potentially involved in lung and vascular development.

Proceedings of the National Academy of Sciences of the United States of America **94**(9):4273.

Epstein ACR, Gleadle JM, McNeill LA, Hewitson KS, O'Rourke J, Mole DR, Mukherji M, Metzen E, Wilson MI, Dhanda A, Tian Y-M, Masson N, Hamilton DL, Jaakkola P, Barstead R, Hodgkin J, Maxwell PH, Pugh CW, Schofield CJ and Ratcliffe PJ (2001) C. elegans EGL-9 and Mammalian Homologs Define a Family of Dioxygenases that Regulate HIF by Prolyl Hydroxylation. *Cell* **107**(1):43-54.

Feldser D, Agani F, Iyer NV, Pak B, Ferreira G and Semenza GL (1999) Reciprocal Positive Regulation of Hypoxia-inducible Factor 1α and Insulin-like Growth Factor 2. *Cancer Research* **59**(16):3915-3918.

Fetter JR, Qian J, Shapleigh J, Thomas JW, García-Horsman A, Schmidt E, Hosler J, Babcock GT, Gennis RB and Ferguson-Miller S (1995) Possible proton relay pathways in cytochrome c oxidase. *Proceedings of the National Academy of Sciences of the United States of America* **92**(5):1604-1608.

Firth JD, Ebert BL, Pugh CW and Ratcliffe PJ (1994) Oxygen-regulated control elements in the phosphoglycerate kinase 1 and lactate dehydrogenase A genes: similarities with the erythropoietin 3' enhancer. *Proceedings of the National Academy of Sciences of the United States of America* **91**(14):6496-6500.

Firth JD, Ebert BL and Ratcliffe PJ (1995) Hypoxic regulation of lactate dehydrogenase A. *Journal of Biological Chemistry* **270**(36):21021.

Flamme I, Fröhlich T, von Reutern M, Kappel A, Damert A and Risau W (1997) HRF, a putative basic helix-loop-helix-PAS-domain transcription factor is closely related to hypoxia-inducible factor-1[alpha] and developmentally expressed in blood vessels. *Mechanisms of Development* **63**(1):51-60.

Freedman SJ, Sun Z-YJ, Kung AL, France DS, Wagner G and Eck MJ (2003) Structural basis for negative regulation of hypoxia-inducible factor-1[alpha] by CITED2. *Nat Struct Mol Biol* **10**(7):504-512.

Frolov MV and Dyson NJ (2004) Molecular mechanisms of E2F-dependent activation and pRB-mediated repression. *Journal of Cell Science* **117**(11):2173-2181.

Fukuda R, Zhang H, Kim JW, Shimoda L, Dang CV and Semenza GL (2007) HIF-1 regulates cytochrome oxidase subunits to optimize efficiency of respiration in hypoxic cells. *Cell* **129**(1):111-122.

Garber K (2004) Energy Boost: The Warburg Effect Returns in a New Theory of Cancer. *Journal of the National Cancer Institute* **96**(24):1805-1806.

Gatenby R and Gillies R (2004) Why do cancers have high aerobic glycolysis? *Nature Reviews Cancer* **4**(11):891-899.

Gess B, Hofbauer K-H, Deutzmann R and Kurtz A (2004) Hypoxia up-regulates triosephosphate isomerase expression via a HIF-dependent pathway. *Pflügers Archiv European Journal of Physiology* **448**(2):175-180.

Gibson SL, Bindra RS and Glazer PM (2005) Hypoxia-Induced Phosphorylation of Chk2 in an Ataxia Telangiectasia Mutatedâ€“Dependent Manner. *Cancer Research* **65**(23):10734-10741.

Goldberg M, Dunning S and Bunn H (1988) Regulation of the erythropoietin gene: evidence that the oxygen sensor is a heme protein. *Science* **242**(4884):1412-1415.

Goldin N, Arzoine L, Heyfets A, Israelson A, Zaslavsky Z, Bravman T, Bronner V, Notcovich A, Shoshan-Barmatz V and Flescher E (2008) Methyl jasmonate binds to and detaches mitochondria-bound hexokinase. *Oncogene* **27**(34):4636-4643.

Gothié E, Richard DE, Berra E, Pagès G and Pouysségur J (2000) Identification of Alternative Spliced Variants of Human Hypoxia-inducible Factor-1α. *Journal of Biological Chemistry* **275**(10):6922-6927.

Gottifredi V and Prives C (2001) Molecular Biology: Getting p53 Out of the Nucleus. *Science* **292**(5523):1851-1852.

Gradin K, McGuire J, Wenger R, Kvietikova I, fhitelaw M, Toftgard R, Tora L, Gassmann M and Poellinger L (1996) Functional interference between hypoxia and dioxin signal transduction pathways: competition for recruitment of the Arnt transcription factor. *Mol Cell Biol* **16**(10):5221-5231.

Graeber TG, Peterson JF, Tsai M, Monica K, Fornace AJ, Jr. and Giaccia AJ (1994) Hypoxia induces accumulation of p53 protein, but activation of a G1-phase checkpoint by low-oxygen conditions is independent of p53 status. *Mol Cell Biol* **14**(9):6264-6277.

Grossman SR, Deato ME, Brignone C, Chan HM, Kung AL, Tagami H, Nakatani Y and Livingston DM (2003) Polyubiquitination of p53 by a Ubiquitin Ligase Activity of p300. *Science* **300**(5617):342-344.

Gu J, Nie L, Wiederschain D and Yuan Z-M (2001) Identification of p53 Sequence Elements That Are Required for MDM2-Mediated Nuclear Export. *Mol Cell Biol* **21**(24):8533-8546.

Gu W and Roeder RG (1997) Activation of p53 Sequence-Specific DNA Binding by Acetylation of the p53 C-Terminal Domain. *Cell* **90**(4):595-606.

Gu YZ, Moran SM, Hogenesch JB, Wartman L and Bradfield CA (1998) Molecular characterization and chromosomal localization of a third alpha-class hypoxia inducible factor subunit, HIF3alpha. *Gene Expr* **7**(3):205-213.

Halterman MW, Miller CC and Federoff HJ (1999) Hypoxia-Inducible Factor-1Î± Mediates Hypoxia-Induced Delayed Neuronal Death That Involves p53. *The Journal of Neuroscience* **19**(16):6818-6824.

Hanahan D (2000) The hallmarks of cancer. *Cell* **100**(1):57-70.

Hanahan D and Weinberg RA (2011) Hallmarks of cancer: the next generation. *Cell* **144**(5):646-674.

Hara S, Hamada J, Kobayashi C, Kondo Y and Imura N (2001) Expression and Characterization of Hypoxia-Inducible Factor (HIF)-3[alpha] in Human Kidney: Suppression of HIF-Mediated Gene Expression by HIF-3[alpha]. *Biochemical and Biophysical Research Communications* **287**(4):808-813.

Heimburg D, Hemmrich K, Zachariah S, Staiger H and Pallua N (2005) Oxygen consumption in undifferentiated versus differentiated adipogenic mesenchymal precursor cells. *Respiratory physiology & neurobiology* **146**(2-3):107-116.

Hellwig-Burgel T, Rutkowski K, Metzen E, Fandrey J and Jelkmann W (1999) Interleukin-1Î² and Tumor Necrosis Factor-îœ€ Stimulate DNA Binding of Hypoxia-Inducible Factor-1. *Blood* **94**(5):1561-1567.

Herrera JE, Bergel M, Yang X-J, Nakatani Y and Bustin M (1997) The Histone Acetyltransferase Activity of Human GCN5 and PCAF Is Stabilized by Coenzymes. *Journal of Biological Chemistry* **272**(43):27253-27258.

Hervouet E, Demont J, Pecina P, VojtÃ-skovÃ¡ A, Houstek J, Simonnet Hln and Godinot C (2005) A new role for the von Hippel-Lindau tumor suppressor protein: stimulation of mitochondrial oxidative phosphorylation complex biogenesis. *Carcinogenesis* **26**(3):531-539.

Hewitson KS, McNeill LA, Riordan MV, Tian Y-M, Bullock AN, Welford RW, Elkins JM, Oldham NJ, Bhattacharya S, Gleadle JM, Ratcliffe PJ, Pugh CW and Schofield CJ (2002) Hypoxia-inducible Factor (HIF) Asparagine Hydroxylase Is Identical to Factor Inhibiting HIF (FIH) and Is Related to the Cupin Structural Family. *Journal of Biological Chemistry* **277**(29):26351-26355.

Higuchi R, Dollinger G, Walsh PS and Griffith R (1992) Simultaneous Amplification and Detection of Specific DNA Sequences. *Nat Biotech* **10**(4):413-417.

Hirano G, Izumi H, Kidani A, Yasuniwa Y, Han B, Kusaba H, Akashi K, Kuwano M and Kohno K (2010) Enhanced Expression of PCAF Endows Apoptosis Resistance in Cisplatin-Resistant Cells. *Molecular Cancer Research* **8**(6):864-872.

Hirose K, Morita M, Ema M, Mimura J, Hamada H, Fujii H, Saijo Y, Gotoh O, Sogawa K and Fujii-Kuriyama Y (1996) cDNA cloning and tissue-specific expression of a novel basic helix-loop- helix/PAS factor (Arnt2) with close sequence similarity to the aryl hydrocarbon receptor nuclear translocator (Arnt). *Mol Cell Biol* **16**(4):1706-1713.

Honda R, Tanaka H and Yasuda H (1997) Oncoprotein MDM2 is a ubiquitin ligase E3 for tumor suppressor p53. *FEBS Letters* **420**(1):25-27.

Honda R and Yasuda H (1999) Association of p19ARF with Mdm2 inhibits ubiquitin ligase activity of Mdm2 for tumor suppressor p53. *EMBO J* **18**(1):22-27.

Horn D and Barrientos A (2008) Mitochondrial copper metabolism and delivery to cytochrome c oxidase. *IUBMB Life* **60**(7):421-429.

Horng Y-C, Leary SC, Cobine PA, Young FBJ, George GN, Shoubridge EA and Winge DR (2005) Human Sco1 and Sco2 Function as Copper-binding Proteins. *Journal of Biological Chemistry* **280**(40):34113-34122.

Hu C-J, Wang L-Y, Chodosh LA, Keith B and Simon MC (2003) Differential Roles of Hypoxia-Inducible Factor 1{alpha} (HIF-1{alpha}) and HIF-2{alpha} in Hypoxic Gene Regulation. *Mol Cell Biol* **23**(24):9361-9374.

Hu W, Zhang C, Wu R, Sun Y, Levine A and Feng Z (2010) Glutaminase 2, a novel p53 target gene regulating energy metabolism and antioxidant function. *Proceedings of the National Academy of Sciences* **107**(16):7455-7460.

Huang LE, Gu J, Schau M and Bunn HF (1998) Regulation of hypoxia-inducible factor 1α is mediated by an O2-dependent degradation domain via the ubiquitin-proteasome pathway. *Proceedings of the National Academy of Sciences of the United States of America* **95**(14):7987-7992.

Invitrogen (2007) *TOPO cloning technology*. Invitrogen.

Isobe M, Emanuel BS, Givol D, Oren M and Croce CM (1986) Localization of gene for human p53 tumour antigen to band 17p13. *Nature* **320**(6057):84-85.

Ivan M, Kondo K, Yang H, Kim W, Valiando J, Ohh M, Salic A, Asara JM, Lane WS and Kaelin Jr. WG (2001) HIFα Targeted for VHL-Mediated Destruction by Proline Hydroxylation: Implications for O2 Sensing. *Science* **292**(5516):464-468.

Iyer NV, Kotch LE, Agani F, Leung SW, Laughner E, Wenger RH, Gassmann M, Gearhart JD, Lawler AM, Yu AY and Semenza GL (1998) Cellular and developmental control of O2 homeostasis by hypoxia-inducible factorâ€‰1Î±. *Genes & Development* **12**(2):149-162.

Jaakkola P, Mole DR, Tian YM, Wilson MI, Gielbert J, Gaskell SJ, Kriegsheim A, Hebestreit HF, Mukherji M and Schofield CJ (2001) Targeting of HIF- to the von Hippel-Lindau ubiquitylation complex by O2-regulated prolyl hydroxylation. *Science* **292**(5516):468.

Jain S, Maltepe E, Lu MM, Simon C and Bradfield CA (1998) Expression of ARNT, ARNT2, HIF1 alpha, HIF2 alpha and Ah receptor mRNAs in the developing mouse. *Mech Dev* **73**(1):117-123.

Jeong J-W, Bae M-K, Ahn M-Y, Kim S-H, Sohn T-K, Bae M-H, Yoo M-A, Song EJ, Lee K-J and Kim K-W (2002) Regulation and Destabilization of HIF-1[alpha] by ARD1-Mediated Acetylation. *Cell* **111**(5):709-720.

Jiang B-H, Agani F, Passaniti A and Semenza GL (1997a) V-SRC Induces Expression of Hypoxia-inducible Factor 1 (HIF-1) and Transcription of Genes Encoding Vascular Endothelial Growth Factor and Enolase 1: Involvement of HIF-1 in Tumor Progression. *Cancer Research* **57**(23):5328-5335.

Jiang B-H, Rue E, Wang GL, Roe R and Semenza GL (1996) Dimerization, DNA Binding, and Transactivation Properties of Hypoxia-inducible Factor 1. *Journal of Biological Chemistry* **271**(30):17771-17778.

Jiang B-H, Zheng JZ, Leung SW, Roe R and Semenza GL (1997b) Transactivation and Inhibitory Domains of Hypoxia-inducible Factor 1α. *Journal of Biological Chemistry* **272**(31):19253-19260.

Jin Y, Zeng SX, Dai MS, Yang XJ and Lu H (2002) MDM2 inhibits PCAF (p300/CREB-binding protein-associated factor)-mediated p53 acetylation. *Journal of Biological Chemistry* **277**(34):30838.

Jones RG and Thompson CB (2009) Tumor suppressors and cell metabolism: a recipe for cancer growth. *Genes & Development* **23**(5):537-548.

Kadenbach B, Jarausch J, Hartmann R and Merle P (1983) Separation of mammalian cytochrome c oxidase into 13 polypeptides by a sodium dodecyl sulfate-gel electrophoretic procedure. *Analytical Biochemistry* **129**(2):517-521.

Kallio PJ, Okamoto K, O'Brien S, Carrero P, Makino Y, Tanaka H and Poellinger L (1998) Signal transduction in hypoxic cells: inducible nuclear translocation and recruitment of theCBP/p300 coactivator by the hypoxia-inducible factor-1. *EMBO J* **17**(22):6573-6586.

Kallio PJ, Pongratz I, Gradin K, McGuire J and Poellinger L (1997) Activation of hypoxia-inducible factor 1α: Posttranscriptional regulation and conformational change by recruitment of the Arnt transcription factor. *Proceedings of the National Academy of Sciences of the United States of America* **94**(11):5667-5672.

Kallio PJ, Wilson WJ, O'Brien S, Makino Y and Poellinger L (1999) Regulation of the Hypoxia-inducible Transcription Factor 1α by the Ubiquitin-Proteasome Pathway. *Journal of Biological Chemistry* **274**(10):6519-6525.

Kamura T, Koepp DM, Conrad MN, Skowyra D, Moreland RJ, Iliopoulos O, Lane WS, Kaelin WG, Elledge SJ, Conaway RC, Harper JW and Conaway JW (1999) Rbx1, a Component of the VHL Tumor Suppressor Complex and SCF Ubiquitin Ligase. *Science* **284**(5414):657-661.

Kamura T, Sato S, Iwai K, Czyzyk-Krzeska M, Conaway RC and Conaway JW (2000) Activation of HIF1α ubiquitination by a reconstituted von Hippel-Lindau (VHL) tumor suppressor complex. *Proceedings of the National Academy of Sciences* **97**(19):10430-10435.

Karnoub AE and Weinberg RA (2008) Ras oncogenes: split personalities. *Nat Rev Mol Cell Biol* **9**(7):517-531.

Ke Q and Costa M (2006) Hypoxia-Inducible Factor-1 (HIF-1). *Molecular Pharmacology* **70**(5):1469-1480.

Kim J-w and Dang CV (2006) Cancer's Molecular Sweet Tooth and the Warburg Effect. *Cancer Research* **66**(18):8927-8930.

Kim J-w, Gao P, Liu Y-C, Semenza GL and Dang CV (2007) HIF-1 and Dysregulated c-Myc Cooperatively Induces VEGF and Metabolic Switches, HK2 and PDK1. *Mol Cell Biol*:MCB.00440-00407.

Kim J-w, Zeller KI, Wang Y, Jegga AG, Aronow BJ, O'Donnell KA and Dang CV (2004a) Evaluation of Myc E-Box Phylogenetic Footprints in Glycolytic Genes by Chromatin Immunoprecipitation Assays. *Mol Cell Biol* **24**(13):5923-5936.

Kim JW, Tchernyshyov I, Semenza GL and Dang CV (2006) HIF-1-mediated expression of pyruvate dehydrogenase kinase: a metabolic switch required for cellular adaptation to hypoxia. *Cell Metab* **3**(3):177-185.

Kim JY, Ahn HJ, Ryu JH, Suk K and Park JH (2004b) BH3-only protein Noxa is a mediator of hypoxic cell death induced by hypoxia-inducible factor 1. *The Journal of Experimental Medicine* **199**(1):113.

Kimata M, Matoba S, Iwai-Kanai E, Nakamura H, Hoshino A, Nakaoka M, Katamura M, Okawa Y, Mita Y, Okigaki M, Ikeda K, Tatsumi T and Matsubara H (2010) p53 and TIGAR

regulate cardiac myocyte energy homeostasis under hypoxic stress. *Am J Physiol Heart Circ Physiol* **299**(6):H1908-1916.

Knies-Bamforth UE, Fox SB, Poulsom R, Evan GI and Harris AL (2004) c-Myc Interacts with Hypoxia to Induce Angiogenesis In vivo by a Vascular Endothelial Growth Factor-Dependent Mechanism. *Cancer Research* **64**(18):6563-6570.

Knights CD, Jason C, Giovanni SD, Muratoglu S, Perez R, Swartzbeck A, Quong AA, Zhang X, Beerman T, Pestell RG and Avantaggiati ML (2006) Distinct p53 Acetylation Cassettes Differentially Influence Gene-Expression Patterns and Cell Fate. *The Journal of Cell Biology* **173**(4):533-544.

Koh MY, Darnay BG and Powis G (2008) HAF, a novel E3-ubiquitin ligase, binds and ubiquitinates HIF-1 {alpha} leading to its oxygen-independent degradation. *Mol Cell Biol*:MCB. 00773-00708v00771.

Kondoh H, Lleonart ME, Gil J, Wang J, Degan P, Peters G, Martinez D, Carnero A and Beach D (2005) Glycolytic Enzymes Can Modulate Cellular Life Span. *Cancer Research* **65**(1):177-185.

Koong AC, Chen EY and Giaccia AJ (1994) Hypoxia Causes the Activation of Nuclear Factor ÎºB through the Phosphorylation of IÎºBÎ± on Tyrosine Residues. *Cancer Research* **54**(6):1425-1430.

Kroemer G and Pouyssegur J (2008) Tumor Cell Metabolism: Cancer's Achilles' Heel. *Cancer Cell* **13**(6):472-482.

Kung AL, Wang S, Klco JM, Kaelin WG and Livingston DM (2000) Suppression of tumor growth through disruption of hypoxia-inducible transcription. *Nature medicine* **6**(12):1335-1340.

Lamb P and Crawford L (1986) Characterization of the human p53 gene. *Mol Cell Biol* **6**(5):1379-1385.

Lambert PF, Kashanchi F, Radonovich MF, Shiekhattar R and Brady JN (1998) Phosphorylation of p53 Serine 15 Increases Interaction with CBP. *Journal of Biological Chemistry* **273**(49):33048-33053.

Lando D, Peet DJ, Gorman JJ, Whelan DA, Whitelaw ML and Bruick RK (2002a) FIH-1 is an asparaginyl hydroxylase enzyme that regulates the transcriptional activity of hypoxia-inducible factor. *Genes & Development* **16**(12):1466-1471.

Lando D, Peet DJ, Whelan DA, Gorman JJ and Whitelaw ML (2002b) Asparagine Hydroxylation of the HIF Transactivation Domain: A Hypoxic Switch. *Science* **295**(5556):858-861.

Lane DP (1992) p53, guardian of the genome. *Nature* **358**(6381):15-16.

Leary SC, Cobine PA, Kaufman BA, Guercin G-H, Mattman A, Palaty J, Lockitch G, Winge DR, Rustin P, Horvath R and Shoubridge EA (2007) The Human Cytochrome c Oxidase Assembly Factors SCO1 and SCO2 Have Regulatory Roles in the Maintenance of Cellular Copper Homeostasis. *Cell Metabolism* **5**(1):9-20.

Leary SC, Kaufman BA, Pellecchia G, Guercin G-H, Mattman A, Jaksch M and Shoubridge EA (2004) Human SCO1 and SCO2 have independent, cooperative functions in copper delivery to cytochrome c oxidase. *Human Molecular Genetics* **13**(17):1839-1848.

Lee EYHP and Muller WJ (2010) Oncogenes and Tumor Suppressor Genes. *Cold Spring Harbor Perspectives in Biology* **2**(10).

Lee K-H, Park J-W and Chun Y-S (2004) Non-hypoxic transcriptional activation of the aryl hydrocarbon receptor nuclear translocator in concert with a novel hypoxia-inducible factor-1alpha isoform. *Nucleic Acids Research* **32**(18):5499-5511.

Lee SK, Kim HJ, Kim JW and Lee JW (1999) Steroid receptor coactivator-1 and its family members differentially regulate transactivation by the tumor suppressor protein p53. *Molecular Endocrinology* **13**(11):1924.

Lee SM, Kim JH, Cho EJ and Youn HD (2009) A nucleocytoplasmic malate dehydrogenase regulates p53 transcriptional activity in response to metabolic stress. *Cell Death Differ* **16**(5):738-748.

Lehninger AL, Nelson DL and Cox MM (2005) *Lehninger principles of biochemistry*. WH Freeman & Company.

Levy AP, Levy NS, Wegner S and Goldberg MA (1995) Transcriptional Regulation of the Rat Vascular Endothelial Growth Factor Gene by Hypoxia. *Journal of Biological Chemistry* **270**(22):13333-13340.

Li F, Wang Y, Zeller KI, Potter JJ, Wonsey DR, O'Donnell KA, Kim J-w, Yustein JT, Lee LA and Dang CV (2005) Myc Stimulates Nuclearly Encoded Mitochondrial Genes and Mitochondrial Biogenesis. *Mol Cell Biol* **25**(14):6225-6234.

Li H and Jogl G (2009) Structural and biochemical studies of TIGAR (TP53-induced glycolysis and apoptosis regulator). *Journal of Biological Chemistry* **284**(3):1748-1754.

Li M, Brooks CL, Wu-Baer F, Chen D, Baer R and Gu W (2003) Mono- Versus Polyubiquitination: Differential Control of p53 Fate by Mdm2. *Science* **302**(5652):1972-1975.

Li M, Chen D, Shiloh A, Luo J, Nikolaev AY, Qin J and Gu W (2002a) Deubiquitination of p53 by HAUSP is an important pathway for p53 stabilization. *Nature* **416**(6881):648-653.

Li M, Luo J, Brooks CL and Gu W (2002b) Acetylation of p53 inhibits its ubiquitination by Mdm2. *Journal of Biological Chemistry* **277**(52):50607.

Lim J-H, Lee Y-M, Chun Y-S, Chen J, Kim J-E and Park J-W (2010) Sirtuin 1 Modulates Cellular Responses to Hypoxia by Deacetylating Hypoxia-Inducible Factor 1alpha. *Molecular Cell* **38**(6):864-878.

Lin J, Chen J, Elenbaas B and Levine AJ (1994) Several hydrophobic amino acids in the p53 amino-terminal domain are required for transcriptional activation, binding to mdm-2 and the adenovirus 5 E1B 55-kD protein. *Genes & Development* **8**(10):1235-1246.

Lin S-J and Guarente L (2003) Nicotinamide adenine dinucleotide, a metabolic regulator of transcription, longevity and disease. *Current Opinion in Cell Biology* **15**(2):241-246.

Lin W-C, Lin F-T and Nevins JR (2001) Selective induction of E2F1 in response to DNA damage, mediated by ATM-dependent phosphorylation. *Genes & Development* **15**(14):1833-1844.

Linares LK, Kiernan R, Triboulet R, Chable-Bessia C, Latreille D, Cuvier O, Lacroix M, Le Cam L, Coux O and Benkirane M (2007) Intrinsic ubiquitination activity of PCAF controls the stability of the oncoprotein Hdm2. *Nat Cell Biol* **9**(3):331-338.

Ling B and Wei-Guo Z (2006) p53: Structure, Function and Therapeutic Applications. *Journal of Cancer Molecule* **2**(4):141-153.

Liu L, Scolnick DM, Trievel RC, Zhang HB, Marmorstein R, Halazonetis TD and Berger SL (1999) p53 sites acetylated in vitro by PCAF and p300 are acetylated in vivo in response to DNA damage. *Mol Cell Biol* **19**(2):1202.

Liu Y, Colosimo AL, Yang X-J and Liao D (2000) Adenovirus E1B 55-Kilodalton Oncoprotein Inhibits p53 Acetylation by PCAF. *Mol Cell Biol* **20**(15):5540-5553.

Liu YV, Baek JH, Zhang H, Diez R, Cole RN and Semenza GL (2007) RACK1 Competes with HSP90 for Binding to HIF-1[alpha] and Is Required for O2-Independent and HSP90 Inhibitor-Induced Degradation of HIF-1[alpha]. *Molecular Cell* **25**(2):207-217.

Lowe S (1999) Activation of p53 by oncogenes. *Endocrine-related cancer* **6**(1):45.

Lozano G and Elledge SJ (2000) Cancer: p53 sends nucleotides to repair DNA. *Nature* **404**(6773):24-25.

Lu H and Levine AJ (1995) Human TAFII31 protein is a transcriptional coactivator of the p53 protein. *Proceedings of the National Academy of Sciences of the United States of America* **92**(11):5154-5158.

Lu T and Finkel T (2008) Free radicals and senescence. *Experimental Cell Research* **314**(9):1918-1922.

Lukashev D and Sitkovsky M (2008) Preferential expression of the novel alternative isoform I.3 of hypoxia-inducible factor 1[alpha] in activated human T lymphocytes. *Human Immunology* **69**(7):421-425.

Luo J and Shibuya M (2001) A variant of nuclear localization signal of bipartite-type is required for the nuclear translocation of hypoxia inducible factors (1alpha, 2alpha and 3alpha). *Oncogene* **20**(12):1435.

Mabjeesh NJ, Escuin D, LaVallee TM, Pribluda VS, Swartz GM, Johnson MS, Willard MT, Zhong H, Simons JW and Giannakakou P (2003) 2ME2 inhibits tumor growth and angiogenesis by disrupting microtubules and dysregulating HIF. *Cancer Cell* **3**(4):363-375.

MacDonald MJ and Marshall LK (2000) Mouse Lacking NAD+-Linked Glycerol Phosphate Dehydrogenase Has Normal Pancreatic Beta Cell Function But Abnormal Metabolite Pattern in Skeletal Muscle. *Archives of Biochemistry and Biophysics* **384**(1):143-153.

Macey MG (2007) *Flow cytometry: Principles and applications*.

Mahon PC, Hirota K and Semenza GL (2001) FIH-1: a novel protein that interacts with HIF-1α and VHL to mediate repression of HIF-1 transcriptional activity. *Genes & Development* **15**(20):2675-2686.

Maki CG, Huibregtse JM and Howley PM (1996) In Vivo Ubiquitination and Proteasome-mediated Degradation of p53. *Cancer Research* **56**(11):2649-2654.

Marín-Hernández A, Rodríguez-Enríquez S, Vital-González PA, Flores-Rodríguez FL, Macías-Silva M, Sosa-Garrocho M and Moreno-Sánchez R (2006) Determining and understanding the control of glycolysis in fast-growth tumor cells. *FEBS Journal* **273**(9):1975-1988.

Martínez-Balbas MA, Bauer UM, Nielsen SJ, Brehm A and Kouzarides T (2000) Regulation of E2F1 activity by acetylation. *EMBO J* **19**(4):662-671.

Masson N, Willam C, Maxwell PH, Pugh CW and Ratcliffe PJ (2001) Independent function of two destruction domains in hypoxia-inducible factor- chains activated by prolyl hydroxylation. *EMBO J* **20**(18):5197-5206.

Mathupala SP, Heese C and Pedersen PL (1997) Glucose Catabolism in Cancer Cells. *Journal of Biological Chemistry* **272**(36):22776-22780.

Matoba S, Kang JG, Patino WD, Wragg A, Boehm M, Gavrilova O, Hurley PJ, Bunz F and Hwang PM (2006) p53 regulates mitochondrial respiration. *Science* **312**(5780):1650-1653.

Maxwell PH, Wiesener MS, Chang G-W, Clifford SC, Vaux EC, Cockman ME, Wykoff CC, Pugh CW, Maher ER and Ratcliffe PJ (1999) The tumour suppressor protein VHL targets hypoxia-inducible factors for oxygen-dependent proteolysis. *Nature* **399**(6733):271-275.

Maynard MA and Evans AJ (2007) Dominant-negative HIF-3a4 suppresses VHL-null renal cell carcinoma progression. *Cell Cycle* **6**(22):2810-2816.

Maynard MA, Evans AJ, Hosomi T, Hara S, Jewett MAS and Ohh M (2005) Human HIF-3α4 is a dominant-negative regulator of HIF-1 and is down-regulated in renal cell carcinoma. *The FASEB Journal* **19**(11):1396-1406.

Maynard MA, Qi H, Chung J, Lee EHL, Kondo Y, Hara S, Conaway RC, Conaway JW and Ohh M (2003) Multiple Splice Variants of the Human HIF-3α Locus Are Targets of the von Hippel-Lindau E3 Ubiquitin Ligase Complex. *Journal of Biological Chemistry* **278**(13):11032-11040.

Meek DW and Anderson CW (2009) Posttranslational Modification of p53: Cooperative Integrators of Function. *Cold Spring Harbor Perspectives in Biology* **1**(6).

Mendonça DBS, Mendonça G, Aragão FJL and Cooper LF (2011) NF-[kappa]B suppresses HIF-1[alpha] response by competing for P300 binding. *Biochemical and Biophysical Research Communications* **404**(4):997-1003.

Minamino T, Orimo M, Shimizu I, Kunieda T, Yokoyama M, Ito T, Nojima A, Nabetani A, Oike Y, Matsubara H, Ishikawa F and Komuro I (2009) A crucial role for adipose tissue p53 in the regulation of insulin resistance. *Nat Med* **15**(9):1082-1087.

Minchenko A, Leshchinsky I, Opentanova I, Sang N, Srinivas V, Armstead V and Caro J (2002) Hypoxia-inducible factor-1-mediated expression of the 6-phosphofructo-2-kinase/fructose-2, 6-bisphosphatase-3 (PFKFB3) gene. *Journal of Biological Chemistry* **277**(8):6183.

Minchenko O, Opentanova I and Caro J (2003) Hypoxic regulation of the 6-phosphofructo-2-kinase/fructose-2,6-bisphosphatase gene family (PFKFB-1-4) expression in vivo. *FEBS Letters* **554**(3):264-270.

Minchenko O, Opentanova I, Minchenko D, Ogura T and Esumi H (2004) Hypoxia induces transcription of 6-phosphofructo-2-kinase/fructose-2, 6-biphosphatase-4 gene via hypoxia-inducible factor-1alpha activation. *FEBS Letters* **576**(1-2):14.

Moll UM and Petrenko O (2003) The MDM2-p53 Interaction. *Molecular Cancer Research* **1**(14):1001-1008.

Mongan PD, Capacchione J, West S, Karaian J, Dubois D, Keneally R and Sharma P (2002) Pyruvate improves redox status and decreases indicators of hepatic apoptosis during hemorrhagic shock in swine. *American Journal of Physiology - Heart and Circulatory Physiology* **283**(4):H1634-H1644.

Morotti A, Cilloni D, Pautasso M, Messa F, Arruga F, Defilippi I, Carturan S, Catalano R, Rosso V, Chiarenza A, Taulli R, Bracco E, Rege-Cambrin G, Gottardi E and Saglio G (2006) NF-kB inhibition as a strategy to enhance etoposide-induced apoptosis in K562 cell line. *American Journal of Hematology* **81**(12):938-945.

Müller L, Schaupp A, Walerych D, Wegele H and Buchner J (2004) Hsp90 Regulates the Activity of Wild Type p53 under Physiological and Elevated Temperatures. *Journal of Biological Chemistry* **279**(47):48846-48854.

Mullis K (1983) Polymerase chain reaction.

Murray RK, Granner DK and Rodwell VW (2003) *Harper's illustrated biochemistry*. McGraw-Hill New York.

Naito AT, Okada S, Minamino T, Iwanaga K, Liu M-L, Sumida T, Nomura S, Sahara N, Mizoroki T, Takashima A, Akazawa H, Nagai T, Shiojima I and Komuro I (2010) Promotion of CHIP-Mediated p53 Degradation Protects the Heart From Ischemic Injury. *Circ Res* **106**(11):1692-1702.

Nakano K and Vousden KH (2001) PUMA, a Novel Proapoptotic Gene, Is Induced by p53. *Molecular Cell* **7**(3):683-694.

Nardinocchi L, Puca R and D'Orazi G (2011) HIF-1 antagonizes p53-mediated apoptosis by triggering HIPK2 degradation. *Aging (Albany NY)* **3**(1):33.

Nisselbaum JS and Green S (1969) A simple ultramicro method for determination of pyridine nucleotides in tissues. *Analytical Biochemistry* **27**(2):212-217.

Obach M, Navarro-Sabaté À, Caro J, Kong X, Duran J, Gómez M, Perales J, Ventura F, Rosa J and Bartrons R (2004) 6-Phosphofructo-2-kinase (pfkfb3) gene promoter contains hypoxia-inducible factor-1 binding sites necessary for transactivation in response to hypoxia. *Journal of Biological Chemistry* **279**(51):53562.

Oda E, Ohki R, Murasawa H, Nemoto J, Shibue T, Yamashita T, Tokino T, Taniguchi T and Tanaka âN (2000) Noxa, a BH3-Only Member of the Bcl-2 Family and Candidate Mediator of p53-Induced Apoptosis. *Science* **288**(5468):1053-1058.

Oehme F, Ellinghaus P, Kolkhof P, Smith TJ, Ramakrishnan S, HÃ¼tter J, Schramm M and Flamme I (2002) Overexpression of PH-4, a novel putative proline 4-hydroxylase, modulates activity of hypoxia-inducible transcription factors. *Biochemical and Biophysical Research Communications* **296**(2):343-349.

Ohh M, Park CW, Ivan M, Hoffman MA, Kim T-Y, Huang LE, Pavletich N, Chau V and Kaelin WG (2000) Ubiquitination of hypoxia-inducible factor requires direct binding to the [bgr]-domain of the von Hippel-Lindau protein. *Nat Cell Biol* **2**(7):423-427.

Okorokov AL and Milner J (1999) An ATP/ADP-Dependent Molecular Switch Regulates the Stability of p53-DNA Complexes. *Mol Cell Biol* **19**(11):7501-7510.

Okumura K, Mendoza M, Bachoo RM, DePinho RA, Cavenee WK and Furnari FB (2006) PCAF Modulates PTEN Activity. *Journal of Biological Chemistry* **281**(36):26562-26568.

Oliner JD, Kinzler KW, Meltzer PS, George DL and Vogelstein B (1992) Amplification of a gene encoding a p53-associated protein in human sarcomas. *Nature* **358**(6381):80-83.

Oliner JD, Pietenpol JA, Thiagalingam S, Gyuris J, Kinzler KW and Vogelstein B (1993) Oncoprotein MDM2 conceals the activation domain of tumour suppressor p53. *Nature* **362**(6423):857-860.

Ostrakhovitch E and Cherian M (2005) Role of p53 and reactive oxygen species in apoptotic response to copper and zinc in epithelial breast cancer cells. *Apoptosis* **10**(1):111-121.

Papandreou I, Cairns RA, Fontana L, Lim AL and Denko NC (2006) HIF-1 mediates adaptation to hypoxia by actively downregulating mitochondrial oxygen consumption. *Cell Metab* **3**(3):187-197.

Pastorino JG, Shulga N and Hoek JB (2002) Mitochondrial Binding of Hexokinase II Inhibits Bax-induced Cytochrome c Release and Apoptosis. *Journal of Biological Chemistry* **277**(9):7610-7618.

Pedersen PL (2007) Warburg, me and Hexokinase 2: Multiple discoveries of key molecular events underlying one of cancers' most common phenotypes, the "Warburg Effect", ie, elevated glycolysis in the presence of oxygen. *Journal of bioenergetics and biomembranes* **39**(3):211-222.

Pedersen PL, Mathupala S, Rempel A, Geschwind JF and Ko YH (2002) Mitochondrial bound type II hexokinase: a key player in the growth and survival of many cancers and an ideal prospect for therapeutic intervention. *Biochimica et Biophysica Acta (BBA)-Bioenergetics* **1555**(1-3):14-20.

Pediconi N, Guerrieri F, Vossio S, Bruno T, Belloni L, Schinzari V, Scisciani C, Fanciulli M and Levrero M (2009) hSirT1-Dependent Regulation of the PCAF-E2F1-p73 Apoptotic Pathway in Response to DNA Damage. *Mol Cell Biol* **29**(8):1989-1998.

Pietenpol JA, Tokino T, Thiagalingam S, el-Deiry WS, Kinzler KW and Vogelstein B (1994) Sequence-specific transcriptional activation is essential for growth suppression by p53. *Proceedings of the National Academy of Sciences of the United States of America* **91**(6):1998-2002.

Pilkis SJ, El-Maghrabi MR, Pilkis J, Claus TH and Cumming DA (1981) Fructose 2,6-bisphosphate. A new activator of phosphofructokinase. *Journal of Biological Chemistry* **256**(7):3171-3174.

Pillai S, Kovacs M and Chellappan S (2010) Regulation of Vascular Endothelial Growth Factor Receptors by Rb and E2F1: Role of Acetylation. *Cancer Research*.

Promega (2007) PGL3 promoter vector.

Pugh CW, O'Rourke JF, Nagao M, Gleadle JM and Ratcliffe PJ (1997) Activation of Hypoxia-inducible Factor-1; Definition of Regulatory Domains within the α Subunit. *Journal of Biological Chemistry* **272**(17):11205-11214.

Pugh CW, Tan CC, Jones RW and Ratcliffe PJ (1991) Functional analysis of an oxygen-regulated transcriptional enhancer lying 3' to the mouse erythropoietin gene. *Proceedings of the National Academy of Sciences of the United States of America* **88**(23):10553-10557.

Qiagen (2000) Polyfect Transfection Reagent Handbook, Qiagen.

Qiagen (2006) Critical factors for successful real time PCR.

Racker E (1983) The Warburg effect: two years later. *Science* **222**(4621):232.

Ramasamy R, Trueblood N and Schaefer S (1998) Metabolic effects of aldose reductase inhibition during low-flow ischemia and reperfusion. *American Journal of Physiology - Heart and Circulatory Physiology* **275**(1):H195-H203.

Ramkumar R, Garva R, Demonacos MK and Demonacos C (2011) Sirtuins: molecular traffic lights in the crossroad of oxidative stress, chromatin remodelling and transcription. *Journal Biotechnoligy and Biomedicine*.

Ravi R, Mookerjee B, Bhujwalla ZM, Sutter CH, Artemov D, Zeng Q, Dillehay LE, Madan A, Semenza GL and Bedi A (2000) Regulation of tumor angiogenesis by p53-induced degradation of hypoxia-inducible factor 1α. *Genes & Development* **14**(1):34-44.

Richard DE, Berra E, Gothié E, Roux D and Pouysségur J (1999) p42/p44 Mitogen-activated Protein Kinases Phosphorylate Hypoxia-inducible Factor 1α (HIF-1α) and Enhance the Transcriptional Activity of HIF-1. *Journal of Biological Chemistry* **274**(46):32631-32637.

Roe J-S, Kim H, Lee S-M, Kim S-T, Cho E-J and Youn H-D (2006) p53 Stabilization and Transactivation by a von Hippel-Lindau Protein. *Molecular Cell* **22**(3):395-405.

Ruddon RW (2007) *Cancer biology*. Oxford University Press, USA.

Ryan J (2004) General guide for cryogenically storing animal cell cultures. *Corning Life Sciences Technical Monograph TC-306: PDF can be downloaded from Technical Information/Cell Culture at www corning com/lifesciences*.

Sakaguchi K, Herrera JE, Saito Si, Miki T, Bustin M, Vassilev A, Anderson CW and Appella E (1998) DNA damage activates p53 through a phosphorylationâ€“acetylation cascade. *Genes & Development* **12**(18):2831-2841.

Sakaguchi K, Sakamoto H, Lewis MS, Anderson CW, Erickson JW, Appella E and Xie D (1997) Phosphorylation of serine 392 stabilizes the tetramer formation of tumor suppressor protein p53. *Biochemistry* **36**(33):10117-10124.

Sakakibara R, Kato M, Okamura N, Nakagawa T, Komada Y, Tominaga N, Shimojo M and Fukasawa M (1997) Characterization of a human placental fructose-6-phosphate, 2-kinase/fructose-2, 6-bisphosphatase. *Journal of biochemistry* **122**(1):122.

Sakamuro D, Sabbatini P, White E and Prendergast GC (1997) The polyproline region of p53 is required to activate apoptosis but not growth arrest. *Oncogene* **15**(8):887-898.

Salceda S and Caro J (1997) Hypoxia-inducible Factor 1α (HIF-1α) Protein Is Rapidly Degraded by the Ubiquitin-Proteasome System under Normoxic Conditions. *Journal of Biological Chemistry* **272**(36):22642-22647.

Sang N, Stiehl DP, Bohensky J, Leshchinsky I, Srinivas V and Caro J (2003) MAPK signaling up-regulates the activity of hypoxia-inducible factors by its effects on p300. *Journal of Biological Chemistry* **278**(16):14013.

Sanni LA, Rae C, Maitland A, Stocker R and Hunt NH (2001) Is Ischemia Involved in the Pathogenesis of Murine Cerebral Malaria? *The American Journal of Pathology* **159**(3):1105-1112.

Santos Rosa H, Valls E, Kouzarides T and Martínez Balbás M (2003) Mechanisms of P/CAF auto acetylation. *Nucleic acids research* **31**(15):4285.

Schmid T, Zhou J, Köhl R and Brüne B (2004) p300 relieves p53-evoked transcriptional repression of hypoxia-inducible factor-1 (HIF-1). *Biochem J* **380**(1):289-295.

Schroedl C, McClintock DS, Budinger GRS and Chandel NS (2002) Hypoxic but not anoxic stabilization of HIF-1α requires mitochondrial reactive oxygen species. *American Journal of Physiology - Lung Cellular and Molecular Physiology* **283**(5):L922-L931.

Schwartz JP, Passonneau JV, Johnson GS and Pastan I (1974) The Effect of Growth Conditions on NAD+ and NADH Concentrations and the NAD+:NADH Ratio in Normal and Transformed Fibroblasts. *Journal of Biological Chemistry* **249**(13):4138-4143.

Schwartzenberg-Bar-Yoseph F, Armoni M and Karnieli E (2004a) The tumor suppressor p53 down-regulates glucose transporters GLUT1 and GLUT4 gene expression. *Cancer research* **64**(7):2627.

Schwartzenberg-Bar-Yoseph F, Armoni M and Karnieli E (2004b) The Tumor Suppressor p53 Down-Regulates Glucose Transporters GLUT1 and GLUT4 Gene Expression. *Cancer Research* **64**(7):2627-2633.

Seagroves TN, Ryan HE, Lu H, Wouters BG, Knapp M, Thibault P, Laderoute K and Johnson RS (2001) Transcription Factor HIF-1 Is a Necessary Mediator of the Pasteur Effect in Mammalian Cells. *Mol Cell Biol* **21**(10):3436-3444.

Selak MA, Armour SM, MacKenzie ED, Boulahbel H, Watson DG, Mansfield KD, Pan Y, Simon MC, Thompson CB and Gottlieb E (2005) Succinate links TCA cycle dysfunction to oncogenesis by inhibiting HIF-± prolyl hydroxylase. *Cancer Cell* **7**(1):77-85.

Selvakumaran M, Lin HK, Miyashita T, Wang HG, Krajewski S, Reed JC, Hoffman B and Liebermann D (1994) Immediate early up-regulation of bax expression by p53 but not TGF beta 1: a paradigm for distinct apoptotic pathways. *Oncogene* **9**(6):1791-1798.

Semenza GL (1998) Hypoxia-inducible factor 1: master regulator of O2 homeostasis. *Current Opinion in Genetics & Development* **8**(5):588-594.

Semenza GL (2003) Targeting HIF-1 for cancer therapy. *Nature Reviews Cancer* **3**(10):721-732.

Semenza GL (2009) Involvement of oxygen-sensing pathways in physiologic and pathologic erythropoiesis. *Blood* **114**(10):2015-2019.

Semenza GL, Nejfelt MK, Chi SM and Antonarakis SE (1991) Hypoxia-inducible nuclear factors bind to an enhancer element located 3' to the human erythropoietin gene. *Proceedings of the National Academy of Sciences of the United States of America* **88**(13):5680-5684.

Semenza GL, Roth PH, Fang HM and Wang GL (1994) Transcriptional regulation of genes encoding glycolytic enzymes by hypoxia-inducible factor 1. *Journal of Biological Chemistry* **269**(38):23757-23763.

Semenza GL and Wang GL (1992) A nuclear factor induced by hypoxia via de novo protein synthesis binds to the human erythropoietin gene enhancer at a site required for transcriptional activation. *Mol Cell Biol* **12**(12):5447-5454.

Sermeus A and Michiels C (2011) Reciprocal influence of the p53 and the hypoxic pathways. *Cell Death and Dis* **2**:e164.

Seton-Rogers S (2009) Metastasis: Attack of the mutant p53. *Nat Rev Cancer* **9**(6):384-385.

Sheppard K-A, Rose DW, Haque ZK, Kurokawa R, McInerney E, Westin S, Thanos D, Rosenfeld MG, Glass CK and Collins T (1999) Transcriptional Activation by NF-kappa B Requires Multiple Coactivators. *Mol Cell Biol* **19**(9):6367-6378.

Shew JY, Lin BT, Chen PL, Tseng BY, Yang-Feng TL and Lee WH (1990) C-terminal truncation of the retinoblastoma gene product leads to functional inactivation. *Proceedings of the National Academy of Sciences* **87**(1):6-10.

Shi D, Pop MS, Kulikov R, Love IM, Kung AL and Grossman SR (2009) CBP and p300 are cytoplasmic E4 polyubiquitin ligases for p53. *Proceedings of the National Academy of Sciences* **106**(38):16275-16280.

Shima DT, Kuroki M, Deutsch U, Ng Y-S, Adamis AP and D'Amore PA (1996) The Mouse Gene for Vascular Endothelial Growth Factor. *Journal of Biological Chemistry* **271**(7):3877-3883.

Shvarts A, Bazuine M, Dekker P, Ramos YFM, Steegenga WT, Merckx G, van Ham RCA, van der Houven van Oordt W, van der Eb AJ and Jochemsen AG (1997) Isolation and Identification of the Human Homolog of a New p53-Binding Protein, Mdmx. *Genomics* **43**(1):34-42.

Shvarts A, Steegenga WT, Riteco N, van Laar T, Dekker P, Bazuine M, van Ham RC, van der Houven van Oordt W, Hateboer G, van der Eb AJ and Jochemsen AG (1996) MDMX: a novel p53-binding protein with some functional properties of MDM2. *EMBO J* **15**(19):5349-5357.

Simon HU, Haj-Yehia A and Levi-Schaffer F (2000) Role of reactive oxygen species (ROS) in apoptosis induction. *Apoptosis* **5**(5):415-418.

Singh KK and Costello L (2009) *Mitochondria and cancer*. Springer Verlag.

Smits PHM, de Haan M, Maat C and Grivell LA (1994) II. Yeast sequencing reports. The complete sequence of a 33 kb fragment on the right arm of chromosome II from Saccharomyces cerevisiae reveals 16 open reading frames, including ten new open reading frames, five previously identified genes and a homologue of the SCO1 gene. *Yeast* **10**(S1994A):S75-S80.

Sone N, Yoshida M, Hirata H and Kagawa Y (1977) Adenosine triphosphate synthesis by electrochemical proton gradient in vesicles reconstituted from purified adenosine triphosphatase and phospholipids of thermophilic bacterium. *Journal of Biological Chemistry* **252**(9):2956.

Soussi T (2007) *Handbook of p53 mutation in cell lines*.

Soussi T (2010) The history of p53. *EMBO Rep* **11**(11):822-826.

Soussi T, Ishioka C, Claustres M and Beroud C (2006) Locus-specific mutation databases: pitfalls and good practice based on the p53 experience. *Nat Rev Cancer* **6**(1):83-90.

Stad R, Little NA, Xirodimas DP, Frenk R, van der Eb AJ, Lane DP, Saville MK and Jochemsen AG (2001) Mdmx stabilizes p53 and Mdm2 via two distinct mechanisms. *EMBO Rep* **2**(11):1029-1034.

Sung HJ, Ma W, Wang PY, Hynes J, O'Riordan TC, Combs CA, McCoy JP, Jr., Bunz F, Kang JG and Hwang PM (2010) Mitochondrial respiration protects against oxygen-associated DNA damage. *Nat Commun* **1**(1):1-8.

Sutter CH, Laughner E and Semenza GL (2000) Hypoxia-inducible factor 1α protein expression is controlled by oxygen-regulated ubiquitination that is disrupted by deletions and missense mutations. *Proceedings of the National Academy of Sciences* **97**(9):4748-4753.

Tang H-y, Zhao K, Pizzolato JF, Fonarev M, Langer JC and Manfredi JJ (1998) Constitutive Expression of the Cyclin-dependent Kinase Inhibitor p21 Is Transcriptionally Regulated by the Tumor Suppressor Protein p53. *Journal of Biological Chemistry* **273**(44):29156-29163.

Tang Y, Luo J, Zhang W and Gu W (2006) Tip60-Dependent Acetylation of p53 Modulates the Decision between Cell-Cycle Arrest and Apoptosis. *Molecular Cell* **24**(6):827-839.

Tang Y, Zhao W, Chen Y, Zhao Y and Gu W (2008) Acetylation Is Indispensable for p53 Activation. *Cell* **133**(4):612-626.

Tanimoto K, Makino Y, Pereira T and Poellinger L (2000) Mechanism of regulation of the hypoxia-inducible factor-1[alpha] by the von Hippel-Lindau tumor suppressor protein. *EMBO J* **19**(16):4298-4309.

Tian H, McKnight SL and Russell DW (1997) Endothelial PAS domain protein 1 (EPAS1), a transcription factor selectively expressed in endothelial cells. *Genes & Development* **11**(1):72.

Tian Y-M, Yeoh KK, Lee MK, Eriksson T, Kessler BM, Kramer HB, Edelmann MJ, Willam C, Pugh CW, Schofield CJ and Ratcliffe PJ (2011) Differential Sensitivity of Hypoxia Inducible Factor Hydroxylation Sites to Hypoxia and Hydroxylase Inhibitors. *Journal of Biological Chemistry* **286**(15):13041-13051.

Toledo F and Wahl GM (2006) Regulating the p53 pathway: in vitro hypotheses, in vivo veritas. *Nat Rev Cancer* **6**(12):909-923.

Toshiyuki M and Reed JC (1995) Tumor suppressor p53 is a direct transcriptional activator of the human bax gene. *Cell* **80**(2):293-299.

Trimarchi JM and Lees JA (2002) Sibling rivalry in the E2F family. *Nat Rev Mol Cell Biol* **3**(1):11-20.

Tsvetkov P, Reuven N and Shaul Y (2009) Ubiquitin-independent p53 proteasomal degradation. *Cell Death Differ* **17**(1):103-108.

Unger T, Juven-Gershon T, Moallem E, Berger M, Sionov RV, Lozano G, Oren M and Haupt Y (1999) Critical role for Ser20 of human p53 in the negative regulation of p53 by Mdm2. *The EMBO Journal* **18**(7):1805-1814.

Uyeda K, Furuya E and Luby LJ (1981) The effect of natural and synthetic D-fructose 2, 6-bisphosphate on the regulatory kinetic properties of liver and muscle phosphofructokinases. *Journal of Biological Chemistry* **256**(16):8394.

Van Schaftingen E, Hue L and Hers HG (1980) Fructose 2,6-bisphosphate, the probable structure of the glucose- and glucagon-sensitive stimulator of phosphofructokinase. *Biochem J* **192**(3):897-901.

Vassilev A, Yamauchi J, Kotani T, Prives C, Avantaggiati ML, Qin J and Nakatani Y (1998) The 400 kDa Subunit of the PCAF Histone Acetylase Complex Belongs to the ATM Superfamily. *Molecular Cell* **2**(6):869-875.

Verdin E (2006) *Histone deacetylases: Transcriptional regulation and other cellular functions*. Humana Pr Inc.

Vleugel MM, Shvarts D, van der Wall E and van Diest PJ (2006) p300 and p53 levels determine activation of HIF-1 downstream targets in invasive breast cancer. *Human Pathology* **37**(8):1085-1092.

Vousden KH and Ryan KM (2009) p53 and metabolism. *Nature Reviews Cancer* **9**(10):691-700.

Wang G and Semenza G (1993a) Desferrioxamine induces erythropoietin gene expression and hypoxia- inducible factor 1 DNA-binding activity: implications for models of hypoxia signal transduction. *Blood* **82**(12):3610-3615.

Wang GL, Jiang BH, Rue EA and Semenza GL (1995) Hypoxia-inducible factor 1 is a basic-helix-loop-helix-PAS heterodimer regulated by cellular O2 tension. *Proceedings of the National Academy of Sciences of the United States of America* **92**(12):5510-5514.

Wang GL and Semenza GL (1993b) Desferrioxamine induces erythropoietin gene expression and hypoxia- inducible factor 1 DNA-binding activity: implications for models of hypoxia signal transduction. *Blood* **82**(12):3610-3615.

Wang GL and Semenza GL (1995) Purification and Characterization of Hypoxia-inducible Factor 1. *Journal of Biological Chemistry* **270**(3):1230-1237.

Wang Y-H, Tsay Y-G, Tan BC-M, Lo W-Y and Lee S-C (2003) Identification and Characterization of a Novel p300-mediated p53 Acetylation Site, Lysine 305. *Journal of Biological Chemistry* **278**(28):25568-25576.

Warburg O (1956) On the origin of cancer cells. *Science* **123**(3191):309-314.

Warburg O, Posener K and Negelein E (1924) The metabolism of cancer cells. *Biochem Zeitschr* **152**:129-169.

Weber JD, Taylor LJ, Roussel MF, Sherr CJ and Bar-Sagi D (1999) Nucleolar Arf sequesters Mdm2 and activates p53. *Nat Cell Biol* **1**(1):20-26.

Weinhouse S (1976) The Warburg hypothesis fifty years later. *Journal of Cancer Research and Clinical Oncology* **87**(2):115-126.

Wenger RH and Gassmann M (1997) Oxygen(es) and the hypoxia-inducible factor-1. *Biol Chem* **378**(7):609-616.

Wenger RH, Stiehl DP and Camenisch G (2005) Integration of Oxygen Signaling at the Consensus HRE. *Sci STKE* **2005**(306):re12-.

Wiesener MS, JÜRGENSEN JS, ROSENBERGER C, SCHOLZE CK, HÖRSTRUP JH, WARNECKE C, MANDRIOTA S, BECHMANN I, FREI UA, PUGH CW, RATCLIFFE PJ, BACHMANN S, MAXWELL PH and ECKARDT K-U (2003) Widespread hypoxia-inducible expression of HIF-2α in distinct cell populations of different organs. *The FASEB Journal* **17**(2):271-273.

Wilkinson JH and Walter SJ (1972) Oxamate as a differential inhibitor of lactate dehydrogenase isoenzymes. *Enzyme* **13**(4):170.

Wines ME, Lee L, Katari MS, Zhang L, DeRossi C, Shi Y, Perkins S, Feldman M, McCombie WR and Holdener BC (2001) Identification of Mesoderm Development (mesd) Candidate Genes by Comparative Mapping and Genome Sequence Analysis. *Genomics* **72**(1):88-98.

Won KY, Lim S-J, Kim GY, Kim YW, Han S-A, Song JY and Lee D-K (2011) Regulatory role of p53 in cancer metabolism via SCO2 and TIGAR in human breast cancer. *Human Pathology*(0).

Wu C, Khan SA, Peng L-J and Lange AJ (2006) Roles for fructose-2,6-bisphosphate in the control of fuel metabolism: Beyond its allosteric effects on glycolytic and gluconeogenic enzymes. *Advances in Enzyme Regulation* **46**(1):72-88.

Wykoff CC, Beasley NJ, Watson PH, Turner KJ, Pastorek J, Sibtain A, Wilson GD, Turley H, Talks KL, Maxwell PH, Pugh CW, Ratcliffe PJ and Harris AL (2000) Hypoxia-inducible expression of tumor-associated carbonic anhydrases. *Cancer Research* **60**(24):7075-7083.

Xenaki G, Ontikatze T, Rajendran R, Stratford IJ, Dive C, Krstic-Demonacos M and Demonacos C (2008) PCAF is an HIF-1 cofactor that regulates p53 transcriptional activity in hypoxia. *Oncogene* **27**(44):5785-5796.

Xiangbing M (1999) Mechanism of p53 downstream effectors p21 and Gadd45 in DNA damage surveillance.

Xu R, Pelicano H, Zhou Y, Carew JS, Feng L, Bhalla KN, Keating MJ and Huang P (2005) Inhibition of glycolysis in cancer cells: a novel strategy to overcome drug resistance associated with mitochondrial respiratory defect and hypoxia. *Cancer research* **65**(2):613.

Xu Y (2003) Regulation of p53 responses by post-translational modifications. *Cell Death Differ* **10**(4):400-403.

Yamauchi T, Yamauchi J, Kuwata T, Tamura T, Yamashita T, Bae N, Westphal H, Ozato K and Nakatani Y (2000) Distinct but overlapping roles of histone acetylase PCAF and of the closely related PCAF-B/GCN5 in mouse embryogenesis. *Proceedings of the National Academy of Sciences* **97**(21):11303-11306.

Yang PC and Schwert GW (1972) Inactivation of lactate dehydrogenase by butanedione. *Biochemistry* **11**(12):2218-2224.

Yang XJ, Ogryzko VV, Nishikawa J, Howard BH and Nakatani Y (1996) A p300/CBP-associated factor that competes with the adenoviral oncoprotein E1A.

Yeo EJ, Chun YS, Cho YS, Kim J, Lee JC, Kim MS and Park JW (2003) YC-1: a potential anticancer drug targeting hypoxia-inducible factor 1. *Journal of the National Cancer Institute* **95**(7):516.

Yeung F, Hoberg JE, Ramsey CS, Keller MD, Jones DR, Frye RA and Mayo MW (2004) Modulation of NF-[kappa]B-dependent transcription and cell survival by the SIRT1 deacetylase. *EMBO J* **23**(12):2369-2380.

Yeung S, Pan J and Lee MH (2008) Roles of p53, Myc and HIF-1 in Regulating Glycolysis — the Seventh Hallmark of Cancer. *Cellular and Molecular Life Sciences* **65**(24):3981-3999.

Yoshida M, Muneyuki E and Hisabori T (2001) ATP synthase — a marvellous rotary engine of the cell. *Nat Rev Mol Cell Biol* **2**(9):669-677.

Yu F, White SB, Zhao Q and Lee FS (2001) HIF-1α binding to VHL is regulated by stimulus-sensitive proline hydroxylation. *Proceedings of the National Academy of Sciences of the United States of America* **98**(17):9630-9635.

Yuan J, Luo K, Zhang L, Cheville JC and Lou Z (2010) USP10 Regulates p53 Localization and Stability by Deubiquitinating p53. *Cell* **140**(3):384-396.

Zamanian M and La Thangue NB (1992) Adenovirus E1a prevents the retinoblastoma gene product from repressing the activity of a cellular transcription factor. *EMBO J* **11**(7):2603-2610.

Zelzer E, Levy Y, Kahana C, Shilo B-Z, Rubinstein M and Cohen B (1998) Insulin induces transcription of target genes through the hypoxia-inducible factor HIF-1[alpha]/ARNT. *EMBO J* **17**(17):5085-5094.

Zhang H, Bosch-Marce M, Shimoda LA, Tan YS, Baek JH, Wesley JB, Gonzalez FJ and Semenza GL (2008) Mitochondrial Autophagy Is an HIF-1-dependent Adaptive Metabolic Response to Hypoxia. *Journal of Biological Chemistry* **283**(16):10892-10903.

Zhang Y and Xiong Y (2001) A p53 Amino-Terminal Nuclear Export Signal Inhibited by DNA Damage-Induced Phosphorylation. *Science* **292**(5523):1910-1915.

Zhong H, Chiles K, Feldser D, Laughner E, Hanrahan C, Georgescu M-M, Simons JW and Semenza GL (2000) Modulation of Hypoxia-inducible Factor 1α Expression by the Epidermal Growth Factor/Phosphatidylinositol 3-Kinase/PTEN/AKT/FRAP Pathway in Human Prostate Cancer Cells: Implications for Tumor Angiogenesis and Therapeutics. *Cancer Research* **60**(6):1541-1545.

Zhong H, Voll RE and Ghosh S (1998) Phosphorylation of NF-[kappa]B p65 by PKA Stimulates Transcriptional Activity by Promoting a Novel Bivalent Interaction with the Coactivator CBP/p300. *Molecular Cell* **1**(5):661-671.

Zhou R, Vitols S, Gruber A, Liliemark J, Wang Y and Liliemark E (1999) Etoposide-induced DNA strand breaks in relation to p-glycoprotein and topoisomerase II protein expression in leukaemic cells from patients with AML and CLL. *British Journal of Haematology* **105**(2):420-427.

Zundel W, Schindler C, Haas-Kogan D, Koong A, Kaper F, Chen E, Gottschalk AR, Ryan HE, Johnson RS, Jefferson AB, Stokoe D and Giaccia AJ (2000) Loss of PTEN facilitates HIF-1-mediated gene expression. *Genes & Development* **14**(4):391-396.

Appendix

The following publications are available online in which Ramkumar Rajendran has involved in some parts of the work.

1. Ramkumar Rajendran, Richa Garva, Marija Krstic-Demonacos, Constantinos Demonacos; Sirtuins: molecular traffic lights in the crossroad of oxidative stress, chromatin remodelling and transcription; ***Journal of biomedicine and biotechnology***, 2011, Special issue on Protein Acetylation and the Physiological Role of HDACs.

2. G Xenaki, T Ontikatze, R Rajendran, I J Stratford, C Dive, M Krstic-Demonacos and C Demonacos; PCAF is an HIF-1α cofactor that regulates p53 transcriptional activity in hypoxia**;** ***Oncogene*** (2008) **27,** 5785–5796

3. James T Lynch, Ramkumar Rajendran, Georgia Xenaki, Ilhem Berrou, Constantinos Demonacos, Marija Krstic-Demonacos; The role of glucocorticoid receptor phosphorylation in Mcl-1 and NOXA gene expression; ***Molecular Cancer*** 2010, **9**:38

4. Yamini Arthanari, Alain Pluen, Ramkumar Rajendran, Harmesh Aojula, Constantinos Demonacos; Delivery of therapeutic shRNA and siRNA by Tat fusion peptide targeting bcr–abl fusion gene in Chronic Myeloid Leukemia cells; ***Journal of Controlled Release,*** 2010, 145(3), 272-280

5. Manikandan Kadirvel, Nicholas J. W. Rattray, Ramkumar Rajendran, Waleed A. Zalloum, Abdul Gbaj, Constantinos Demonacos, Elena V. Bichenkova and Sally Freeman Bioreductive molecular probe: fluorescence signalling upon reduction of an azo group; ***New J. Chem.***, 2011, **35**, 701-708

Oncogene (2008) 27, 5785–5796

www.nature.com/onc

ORIGINAL ARTICLE

PCAF is an HIF-1α cofactor that regulates p53 transcriptional activity in hypoxia

G Xenaki[1], T Ontikatze[1], R Rajendran[1], IJ Stratford[1], C Dive[1,2], M Krstic-Demonacos[3] and C Demonacos[1]

[1]*School of Pharmacy and Pharmaceutical Sciences, University of Manchester, Manchester, UK;* [2]*Paterson Institute for Cancer Research, University of Manchester, Manchester, UK and* [3]*Faculty of Life Sciences, University of Manchester, Manchester, UK*

The p53 tumour suppressor is involved in several crucial cellular functions including cell-cycle arrest and apoptosis. p53 stabilization occurs under hypoxic and DNA damage conditions. However, only in the latter scenario is stabilized p53 capable of inducing the expression of its pro-apoptotic targets. Here we present evidence that under hypoxia-mimicking conditions p53 acetylation is reduced to a greater extent at K320 site targeted by P300/CBP-associated factor (PCAF) than at K382 site targeted by p300/CBP. The limited amounts of acetylated p53 at K320 are preferentially recruited to the promoter of the *p21*$^{WAF-1/CIP-1}$ gene, which appears to be unaffected by hypoxia, but are not recruited to the BID promoter and hence p53 is incapable of upregulating pro-apoptotic BID in hypoxic conditions. As the K320 p53 acetylation is the site predominantly affected in hypoxia, the PCAF histone acetyltransferase activity is the key regulator of the cellular fate modulated by p53 under these conditions. In addition, we provide evidence that PCAF acetylates hypoxia-inducible factor-1α (HIF-1α) in hypoxic conditions and that the acetylated HIF-1α is recruited to a particular subset of its targets. In conclusion, PCAF regulates the balance between cell-cycle arrest and apoptosis in hypoxia by modulating the activity and protein stability of both p53 and HIF-1α.
Oncogene (2008) **27,** 5785–5796; doi:10.1038/onc.2008.192; published online 23 June 2008

Keywords: transcription; p53; hypoxia-inducible factor; PCAF; apoptosis

Introduction

The transcriptional activity of the tumour suppressor protein p53 is crucial for the mediation of its physiological functions (Vousden and Prives, 2005). Cells adapt to various forms of stress by mechanisms orchestrated by p53, which interacts with specific classes of genes, ultimately leading to differential susceptibility to diverse types of stress (Vousden and Lane, 2007). Modulation of the p53 transcriptional activity is achieved by stabilization of the protein and binding to various cofactors such as p300 and the P300/CBP-associated factor (PCAF). These cofactors contribute to the regulation of the p53 transcriptional activity by acetylating different lysine residues in its C-terminal region (Liu *et al.*, 1999).

During tumourigenesis, cells encounter hypoxia as a major stress and most if not all human solid tumours contain subpopulations of hypoxic cells. Among these tumour types, those showing greater levels of hypoxia show resistance to therapy, greater malignancy and increased metastatic potential (Vaupel and Harrison, 2004). One reason that hypoxic tumours are resistant to DNA-damaging therapies is because of alterations in the p53 transcriptional activity (Achison and Hupp, 2003). Under hypoxic conditions, increased p53 protein stability has been shown to occur in a hypoxia-inducible factor-1α (HIF-1α)-dependent (An *et al.*, 1998; Hansson *et al.*, 2002) and -independent manner (Pan *et al.*, 2004). Furthermore, under hypoxic conditions p53 is incapable of inducing the expression of several of its transcription targets including pro-apoptotic members of the Bcl-2 family, due to failure to recruit the p300/CBP co-activator proteins to their promoters (Koumenis *et al.*, 2001), although enhanced p53 transcriptional activity in anoxic conditions has also been reported (Zhu *et al.*, 2002).

Functional crosstalk between the HIF-1α and p53 pathways occurs at several levels, including p53 protein stability (Ravi *et al.*, 2000), attenuated HIF-1 transcriptional activity by p53 (Blagosklonny *et al.*, 1998) and *vice versa* (Chen *et al.*, 2003). Interference of each one of these transcription factors with the transcriptional activity of the other has been attributed to the availability of the transcriptional co-activator p300 (Arany *et al.*, 1996; Schmid *et al.*, 2004), as the binding site of p300 for both p53 and HIF-1α is the CH1 domain (Freedman *et al.*, 2002). Differential acetylation of p53 by p300 and other histone acetyltransferases (HATs)

Correspondence: Dr C Demonacos, School of Pharmacy and Pharmaceutical Sciences, University of Manchester, Stopford building, Oxford Road, Manchester, M13 9PT, UK.
E-mail: cdemonacos@manchester.ac.uk
Received 12 July 2007; revised 25 April 2008; accepted 19 May 2008; published online 23 June 2008

mediates explicit responses to diverse signals and adjustment to the cellular requirements depending on the environmental conditions (Liu *et al*., 1999). p300-mediated acetylation of p53 at K373 and K382 (Sakaguchi *et al*., 1998; Liu *et al*., 1999; Luo *et al*., 2004) occurs under severe and irreparable DNA damage leading to the induction of pro-apoptotic p53 targets and cellular death. Milder stress conditions stimulate acetylation of the p53-K320 by PCAF and result in the induction of the expression of the cyclin/cdk inhibitor $p21^{WAF-1/CIP-1}$ and cell-cycle arrest (Knights *et al*., 2006). The general consensus of all the above-mentioned reports is that site-specific acetylation of p53 leads to selective response to various signals (Roy and Tenniswood, 2007).

HIF-1α has a key role in cellular responses to hypoxia (Wenger, 2002). The half-life and transcriptional activity of HIF-1α is controlled by several post-translational modifications including prolyl hydroxylations, which regulate both stability and transactivation by governing the interaction of HIF-1α with the von Hippel-Lindau ubiquitin E3 ligase (pVHL), and the p300 (Mahon *et al*., 2001; Lando *et al*., 2002; Freedman *et al*., 2004; Kaelin, 2005). It is clear that p300 is required for the transactivation of both HIF-1α and p53 and there is competition for limiting amounts of this cofactor in hypoxia between HIF-1α and p53 (Freedman *et al*., 2002).

ARD1-mediated acetylation of HIF-1α has also been reported (Jeong *et al*., 2002), although contradictory results have been presented with regard to the effect of acetylation on HIF-1α transcriptional activity and protein stability (Bilton *et al*., 2006). Other post-translational modifications regulating HIF-1α and p53 function by the same enzymatic cascades include phosphorylation, nitrosylation and SUMOylation (Brahimi-Horn *et al*., 2005).

The above observations increasingly support the notion that similar and in many cases common regulatory mechanisms exist that modulate the transcriptional activity and protein stability of both HIF-1α and p53. To decipher the molecular mechanisms by which p300 and PCAF regulate p53 transcriptional activity under hypoxic conditions and define the mechanisms underlying selective activation by p53 in these conditions, we studied the expression of the pro-apoptotic p53 target BID, which is known to contain in its promoter region regulatory sequences targeted by both p53 (Sax *et al*., 2002) and HIF-1α (Erler *et al*., 2004). We asked whether p53 binds preferentially to upstream regulatory regions of genes involved in cell-cycle arrest or control of apoptosis and if this involves the function of PCAF. Furthermore, in this report we present evidence that PCAF acetylates HIF-1α under hypoxic conditions and directs it selectively to a subset of its transcription targets. Our results provide an additional evidence for the importance of co-activator function in determining the cell fate under hypoxia by modulating both p53 and HIF-1α responses.

Results

PCAF and p300 differentially occupy the promoters of p53 target genes in hypoxia

Studies by Erler *et al*. (2004) have shown that the protein levels of several anti-apoptotic members of the Bcl-2 family remain unchanged under normoxic, hypoxic (1% O_2) or anoxic (0.1% O_2) conditions. In contrast, pro-apoptotic Bcl-2 family members such as Bax and BID are downregulated despite of the fact that both of these genes are p53 transcriptional targets and p53 is stabilized under anoxic and hypoxic conditions (An *et al*., 1998). The altered affinity or lack of binding between p53 and the transcriptional co-activator p300 under anoxic conditions has been suggested as the reason for the inability of p53 to activate its targets under these conditions (Hammond and Giaccia, 2005).

To test whether other p53 cofactors are implicated in the determination of p53 transcriptional activity under these conditions we carried out chromatin immunoprecipitation (ChIP) experiments and monitored the occupancy of the p53-binding sites of BID, PUMA, Bax and $p21^{WAF-1/CIP-1}$ promoter regions by the p300/CBP complex component PCAF in cells treated with the hypoxia-mimicking agent desferrioxamine (DSFX). PCAF/chromatin complexes were precipitated and the promoter regions containing the p53-binding sites of the above-mentioned genes were amplified with specific primers. PCAF recruitment to the promoters of the pro-apoptotic p53 target genes BID, PUMA and Bax was substantially lower (10-fold or more) in the cells treated with DSFX compared to the non-treated cells (Figure 1a). Interestingly, the recruitment of PCAF to the $p21^{WAF-1/CIP-1}$ promoter was reduced to a lesser extent, indicating preferential PCAF promoter occupancy of the cell-cycle arrest $p21^{WAF-1/CIP-1}$ gene rather than the pro-apoptotic p53 targets in hypoxia-mimicking conditions. In contrast, recruitment of p300 to the promoters of the same p53 target genes exhibited a different occupancy profile. In the case of PUMA and $p21^{WAF-1/CIP-1}$ the p300-binding efficiency was 40% lower, in the case of BID was 10-fold higher and no change was observed in Bax promoter occupancy in DSFX-treated U2OS cells (Figure 1c). These differences in PCAF or p300 promoter recruitment were not due to differences in the amount of the cofactors precipitated as equal quantity of PCAF and p300 were precipitated in DSFX-treated or not treated cells (Figures 1b and d).

BID, PUMA, Bax and $p21^{WAF-1/CIP-1}$ gene expression profiles indicated that PCAF promoter occupancy of these genes was closely related to their mRNA levels followed by qRT-PCR (Supplementary Figure 2).

Acetylation of p53 at K320 by PCAF is not efficient in hypoxia

Next we investigated whether the PCAF-mediated acetylation of p53 at K320 occurs with the same efficiency in normoxic and DSFX-treated cells. Immunoprecipitation of total endogenous p53 from U2OS cells and blotting with a specific antibody recognizing

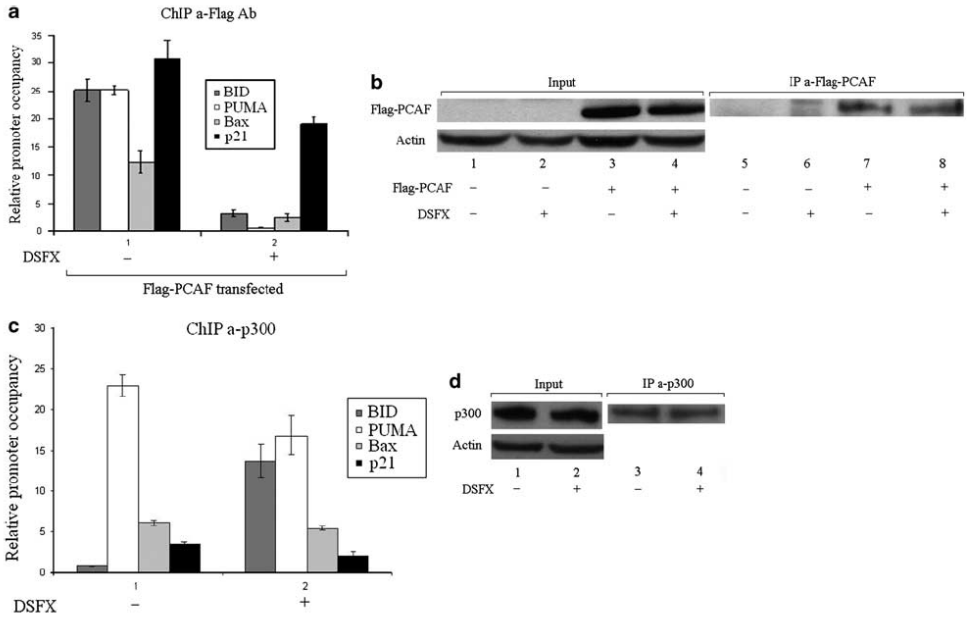

Figure 1 P300/CBP-associated factor (PCAF) and p300 differentially occupy the promoters of p53 target genes in hypoxia. U2OS cells were transfected with Flag-PCAF (**a**) or cytomegalovirus (CMV)-p300 expression plasmids (**c**), and processed for chromatin immunoprecipitation (ChIP). Flag-PCAF (**a**, **b**) and p300 (**c**, **d**) antibodies were used to immunoprecipitate cross-linked DNA–protein complexes and primers for BID, BAX, Puma and p21$^{WAF-1/CIP-1}$ promoters (Supplementary Figure 1) to amplify precipitated DNA by real-time qPCR. Standard error bars represent the deviations between at least two independent experiments. (**b**) Flag antibody recognizes specifically the Flag-PCAF-expressed protein and equal amounts of PCAF are precipitated from desferrioxamine (DSFX)-treated or not treated cells. (**d**) Equal amounts of p300 are precipitated by the p300 antibody in DSFX-treated or not treated cells.

the p53 K320 acetylated isoform revealed a significant reduction (~70%) of p53 acetylation at K320 in cells exposed to DSFX versus those treated with etoposide (Figure 2a, compare tracks 5 and 6). In contrast, the level of reduction of p53 acetylation at K382 by p300 was not as dramatic (~30% reduction) after 16 h of DSFX treatment (Figure 2a, compare tracks 5 and 6).

PCAF enhances the expression of the p21$^{WAF-1/CIP-1}$ p53 target in hypoxia

The recruitment of the two acetyl isoforms K320 and K382 of p53 to the p53-binding sites present within the promoters of the cell-cycle arrest gene *p21$^{WAF-1/CIP-1}$* and the pro-apoptotic p53 target BID was followed using ChIP assays (Figures 2b–d). BID promoter occupancy by the p53 acetylated at K320 was considerably lower (~40%) in the DSFX- versus the etoposide-treated cells and higher (~300%) in the case of *p21$^{WAF-1/CIP-1}$* (Figure 2b). In contrast, the p53 acetylated at K382 by p300 exhibited higher affinity for both the p53-binding sites of BID and p21$^{WAF-1/CIP-1}$ promoters in cells treated with DSFX (Figure 2c). The anti-acetyl p53 antibodies were specific for the acetylated p53 isoforms as no p53 was precipitated in the non-treated cells with these antibodies (Figure 2d, tracks 4 and 7). The amount of the precipitated p53 in etoposide- and DSFX-treated cells was normalized to the input p53 protein.

The same conclusions were reached following studies using BID and p21$^{WAF-1/CIP-1}$ luciferase reporter assays (Figures 3a and b, respectively). Indeed, both BID-p53bs-Luc and p21-p53bs-Luc reporters were not induced to the same extent in DSFX-treated (where K320 is not efficiently acetylated) versus untreated cells (Figures 3a and b, compare bars 3 and 4). Notably, the reduction in BID luciferase reporter expression in DSFX-treated compared to the untreated cells was 36% (Figure 3a, compare bars 3 and 4) and in the case of p21$^{WAF-1/CIP-1}$ reporter much less (19%; Figure 3b compare bars 3 and 4). The non-acetylatable p53K320R mutant was unable to induce luciferase expression driven by either BID or p21$^{WAF-1/CIP-1}$ reporters (Figures 3a and b, bars 5 and 6). In cells transfected with the constitutively acetylated K320Q mutant there was no difference in the expression of BID and p21$^{WAF-1/CIP-1}$ reporters in DSFX-treated or untreated cells as p53 K320 acetylation of this mutant is not affected by DSFX in this case (Figures 3a and b, bars 7 and 8).

Results in Figures 2 and 3 suggest that PCAF binding and partial acetylation of p53 at K320 might explain the

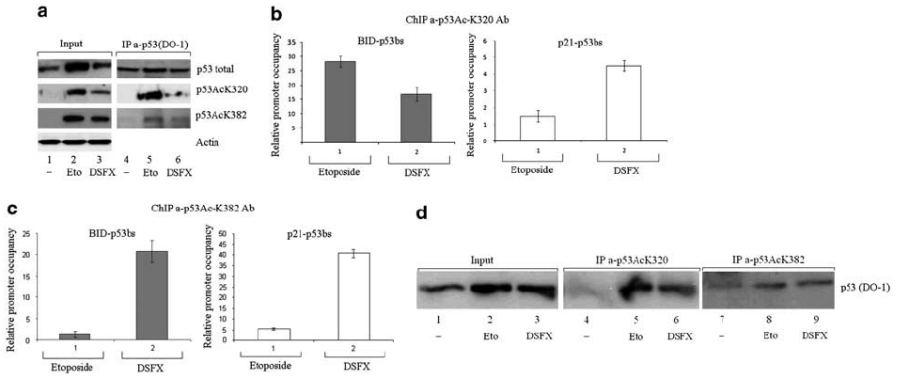

Figure 2 p53 K320 is not acetylated efficiently in desferrioxamine (DSFX)-treated cells. (**a**) U2OS cells were subjected to etoposide or DSFX treatment or left untreated, and cellular extract submitted to immunoprecipitation with antibody against endogenous p53 (DO-1). Precipitates were blotted with antibodies against p53 anti-human rabbit polyclonal PC-100, p53 acetylated at K320 and p53 acetylated at K382. Actin was used as loading control and input lysates are shown in the left panel. (**b**) p53 acetylated at K320 is preferentially recruited to the $p21^{WAF-1/CIP-1}$ promoter. U2OS cells treated as in Figure 1 were processed for chromatin immunoprecipitation (ChIP) using antibodies against p53 acetylated at K320 (**b**) or at K382 (**c**). Primers flanking a 200 bp fragment containing the p53-binding sites of the BID and $p21^{WAF-1/CIP-1}$ promoters (Supplementary Figure 1) were used to amplify precipitated DNA by real-time qPCR. Standard error bars represent the deviations between at least two independent experiments. (**d**) The specificity of the antibodies and the amounts of the precipitated p53 protein are shown.

inability of p53 to induce the expression of its pro-apoptotic targets in cells treated with DSFX in accordance with published observations (Chao *et al*., 2006).

PCAF-dependent acetylation of p53 regulates cell proliferation

The role of the HAT activity of PCAF on cell-cycle progression and apoptosis was investigated by fluorescence-activated cell sorting (FACS) analysis performed in DSFX-treated or untreated U2OS and SAOS2 cells transfected with either empty vector, Flag-PCAFwt or Flag-PCAF-ΔHAT expression constructs as indicated in Figures 4a and b. The ratio between apoptotic versus arrested cells in G_1 phase of the cell cycle is presented in Figure 4a for U2OS and in 4B for SAOS2 cells. PCAFwt-transfected cells exhibited higher apoptotic potential compared to PCDNA3 or PCAF-ΔHAT-overexpressing and DSFX-treated cells. In agreement with previously published observations (Cohen *et al*., 2004), this induction of cell death was dependent on the HAT activity of PCAF, as apoptosis was not efficiently stimulated in the PCAF-ΔHAT-expressing cells (Figure 4a, compare bars 5 and 8). The lesser extent to which apoptosis was stimulated in SAOS2 cells under the same conditions indicates that at least in part and to the measure permitted by these correlative experiments the cell-cycle events were p53 dependent (compare Figure 4a, bar 5 to 4b, bar 5). In addition, the caspase 3 assay shown in Supplementary Figure 3 confirmed that the population of cells in sub-G_1 phase represented apoptotic cells.

To investigate the contribution of HIF-1α to the cell-cycle events in U2OS (Figure 4a) and SAOS2 cells (Figure 4b) expressing the same Flag-PCAFwt, Flag-PCAF-ΔHAT or empty (PCDNA3) expression vectors we co-transfected RNAi against HIF-1α to silence its expression. The ratio of apoptotic versus G_1-arrested cells ectopically expressing PCAFwt in correlation to the respective ratio of RNAi-HIF-1α-co-transfected cells was 2.9 times higher for the U2OS and 1.3 for the SAOS2 cells (compare Figure 4a, ratio of bars 5 and 6 with 4b, bars 5 and 6) indicating that p53 acetylated at K320 in the absence of HIF-1α favours cell survival and in the presence of HIF-1α apoptosis. In a similar manner HIF-1α in the presence of non-acetylated p53 at K320 (PCAF-ΔHAT-transfected cells) stimulated cell survival whereas the complete absence of p53 initiated apoptosis (compare Figure 4a, ratio of bars 8 and 9 (1.8) with 4b, bars 8 and 9 (2.7)).

Results shown in Figure 4 imply that the HAT activity of PCAF functions as a coordinating factor in the regulation of HIF-1α and p53-dependent cell-cycle progression in addition to other known p53- and HIF-1α-independent effects on apoptosis (Cohen *et al*., 2004).

PCAF is an HIF-1α cofactor

Taken together the results shown in Figure 4 with the fact that both HIF-1α and p53 share the common cofactor p300 (Freedman *et al*., 2002) prompted us to investigate whether PCAF as another p53 cofactor, which associates with p300, was also involved in the regulation of HIF-1α transcriptional activity. Towards this end, we performed ChIP assays monitoring the PCAF recruitment to the promoters of known HIF-1 targets such as BID (Erler *et al*., 2004; Supplementary Figure 5), erythropoietin (Epo; Semenza *et al*., 1996) and vascular endothelial growth factor (VEGF; Forsythe *et al*., 1996) in U2OS cells ectopically

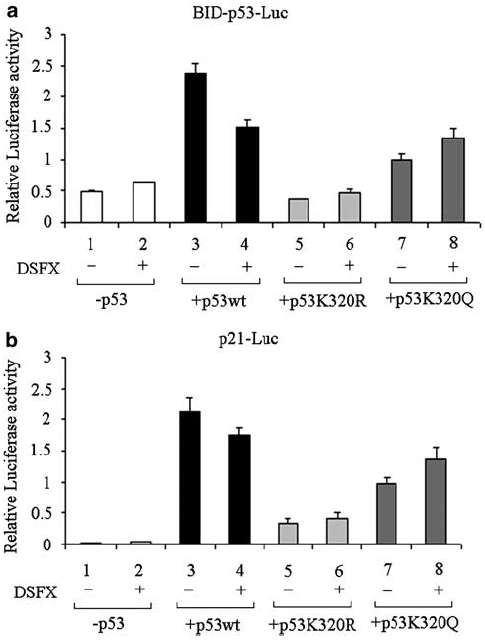

Figure 3 Acetylation of p53 at K320 induces preferentially the expression of the p21$^{WAF-1/CIP-1}$-Luc-reporter. SAOS2 cells transfected with either the BID-p53bs-Luc (**a**) or the p21$^{WAF-1/CIP-1}$-Luc (**b**) reporters together with cytomegalovirus (CMV) empty vector (bars 1, 2), pCMV-p53wt (bars 3, 4), pCMV-p53K320R (bars 5, 6), or pCMV-p53K320Q (bars 7, 8) expression plasmids were submitted to luciferase reporter assay. Relative luciferase activity was monitored as mentioned in 'Materials and methods'. Cells submitted to desferrioxamine (DSFX) treatment for 20 h are indicated with (+).

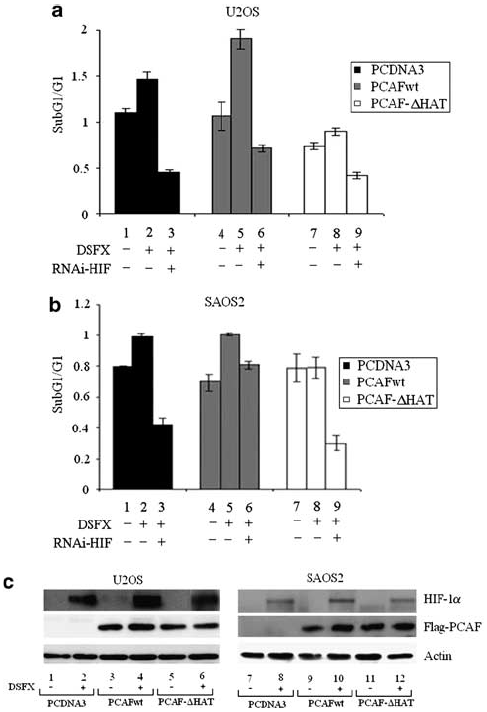

Figure 4 Hypoxia-inducible factor-1α (HIF-1α) and p53-dependent cell-cycle progression is coordinated by P300/CBP-associated factor (PCAF). U2OS (**a**) and SAOS2 cells (**b**) were transfected with vectors expressing either PCAFwt or PCAF-ΔHAT together with a plasmid-expressing CD20. In some cases RNAi for HIF-1α was co-transfected (**a**, **b**, bars 3, 6 and 9) and cells were treated with desferrioxamine (DSFX) where indicated. The ratio of the fraction of cells accumulated in sub-G_1 versus the percentage of cells arrested in G_1 phase of the cell cycle is presented in the diagrams (**a**, **b**). Results are the average of two independent experiments. (**c**) Western blot showing the equal expression of transfected PCAFwt and PCAF-ΔHAT in U2OS and SAOS2 cells.

expressing PCAF and treated with or without DSFX. Results shown in Figure 5a confirmed that PCAF acts as HIF cofactor as it is recruited with high efficiency in both BID and VEGF promoters in hypoxic conditions. In agreement with recently published observations showing that Epo is primarily an HIF-2-specific target (Warnecke *et al*., 2004), PCAF was not recruited to the Epo promoter with the same efficiency as to BID and VEGF promoters in DSFX-treated cells. PCAF recruitment to the BID HIF-1α response element (HRE) is reflected in increased BID protein levels of both the truncated and the non-truncated forms of BID in U2OS cells over-expressing PCAF and treated for 20 h with DSFX (Figure 5b, track 3).

In addition, PCAF was found to regulate the expression of other known HIF-1α transcription targets such as carbonic anhydrase IX (CA-IX; Wykoff *et al*., 2000), VEGF (Forsythe *et al*., 1996), phosphoglycerate kinase-1 (PGK-1) and lactate dehydrogenase A (LDH-A; Semenza *et al*., 1996). Luciferase reporter assays shown in Figure 6 point out that PCAF functioned as HIF-1α co-activator in the case of the CA-IX-Luc and VEGF-Luc reporters (Figures 6a and b), but did not have any effect in the expression of PGK-Luc and LDH-A-Luc reporters (Figures 6c and d). In addition, PCAF HAT activity played an important role in the co-activation of CA-IX-Luc reporter (Figure 6a) but did not appear to have significant effect on the VEGF-Luc and PGK-Luc reporters (Figures 6b and c) and exerted a negative effect on the expression of LDH-A-Luc reporter (Figure 6d). The observed PCAFwt- or PCAF-ΔHAT-mediated effects on these HIF-1α targets were not a result of unequal HIF-1α expression levels in cells expressing Flag-PCAFwt or Flag-PCAF-ΔHAT (Figure 6e). In addition, the expression of wild-type (wt) or mutated cofactor was not affected by DSFX treatment (Figure 6e).

Results shown in Figures 4–6 imply that PCAF functions as an HIF-1α cofactor, is involved in the HIF-1α-mediated apoptosis and that PCAF HAT activity regulates HIF-1α transcriptional selectivity.

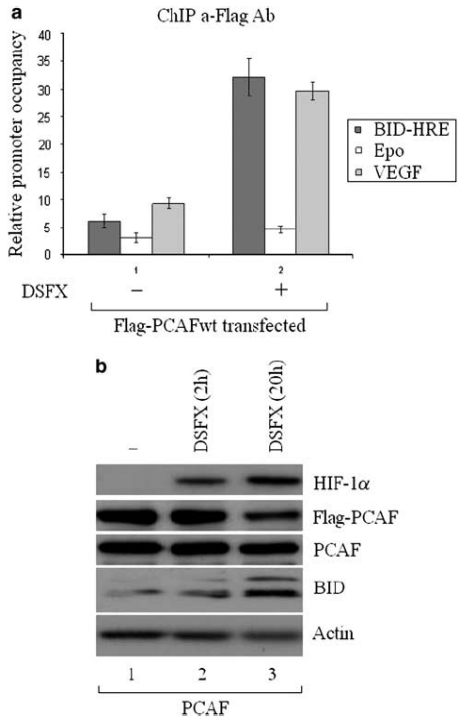

Figure 5 P300/CBP-associated factor (PCAF) is recruited to the hypoxia responsive elements (HREs) of known hypoxia-inducible factor-1α (HIF-1α) targets. (**a**) Chromatin immunoprecipitation (ChIP) assays were performed in U2OS cells treated as in Figure 1. Primers flanking the HREs of BID, Epo and vascular endothelial growth factor (VEGF) promoters (Supplementary Figure 1) were used to amplify the cross-linked DNA by real-time qPCR. (**b**) Whole-cell lysates from U2OS cells over-expressing PCAF and treated with desferrioxamine (DSFX) for 0, 2 and 20 h were submitted to western blot analysis and the protein levels of HIF-1α, Flag-PCAF, PCAF and BID were followed with specific antibodies against these proteins. Actin served as loading control.

PCAF interacts with and acetylates HIF-1α

Next we determined whether endogenous PCAF interacts with HIF-1α in untreated (Figure 7, tracks 1 and 5), DSFX (tracks 2 and 6), etoposide (tracks 3 and 7) or both DSFX- and etoposide-treated U2OS cells (tracks 4 and 8). The interaction between the two proteins was evident in the DSFX-treated cells and with lower affinity in the cells treated with both DSFX and etoposide (Figure 7, tracks 6 and 8).

To study whether PCAF acetylates HIF-1α, acetylated proteins were precipitated from DSFX-treated SAOS2 cells with the pan-acetyl-lysine antibody and higher levels of acetylated HIF-1α were detected among the precipitated proteins in the extract of the cells ectopically expressing Flag-PCAF (Figure 8a, track 6). A low level of HIF-1α acetylation was detected in the non-transfected Flag-PCAF cells (Figure 8a, track 4) possibly representing HIF-1α acetylated by ARD-1 (Jeong *et al.*, 2002) or other unidentified HAT(s).

The same results were obtained by precipitating PCAF acetylation targets from DSFX-treated U2OS cells using another antibody that recognizes the histone H3 acetylated lysine, previously reported to be a specific PCAF acetylation substrate (Poux and Marmorstein, 2003). Acetylation of HIF-1α was evident in the DSFX and both DSFX- and etoposide-treated cells, although in the latter case PCAF exhibited lower acetylation efficiency for HIF-1α, and slightly higher for p53 (Figure 8b, compare tracks 7 and 8), possibly due to weaker association between HIF-1α and PCAF under these conditions (Figure 7, track 8). The observed HIF-1α acetylation was PCAF dependent as the PCAF-ΔHAT mutant failed to acetylate the transcription factor (Figure 8c, compare tracks 2–4).

To confirm that the pan-acetyl-lysine antibody immunoprecipitated acetylated HIF-1α and not another acetylated protein that interacts with HIF-1α and coprecipitates with the transcription factor, we performed immunoprecipitation experiments in U2OS cells ectopically expressing HA-HIF-1α using an anti-HA-specific antibody. Precipitated HIF-1α was recognized by the acetyl-lysine antibody (Figure 8d, tracks 2 and 4).

Furthermore, to identify the HIF-1α sites that are PCAF acetylation targets we mutated the ARD1 target K532 and K389 to arginine. Immunoprecipitation of the mutated HA-HIF-1α-K532R and HA-HIF-1α-K389R with haemagglutinin (HA) antibody and immunoblotting with the acetyl-lysine antibody confirmed that HIF-1α was acetylated and revealed that K532 is not the only acetylated site in HIF-1α (Figures 8e and f, tracks 2 and 4).

To test the effect of PCAF-dependent acetylation of HIF-1α on its protein stability we followed HIF-1α half-life in SAOS2 cells transfected with either PCAFwt- or PCAF-ΔHAT-expressing vectors or untransfected cells treated with cyclohexamide for different time points from 0 to 6 h (Figure 8g). As shown with densitometric analysis (Figure 8h) HIF-1α in PCAFwt-transfected cells could still be detected after 6 h of cyclohexamide treatment and its half-life was approximately 4 h, whereas in PCAF-ΔHAT-, or PCDNA3-transfected cells the HIF-1α half-life was shorter (approximately 2 h; Figure 8g). The intensity of the HIF-1α bands in the cells transfected with different expression vectors (PCDNA3, PCAFwt, PCAF-ΔHAT) has been normalized to the intensity of the actin bands in the respective cells (Figure 8h).

Discussion

In this study, we provide insight into the molecular mechanisms regulating p53 transcriptional selectivity in the apoptotic response to treatment with the hypoxia-mimicking agent DSFX. Despite the recently published analysis of the p53 transcriptional activity under

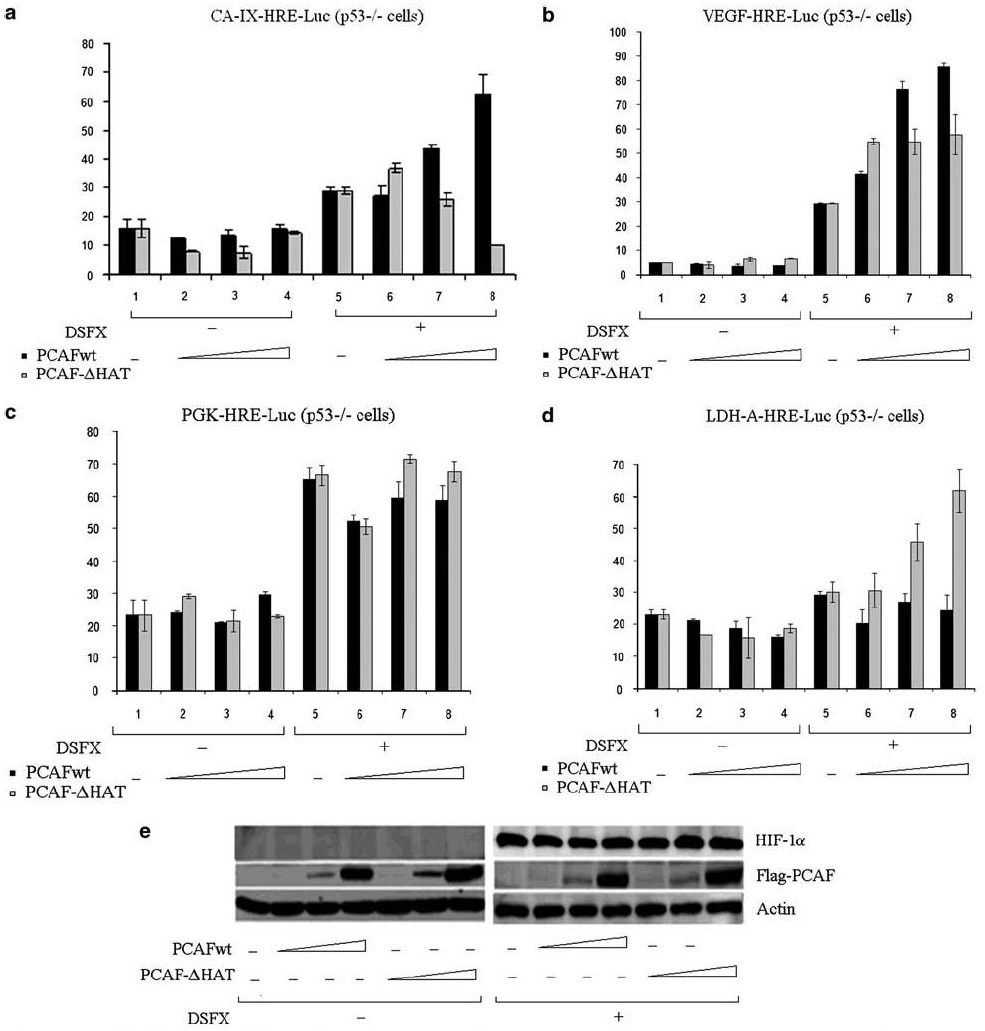

Figure 6 P300/CBP-associated factor (PCAF) directs hypoxia-inducible factor-1α (HIF-1α) to a specific subset of its targets. PCAFwt or PCAF-ΔHAT over-expressing SAOS2 cells were subjected to 20 h desferrioxamine (DSFX) treatment and the luciferase activity of carbonic anhydrase IX (CA-IX) (**a**), vascular endothelial growth factor (VEGF) (**b**), phosphoglycerate kinase-1 (PGK-1) (**c**) and lactate dehydrogenase A (LDH-A) (**d**) was analysed as described in 'Materials and methods'. Values represent means of four experiments. (**e**) Equal levels of HIF-1α expression in cells transfected either with PCAFwt or with PCAF-ΔHAT. In addition, the expression of Flag-PCAFwt and Flag-PCAF-ΔHAT proteins was not affected by DSFX treatment.

hypoxic conditions by genome-wide expression profile techniques (Hammond *et al*., 2006) the detailed and subtle mechanisms involved in the p53 selectivity to transactivate its downstream targets in hypoxic conditions remain imprecisely defined. The most likely explanation of p53 incompetence to activate its pro-apoptotic targets under hypoxia is based on an inability to form requisite networks with specific co-activators (Hammond and Giaccia, 2005). A precedent for this thinking is that p53 fails to induce the expression of Bnip3L under hypoxia because the binding between p53 and the p300/CBP co-activators is weak and unable to support Bnip3L expression in these conditions (Fei *et al*., 2004). Considering these observations we wanted

to define the composition of the transcription co-activator complexes that bind p53 and fine-tune its transcriptional activity under hypoxia.

The molecular mechanisms of p53- and HIF-1α-mediated apoptosis mostly operate through the activation of pro-apoptotic genes that bear binding sites for these transcription factors in their promoter such as the Bcl-2 family members that are important in the initiation and execution of the intrinsic pathway of apoptosis (Cory *et al*., 2003). The expression and activity of anti- and pro-apoptotic members of this family is delicately balanced by several mechanisms. The expression of the pro-apoptotic *Bax*, *PUMA*, *Noxa* and *BID* genes can be regulated by the transcriptional activity of the p53 tumour suppressor (Vousden and Lane, 2007). Recently published observations reported that the basis of the p53 promoter selectivity lies on its differential post-translational modifications. For example, activation of the Bax promoter requires participation of p53 acetylated at Lys320 by PCAF and Lys373 by p300, whereas the p53-dependent induction of p21 requires the participation of p53 acetylated at either site (Roy *et al*., 2005). In addition, acetylation of p53 by TIP-60 at K120 promotes apoptosis and not cell-cycle arrest (Tyteca *et al*., 2006), whereas acetylation at p53 K373 and K382 by p300 results in the induction of pro-apoptotic p53 targets (Knights *et al*., 2006). The existence of HREs in the regulatory regions of the gene promoters of several Bcl-2 family members and thus regulation of their expression by HIF-1α has also been demonstrated (Greijer and van der Wall, 2004). These observations imply that selectivity of p53 transcriptional activity under hypoxia is regulated by upstream events such as post-translational modifications, specific protein–protein interactions with co-activators (Demonacos *et al*., 2004) and other transcription factors such as HIF-1α (An *et al*., 1998). To gain further mechanistic insight into apoptosis in hypoxic cells and provide details on how it is regulated we investigated the function of the known p53 co-regulator PCAF and how this factor orchestrates the coordination of regulatory events leading to the selective pattern of gene expression of both p53 and HIF-1α under hypoxia.

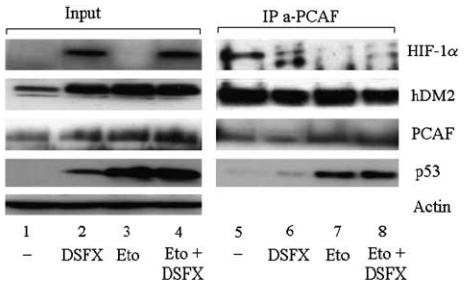

Figure 7 P300/CBP-associated factor (PCAF) interacts with hypoxia-inducible factor-1α (HIF-1α). U2OS cells were treated with desferrioxamine (DSFX, 20 h) and etoposide (6 h) or both DSFX and etoposide or left untreated as indicated. Whole-cell extracts were immunoprecipitated using an anti-PCAF antibody against the endogenous protein and blotted for HIF-1α, hDM2, PCAF and p53.

In this study we show that the transcriptional co-activator PCAF directs p53 preferentially to the $p21^{WAF-1/CIP-1}$ promoter in DSFX-treated cells. In addition, we established that PCAF-dependent acetylation of p53 K320 is deficient in DSFX-treated cells and this correlates with the reduction of the recruitment of this acetylated p53 isoform to its pro-apoptotic targets. These observations are in agreement with recently published reports showing that K320Q prevents cell death and induces G_1 arrest (Knights *et al*., 2006) and could explain the predominance of surviving and growth arrested versus dying cells in hypoxic tumour subpopulations (Bunz *et al*., 1998). Earlier studies (Koumenis *et al*., 2001) have shown that hypoxia primarily induces the interaction of p53 with mSin3A, but not with p300. These data suggest that different levels of hypoxia or tissue specificity are involved in the differential interactions of p53 with specific co-activators or co-repressors modulating its transcriptional activity under diverse stress conditions.

Figure 8 P300/CBP-associated factor (PCAF) acetylates hypoxia-inducible factor-1α (HIF-1α) and regulates its protein stability. (**a**) SAOS2 cells were transfected with Flag-PCAF expression vector and treated with desferrioxamine (DSFX) for 20 h as indicated. Whole-cell extract was immunoprecipitated with pan-acetyl-lysine antibody, resolved on polyacrylamide gel electrophoresis (PAGE) and blotted for HIF-1α and PCAF antibodies. Actin was used as loading control. (**b**) Whole-cell extract from transiently transfected with Flag-PCAFwt U2OS cells was submitted to immunoprecipitation with the anti-H3-K14 Ac-lysine antibody and western blotted with anti-HIF-1α, anti-p53 and anti-Flag-specific antibodies. Lysate (10%) was loaded as input and is shown in the left panel. Actin was used as loading control. (**c**) U2OS cells were transfected with Flag-PCAFwt and Flag-PCAF-ΔHAT and exposed to DSFX treatment for 20 h. At 48 h after transfection the whole-cell extract from these cells was submitted to immunoprecipitation with the pan-acetyl-lysine antibody and immunoblotted with anti-HIF-1α antibody. U2OS transfected with empty cytomegalovirus (CMV) or Flag-PCAFwt expression vectors co-transfected with plasmids expressing HA-HIF-1α(wt) (**d**) HA-HIF-1α-K532R (**e**) or HA-HIF-1α-K389R (**f**) were submitted to immunoprecipitation with HA antibody after 20 h of DSFX treatment as indicated. Pan-acetyl-lysine antibody was used to detect acetylated proteins in the immunoprecipitations, anti-HA antibody against transfected HA-HIF-1α and anti-HIF-1α to detect total HIF-1α in the inputs. Actin was used as loading control. (**g**) PCAF-dependent acetylation of HIF-1α regulates its protein stability. Empty PCDNA3 vector, Flag-PCAFwt or Flag-PCAF-ΔHAT was transiently expressed in SAOS2 cells and incubated with DSFX for 20 h and cyclohexamide for the indicated time points. Cell extracts were analysed with PAGE and subjected to immunoblot analysis with anti-HIF-1α, Flag and actin antibodies. (**h**) The diagram represents the ratio of the intensity of the HIF-1α bands in the cells transfected with different expression vectors (PCDNA3, PCAFwt, PCAF-ΔHAT) and the intensity of the actin bands in the respective cells. The intensity of HIF-1α divided by the intensity of actin at 0 time points was regarded as 100%. Densitometric analysis was performed using the AIDA 3.52.046 quantification software.

To provide additional insight in the regulation of the cell growth programme regulated by PCAF we performed FACS analysis. We observed increased number of U2OS cells expressing Flag-PCAF-ΔHAT arresting in G_1 phase of the cell cycle (Figures 4a and b, compare bar 8 to 5), which could be explained by the fact that p53 was preferentially recruited to the $p21^{WAF-1/CIP-1}$ promoter (Figure 3b). On the other hand the accumulation of PCAFwt-expressing U2OS cells in sub-G_1 phase (Figure 4a) was at least in part a result of the

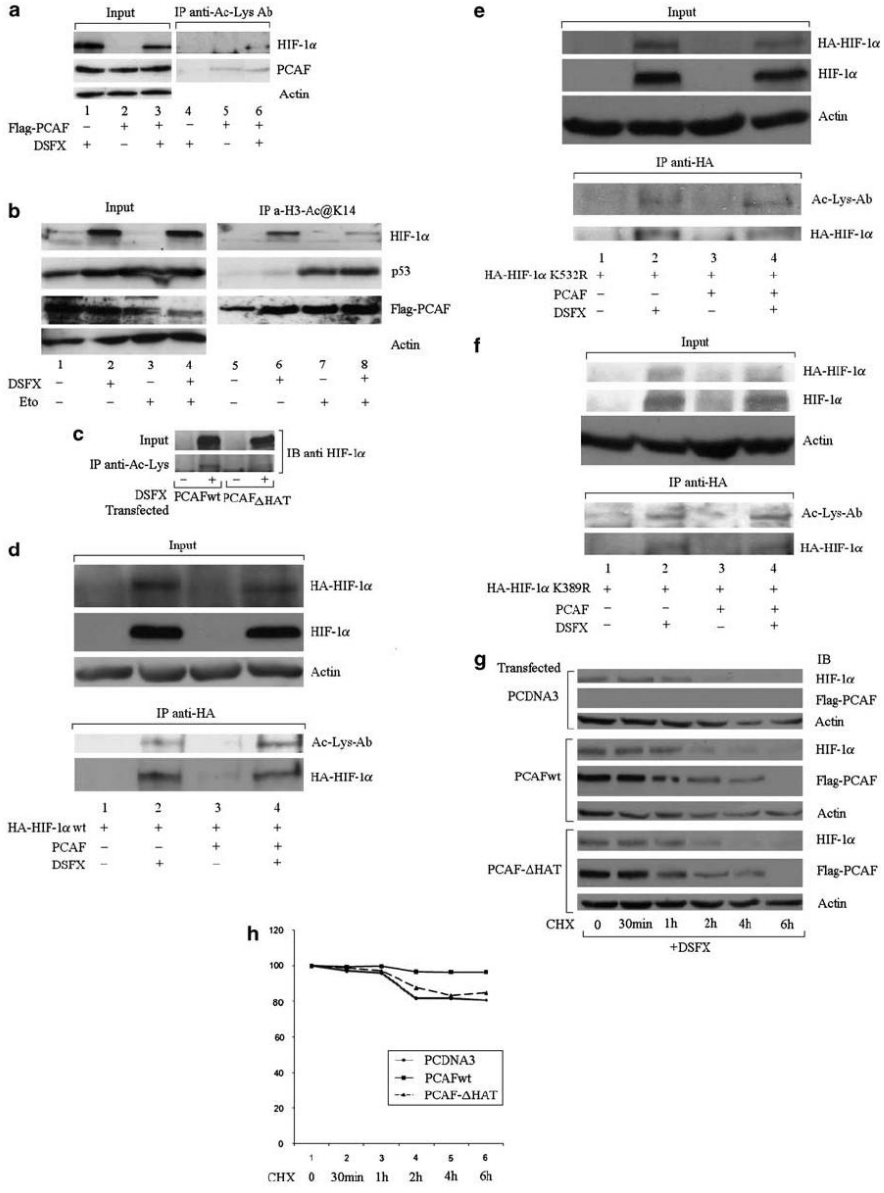

upregulation of BID expression in these cells after DSFX treatment (Figure 5b). Furthermore, FACS analysis showed that p53 and HIF-1α cooperate in inducing apoptosis and they have opposing functions in the G_1 cell-cycle arrest in accord with previously published observations (Goda *et al*., 2003).

Alternative pathways involving transcription factors activated in DSFX-treated cells, such as FOXO3a (You *et al*., 2006) mediate induction of p53- and HIF-1α-independent apoptosis. PCAF as a FOXO3a HAT (Brunet *et al*., 2004) might be implicated in the execution of apoptosis induced by this transcription factor. Another pathway through which the PCAF HAT activity induces p53-independent apoptosis is through PCAF-dependent acetylation of Ku70, which results in the disruption of the complex of this DNA damage repair protein with Bax, stimulating initiation of programmed cell death (Cohen *et al*., 2004).

To explore further these observations and investigate whether PCAF has any effect on HIF-1α transactivation we followed the promoter occupancy of known HIF-1α targets by PCAF. These experiments showed that PCAF is recruited to the HRE sites of two HIF-1α targets, the pro-apoptotic BID (Erler *et al*., 2004) and the angiogenic VEGF gene (Pescador *et al*., 2005). Interestingly, the expression of the pro-apoptotic truncated variant of BID was identified in the DSFX-treated cells over-expressing PCAF, implying that PCAF is involved in the regulation of HIF-1α-mediated apoptosis. Other assays showed that PCAF is an HIF-1α transcriptional cofactor and through its HAT activity it specifically and selectively directs HIF-1α to a subset of its target genes. There are several potential explanations for this distinction in the PCAF function. First, differences in the structure of the promoter between the different HIF-1α targets could be responsible for preferential binding of particular subset of these targets by differently modified HIF-1α isoforms. Indeed, the gene encoding CA-IX conforms to a pattern first described among genes encoding glycolytic enzymes (Hu *et al*., 2003), and is specifically responsive to HIF-1α, showing no response to HIF-2α in any cell type (Raval *et al*., 2005). The gene encoding VEGF is rather similar to a pattern previously reported for genes encoding proteins such as PHD3 and GLUT-1 (Raval *et al*., 2005). Therefore, PCAF-dependent acetylation of HIF-1α might be the mechanism by which HIF-1α subunit distinguishes between its target promoters or even between targets that are specifically responsive to HIF-1α or to HIF-2α transcription factors (Gordan *et al*., 2007), a possibility that we are currently investigating in our laboratory. Second, PCAF might help the recruitment of different transcription factors to distinct regions of the genome. In turn, these associations could allow different transcription factors to carry out specialized functions determining the cellular fate (survival or apoptosis). In line with these observations previous reports have indicated that the p300 co-activator is vital for the induction of a part of HIF-responsive genes and dispensable for others (Kasper *et al*., 2005).

Further study of the effects of PCAF on HIF-1α revealed that the two proteins interact in DSFX-treated cells (Figure 7) and this interaction results in the PCAF-dependent acetylation of HIF-1α (Figure 8). To exclude the possibility that HIF-1α coprecipitated with other acetylated proteins such as other HAT(s), acetylated p53 or auto-acetylated PCAF (Liang *et al*., 2006) we followed two approaches. First, we immunoprecipitated acetylated proteins from the extract of U2OS cells expressing either PCAFwt or PCAF-ΔHAT and immunoblotted with antibodies recognizing HIF-1α. HIF-1α was more efficiently acetylated in the PCAFwt-transfected cells and was acetylated to a lesser extent in the PCAF-ΔHAT-expressing cells. The same conclusion was reached when we used an antibody that recognizes PCAF-specific acetylation targets to perform the precipitation of PCAF acetylation targets (Poux and Marmorstein, 2003). Second, we mutated two possible acetylation targets in HIF-1α namely K532 and K389. Precipitation of HIF-1α with HA antibodies and blot with the acetyl-lysine antibody confirmed that HIF-1α was acetylated.

Although the effect of ARD1-mediated acetylation of HIF-1α is a controversial issue, it has been linked to HIF transcriptional activity and protein stability (Bilton *et al*., 2006). We tested whether PCAF mediated similar effect on HIF-1α by following its half-life and we observed that HIF-1α acetylated by PCAF was a more stable protein (Figures 8g and h). Studies to identify the possible site(s) of HIF-1α acetylated by PCAF are currently ongoing in our laboratory.

In conclusion, our study provides an additional molecular mechanism explaining the inability of p53 to activate its pro-apoptotic targets in hypoxia and implicates PCAF in the regulation of the fine-tuning of the transcriptional activity of both p53 and HIF-1α in hypoxic conditions as well as regulating protein stability of both transcription factors (Jin *et al*., 2002; Linares *et al*., 2007).

Materials and methods

Cell lines, culture conditions and constructs

Dulbecco's modified Eagle's medium (Gibco, Paisley, Scotland, UK) supplemented with 10% fetal calf serum and 1% 10 U/ml penicillin and streptomycin was used to maintain human osteosarcoma U2OS (p53+/+) and SAOS2 (p53−/−) cell lines at 37 °C and 5% CO_2. Cells were collected 20 h after 250 μM DSFX treatment (Sigma, Gillingham, England, UK) and 16 h after incubation with 10 μM etoposide (Sigma) unless otherwise indicated.

The p53K320R expression vector was a gift from Dr Halazonetis, the pCiFlag-PCAF(wt) and pCiFlag-PCAF(ΔHAT) from Dr Talianidis. Human BID luciferase reporter consisting the consensus p53-binding site has been provided by Dr El-Deiry and is described in Sax *et al*. (2002). The $p21^{WAF-1/CIP-1}$ (El-Deiry *et al*., 1993) and CA-IX-HRE-luc (Wykoff *et al*., 2000) have been previously described. Silencing of HIF-1α with RNAi was performed as described previously (Erler *et al*., 2004).

Site-directed mutagenesis was performed by amplifying the HA-HIF-1α(wt) plasmid with two sets of primers to achieve the desired mutations. The mutagenesis was performed using the QuickChange Site Directed Mutagenesis Kit (Stratagene, La Jolla, CA, USA) following the manufacturer's instructions.

The calcium phosphate method (Demonacos *et al*., 2001) and the polyfect transfection system (Qiagen, Crawley, UK) were used to transfect cells. Luciferase reporter assays were carried out as described previously (Demonacos *et al*., 2001).

Immunoprecipitation and immunoblotting

Total cellular protein extract was immunoprecipitated with the following antibodies: mouse monoclonal anti-p53 (DO-1; Santa Cruz, Santa Cruz, CA, USA), anti-human rabbit polyclonal p53 (2381-PC-100; Trevigen, Gaithersburg, MD, USA), mouse monoclonal anti-Flag (M2; Sigma), mouse monoclonal anti-acetyl-lysine (4G12; Upstate, Watford, England, UK), rabbit polyclonal anti-acetyl-histone H3 at Lys14 (Upstate), anti-PCAF rabbit polyclonal (H-369; Santa Cruz), Anti-HIF-1α (H1α67; Calbiochem, San Diego, CA, USA) and goat polyclonal anti-BID (R&D, Minneapolis, MN, USA). For detection of acetylated forms of p53, cells were treated with Na-butyrate (1 mM) for 2 h before lysis. IP extracts were analysed accordingly by western blotting with anti-acetyl K320 p53 (Upstate) and anti-acetyl-p53 at Lys382 (no. 2525; Cell Signaling, Danvers, MA, USA). Proteins were visualized using ECL (Pierce, Rockford, IL, USA) according to the manufacturer's instructions.

Chromatin immunoprecipitation

ChIP analysis was performed in U2OS cells using the Active Motif (Rixensart, Belgium) ChIP express kit. Briefly, after chromatin cross-linking with 1% formaldehyde, chromatin complexes were immunoprecipitated from DSFX-treated or not treated cells with antibodies against p53 acetylated at K320 and K382, anti-p300 NM-11 (Santa Cruz), anti-Flag M-20 (Sigma) or irrelevant (horseradish peroxidase-conjugated anti-rabbit). Quantitative PCR analysis was performed with the oligonucleotides described in Supplementary Figure 1. Values obtained from the ChIP assay analysis (Opticon Monitor 3 software) were normalized to the background obtained from the precipitation with a non-specific antibody. Figures 1a, c, 2b, c and 5a indicate values obtained by subtracting the amount of the non-specifically precipitated immunocomplexes from the amount of the specifically precipitated ones.

Flow cytometry

Cells were transfected with the indicated expression vectors, treated with DSFX as specified in Figure 4, harvested 48 h after transfection and fixed in 50% ethanol. Propidium iodide and RNase A were added to final concentrations of 50 and 100 μg/ml, respectively and transfected cells were stained with a CD-20-FITC antibody for CD20 expression. Cell-cycle profile was determined by FACScan flow cytometry and analysed by CellQuest software (Becton Dickinson) as previously described (Demonacos *et al*., 2001). Cell count represents the cells exhibiting the CD20 antigen used as a transfection efficiency control. The average transfection efficiency was 30% for U2OS and 12% for SAOS2 cells. Only the CD20-transfected population of cells (sorted by CD20-FITC-conjugated antibody) has been taken into account for the FACS analysis. The average of two independent FACS experiments is shown in Figures 4a and b and the cell-cycle profiles from one experiment in Supplementary Figure 3.

Acknowledgements

We thank W El-Deiry for providing the BID-p53-Luc reporter construct; I Talianidis for the Flag-PCAF and Flag-PCAF-ΔHAT constructs; T Halazonetis for the p53K320R expression vector; K Williams for the HIF-1α-responsive reporters of VEGF-Luc, CA-IX-Luc, PGK-1-Luc and LDH-A-Luc; M Blaylock and the Paterson Institute for Cancer Research for assistance with FACS analysis. Our research was supported by the School of Pharmacy, University of Manchester (CD), Cancer Research UK (CDive), MRC programme grant (G0500366) to IJS and Wellcome Trust (069024) to MKD.

References

An WG, Kanekal M, Simon MC, Maltepe E, Blagosklonny MV, Neckers LM. (1998). Stabilization of wild-type p53 by hypoxia-inducible factor 1α. *Nature* **392**: 405–408.

Achison M, Hupp TP. (2003). Hypoxia attenuates the p53 response to cellular damage. *Oncogene* **22**: 3431–3440.

Arany Z, Huang LE, Eckner R, Bhattacharya S, Jiang C, Goldberg MA *et al*. (1996). An essential role for p300/CBP in the cellular response to hypoxia. *Proc Natl Acad Sci USA* **93**: 12969–12973.

Bilton R, Trottier E, Pouyssegur J, Brahimi-Horn MC. (2006). ARDent about acetylation and deacetylation in hypoxia signalling. *Trends Cell Biol* **16**: 616–621.

Blagosklonny MV, An WG, Romanova LY, Trepel J, Fojo T, Neckers L. (1998). p53 inhibits hypoxia-inducible factor-stimulated transcription. *J Biol Chem* **273**: 11995–11998.

Brahimi-Horn C, Mazure N, Pouysségur J. (2005). Signalling via the hypoxia-inducible factor-1α requires multiple posttranslational modifications. *Cell Signalling* **17**: 1–9.

Brunet A, Sweeney LB, Sturgill JF, Chua KF, Greer PL, Lin Y *et al*. (2004). Stress-dependent regulation of FOXO transcription factors by the SIRT1 deacetylase. *Science* **303**: 2011–2015.

Bunz F, Dutriaux A, Lengauer C, Waldman T, Zhou S, Brown JP *et al*. (1998). Requirement for p53 and p21 to sustain G_2 arrest after DNA damage. *Science* **282**: 1497–1501.

Chao C, Wu Z, Mazur SJ, Borges H, Rossi M, Lin T *et al*. (2006). Acetylation of mouse p53 at lysine 317 negatively regulates p53 apoptotic activities after DNA damage. *Mol Cell Biol* **26**: 6859–6869.

Chen D, Li M, Luo J, Gu W. (2003). Direct interactions between HIF-1α and Mdm2 modulate p53 function. *J Biol Chem* **278**: 13595–13598.

Cohen HY, Lavu S, Bitterman KJ, Hekking B, Imahiyerobo TA, Miller C *et al*. (2004). Acetylation of the C terminus of Ku70 by CBP and PCAF controls Bax-mediated apoptosis. *Mol Cell* **13**: 627–638.

Cory S, Huang DCS, Adams JM. (2003). The Bcl-2 family: roles in cell cycle survival and oncogenesis. *Oncogene* **22**: 8590–8607.

Demonacos C, Krstic-Demonacos M, La Thangue NB. (2001). A novel TPR-motif co-factor contributes to p300 activity in the p53 response. *Mol Cell* **8**: 71–84.

Demonacos C, Krstic-Demonacos M, Smith L, Xu D, O'Connor DP, Jansson M *et al*. (2004). A new effector pathway links ATM kinase with the DNA damage response. *Nat Cell Biol* **6**: 968–976.

El-Deiry WS, Tokino T, Velculescu VE, Levy DB, Parsons R, Trent JM *et al*. (1993). WAF1, a potential mediator of p53 tumor suppression. *Cell* **75**: 817–825.

Erler JT, Cawthorne CJ, Williams KJ, Koritzinksy M, Wouters B, Wilson C *et al*. (2004). Hypoxia mediated down regulation of Bid and Bax in tumours occurs via HIF-1 dependent and independent mechanisms and contributes to drug resistance. *Mol Cell Biol* **24**: 2875–2889.

Fei P, Wang W, Kim S, Wang S, Burns TF, Sax JK *et al*. (2004). Bnip3L is induced by p53 under hypoxia, and its knockdown promotes tumor growth. *Cancer Cell* **6**: 597–609.

Forsythe JA, Jiang BH, Iyer NV, Agani F, Leung SW, Koos RD *et al.* (1996). Activation of vascular endothelial growth factor gene transcription by hypoxia-inducible factor 1. *Mol Cell Biol* **16**: 4604–4613.

Freedman SJ, Sun Z-YJ, Kung AL, France DS, Wagner G, Eck MJ. (2004). Structural basis for negative regulation of hypoxia-inducible factor-1α by CITED2. *Nat Struct Biol* **10**: 504–512.

Freedman SJ, Sun Z-YJ, Poy F, Kung AL, Livingston DM, Wagner G *et al*. (2002). Structural basis for recruitment of CBP/p300 by hypoxia-inducible factor-1α. *Proc Natl Acad Sci USA* **99**: 5367–5372.

Goda N, Dozier S, Johnson RS. (2003). HIF-1 in cell cycle regulation, apoptosis, and tumor progression. *Antioxid Redox Signal* **5**: 467–473.

Gordan JD, Bertout JA, Hu C-J, Diehl JA, Simon MC. (2007). HIF-2a promotes hypoxic cell proliferation by enhancing c-Myc transcriptional activity. *Cancer Cell* **11**: 335–347.

Greijer AE, van der Wall E. (2004). The role of hypoxia inducible factor 1 (HIF-1) in hypoxia induced apoptosis. *J Clin Pathol* **57**: 1009–1014.

Hammond EM, Giaccia AJ. (2005). The role of p53 in hypoxia-induced apoptosis. *Biochem Biophys Res Comm* **331**: 718–725.

Hammond EM, Mandell DJ, Salim A, Krieg AJ, Johnson TM, Shirazi HA *et al.* (2006). Genome-wide analysis of p53 under hypoxic conditions. *Mol Cell Biol* **26**: 3492–3504.

Hansson LO, Friedler A, Freund S, Rudiger S, Fersht AR. (2002). Two sequence motifs from HIF-1α bind to the DNA-binding site of p53. *Proc Natl Acad Sci USA* **99**: 10305–10309.

Hu CJ, Wang LY, Chodosh LA, Keith B, Simon MC. (2003). Differential roles of hypoxia inducible factor 1alpha (HIF-1alpha) and HIF-2alpha in hypoxic gene regulation. *Mol Cell Biol* **23**: 9361–9374.

Jeong J-W, Bae M-K, Ahn M-Y, Kim S-H, Sohn T-K, Bae M-H *et al.* (2002). Regulation and destabilization of HIF-1α by ARD1-mediated acetylation. *Cell* **111**: 709–720.

Jin Y, Zeng SX, Dai M-S, Yang X-J, Lu H. (2002). MDM2 Inhibits PCAF-mediated p53 acetylation. *J Biol Chem* **277**: 30838–30843.

Kaelin Jr WG. (2005). Proline hydroxylation and gene expression. *Annu Rev Biochem* **74**: 115–128.

Kasper LH, Boussouar F, Boyd K, Xu W, Biesen M, Rehg J *et al.* (2005). Two transactivation mechanisms cooperate for the bulk of HIF-1 responsive gene expression. *EMBO J* **24**: 3846–3858.

Knights CD, Catania J, Di Giovani S, Muratoglu S, Perez R, Swartzbeck A *et al.* (2006). Distinct p53 acetylation cassettes differentially influence gene-expression patterns and cell fate. *J Cell Biol* **173**: 533–544.

Koumenis C, Alarcon R, Hammond E, Sutphin P, Hoffman W, Murphy M *et al.* (2001). Regulation of p53 by hypoxia: dissociation of transcriptional repression and apoptosis from p53-dependent transactivation. *Mol Cell Biol* **21**: 1297–1310.

Lando D, Peet DJ, Whelan DA, Gorman JJ, Whitelaw ML. (2002). Asparagine hydroxylation of the HIF transactivation domain: a hypoxic switch. *Science* **295**: 858–861.

Liang D, Kong X, Sang N. (2006). Effects of histone deacetylase inhibitors on HIF-1. *Cell Cycle* **5**: 2430–2435.

Linares LK, Kiernan R, Triboulet R, Chable-Bessia C, Latreille D, Cuvier O *et al.* (2007). Intrinsic ubiquitination activity of PCAF controls the stability of the oncoprotein Hdm2. *Nat Cell Biol* **9**: 331–338.

Liu L, Scolnick DM, Trievel RC, Zhang HB, Marmorstein R, Halazonetis TD *et al*. (1999). p53 sites acetylated *in vitro* by PCAF and p300 are acetylated *in vivo* in response to DNA damage. *Mol Cell Biol* **19**: 1202–1209.

Luo J, Li M, Tang Y, Laszkowska M, Roeder RG, Gu W. (2004). Acetylation of p53 augments its site-specific DNA binding both *in vitro* and *in vivo*. *Proc Natl Acad Sci USA* **101**: 2259–2264.

Mahon PC, Hirota K, Semenza GL. (2001). FIH-1: a novel protein that interacts with HIF-1α and VHL to mediate repression of HIF-1 transcriptional activity. *Genes Dev* **15**: 2675–2686.

Pan Y, Ogrysko PR, Arsham AM, Koch CJ, Simon MC. (2004). p53 cannot be induced by hypoxia alone but responds to the hypoxic microenvironment. *Oncogene* **23**: 4975–4983.

Pescador N, Cuervas Y, Naranjo S, Alcaide M, Villar D, Landazuri MD *et al.* (2005). Identification of a functional hypoxia-responsive element that regulates the expression of egl nine homologue 3 (egln/phd3) gene. *Biochem J* **390**: 189–197.

Poux AN, Marmorstein R. (2003). Molecular basis for Gcn5/PCAF histone acetyltransferase selectivity for histone and non-histone substrates. *Biochemistry* **42**: 14366–14372.

Ravi R, Mookerjee B, Bhujwalla ZM, Sutter CH, Artemov D, Zeng Q *et al.* (2000). Regulation of tumor angiogenesis by p53-induced degradation of hypoxia-inducible factor 1α. *Genes Dev* **14**: 34–44.

Raval RR, Lau KW, Tran MG, Sowter HM, Mandriota SJ, Li JL *et al.* (2005). Contrasting properties of hypoxia-inducible factor 1 (HIF-1) and HIF-2 in von-Hippel-Lindau-associated renal cell carcinoma. *Mol Cell Biol* **25**: 5675–5686.

Roy S, Packman K, Jeffrey R, Tenniswood M. (2005). Histone deacetylase inhibitors differentially stabilise acetylated p53 and induce cell cycle arrest or apoptosis in prostate cancer cells. *Cell Death Diff* **12**: 482–491.

Roy S, Tenniswood M. (2007). Site-specific acetylation of p53 directs selective transcription complex assembly. *J Biol Chem* **282**: 4765–4771.

Sakaguchi KJ, Herrera S, Saito T, Miki M, Bustin A, Vassilev A *et al.* (1998). DNA damage activates p53 through a phosphorylation-acetylation cascade. *Genes Dev* **12**: 2831–2841.

Sax JK, Fei P, Murphy ME, Bernhard E, Korsmeyer SJ, El-Deiry WS. (2002). BID regulation by ER contributes to chemosensitivity. *Nat Cell Biol* **4**: 842–849.

Schmid T, Zhou J, Köhl R, Brüne B. (2004). p300 relieves p53-evoked transcriptional repression of hypoxia-inducible factor-1 (HIF-1). *Biochem J* **380**: 289–295.

Semenza GL, Jiang B-H, Leung SW, Passantino R, Concordet J-P, Maire P *et al.* (1996). Hypoxia response elements in the aldolase A, enolase 1, and lactate dehydrogenase a gene promoters contain essential binding sites for hypoxia-inducible factor 1. *J Biol Chem* **271**: 32529–32537.

Tyteca S, Legube G, Trouche D. (2006). To die or not to die: A HAT trick. *Mol Cell* **24**: 807–812.

Vaupel P, Harrison L. (2004). Tumor hypoxia: causative factors, compensatory mechanisms, and cellular response. *Oncologist* **9**(Suppl 5): 4–9.

Vousden KH, Lane DP. (2007). p53 in health and disease. *Nat Rev Mol Cell Biol* **8**: 275–283.

Vousden KH, Prives C. (2005). p53 and prognosis; new insights and further complexity. *Cell* **120**: 7–10.

Warnecke C, Zaborowska Z, Kurreck J, Erdmann VA, Frei U, Wiesener M *et al.* (2004). Differentiating the functional role of hypoxia-inducible factor (HIF)-1a and HIF-2a (EPAS-1) by the use of RNA interference: erythropoietin is a HIF-2alpha target gene in Hep3B and Kelly cells. *FASEB J* **18**: 1462–1464.

Wenger RH. (2002). Cellular adaptation to hypoxia: O2-sensing protein hydroxylases, hypoxia-inducible transcription factors, and O2-regulated gene expression. *FASEB J* **16**: 1151–1162.

Wykoff CC, Beasley NJP, Watson PH, Turner KJ, Pastorek J, Sibtain A *et al*. (2000). Hypoxia-inducible expression of tumor-associated carbonic anhydrases. *Cancer Res* **60**: 7075–7083.

You H, Pellegrini M, Tsuchihara K, Yamamoto K, Hacker G, Erlacher M *et al*. (2006). FOXO3a-dependent regulation of Puma in response to cytokine/growth factor withdrawal. *J Exp Med* **203**: 1657–1663.

Zhu Y, Mao XO, Sun Y, Xia Z, Greenberg DA. (2002). p38 mitogen-activated protein kinase mediates hypoxic regulation of Mdm2 and p53 in neurons. *J Biol Chem* **277**: 22909–22914.

Supplementary Information accompanies the paper on the Oncogene website (http://www.nature.com/onc)